The Synthesis and Coordination Properties of Heterocyclic Receptors and Sensors for Anions

By

Colin Neil Warriner

A thesis submitted for the degree of

DOCTOR OF PHILOSOPHY

at the

School of Chemistry

University of Southampton

2004

UNIVERSITY OF SOUTHAMPTON

ABSTRACT

FACULTY OF ENGINEERING, SCIENCE AND MATHEMATICS

Doctor of Philosophy

THE SYNTHESIS AND COORDINATION PROPERTIES OF HETEROCYCLIC RECEPTORS AND SENSORS FOR ANIONS

by Colin Neil Warriner

Two calix[4]pyrrole macrocycles have been synthesised containing a ferrocene redox active group in one of the *meso*-positions. These receptors co-ordinate a variety of anions in solution. ^{1}H NMR analysis of the receptors in the presence of anions revealed a downfield shift of one ferrocene proton, this provided evidence for a direct co-ordination mechanism between the anion binding site and the redox reporter group. Electrochemical studies revealed cathodic shifts with all anions, up to 100 mV with dihydrogen phosphate. A pentapyrrolic calix[4]pyrrole was synthesised bearing a single pyrrole pendant arm in the *meso*-position. This receptor displayed an enhanced affinity for all anions when compared to *meso*-octamethylcalix[4]pyrrole. The selectivity displayed by this receptor for carboxylates was investigated using molecular modelling that suggested both of the carboxylate oxygens were simultaneously co-ordinated.

A variety of furan and thiophene based amide and thioamide clefts have been synthesised. Introduction of the thioamide functional group displayed a moderate increase in anion binding affinity when compared to the corresponding amide derivatives, whereas the heteroatom was seen to alter the receptor selectivity. The furan based receptors revealed up to a 40-fold selectivity for fluoride over other anionic guests, while the thiophene receptors selectively bound dihydrogen phosphate. The phenylamide thiophene receptors gave strange titration profiles with fluoride, believed to be caused by multiple equilibria processes occurring in solution. However, addition of fluoride and other basic anions to these receptors produced a colourless to yellow colour change, possibly allowing colourimetric sensing of basic anions by these receptors. A crystal structure revealed the formation of thiophene CH···anion hydrogen bonds in the solid state, while a mono-amide substituted thiophene receptor provided further evidence for this interaction in solution.

Finally, four amido-pyrrole clefts bearing one or two ferrocene reporter groups have been synthesised and crystallographically characterised. The redox active ferrocene moieties are linked to the anion binding site (amido-pyrrole unit) by either a non-conjugated or conjugated pathway. The conjugated receptors are predominantly better anion receptors than their non-conjugated counterparts. The conjugated receptors displayed a selectivity for benzoate over other anionic guests, additionally large cathodic shifts of the ferrocene/ferrocenium redox couple are observed in the presence of this anion.

"I suppose I could make changes in my play
but who am I to tamper with a masterpiece."

Oscar Wilde

Acknowledgments

I would like to start by thanking Dr Phil Gale for letting me work in his research group and for his assistance over the last three and a bit years. Thanks to everyone in the group past and present, you all made everyday lab life more bearable, and sometimes exciting….. Salvo and Graham with the HCl cylinder, Ismael performing magic tricks with fire etc.

I am exceptionally grateful to Dr Mike Paver for the "short term loan" of his lap-top, without which I would probably still be writing my introduction. On the topic of computers, my thanks goes out to everyone who helped me overcome my technophobia problems over the last few years, you know who you are.

I would like to sincerely thank the EPSRC National Crystallography Service based at the University of Southampton for solving all of my crystal structures and giving me advice, principally Dr. Simon Coles and Dr. Mark Light. I appreciated your ability to keep smiling when yet another!! Gale group crystal came down to you.

I would like to thank Dr. Guy Denuault and Rebecca Zimmerman for help with the electrochemistry results, and Prof. Richard Whitby for the molecular modelling on the pentapyrrolic calix[4]pyrrole.

To all of my friends, among them:- Salvo, your rolling ability never failed to amuse me (I can confirm the total number of cigarettes smoked during our breaks reached 233412). Vince, well what can I say drinking partner extraordinaire, miss the Gate and that healthy pint after circuits. Bav, for going out and making a normal night, well a big night. Rob, after playing many hours of pool in the staff club, I think we're about even?! Jo, where would the quiz team have been without you? Graham, always certain that you had the ability to talk and talk… and Matt the worlds greatest diplomat.

Finally, I would like to thank my parents for there support and encouragement over the years, and to thank Caroline for being hugely supportive both emotionally and financially. I am grateful for everything that you have done.

Contents

Chapter 3: *Heterocyclic amide clefts*

Chapter 4: *Ferrocene appended pyrrole amide clefts*

Chapter 5: *Experimental*

Glossary

ADP	Adenosine 5-diphosphate
AMP	Adenosine 5-monophosphate
Anal.	Analysis (elemental)
ATP	Adenosine 5-triphosphate
br	Broad resonance (NMR)
Bu	Butyl
Calcd.	Calculated
CV	Cyclic Voltammetry
d	Doublet (NMR)
Δ	Standard Error on HRMS Analysis
DCM	Dichloromethane
Decomp.	Decomposition
DMAP	4,4'-Dimethylaminopyridine
DMF	Dimethyl Formamide
DMSO	Dimethyl Sulfoxide
DNA	Deoxyribonucleic Acid
e.g.	*Exempli gratia* (Latin: 'for the sake of example')
ES^+/ES^-	Positive/Negative Electrospray
Et	Ethyl
Fc	Ferrocene
g	Grams
He	Hexyl
HIV-1	Human Immunodeficiency Virus (strain 1)
HOBt	1-Hydroxybenzotriazole hydrate
HRMS	High Resolution Mass Spectrometry
Hz	Hertz
i.e.	*Id est* (Latin: 'that is')
ITC	Isothermal Titration Microcalorimetry
m	Multiplet (NMR)
M	Molecular Ion (MS) or Molar concentration
Me	Methyl

mg	Milligram
ml	Millilitre
Mp	Melting Point
MS	Mass Spectrometry
NMR	Nuclear Magnetic Resonance
PBP	Phosphate Binding Protein
Ph	Phenyl
ppm	Part per million
PyBOP	Benzotriazol-1-yloxytripyrrolidinophosphonium Hexafluorophosphate
RNA	Ribonucleic Acid
s	Singlet (NMR)
SBP	Sulfate Binding Protein
SWV	Square Wave Voltammetry
t	Triplet (NMR)
TBA	Tetrabutylammonium
TFA	Trifluoroacetic Acid
THF	Tetrahydrofuran
Tos	Tosyl
UV/Vis	Ultraviolet/Visable

1. *Introduction*

1.1 Supramolecular Chemistry

"One may say that supermolecules are to molecules and the intermolecular bond what molecules are to atoms and the covalent bond" Jean-Marie Lehn.[1]

Synthetic chemistry involves the making and breaking of covalent bonds to produce a desired compound from which intrinsic physical and chemical properties may be derived. Supramolecular chemistry is the study of supermolecules, molecular systems held together by reversible intermolecular forces much weaker than a covalent bond.

A supermolecule can be thought of as an organised structure constituted from two or more chemical species and the intermolecular interactions between them (Figure1.1), or alternatively, a host (deemed to be the larger component) binding a guest (neutral or ionic in nature). Although these species are not covalently bound they form stable complexes both in solution and in the solid state, due to the formation of complementary interactions between the individual components.

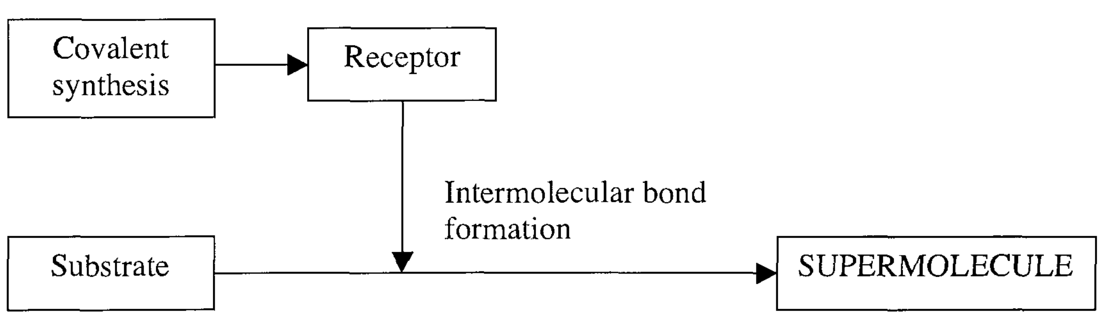

Figure 1.1: Schematic representation for the formation of a supermolecule.

The biological world provides supramolecular chemists with elegant complementary systems setting a standard for them to match synthetically. The DNA double helix is a natural structure that self assembles through formation of hydrogen-bonds between two complementary polynucleotide strands. The synthetic chemist has shown examples of self assembly within the literature although these systems will not be discussed here.[2,3]

An enzyme host may catalyse a single reaction with very high or total specificity, the active site in the enzyme is complementary to the guest substrate (or stabilises the transition state of the reaction). The size, position and shape of the binding sites within the active site of the enzyme are perfect for specific substrate recognition. This concept was described as the *"Lock and Key" principle*[4] (Figure 1.2) by Emil Fischer in 1894; a host and guest that complement each other in size, geometric shape and type of electronic interaction, will form the strongest complexes.

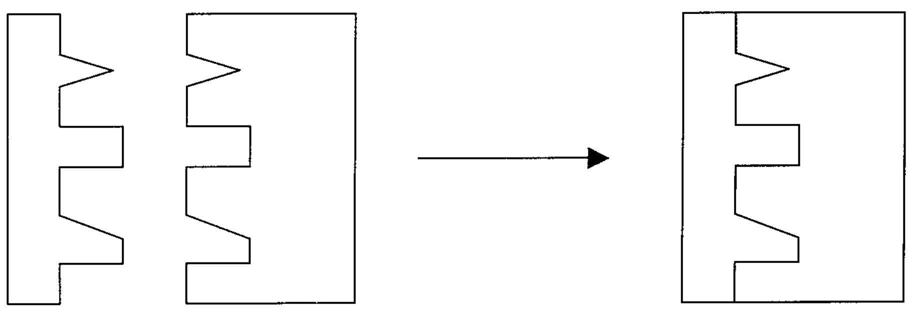

Key Lock Complex

Figure 1.2: The *"Lock and Key" principle* :- The receptor sites present in the lock (host) are complementary to the key (guest) forming a complex.

Supramolecular chemists use synthetic chemistry to produce a molecule that will form optimum interactions with a guest. The chemist has various non-covalent interactions (hydrogen bonding, electrostatics, Lewis acids, hydrophobic effects, π–π stacking and Van der Waals) available, and may use them either individually or in combination to make selective receptors. It is this flexibility and diversity, tied in with the broad applications, that interests and drives chemists to synthesise new selective receptors.

The field now known as supramolecular chemistry began when anion and alkali metal cation co-ordination almost concurrently came to light in the late 1960's. Yet the inspiring work on cation co-ordination by Pedersen,[5,6] Lehn,[1] and Cram[7] by crown ethers, cryptands and spherands respectively took precedence. This work inspired supramolecular chemists the world over, who developed novel cation integrated structures, such as racks,[8] helicates[9] and grids[10] or templated structures such as trefoil knots.[11] After the initial foundations were laid in metal cation co-ordination, the area of molecular recognition was formed with the inclusion of co-ordination of anions, neutral molecules and complex biomolecules.[3]

1.2 Anion binding

In 1968, Park and Simmons'[12] reported the first synthetic anion receptor, although it has only been in the last twenty years that significant attention has been paid to the co-ordination chemistry of anionic species. This may be due to the intrinsic properties of anions that create challenges in the design of new anion receptors or sensors.

Anions are larger than their iso-electronic cation counterparts, with the resultant effect of a lower charge to radius ratio. As a consequence, electrostatic interactions are relatively weaker when binding anions. Complementarity between the host and guest is an important consideration in the design of a receptor. Anions exhibit an array of geometries (e.g. spherical for halides, linear for hydroxide, tetrahedral for phosphate etc) requiring a receptor to be tailored to the guest of choice. Anions may also become protonated at lower pH values and lose their negative charge, requiring the receptor to function within the pH window of the desired anion.

The choice of solvent can also have a dramatic effect on the selectivity and binding strength of the receptor. Solvents that are able to accept or donate hydrogen bonds may compete with the anion for the binding site or form strong hydrogen bonds to the anion itself. Therefore a receptor must be able to effectively compete with the solvent media in which the anion recognition process is to occur. And finally the hydrophobicity of the anion can influence the affinity shown by a receptor. A hydrophobic anion will be bound more tightly in a hydrophobic binding site. Consideration of these design principles can hopefully lead to the generation of highly selective anion receptors.

Nature provides examples of highly selective anion recognition in the form of the transport proteins phosphate binding protein (PBP) and sulfate binding protein (SBP) (Figure 1.3) that are found in certain bacteria.[13]

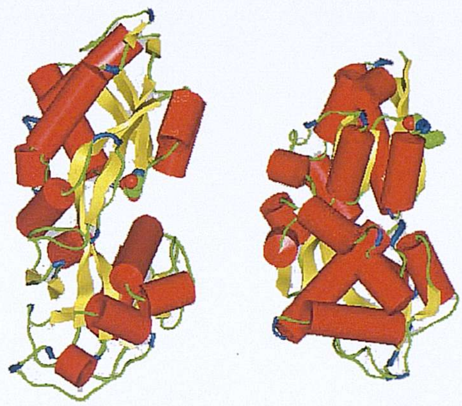

Figure 1.3: Crystal structures of the PBP (left) and SBP (right)

These proteins are able to distinguish between the two tetrahedral anions (phosphate being mono-protonated at physiological pH whilst sulfate is not) through the formation of hydrogen bonds. The PBP forms twelve hydrogen bonds to the anion, including the acceptance of a hydrogen bond from the phosphate by a negatively charged carboxylate group[14] enabling the protein to discriminate between protonated (phosphate) and fully deprotonated anions (sulfate). The SBP does not have any hydrogen bond acceptor groups in the binding site and is only able to co-ordinate fully deprotonated anions through seven hydrogen bonds in the protein cavity.

Anions are involved in many other biological systems, infact 70% of enzyme substrates are anionic. For example, the copper, zinc superoxide dismutase enzyme (CuZnSOD)[13] attracts anionic molecules through a positive field gradient allowing the enzyme to correctly dock the substrate. CuZnSOD is a dimer of two 151 amino acid containing monomers (Figure 1.4), and has a molecular weight of around 32 KDa.

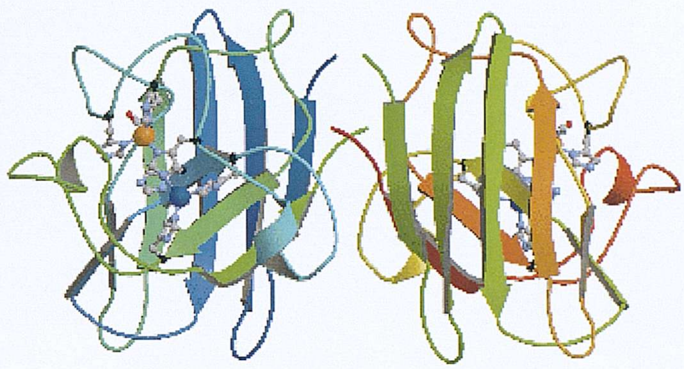

Figure 1.4: The Cu, Zn superoxide dismutase enzyme, an active copper centre is depicted as the blue sphere as seen within the monomer on the left.

A key residue in the active-site cavity is a positively charged arginine group, the absence of this group can lower the enzyme affinity for anions by a factor of ten. Throughout the catalytic process, the anionic guests are bound to the copper centre in both the +1 and +2 oxidation states (Scheme 1.1) whilst maintaining catalytic efficiency.

$$\text{SOD-Cu}^{2+} + O_2^{\cdot -} \longrightarrow \text{SOD-Cu}^{1+} + O_2$$

$$\text{SOD-Cu}^{1+} + O_2^{\cdot -} + 2H^+ \longrightarrow \text{SOD-Cu}^{2+} + H_2O_2$$

Scheme 1.1: The toxic superoxide radical is efficiently removed by the enzyme, remaining catalytic in both of the copper oxidation states.

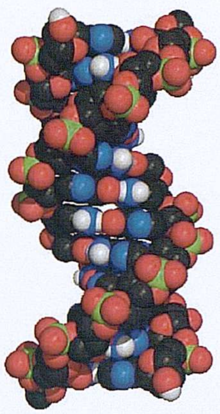

Figure 1.5: The DNA double helix.

Essential for the transfer of genetic information, deoxyribonucleic acid (DNA) is a polyanion. The double helical structure is built up from two strands of polynucleotides, with each nucleotide sub-unit containing a deoxyribose sugar, a nitrogenous base (adenine, guanine, cytosine or thymine) and a phosphate group (Figure 1.5). Alteration of the DNA structure or gene mutation can cause many diseases including cancer. Another phosphate containing anion found within human cells is adenosine 5-triphosphate (ATP) a tetra-anion at physiological pH and essential for life (Figure 1.6). When the terminal phosphate bond is hydrolysed (to form ADP, then AMP) energy is released, this process enables other endothermic reactions to take place that may not otherwise occur. The development of receptors or sensors that selectively bind phosphate may enhance our understanding and even give us control of these processes.

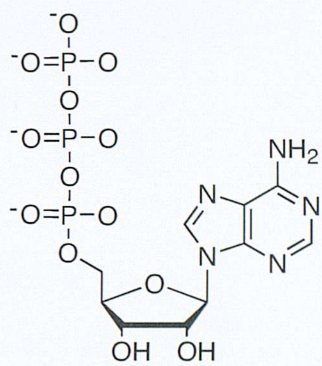

Figure 1.6: The ATP polyanion plays an important biological role.

Cystic fibrosis is a genetically inherited disease that is caused by the mis-regulation of chloride anion channels in cell walls.[15] Although the co-ordination of chloride has been achieved by many receptors, no clinically viable chloride anion transport agent currently exists.

The HIV-1 Tat protein employs a guanidinium group to co-ordinate two phosphate groups that are close together in space, forming a bridging motif known as an 'arginine fork' (Figure 1.7). Frankel and co-workers found that the arginine fork formed a hydrogen bond network near to RNA loops and bulges but not within double stranded A-form RNA allowing the protein to distinguish selectively between the different regions.[16]

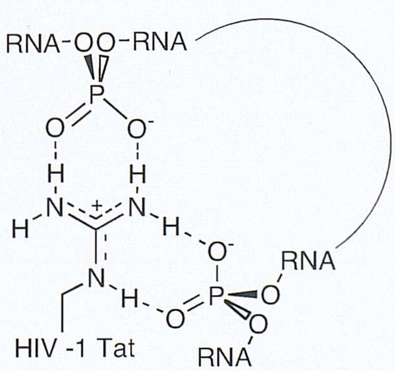

Figure 1.7: The 'arginine fork' motif.

Anionic pollutants can cause serious environmental problems. The anionic substrates phosphate and nitrate can be leached from agricultural land, originally introduced as fertilisers to promote crop growth. Nitrogen sources found in natural bedrock can increase the surface water concentrations of nitrate,[17] whilst the long term use of phosphate derived detergents is contributory to the problem. Increased phosphate and/or nitrate concentrations in lakes and rivers can promote the formation of blue-green algal blooms. This hinders oxygenation of the water, in a process known as eutrophication[18] (Figure 1.8) that has a deleterious effect on aquatic life.

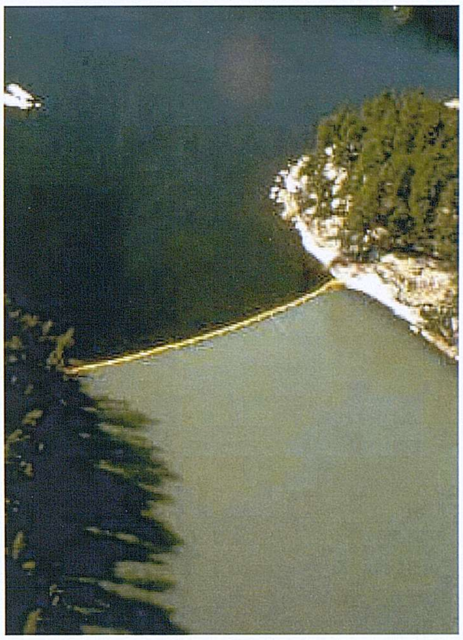

Figure 1.8: Experimentally increased phosphate levels on nearside of the boom show the dramatic effect of eutrophication.

In addition, the industrial reprocessing of nuclear fuel generates pertechnetate, an anionic bi-product that is both toxic and radioactive. It is therefore an important goal to co-ordinate and extract such anions to protect the worlds ecological systems.[19]

Wherever anions are involved be it in an environmental, industrial, medical, biological or chemical application, there are many potential uses for synthetic receptors that can bind and sense anions.

1.3 The expanding field of anion receptors

In recent years there has been interest by many research groups in the co-ordination of anions[2,20,21,22] with many strategies being employed. Incorporation of functional groups that will interact with the anionic guest through complementary contacts form the strongest complexes. Some groups employ the use of hydrogen bonding and/or electrostatic interactions, while others approach the same goal with Lewis acid metal centres.[23]

Hawthorne and co-workers produced the first of their mercuracarborands[24] **1** in 1991[25]. The receptor consists of four mercury Lewis acid centres linking four carborane cages through their carbon atoms. The authors noted that **1** is a charge-reversed analogue of the [12]crown-4[6] macrocycle **2** and hence was named [12]mercuracarborand-4. Solid state analysis revealed a chloride anion was bound within the plane of the macrocycle, equidistant from the four mercury atoms (2.94 Å), in a nearly square planar geometry. The chloride anion was introduced during the synthesis as mercury(II)chloride (compound **1** is formed by reacting mercury(II)chloride with the corresponding dilithiated icosahedral carborane), and was shown to act as a template around which the macrocycle forms.

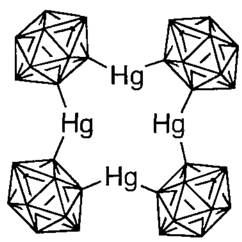

1

= $B_{10}C_2H_{12}$

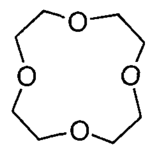

2

Receptors that employ hydrogen bonding and/or electrostatic interactions are far more established. Polarisation of the NH bond in the neutral amide functional group makes it suitable as a hydrogen bond donor for the co-ordination of anions. The receptor selectivity may be modulated and/or enhanced through the orientation and number of the amide groups present. Within the literature there are many examples of anion receptors that make use of the amide functionality, this has been subject to recent review by Loeb and Bondy.[26] Somewhat surprisingly the analogous thioamide, which is more acidic and hence a better hydrogen bond donor, has received very little attention.

The simplest amide is formamide **3**, this small molecule contains both a carbonyl, and an adjacent NH group. An analogous thioformamide **4** can be formed by the replacement of the carbonyl oxygen with sulphur.

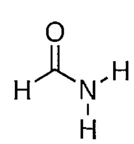

3

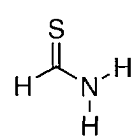

4

A theoretical study on the hydrogen bonding abilities of thioamide has been recently conducted by Choi, Yoon and co-workers[27]. They examined eighteen minimum energy structures generated from **3-3**, **3-4** and **4-4** dimers. The calculated average strength of hydrogen bonds at the B3LYP/6-311++G(2d,2p) level are summarised (Table 1.1), when the basis set superposition error (BSSE) was corrected. In agreement with work by Alemán[28] the results show that thioamide is a better hydrogen bond donor but a worse hydrogen bond acceptor when compared to the amide functionality.

Hydrogen bond interaction	Average strength kcal/mol
OCN-H···O=C	-6.1 ± 0.3
SCN-H···S=C	-5.0 ± 0.1
OCN-H···S=C	-4.8 ± 0.3
SCN-H···O=C	-7.3 ± 0.4

Table 1.1: The average calculated hydrogen bond strengths from amide/thioamide interactions.

Researchers in the anion co-ordination field were astounded in 1997 with the introduction of isophthalamide derivatives **5** and **6** by Crabtree and co-workers.[29] With a one step synthesis from easily purchased starting materials, they had produced two non-preorganised acyclic molecules that displayed an incredible affinity for anions. Very strong and selective 1:1 binding of chloride ($K_a = 6.1 \times 10^4$ M^{-1}) and bromide ($K_a = 7.1 \times 10^3$ M^{-1}) was observed with receptor **6** in dichloromethane-d_2 solution. The solid state bromide complex of receptor **5** revealed the receptor adopts an unfavourable *syn-syn* conformation (over *syn-anti* and *anti-anti*). This conformation enables the formation of two amide NH···Br hydrogen bonds to one bromide anion, however the amide groups have to twist significantly out of the central ring plane.

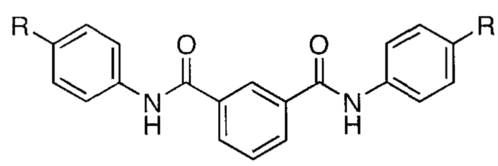

5 R = H
6 R = n-Bu

Szumna and Jurcak synthesised two tetra-amide receptors, macrocycle **7** and acyclic analogue **8**.[30] ^{1}H NMR titrations in dimethyl sulfoxide solution revealed **8** interacted weakly with anions, whilst the macrocycle showed selectivity for bidentate oxy-anions. Receptor **7** formed predominantly 1:1 complexes with anions in solution, however mass spectral analysis showed that a 2:1 complex was formed with acetate as a minor species *ca.* 10%. The crystal structure of the tetrabutylammonium acetate complex shows the formation of this 2:1 species in the solid state although Job plot analysis confirmed a 1:1 stoichiometry in solution for all anions. Interestingly crystal structure analysis provided evidence that the 18-membered macrocycle is unable to contain chloride within the cavity ($K_a = 65\ M^{-1}$), but fluoride fits well ($K_a = 830\ M^{-1}$).

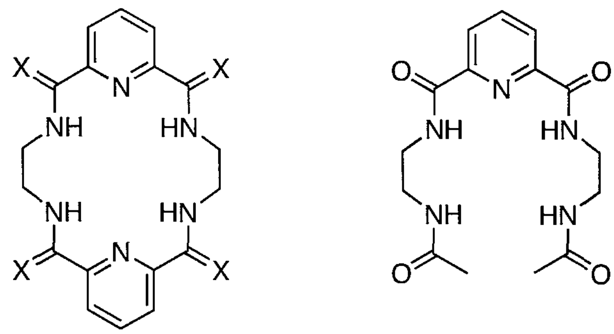

7 X = O
9 X = S

8

Kanbara, Yamamoto and co-workers have produced macrocyclic polythiolactam **9** by thiocarbonylation of **7**.[31] The conversion from amide to thioamide is easily achieved by using a slight excess of Lawessons reagent and refluxing for 48 hours in tetrahydrofuran solution (purification by chromatographic techniques). The receptor **9** displayed an enhanced affinity over the tetra-amide **7** for all of the anions studied. Association constants were obtained by ^1H NMR techniques for both macrocycles in the same solvent system (dimethyl sulfoxide-d_6), selected results are shown (Table 1.2). The increase in anion binding affinity is a direct consequence of the increased acidity of the thioamide NH donors, and hence the formation of stronger hydrogen bonds to the anionic guest.

Anion	**7** K_a (M^{-1})	**9** K_a (M^{-1})
Acetate	2640	14,000
Dihydrogen Phosphate	1680	3900
Fluoride	830	9600*
Chloride	65	1100

Table 1.2: Association constants (K_a) of macrocyclic receptors **7** and **9** with anions (added as their tetrabutylammonium salts, at 298K. * Data collected at 373K.)

Bowman-James and co-workers have very recently reported the anion co-ordinating properties of macrocyclic thioamide receptors.[32] The anion binding ability of receptors **10** to **15** were investigated in dimethyl sulfoxide-d_6 solution, with the ^{1}H NMR titration data fitting a 1:1 binding model. The thioamide monocycles proved to be better receptors for dihydrogen phosphate, hydrogen sulfate and fluoride over the amide anologues. By way of example **10** has a log K_a of 4.97 for dihydrogen phosphate whilst a log K_a of 2.92 is obtained for **13** with the same anion. A selectivity for hydrogen sulfate over other anionic guests was shown by **11**; of all the macrocycles this receptor bound hydrogen sulfate the strongest with a log K_a of 4.99. The bicyclic thioamide and amide cryptands **12** and **15** generally had lowered affinities for anions when compared to the monocyclic derivatives, possibly due to intramolecular hydrogen bonds. However strong and selective binding of fluoride by these receptors was shown with log K_a values of 5.90 and 4.50 respectively.

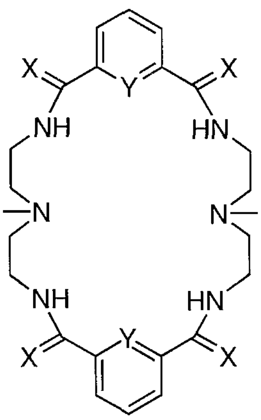

10 X = S, Y = CH
11 X = S, Y = N
13 X = O, Y = CH
14 X = O, Y = N

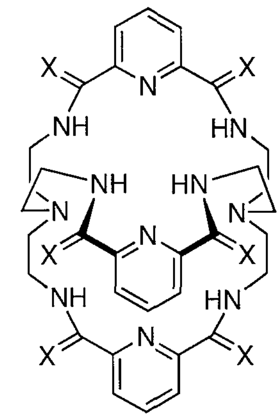

12 X = S
15 X = O

Two cyclohexapeptide macrocycles each containing three amide NH donor groups, have been coupled together via an adipinic acid spacer by Kubik and co-workers forming what they term to be a molecular oyster.[33] Inspired by findings that **16** forms strong 2:1 complexes with a range of anions[34] in 50% water:methanol solution, compound **17** was synthesised in an attempt to form 1:1 complexes. ^{1}H NMR and mass spectrometry techniques confirmed that with halide anions this was indeed the case with little or no other species formed in aqueous solution. The association constants for the various anion complexes were ascertained in the same

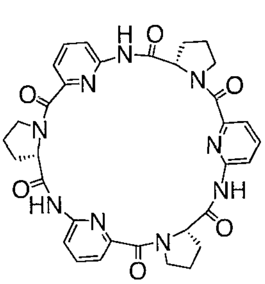

16

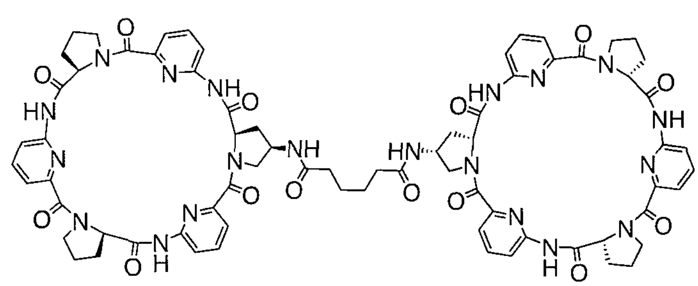

17

solvent mixture used for **16** revealing a strong affinity for sulfate. The following trend of anion binding was observed sulfate> iodide> bromide> chloride, as confirmed by isothermal titration microcalorimetry (ITC). The association constants (^{1}H NMR titrations) ranged from 3.5 x 10^5 down to 1.3 x 10^2 M^{-1} for sulfate and nitrate respectively. The selectivity for larger anions was attributed to a better geometric fit within the defined cavity. However the selectivity for sulfate over iodide (K_a = 8900 M^{-1}) was credited to the fractionally larger ionic radius in conjunction with the ability of sulfate being able to form stronger hydrogen bonds to the NH groups of the receptor.

The urea and thiourea functionalities can form two hydrogen bonds to anionic guest species. They are capable of co-ordinating a variety of anions, although their complementary geometry makes them particularly good for the co-ordination of carboxylates.

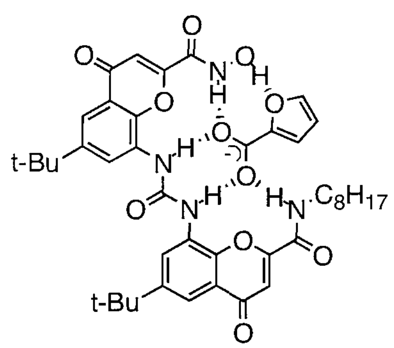

Receptor **18** and 2-furoate

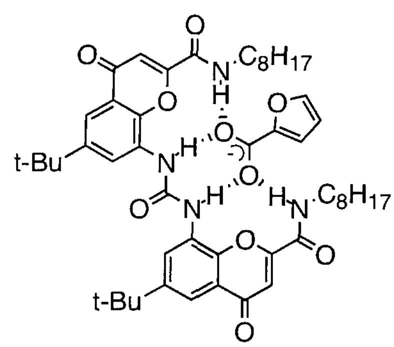

Receptor **19** and 2-furoate

Figure 1.9: The proposed complexes formed between receptors **18** (on left) and **19** (on right) with 2-furoate. The hydroxamic group present in **18** can make an additional hydrogen bond to the guest.

Having already synthesised receptors for chiral recognition of hydroxycarboxylates,[35] Caballero and co-workers produced a series of similar receptors for carboxylates of α-heterocyclic and α-keto acids.[36] A urea head group and two amide groups interact with the carboxylate, whilst a fifth hydrogen bond donor group was incorporated to further complex the guest through a α-heteroatom or carbonyl function. For example, in deuterated chloroform:methanol solution (99:1) hydroxamic receptor **18** has a 36 fold improvement in furan-2-carboxylate binding compared to bisamide receptor **19** (Figure 1.9). Upon finding that the hydroxamic derivative seemed to form the desired fifth hydrogen bond, a selection of carboxylates were studied. Benzoate **20** was experimentally found to have the lowest association constant with $K_a = 1.1 \times 10^3\ M^{-1}$, whilst 2-furoate **21** and fusaric carboxylate **22** had relative constants of 21.6 and 392 respectively. The selectivity can be attributed to the α-heteroatom; unapparent in benzoate (carbon can be assumed to have negligible interaction with the additional H-bond donor), whilst the nitrogen in **22** is relatively more basic than the oxygen in **21** and thus forms the strongest hydrogen bond. A range of α-keto acid carboxylates were also studied, concluding that the carbonyl oxygen does indeed interact with the additional hydrogen bond donor present in **18**.

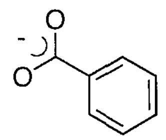

20

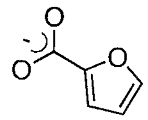

21

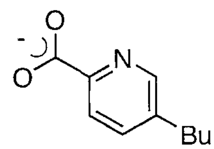

22

Wu and co workers reported the synthesis of several naphthalene appended ureas **23-25**.[37] Addition of α,ω–alkyl dicarboxylate anions resulted in a change in fluorescence spectrum for all receptors, fluorescence and NMR data indicate a 1:1 receptor:dicarboxylate complex being formed in dimethyl sulfoxide solution. Sequential addition of pimelate to the bis-urea system **25** shows a quenching of the fluorescence intensity at 380nm whilst a new long-wavelength emission at 500nm and an isobestic point at 449nm simultaneously develop. The magnitude of the association constant was found to be dependant upon the length of the alkyl chain of the dicarboxylate anion, with pimelate being relatively bound 4.6 times more strongly than malonate.

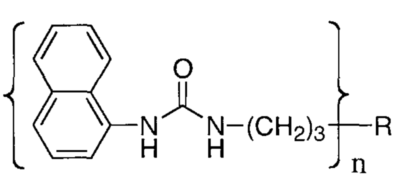

23 n = 1, R = $-CH_2CH_3$

24 n = 1, R = $-N(CH_3)_2$

25 n = 2, R = 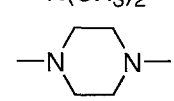

A variety of urea derivatised "cholapods", steroidal type molecules synthesised by the functionalisation of cholic acid, have recently been reported by Davis and co-workers.[38] These receptors form incredibly strong complexes with chloride and bromide anions in wet-chloroform solution (predominantly 1:1 complexes by NMR).

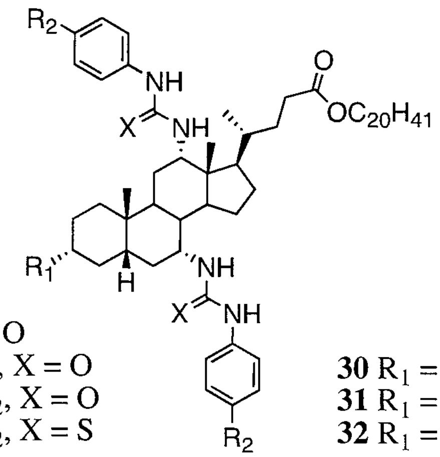

$\mathbf{26}$ $R_1 = R_2 = H, X = O$
$\mathbf{27}$ $R_1 = H, R_2 = CF_3, X = O$
$\mathbf{28}$ $R_1 = H, R_2 = NO_2, X = O$
$\mathbf{29}$ $R_1 = H, R_2 = NO_2, X = S$

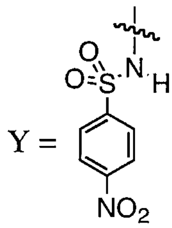

$\mathbf{30}$ $R_1 = Y, R_2 = CF_3, X = O$
$\mathbf{31}$ $R_1 = Y, R_2 = NO_2, X = O$
$\mathbf{32}$ $R_1 = Y, R_2 = NO_2, X = S$

With two (thio)urea groups **26-29** and an additional nitrophenylsulphonamide group **30-32** the receptors have four and five hydrogen bond donors respectively. The attachment of these groups to the axial positions of the steroid skeleton aids pre-organisation, by restricting rotation about the C-N bonds, whilst the electron-withdrawing groups serve to increase the H-bond donor power. The affinities for the said anions were seen to increase through the series **26-29** illustrating the effect of increased acidity of the urea(thiourea) groups. Whilst the additional nitrosulphonamide group included in **30-32** gave further improvements with **32** having an association constant with chloride of $K_a = 1.03 \times 10^{11}$ M^{-1} in wet-chloroform.

Hong and co-workers have synthesised thiourea containing receptors **33** and **34** with one and two chromophores respectively.[39] Receptor **34** is able to differentiate between anions of similar basicity (dihydrogen phosphate, acetate and fluoride) through the cooperativity of the two chromophores present, namely azophenol and nitrophenyl. A pale yellow to violet colour change is observed upon addition of dihydrogen phosphate to a chloroform solution of the receptor. This change is ascribed to the four oxygen atoms of dihydrogen phosphate interacting via hydrogen bonds to both of the chromophores, while fluoride and acetate anions have a relatively weaker effect on the *p*-nitrophenyl group. Model receptor **33** however was unable to discriminate between dihydrogen phosphate, acetate and

$\mathbf{33}$ $R = H$
$\mathbf{34}$ $R = NO_2$

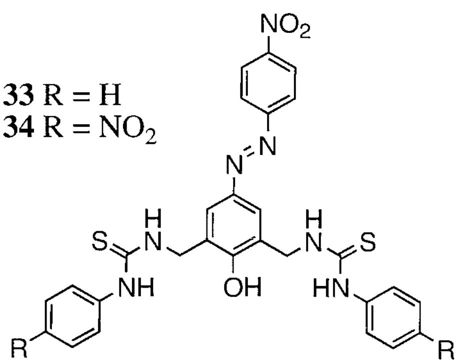

fluoride. This shows that the introduction of *p*-nitrophenylthiourea groups as a co-ordination site are essential for the colour discrimination between the similar basicity anions.

Guanidinium and amidinium in a similar fashion to (thio)urea functional groups are capable of forming two hydrogen bonds to their guest. They are however also able to make an electrostatic contribution to the binding from a delocalised positive charge. [20,21,40]

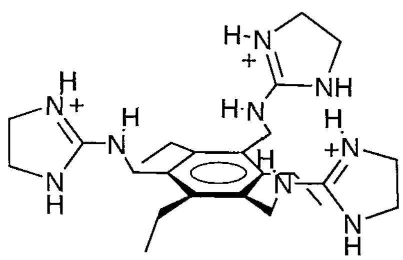

35

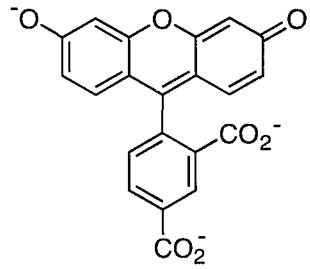

36

Anslyn and Metzger developed a chemosensor for citrate in beverages based upon an ensemble of receptor **35** and 5-carboxy-fluorescein **36**.[41] The receptor consists of three guanidinium groups that are pre-organised on the same face of the benzene ring, achieved through steric gearing. In water, the host is selective for the triple negatively charged citrate ($K_a = 6.8x10^3\ M^{-1}$), over di- and mono-carboxylates and other anionic guests.[42] The pH sensitive fluorescent probe **36**, is co-ordinated by its two carboxylate groups to form a complex with the host. Addition of the more strongly bound citrate, displaces the 5-carboxy-fluorescein into the bulk solution. This lowers the intensity seen in the absorbance spectrum due to increasing protonation of the phenol anion. A change in the absorbance and fluorescence spectrums of a solution of **35** and **36** was observed upon addition of small samples of many drinks. Comparison to calibration curves allowed the concentration of citrate in each to be determined accurately.

The steroidal based receptors **37** and **38** have been synthesised by Davis and co-workers and reported in 2002.[43] Receptor **37** confirmed no loss of enantioselectivity compared to initial studies[44] by extracting *N*-acetyl-α-amino acids from aqueous media into chloroform solution (efficiency~80%) with enantioselectivities (L:D) of 7-10:1. The more lipophillic steroidal guanidine **38** was used in "U-tube" experiments, and was shown to be capable of transporting racemic *N*-acetylphenylanaline through dichloromethane solution in nearly 70% enantiomeric excess in favour of the L

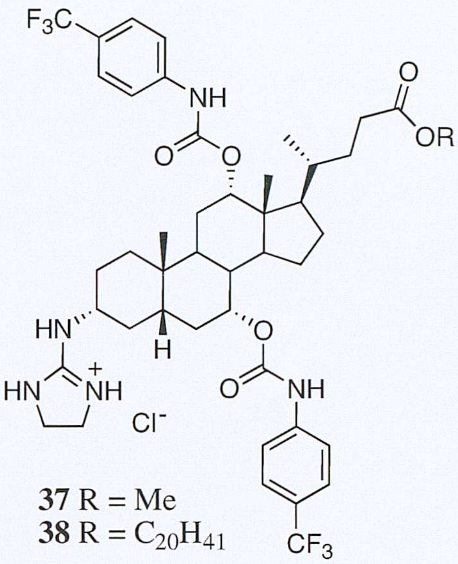

37 R = Me
38 R = $C_{20}H_{41}$

isomer. Over the duration of the experiment about 20 equivalents of the *N*-acetylphenylanaline substrate were transferred.

The first example of a guanidinium group appended to a redox-active moiety was reported by Beer and co-workers.[45] The ferrocene appended host **39** was selective for basic bidentate anionic guests such as dihydrogen phosphate or pyrophosphate in dimethyl sulfoxide solution, through interaction with the charged guanidinium group. NMR studies were conducted in methanol/water (50/50) solution, **39** interacted with pyrophosphate but not dihydrogen phosphate forming 2:1 host:anion complexes with $K_a = 4600\ M^{-2}$. The receptor showed an electrochemical response to pyrophosphate in the same solvent system with a cathodic shift of 70mV for the ferrocene redox couple whilst no response was observed for dihydrogen phosphate.

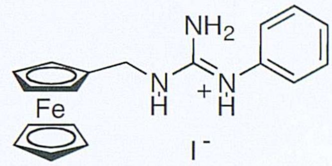

39

The simple ammonium group also uses an electrostatic interaction as well as a hydrogen bonding component in anion binding. The first reported anion receptors were cryptand like ammonium derivatives.[12] ^{1}H NMR investigations suggested the diprotonated compound **40** with both ammonium groups pointing inward (one of three isomers, in-in, in-out, out-out) encapsulated chloride (Figure 1.10), although crystallographic proof did not appear until a few years later.[46]

40

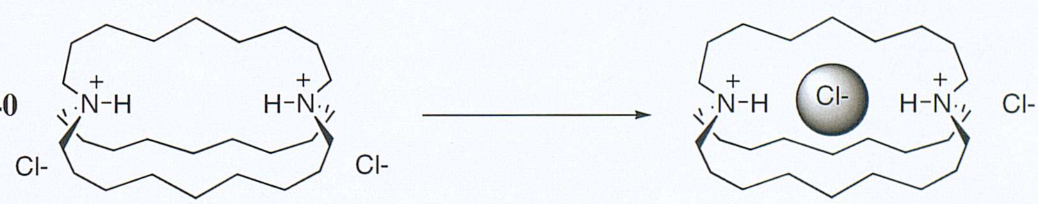

Figure 1.10: Chloride is bound within the defined cavity of the in-in stereoisomer. Crystallographic evidence reveals N(H)···Cl distances of 3.10 Å.

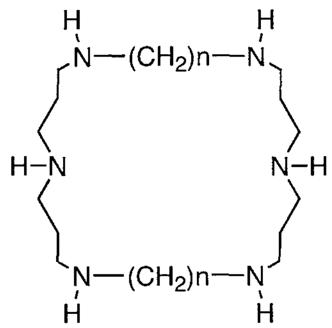

43 n = 7
44 n = 10

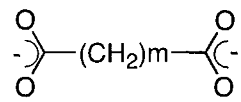

45 m = 2
46 m = 3
47 m = 5
48 m = 6

In 1982 Lehn and co-workers reported ditopic receptors **43** and **44**, these receptors could efficiently bind dicarboxylate species within the hexaaza-macrocyclic cores.[47] The study revealed that the alkyl spacer between the binding sites strongly dictated the selectivity of the receptor. In aqueous solution the hexaprotonated form of **43** was selective for succinate **45** (log K_a= 4.3) and glutarate **46** (log K_a= 4.4), whilst **44**·**6H**$^+$ most strongly bound pimelate **47** (log K_a= 4.4) and suberate **48** (log K_a= 4.2). It should be noted that the selectivity change is due to an increase of three CH_2 groups in alkyl chain length n, which is exactly replicated in the increase of chain length m. This reveals the selectivity arises from a direct correlation between spacer and the length of the di-anionic guest.

Bowman-James and co-workers have studied the complexation properties of the octaazacryptand **49**.[48] Although the "tiny" cryptand displays very little affinity for anions other than fluoride between pH 2.5 and 5, the selectivity changes at values below pH 2.5. Under these more acidic conditions crystallographic evidence reveals that chloride can become encapsulated within the bicyclic cavity. The anion is bound by six ammonium-chloride hydrogen bonds in a non symmetrical hydrogen bond network, with N-Cl distances ranging from 2.99(1) to 3.18(1) Å. This dramatic increase in affinity for chloride at lower pH values has also been confirmed by ^{1}H NMR analysis, even though previous potentiometric studies indicated weak chloride binding (measured at pH *ca.* 4).

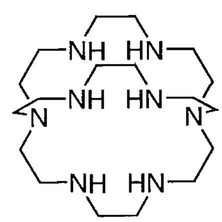

49

The imidazolium group is another functionality that uses both hydrogen bonding and electrostatics to form complexes with anions. The difference from the previously seen examples is the use of $(C\text{-}H)^+\cdots$anion hydrogen bond formation as opposed to $(N\text{-}H)^+$.

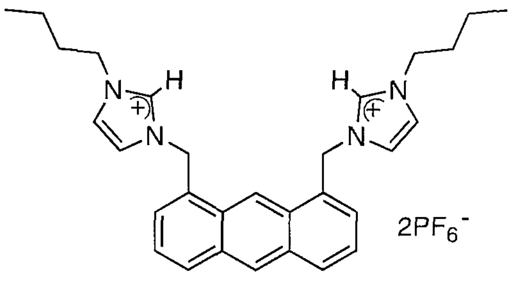

50

In a very recent publication Yoon, Kim and co-workers have used imidazolium moieties bolted onto a rigid anthracene backbone to form **50**, a fluorescent chemosensor with a pre-organised binding site.[49] In strong agreement to *ab initio* calculations the receptor forms strong complexes with dihydrogen phosphate anions, in a predicted tweezer type conformation. ^{1}H NMR titrations in acetonitrile-d_3 and job plot analysis indicate the formation of 1:1 complexes. The association constants as derived from fluorescence titration experiments in acetonitrile for dihydrogen phosphate, chloride and bromide were found to be ~1,300,000, 7900 and 4500 M^{-1} respectively. The selectivity of **50** for dihydrogen phosphate is approximately 200 times that for other anions such as chloride or bromide.

Receptors that co-ordinate anions through predominant electrostatic interactions have also been reported. In 1977, Schmidtchen and co-workers described the synthesis and anion inclusion properties of macrotricyclic quaternary ammonium salts **51** and **52**.[50] These receptors showed selectivity for anions dependant upon size, in relation to the cavity dimensions. The receptors formed 1:1 host:guest complexes with a variety of anions in either water or 95% methanol solutions. The researchers realised that the four counter anions associated with the positively charged host molecules may compete for the anion binding site. To overcome this problem they produced zwitterionic receptors[51] **53** and **54** that are neutral. In aqueous solution ^{1}H NMR experiments showed that **53** forms stronger complexes with chloride, bromide and iodide anions than receptor **51**.

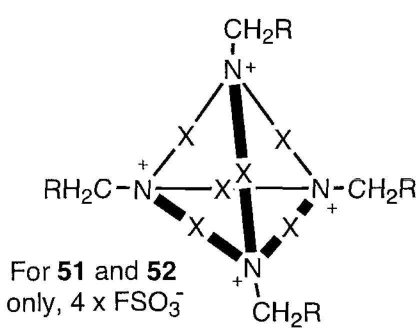

51 R = H, X = $(CH_2)_6$
52 R = H, X = $(CH_2)_8$
53 R = Y, X = $(CH_2)_6$
54 R = Y, X = $(CH_2)_8$

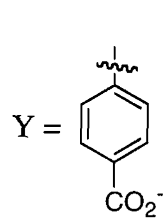

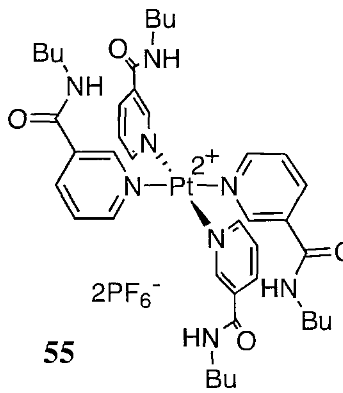

55

The preceding examples have shown various organic functional groups that co-ordinate anions through hydrogen bond and/or electrostatic interactions. Loeb, Gale and co-workers adopted an inorganic approach and synthesised an anion receptor based on a square planar platinum complex.[52] Compound **55** provides nicotinamide hydrogen bond donors and an electrostatic contribution from the platinum (II) metal centre. ^{1}H NMR titration experiments were conducted in various polar solvents and revealed **55** was an effective host for several oxo-anions, but tetrahedral or pseudo-tetrahedral anions are bound relatively weakly in a 1:1 host:guest stoichiometry. However an increase in selectivity was seen for planar bidentate anions, namely nitrate and acetate, with these anions binding in a 2:1 anion:receptor ratio. It is assumed the anions sit above and below the metal square plane in a sandwich type formation, co-ordinated by two *cis* amido groups. There is association constant evidence to suggest that the binding of the first anion promotes co-ordination of the second. With this in mind the same researchers synthesised a pre-organised receptor[53] **56** that was already in the termed 1,2-alternate conformation, derived from the four conformations that can be adopted by calix[4]arene. Interestingly this receptor proved not to be an improvement on the first nicotinamide derivative, with the binding of a second anion being inhibited by the first. The binding sites contain two amide groups, one from each 3,5-di-*n*butylamidopyridine ligand. The binding sites are therefore not independent of each other. The formation of two hydrogen bonds to an anionic guest on one side of the receptor simultaneously causes the other binding site to open up and thus removes the ability of the second binding site to form two hydrogen bonds to the second guest.

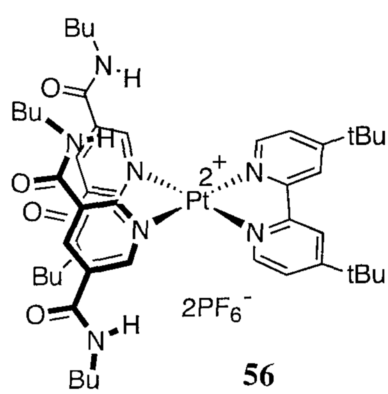

56

The inclusion of a cation within a receptor allows an electrostatic interaction with the anionic guest. This can lead to the formation of strong host:guest complexes. If a receptor has both anion and cation binding sites then a synergic effect may be observed. That is to say that the receptor may behave as an ion pair receptor that is capable of binding and extracting inorganic salts into organic media.

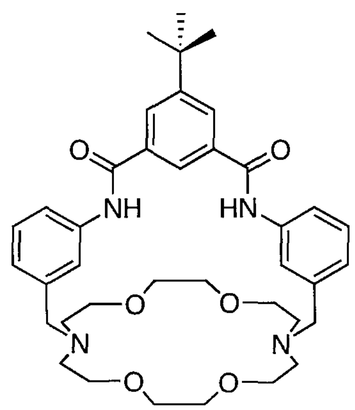

57

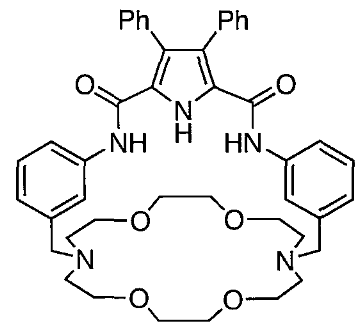

58

Initial work by Smith and co-workers on the synthesis and study of ion pair receptor **57** was conducted in 2001[54]. This receptor could dissolve one equivalent of potassium chloride in chloroform, forming a complex that was stable enough to withstand column chromatography on silica gel eluting with weakly polar solvents. In addition ^{1}H NMR titration experiments in dimethyl sulfoxide-d_6 revealed that potassium chloride was bound more tightly than the free ions. More recently a collaboration with Gale and co-workers[55] yielded analogous ion pair receptor **58**. This receptor displayed an enhanced affinity for chloride and chloride salts (sodium and potassium) compared to the isophthalamide derivative in dimethyl sulfoxide solution. A three fold improvement in chloride binding and an association constant of 540 M^{-1} was recorded for the potassium chloride ion pair. Crystals of the **58**·NaCl complex were isolated; bound as an ion pair the Na-Cl distance in the complex is 0.09Å shorter than the Na-Cl distance found in crystalline sodium chloride. The increased acidity of the amide groups in parallel with the ability of the pyrrole NH to form an additional hydrogen bond to chloride accounts for the increased affinity of **58** compared to **57**.

1.4 Pyrrole derived receptors

Pyrrole is a neutral heterocycle that contains a polarised NH bond suitable for co-ordinating anions ($pK_a \approx 15$, i.e. a weak acid). Inherently, this motif does not contain an inbuilt hydrogen bond acceptor and consequently is unable to form "self-associating" hydrogen bonds. It is possible for groups such as amide or urea to interact with themselves through C=O···HN interactions. This can have an adverse effect on the anion binding abilities of a receptor by competing with potential guests for hydrogen bond formation:-

- intramolecular interactions could close or alter the binding cleft or cavity
- intermolecular interactions may lower solubility or block the binding site

Gale and co-workers have shown that pyrrole is capable of forming hydrogen bonds to chloride in the solid state,[56] although monomeric 2,5-dimethylpyrrole binds anions very weakly in solution.[57] The coupling of several pyrrolic entities, or direct functionalisation is essential to form pyrrole based receptors capable of anion co-ordination.[58]

1.4.1 Acyclic binding agents

Inspired by work from the laboratories of Schmuck[59] and Crabtree,[29,60] Gale and co-workers have produced a variety of simple pyrrole 2,5-amide clefts[61] with **59** and **60** functioning as effective receptors for oxo-anions. In order to investigate the binding mode of these receptors in solution compounds **61** and **62** were synthesised.[62] The monoamide species maintained the selectivity for oxo-anions, with compound **61** binding benzoate with $K_a = 202\ M^{-1}$ in acetonitrile-d_3 compared to that of **59** having an association constant $K_a = 2500\ M^{-1}$. Gale postulated that the higher affinity of the bis-amide species was due to a different binding mode in which the hydrogen bond formation could be in a cleft conformation (not available to the mono-amide species),

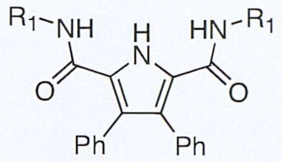

59 R_1 = n-Bu
60 R_1 = Ph

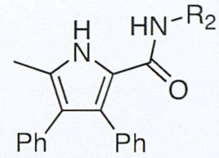

61 R_2 = n-Bu
62 R_2 = Ph

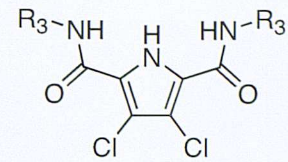

63 R_3 = n-Bu
64 R_3 = Ph

this was recently confirmed in the solid state by analysis of the **59**·benzoate complex showing all three NH donors involved in the co-ordination of the benzoate anion (Figure 1.11).[63]

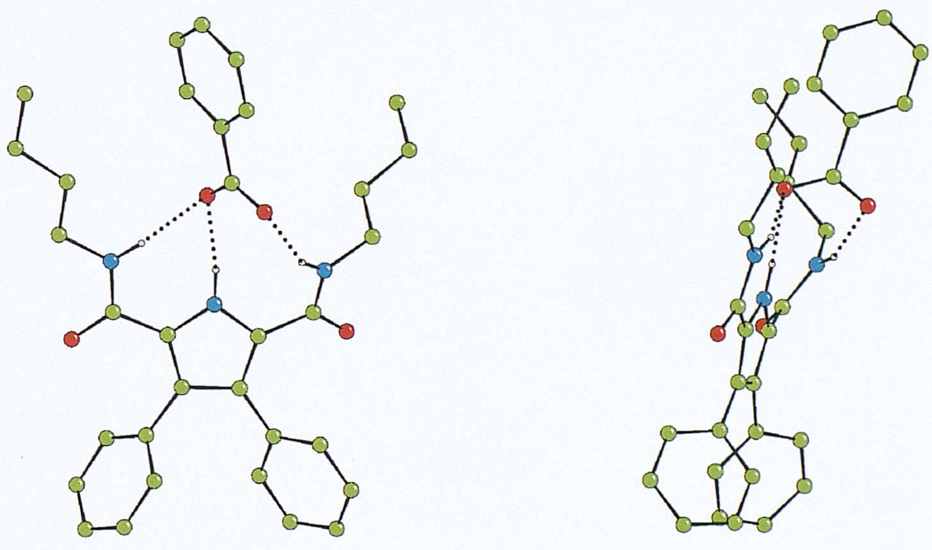

(a) (b)

Figure 1.11: (a) Crystal structure of the complex **59**/benzoate. The receptor adopts a 'cleft' conformation and coordinates the anion via the formation of three hydrogen bonds. One benzoate oxygen interacts with both the pyrrole and one of the amide NH groups via the formation of two hydrogen bonds (distances $N_{amide}\cdots O$ = 2.8638(4)Å, $N_{pyrrole}\cdots O$ = 2.7710(4)Å); the second carboxylate oxygen interact with the remaining amide group through the formation of the third hydrogen bond (distance $N\cdots O$ = 2.7915(6)Å). (b) Side view of the crystal structure.

The introduction of electron withdrawing groups to the pyrrole backbone has been shown to be an effective way to increase the acidity of the NH hydrogen bond donor group thus forming stronger complexes with anions.[64,65,66] Certainly, the 3,4-dichloro pyrrole derivative **63** binds chloride with $K_a = 2015\ M^{-1}$ in acetonitrile-d_3, whereas under the same conditions receptor **59** binds chloride much more weakly with a $K_a = 138\ M^{-1}$. However, in the case of basic anions such as fluoride, receptors **63** and **64** became deprotonated in solution.[67] A dilution study on the tetrabutylammonium salt of compound **64** gave data consistent with the formation of pyrrolate anion dimers in solution over a concentration range between $1x10^{-3}$ M and $4x10^{-2}$ M. Analysis of crystals obtained by slow evaporation of a dichloromethane solution of **64** in the presence of excess tetrabutylammonium fluoride revealed that instead of observing fluoride within the structure, it was the tetrabutylammonium salt of the deprotonated receptor. The deprotonated receptor now in the *syn-syn* conformation forms a dimer with another deprotonated receptor stabilised by the formation of four hydrogen bonds (distances $N_{amide}\cdots N_{pyrrole}$ = 3.218(4), 3.130(4), 3.124(4), 3.072(4)Å) between the amide NH groups and the deprotonated pyrrolic nitrogen (Figure 1.12). The two pyrrolate anions are almost orthogonal to each other (in DNA the hydrogen bond array is almost coplanar), this motif has been incorporated into new interlocking materials.[68]

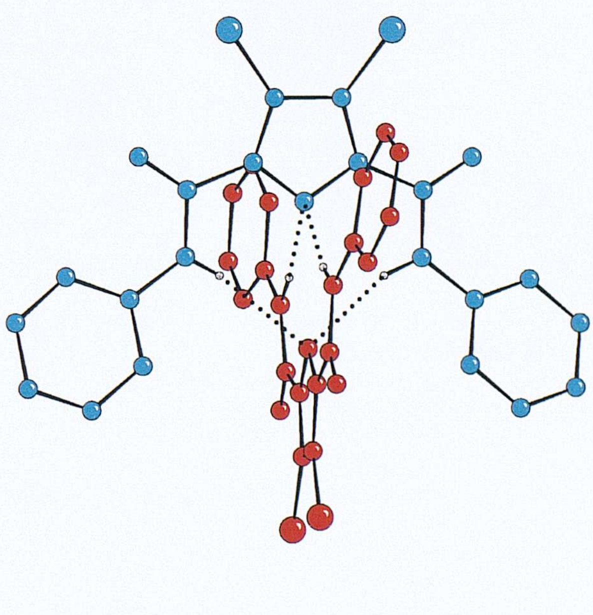

Figure 1.12: Crystal structure of the deprotonated receptor **64**. In the solid state the receptor dimerizes in the deprotonated form, via the formation of four hydrogen bonds. Non acidic hydrogen atoms and tetrabutylammonium counter cations have been omitted for clarity.

Conversely less basic anions such as chloride do not deprotonate the receptor and form 1:1 complexes in solution. Compound **63** binds chloride with a $K_a = 2015\ M^{-1}$ in acetonitrile-d_3 an improvement compared to its phenyl analogue **59** that had an association constant $K_a = 138\ M^{-1}$.

Sessler and co-workers produced a series of quinoxaline derivatives[69] that bind fluoride, chloride and dihydrogen phosphate in dichloromethane solution. The receptors **65**, **66** and **67** contain two, four and six pyrrole subunits respectively.

65 **66** **67**

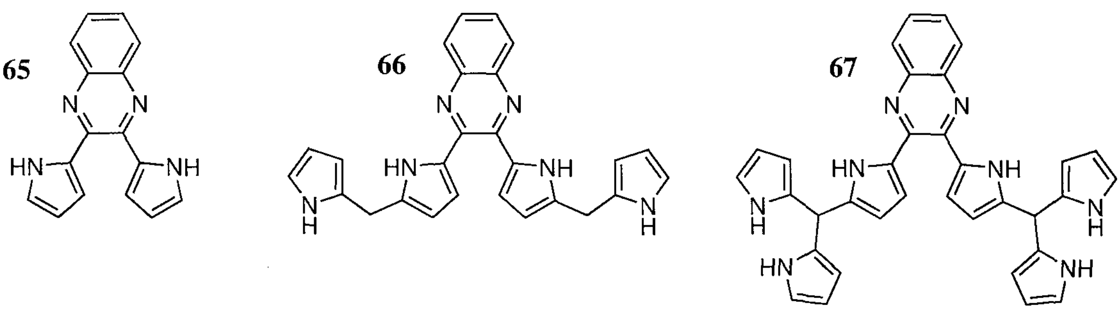

Uniquely a yellow to red colour change was observed upon addition of fluoride to a dilute solution of **66**. Fitting a 1:1 binding curve, the association constant K_a of $3.2 \times 10^4\ M^{-1}$ was determined, a value nearly twice that observed for **65**. For all the anions studied there is an improvement in binding through the series **65** to **67**. The most impressive increase in binding affinity was shown for dihydrogen phosphate, with **67** indicating a 5000 fold increase in affinity compared to **65.** Enhancements of approximately 100 and 50 fold were seen for chloride and fluoride respectively, indicating receptor **67** is more suited to binding larger anions. Comparison of binding constant ratios also suggested that the extra pyrrole units favour the binding of dihydrogen phosphate and chloride relative to fluoride (irrespective of fluoride being bound most strongly by all receptors).

1.4.2 Cyclic binding agents

There are a limited number of acyclic pyrrole based anion receptors within the literature. However the incorporation of pyrrole into macrocyclic structures has generated many more examples, and is still a rapidly expanding area of anion co-ordination.[58]

1.4.2.1 Calix[n]pyrroles

The facile acid catalysed condensation of pyrrole with a ketone yields a tetrapyrrolic macrocycle. This class of compound have been known for over a century[70] and are now better known as calix[4]pyrroles drawing on the structural analogy to calixarenes.[71] Although previous interest was shown in their cation co-ordination chemistry[72], it has only been in recent years that they have been considered as possible anion receptors. Many research groups have employed various methodologies to modify the basic skeleton to increase or adjust the selectivity/affinity of this family of anion receptors.

Sessler and co-workers have shown in the last decade that *meso*-octamethylcalix[4]pyrrole **68** is capable of co-ordinating a variety of anions[57] and neutral molecules[73] both in solution and in the solid state. Co-ordination is achieved through hydrogen bond formation from four pyrrole NH groups. These rotationally free groups form a convergent binding site in the presence of anions or small neutral molecules.

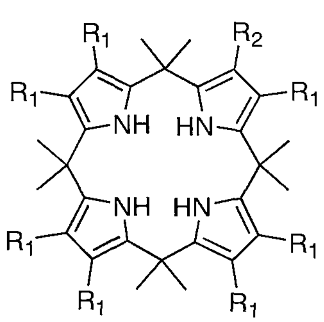

68 $R_1 = R_2 = H$
69 $R_1 = H, R_2 = I$
70 $R_1 = H, R_2 = Br$
71 $R_1 = H, R_2 = Cl$
72 $R_1 = H, R_2 = F$
73 $R_1 = R_2 = Br$

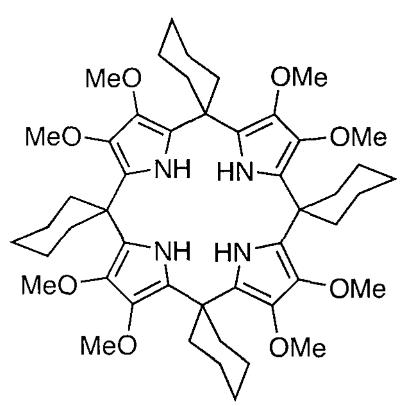

74

Functionalisation of the pyrrole backbone with either electron withdrawing or donating groups has been shown to have a dramatic effect on the receptors affinity for anions.[64,65,66] Sessler and co-workers synthesised calix[4]pyrroles **69-72** and illustrated that substitution of a single β–pyrrolic proton for a halide can enhance the anion co-ordination properties.[74] In dichloromethane-d_2 solution, the parent macrocycle *meso*-octamethylcalix[4]pyrrole has an association constant for chloride of 350 M^{-1}, whilst mono- and octa-bromo substituted calixpyrroles **70** and **73** have K_a values of 650 and 4300 M^{-1} respectively. Whilst the β-octamethoxy-*meso*-tetraspirocyclohexylcalix[4]pyrrole derivative **74** has an association constant of less than 10 M^{-1} for chloride in the same solvent system. The monohalide substituted receptors all showed an increase in affinity for anions over the parent macrocycle with receptor **72** having a K_a for chloride of 870 M^{-1}. However for more weakly bound anions such as bromide, dihydrogen phosphate and hydrogen sulfate, receptor **71** proved to be better than **72** due to interference from intermolecular NH-F interactions.

In 2002 Lee and co-workers reported the synthesis of a "strap" substituted calix[4]pyrrole **75**.[75] This receptor forms a 1:1 complex with chloride (also solid state evidence)[76] with an association constant of 1.01×10^5 M^{-1} in dimethyl sulfoxide solution. Evidence for strong fluoride binding was obtained by proton NMR analysis, although a quantitative value for the association constant was unobtainable. The same researchers have very recently collaborated with Sessler and co-workers producing strapped calixpyrroles **76-78**.[76]

75

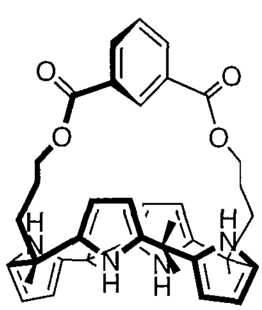

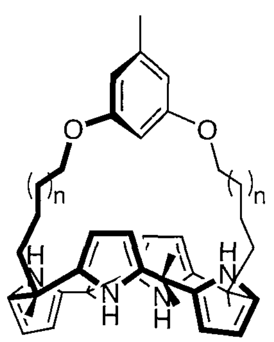

76 n = 1
77 n = 2
78 n = 3

Again attempts to obtain the anion binding properties of these receptors in acetonitrile by NMR methods proved unsuccessful, due to strong binding and slow complexation kinetics. However addition of chloride to **77** strongly perturbed resonances in the ^{1}H NMR spectrum with downfield shifts of up to 3ppm (pyrrolic NH protons). The appearance of the new peaks had completed around the time ~1 equivalent of chloride had been added, suggesting a strong 1:1 binding mode. Isothermal titration calorimetry measurements revealed the very high anion affinity of these compounds. Bearing the shortest strap, receptor **76** binds chloride and bromide anions in acetonitrile solution with a K_a of $3.6x10^6$ and $3x10^4 M^{-1}$ respectively. With the longest strap, **78** showed a increase in affinity for bromide over the other receptors, with $K_a = 1.2 \times 10^5 M^{-1}$ perhaps indicating the better fit of bromide in this cavity.

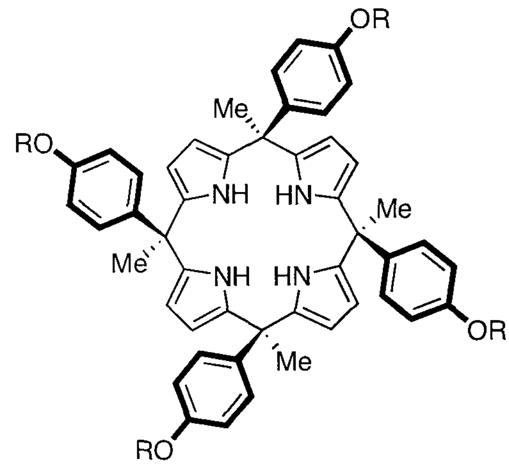

79 R = CH_2COOEt
80 R = CH_2CONEt_2
81 R = COMe

The condensation of *p*-hydroxy-acetophenone with pyrrole forms a calixpyrrole product with four isomers.[77,78] In 2000 Gale and co-workers derivatised the αααα isomer to produce "super-extended cavity" calixpyrroles[79] **79** and **80** that were shown to bind fluoride exclusively in dimethyl sulfoxide-d_6 solution. To further investigate the binding properties of "super-extended cavity" calixpyrroles, Gale and co-workers synthesised compound **81**.[80] The anion binding capabilities were investigated in dimethyl sulfoxide-d_6 using ^1H NMR titration techniques, again showing fluoride selectivity ($K_a = 74 M^{-1}$). The ^1H NMR spectrum in the presence of 100 equivalents of chloride, bromide, iodide, dihydrogen phosphate and hydrogen sulfate revealed no change, indicating these anions do not interact with **81** in this solvent system. To explore the observed selectivity, Monte Carlo free energy perturbation simulations and Poisson calculations were used. In agreement with solid state analysis, these studies indicated that the smaller fluoride anion may gain favourable electrostatic interactions (maximise hydrogen bond strength) by sitting lower in the phenolic cavity of the receptor.

Condensation of acetone with 3,4-difluoropyrrole predominantly forms the corresponding calix[4]pyrrole **82**, however the reaction also forms calix[5]- and calix[8]pyrroles, **83** and **84** as by-products that are stable enough to isolate in their pure form.[65] These larger calixpyrroles by definition have more pyrrolic NH groups and a larger macrocyclic core size. The anion co-ordination properties of compound **83** have been studied

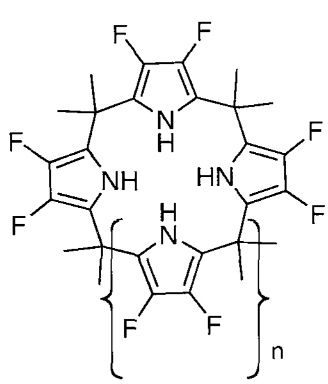

82 n = 1
83 n = 2
84 n = 5

revealing an affinity for chloride with a K_a of 41,000M^{-1} a value four times greater than that shown by **82** in acetonitrile-d_3:D_2O (99.5:0.5).

Eichen and co-workers reported the first calix[6]pyrrole synthesis in 1998,[81] their synthesis involved the reaction of bulky ketones with pyrrole to form di-(2-pyrrolyl)methanes, the subsequent condensation with acetone in the presence of trifluoroacetic acid catalyst yielded the corresponding calix[6]pyrrole such as **85**. A couple of years later Kohnke and co-workers found that *meso*-dodecamethylcalix[6]pyrrole **86** could be made by converting a furan based analogue.[82] The co-ordinating properties of receptor **85** were studied.[83] In contrast to octamethylcalix[4]pyrrole **68**, the bigger macrocycle displayed affinity for larger anionic guests, showing selectivity for iodide K_a = 6600 M^{-1} over fluoride K_a = 1080 M^{-1} and other anionic guests in acetonitrile: chloroform solution (1:9). Transport studies revealed compound **86** can bind and extract bromide and chloride anions from an aqueous phase into dichloromethane solvent, and shows around a six fold selectivity factor for chloride with respect to bromide.[84]

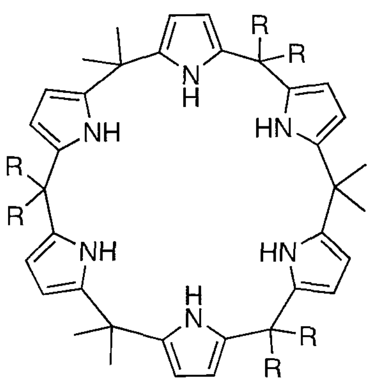

85 R = Ph
86 R = Me

A recent paper by Sessler and co-workers reports the synthesis, solid state analysis and anion co-ordinating properties of the first cryptand like calixpyrrole.[85] Solid state results suggested that the bicyclic nonapyrrole **87** may be able to bind anions within its three identical cavities in a 1:1, 1:2 and 1:3 receptor to anion stoichiometry. However ^{1}H NMR experiments conducted in dichloromethane-d_2 and tetrahydrofuran-d_8 revealed more complex stoichiometric ratios, that were clearly dependant upon the anion in solution. For example, fluoride is bound by six of the nine pyrrolic NH groups in a 1:1 complex, whereas chloride appears to be co-ordinated in a 2:1 receptor:anion ratio with an association constant of 3.08x10^6 M^{-2} in dichloromethane-d_2 solution. In contrast the receptor simultaneously binds two nitrate anions with association constants K_1 and K_2 of 1740 and 420 M^{-1}, respectively in dichloromethane-d_2 solution.

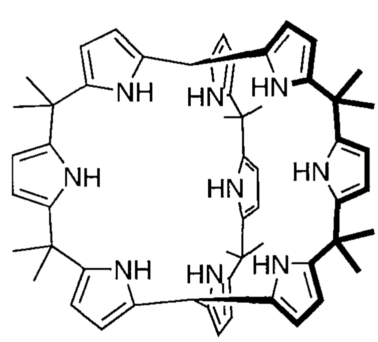

87

1.4.2.2 Other macrocyclic systems

A recent addition to the calixphyrin family (porphyrin/calixpyrrole hybrids) **88** was reported by Sessler and co-workers in 2001.[86] Addition of a variety of anions (chloride, bromide, iodide, nitrate and hydrogen sulfate) to the neutral macrocycle revealed no evidence to support anion binding. The optical properties of diprotonated **88** in acetone solution were found to be perturbed upon addition of bromide, chloride and iodide. Stoichiometric analysis revealed that only iodide formed a clean 1:1 complex with the fully protonated receptor, with an association constant K_a = 25,500 M^{-1} in acetone solution. It was also calculated that in the absence of the competing counter anion (hydrogen sulfate) an association constant K_a of up to *ca.* $8x10^7$ M^{-1} with iodide was potentially viable.

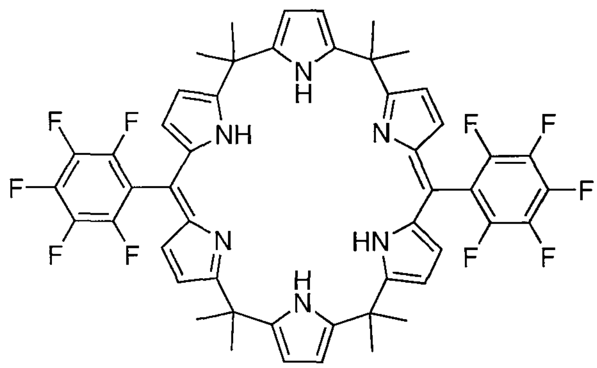

88

In 1998 Sessler, Vögtle and co-workers reported the synthesis and anion binding properties of a novel dipyrrole-based [2]catenane receptor **89**.[87] Condensation of the corresponding bipyrrole acyl chloride and *p*-xylenediamine subunits isolated the [2]catenane in 2% (single step) and 4% (stepwise synthesis) yields. Very high association constants with anions were observed with **89** in 1,1,2,2-tetrachloroethane-d_2 reaching up to 10^7 M^{-1} for dihydrogen phosphate. The association constants for the other anions studied were all greater than $1.48x10^5$ M^{-1} as seen for fluoride. ^1H, ^{13}C and ^{19}F NMR solution studies in 1,1,2,2-tetrachloroethane-d_2 revealed that the addition of anions

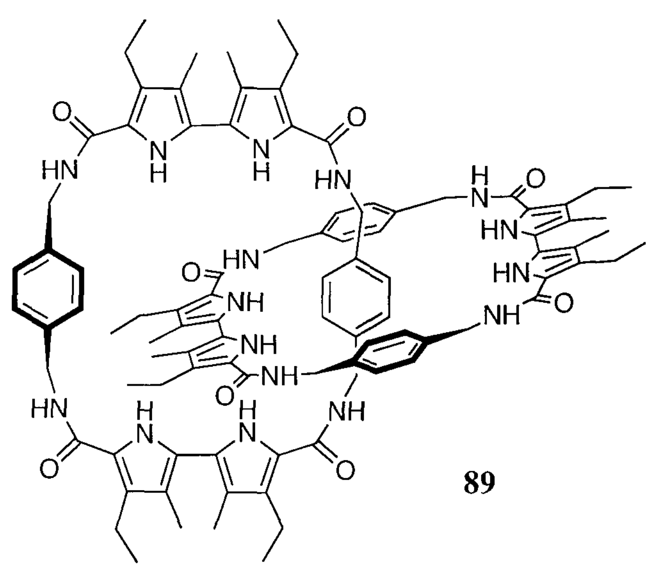

89

induced a conformational change in the receptor. This was attributed to the formation of a tetrahedral cavity between the rings, thus creating a binding site that could accommodate to its anionic guest.

Initially synthesised by Woodward and co-workers[88] sapphyrin is an expanded porphyrin that is planar, rigid and has an aromatic 22 π-electron system. In 1990 Sessler and co-workers found that when diprotonated sapphyrin **90** could accommodate fluoride within its pentapyrrolic core.[89] This serendipitous discovery marked the first example of a pyrrole based anion receptor. The crystal structure revealed that the fluoride and nitrogens were all nearly co-planar, with a mean deviation of only 0.03Å, the fluoride was situated in the 5.5Å diameter core and also found to be in hydrogen bond distance of all five nitrogens. The diprotonated form of **90** is able to interact with a range of anions both in solution and the solid state,[90,91] although the solid state binding motif observed for fluoride was found to be unique. For example chloride is too large and unable to fit within the core, but forms a 2:1 complex in the solid state, with the anions placed 1.8Å above and below the macrocyclic plane.[90] Solution phase studies in dichloromethane and methanol indicated that the diprotonated receptor is selective for fluoride, at least $\geq 10^3$ relative to either chloride or bromide. Various sapphyrin derivatives have been synthesised and the anion binding properties have been subject to recent review.[92,58]

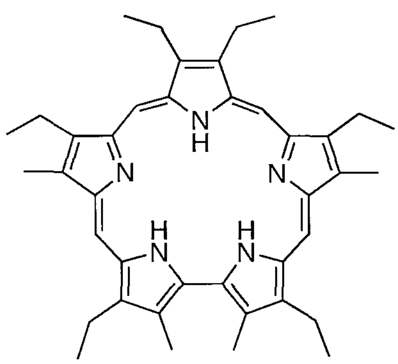

90

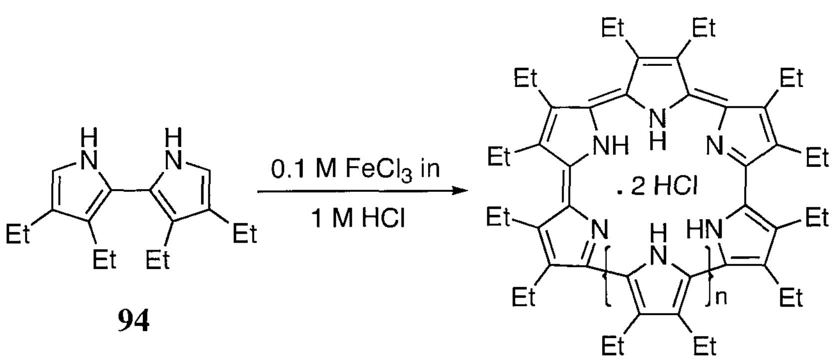

94

91 n = 1
92 n = 2
93 n = 3

Scheme 1.2: Direct coupling of bipyrrolic fragments to form "contracted" expanded porphyrins.

Sessler and co-workers have synthesised other expanded porphyrins and pyrrole based macrocycles.[58] Very recently the same researchers have reported the synthesis of "contracted" expanded porphyrins,[93,94] namely cyclo[6]pyrrole **91**, cyclo[7]pyrrole **92** and cyclo[8]pyrrole **93**. They are so called contracted because there are no *meso* bridging carbon atoms between adjoining pyrrole rings. The products are synthesised from bipyrrole building blocks such as **94** that are oxadatively coupled using ferric chloride in the presence of acid (Scheme 1.2). Interestingly the use of sulphuric acid predominantly forms product **93** in 77% yield (corresponding dihydrogen sulfate salt), whilst hydrochloric acid gives macrocycles **93**, **91** and **92** in 25%, 15% and 5% yields respectively. A diprotonated cyclo[8]pyrrole derivative has been crystallised with a sulfate anion bound centrally within the cavity. The four oxygen atoms of the sulfate are co-ordinated by eight NH hydrogen bonds that range from 1.91-2.49Å, with the macrocycle still very flat and not deviating from planarity.

1.5 Electrochemical sensors for anions

1.5.1 Introduction

It has been shown herein that there is a vast and expanding number of examples within the literature of compounds that are capable of co-ordinating anions. Chemists tailor their host molecules to selectively bind a desired guest giving rise to the area of molecular recognition, whereby a receptor can discriminate between a range of guests. These molecules can be a powerful analytical tool if upon co-ordination of an anion a macroscopic physical response is induced (be it fluorescence, colorimetric or redox-activity)[2,95] and hence behave as a sensor[96].

An electrochemical sensor will therefore consist of a binding site and a redox active species that has a well defined electrochemical behaviour (ferrocene, cobaltocene etc) that is perturbed upon ion co-ordination. This can be achieved through incorporation of a redox active "reporter group" in close proximity to the binding site. There are various known mechanisms[97] (through bond or space, direct co-ordination, conformational change and interference) that communicate the binding process to the "reporter group", although ultimately there is one essential requirement, and that is a response (Figure 1.13).

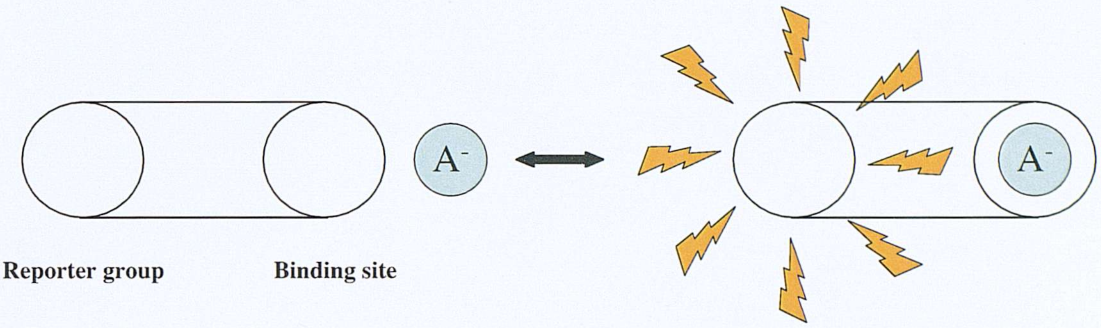

Figure 1.13: The co-ordination of an anion within a binding site of a receptor perturbs the electrochemical properties of a redox active species forming a sensor.

Why are the electrochemical properties of a receptor that contains ferrocene effected upon the addition of some anionic species? The Fe(II) iron centre of the ferrocene group can be reversibly oxidised to Fe(III), giving the mono-positively charged ferrocenium species. This oxidation process involves the loss of an electron and the molecule gaining a net positive charge. Co-ordination of an anion to the receptor introduces a negative charge in close proximity to the redox-active species and can stabilise the oxidation process through ion pairing. It is normal to expect to see a cathodic shift in the Fc/Fc^+ redox couple when the receptor is in presence of anions as less positive potentials are required to oxidise the ferrocene group. It is important to note that the electrochemical response measures the increased affinity of the oxidised receptor for the anion, and cannot be directly correlated to association constants derived from ^1H NMR data or UV-Vis titrations that measure the affinity of the neutral receptor.

1.5.2 Synthetic electrochemical anion sensors.

Sessler and co-workers have reported the synthesis of some bridged dipyrrole ansa-ferrocene derivatives **95-98**.[98,99] ^{1}H NMR titration experiments revealed **95** showed selectivity for fluoride, chloride and dihydrogen phosphate over the other anions studied in acetonitrile-d_3 solution. The complex stoichiometry was found to be dependant upon the size of the anion. Notably fluoride was found to bind in a 2:1 ratio while chloride, bromide, hydrogen sulfate and dihydrogen phosphate were co-ordinated in a 1:1 fashion. Cathodic shifts were observed with **95** in the presence of anions, specifically dihydrogen phosphate (136mV), fluoride (80mV) and chloride (24mV).

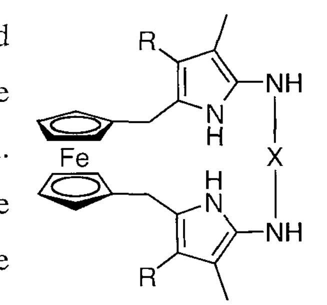

95 X = $CH_2(CH_2OCH_2)_2CH_2$
R = CH_2CH_3
96 X = $(CH_2)_5$
R = CH_3
97 X = $CH_2CH_2OCH_2CH_2$
R = CH_3
98 X = $CH_2(CH_2OCH_2)_2CH_2$
R = CH_3

Sessler showed that the affinity of this class of receptor for dihydrogen phosphate could be modulated through the number of oxygen atoms present in the bridging linker. For example compounds **96**, **97** and **98** had association constants of $K_a = 4050$ M^{-1}, $K_a = 13{,}200$ M^{-1} and $K_a = 81{,}400$ M^{-1} respectively in 2% dimethyl sulfoxide-d_6-dichloromethane-d_2 solution. The massive increase in association constant was not reciprocated in the shift of the ferrocene/ferrocenium redox couple with a negligible increase from 128mV (no ether link) to 140mV (for both ether linked species) in this solvent system.

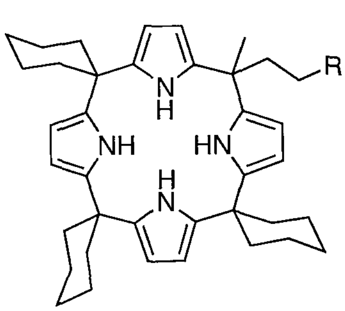

99

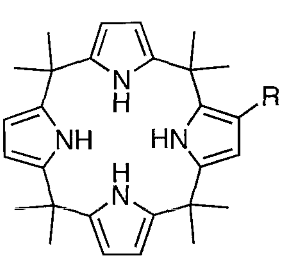

100

R =

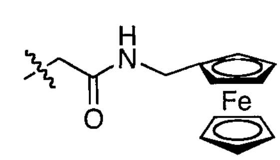

Sessler and co-workers reported the synthesis of two calix[4]pyrrole derivatives with a loosely linked ferrocene moiety. The redox group was appended to the calixpyrrole skeleton at the *meso*-position or to the pyrrole backbone at a *beta*-position,[100] **99** and **100** respectively. Cathodic shifts of 14 and 207mV were observed in the ferrocene/ferrocenium redox couple upon addition of fluoride and chloride anions respectively to a solution of **99**. Whilst the addition of dihydrogen phosphate to the same system resulted in an anodic shift of –9mV. Compound **100** also gave an anodic shift in the ferrocene/ferrocenium redox couple upon addition of chloride (-22mV). Yet addition of dihydrogen phosphate and fluoride anions to the same receptor gave cathodic shifts of 31 and 63mV respectively. The electrochemical properties of the ferrocene group are clearly perturbed upon addition of anions, however rationalisation for the direction of the shift observed remained unexplained.

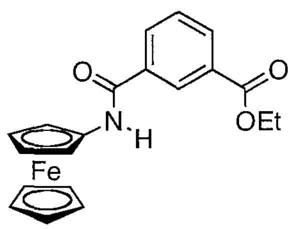

101

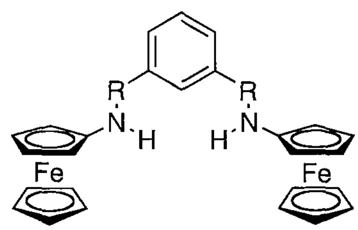

102 R = CO
103 R = SO_2

Crabtree and co-workers have previously reported work on acyclic, non-preorganised diamide receptors[29] with respect to their anion binding abilities. In addition they have produced mono and bisferrocene-amide species **101-103** to investigate if these species may be able to detect anions electrochemically.[101] The study however better illustrated the importance of having two convergent amide sites for the binding of chloride more so than having strong pertubations in the redox couple. Association constants for chloride of 9500 M^{-1} and 30 M^{-1} were observed for **103** and **101** respectively in dichloromethane-d_2. Addition of one equivalent of tetrabutylammonium chloride to **103** slightly perturbed the redox couple with a cathodic shift of 20mV, whilst a negligible shift of <5mV was observed upon addition to **101**.

In comparison to ferrocene, cobaltocenium is positively charged and more stable. The reduction of cobaltocenium gives the nineteen valence electron complex cobaltocene forming a well defined redox couple. The cobaltocenium moiety can potentially introduce an electrostatic component to the binding of anions, whilst still incorporating a redox active group.

In 1999 Beer and co-workers reported the synthesis and anion recognition properties of three upper-rim cobaltocenium substituted calix[4]arene receptors.[102]

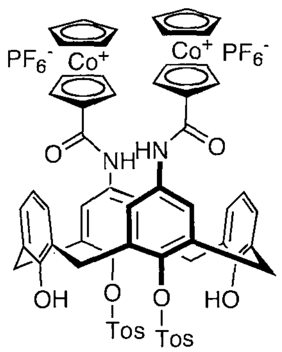

104

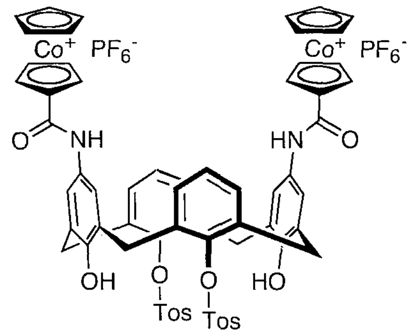

105

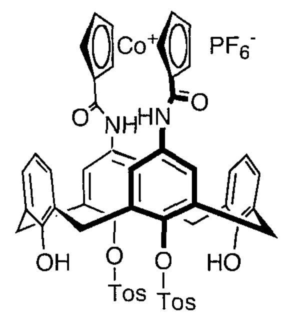

106

The anion co-ordination properties were found to be dependant upon the pre-organisation of the upper-rim substituents. Considering only acetate and dihydrogen phosphate anions, a seven fold preference for acetate ($K_a = 2.1x10^4 M^{-1}$) is shown by **104**, yet isomeric **105** reverses the order and binds dihydrogen phosphate ($K_a = 2.5x10^3 M^{-1}$) three times more strongly in dimethyl sulfoxide-d_6 solution. The cobaltocenium-bridged host **106** proved to bind carboxylate and dihydrogen phosphate anions better than either **104** or **105** with this receptor selectively binding acetate ($K_a = 4.15x10^4 M^{-1}$). The higher affinities can be accounted for by the arrangement of the upper-rim amide groups, through forming a cavity suitable for interaction with bidentate anions. Electrochemical recognition of carboxylate, dihydrogen phosphate and chloride anions was demonstrated by the receptors with cathodic perturbations of up to 155mV for **106** with acetate.

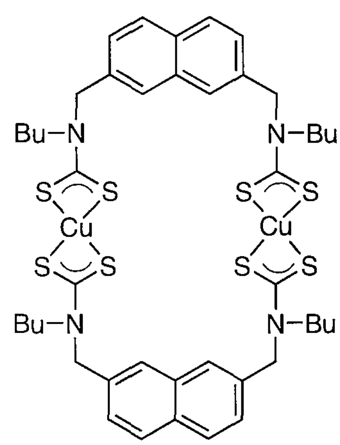

107

In two recent publications Beer and co-workers have reported self assembled dithiocarbamate based anion receptors. Selected examples **107**[103] and **108**[104] contain two copper redox-active centres, that are separated by naphthyl and amide based spacer groups respectively. Both compounds were prepared in a one pot synthesis from the parent secondary amines in a reaction with carbon disulphide, potassium hydroxide

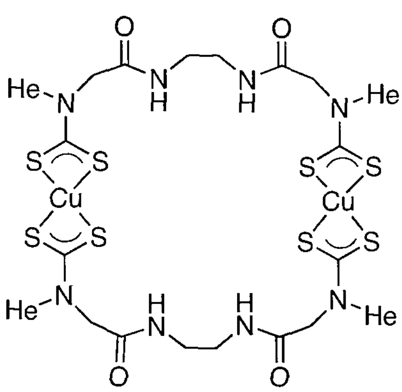

108

and copper(II)acetate. Macrocycle **107** showed selectivity for tetrahedral anions. Identical cathodic shifts of 85mV in the copper(II)/copper(III) redox couple were measured for perhenate and dihydrogen phosphate anions in dichloromethane:acetonitrile (4:1) solution. Addition of anions to electrochemical solutions of tetra-amide species **108** also results in significant perturbations of the copper(II)/copper(III) dithiocarbamate redox couple. This sensor can distinguish various anions by their induced cathodic shifts, of up to 160mV with dihydrogen phosphate.

1.6 Aim of the project

This chapter has shown throughout the various sections the huge variety of receptors and electrochemical sensors that employ different functional groups to co-ordinate anions. Over recent years anionic recognition has drawn much attention from supramolecular chemists, and will continue to do so into the future. It is still a developing field of great interest within the supramolecular chemistry community because of the remaining goal of many researchers to synthesise receptors/sensors that can strongly and selectively bind a single anionic substrate.

In accordance with these goals, the work in this thesis describes the synthesis of new anion receptors. An investigation of the anion complexation properties and in some cases redox activity is also reported. The work can be separated into the following areas of research:-

- A variety of *meso*- substituted calix[4]pyrroles were synthesised. Ferrocene substituted derivatives indicated a direct co-ordination mechanism between the anion and "reporter group". Whilst a calixpyrrole bearing a 3,4,5-tribromopyrrole group displayed a high affinity for carboxylates.

- A range of pyrrole, furan and thiophene amide and thioamide derivatives were synthesised to investigate if the molecules would dimerise. The anion binding properties of these compounds was investigated.
- Finally the solid state assembly, anion complexation and electrochemical properties of mono- and bisferrocene 2,5-diamidopyrrole clefts were studied.

2. *Meso-substituted calix[4]pyrroles*

2.1 Introduction

In the previous chapter we have seen examples of neutral anion receptors[105] that co-ordinate anions through hydrogen bond interactions. Some functional groups that are used to bind anions in this way can self associate through C=O···HN interactions (e.g. amides or ureas). The pyrrole group does not contain an intrinsic hydrogen bond acceptor and is therefore unable to hydrogen bond to itself. Interestingly, Gale and co-workers have shown that a single pyrrole ring can form a hydrogen bond[56] to an anion (Figure 2.1) in the solid state. The crystal structure reveals two pyrrole rings co-ordinating one chloride anion (N···Cl distance 3.241Å), unfortunately this interaction is weak when studied in solution.[57] In 1990 Sessler and co-workers made a serendipitous discovery that sapphyrin (an expanded porphyrin) was able to co-ordinate anions when diprotonated.[89] This can be considered the birth of pyrrole-based anion recognition after which time the anion co-ordination chemistry of other pyrrolic systems was investigated.

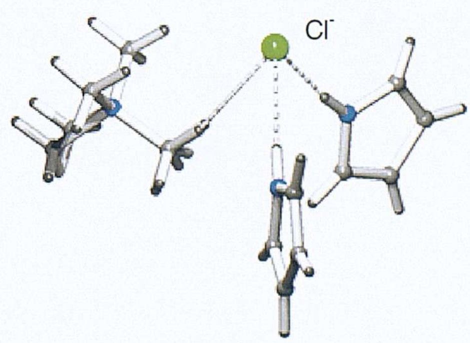

Figure 2.1: Crystal structure of the pyrrole/tetramethyl ammonium chloride complex.

Porphyrinogens are a naturally occurring group of tetrapyrrolic macrocycles, that contain four pyrrole rings linked by sp^3 hybridised carbon atoms at the 2- and 5-positions. Porphyrinogens are precursors to porphyrins, as they are easily oxidised to the corresponding aromatic species. However, the condensation of pyrrole with a ketone, as opposed to an aldehyde, results in a fully substituted bridging carbon. The first porphyrinogen of this type was synthesised by Baeyer over a century ago[70] when he condensed pyrrole with acetone in the presence of hydrochloric acid (Scheme 2.1). This type of porphyrinogen has been renamed 'calix[4]pyrrole' because of the structural similarity to calix[4]arene (a tetraphenolic macrocycle that resembles a Greek calix crater vase).[106] This re-naming emphasizes the analogy between the conformational properties of the pyrrolic macrocycles, and the calixarenes[71] (a group of macrocyles formed by the base induced condensation of certain *para*-substituted phenols and formaldehyde).

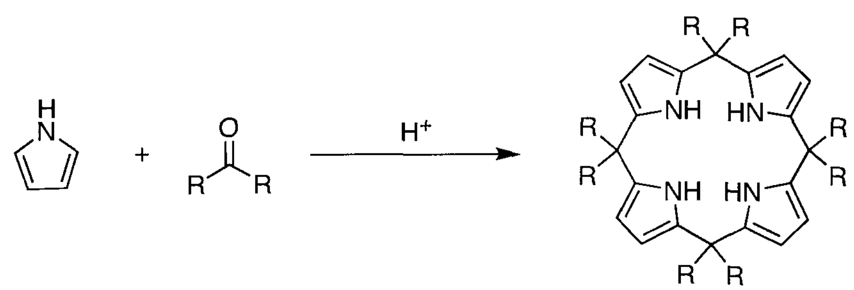

Scheme 2.1: Calix[4]pyrroles can be synthesised by acid catalysed condensation of a ketone with pyrrole.

Calix[4]pyrroles (mainly the *meso*-octaethyl derivative) in their deprotonated form, were used by Floriani and co-workers as co-ordinating agents for various transition-metal cations. The calix[4]pyrrole skeleton allowed them to produce oxidised derivatives of porphyrinogen other than porphyrins (typically obtained upon porphyrinogen oxidation).[107,72] However, in 1996 Sessler and co-workers reported that *meso*-octamethylcalix[4]pyrrole **68** was able to bind a selection of anions through the formation of four pyrrole NH···anion hydrogen bonds. A high selectivity was shown for fluoride with an association constant K_a = 17,170 M^{-1}, a value two orders of magnitude larger than that measured for chloride K_a = 350 M^{-1} in dichloromethane-d_2.[57]

X-ray crystallographic analysis of the free *meso*-octamethylcalix[4]pyrrole **68** revealed that the macrocycle adopted a 1,3-alternate conformation in the solid state.[57] This is in contradistinction to free unsubstituted calix[4]arenes, a phenolic based macrocycle that forms a cone conformation through hydrogen bonding between the four phenol OH groups[71] (unmodified calixpyrroles have no such possibility for hydrogen bonding). However in the presence of chloride the macrocycle adopts a cone conformation, with all four of the pyrrole NH groups pointing towards the chloride anion.[57] Variable temperature NMR revealed that the cone conformation of the host/guest complex is maintained in solution at low temperature.[108]

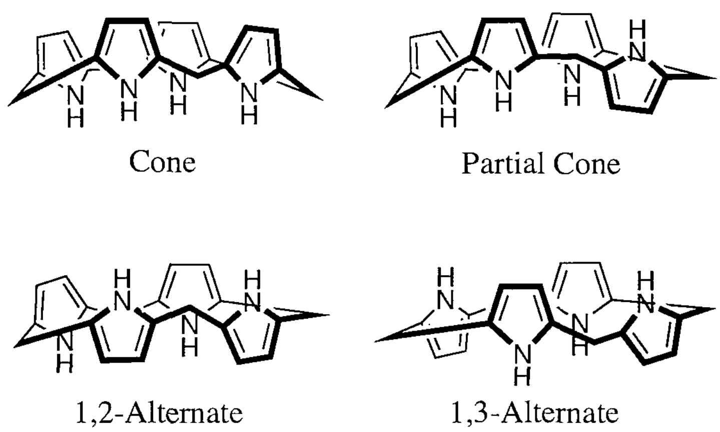

Figure 2.2: A schematic representation of the four major conformations of calix[4]pyrrole. Substituents at the *meso*-position have been omitted for clarity.

In 1999 van Hoorn and Jorgensen conducted modelling studies using Monte Carlo simulations to study the anion selectivities of calix[4]pyrroles.[109] In agreement with experiment they concluded of the four possible conformations (Figure 2.2) the 1,3 – alternate conformation was the most stable in the absence of anions, whilst the cone conformation was the most stable when co-ordinating a halide anion. Free energy calculations on the binding of the halides in dichloromethane were found to be in excellent agreement with experiment excluding fluoride. The calculated affinity of calix[4]pyrrole with fluoride ions was far greater than the experimental value. This inconsistency was attributed to trace quantities of water. The fluoride used to determine the association constant by Sessler and co-workers was added as the tetrabutylammonium salt, which is inherently hygroscopic (altering the actual quantity of fluoride added).

Schmidtchen has shown that calorimetric measurements in acetonitrile solution do not corroborate the values obtained by NMR titration techniques, indicating that the fluoride over chloride selectivity is hugely over-estimated. However these studies did not use the same conditions used in the NMR titration studies.[110] While in a paper by de Namor and co-workers their isothermal titration calorimetry results maintained the selectivity of calix[4]pyrroles for fluoride.[111] More recently Sessler and co-workers conducted a theoretical study on anion binding capabilities of calix[4]pyrrole accounting for solvent, cosolute and water traces. In the case of fluoride, the work suggested that the binding constant is infact an "apparent" binding constant that measures the transfer of fluoride from tetrabutylammonium-$(H_2O)_3^+$ to the calix[4]pyrrole.[112] These studies indicate that association constants obtained between calixpyrroles and fluoride should be treated with a degree of caution.

Unlike many other macrocycles, *meso*-octamethylcalix[4]pyrrole can be made easily in a simple one step synthesis (acid catalysed condensation of pyrrole with acetone). Many research groups have modified the synthesis to produce a variety of new calix[4]pyrrole derivatives.[113] This has been achieved by modification of the ketone and/or pyrrole starting reagents prior to condensation, or by reacting a previously synthesised calix[4]pyrrole at a pyrrole β-position.[114,115] The recent advances in calixpyrrole anion co-ordination have been summarised in the previous chapter, illustrating how different methodologies have been used to modulate the selectivity of this class of receptor. If selective anion co-ordination is coupled with a reporter group then the receptor can behave as a sensor for anions.

Sessler, Gale and co-workers have produced a variety of fluorescent[116] and colorimetric[117] anion sensors[113] based upon calix[4]pyrrole. However their attempts to synthesise electrochemical sensors based upon calix[4]pyrrole and ferrocene conjugates **99** and **100** gave complicated results, that were not easily rationalised.[100] We decided to incorporate a ferrocene moiety at the calixpyrrole *meso*-position, to allow for the possibility of direct co-ordination to the anion from the ferrocene group through C-H hydrogen bond interactions. This chapter reports the synthesis of a variety of *meso*-substituted calix[4]pyrroles. The anion co-ordinating properties were investigated using ^{1}H NMR titration techniques,[118,119] while the electrochemical properties of **110** were obtained using cyclic voltametric and square-wave voltametric techniques.

2.2 Ferrocene substituted calix[4]pyrroles

2.2.1 Synthesis and characterisation

In order to synthesise a calix[4]pyrrole containing a ferrocene moiety at the *meso*-position we condensed acetylferrocene with pyrrole (1:1) using methanesulfonic acid as a reaction catalyst, to form macrocycle **109** bearing four ferrocene groups (Scheme 2.2). The reagents were stirred in methanol under an inert atmosphere of nitrogen to give a mixture of isomeric products (Figure 2.3). After stirring overnight the solution was neutralised with triethylamine and the solvent removed *in vacuo.* When a solution of the crude product was subjected to positive electrospray mass spectrometry, analysis of the spectrum revealed a peak at 1108 Da/e that corresponds to the expected value for M^+. Additionally, a ^1H NMR spectrum showed characteristic peaks that could be designated to the various sites in the molecule (methyl, ferrocene and pyrrolic) indicating that the formation of the desired product had been achieved.

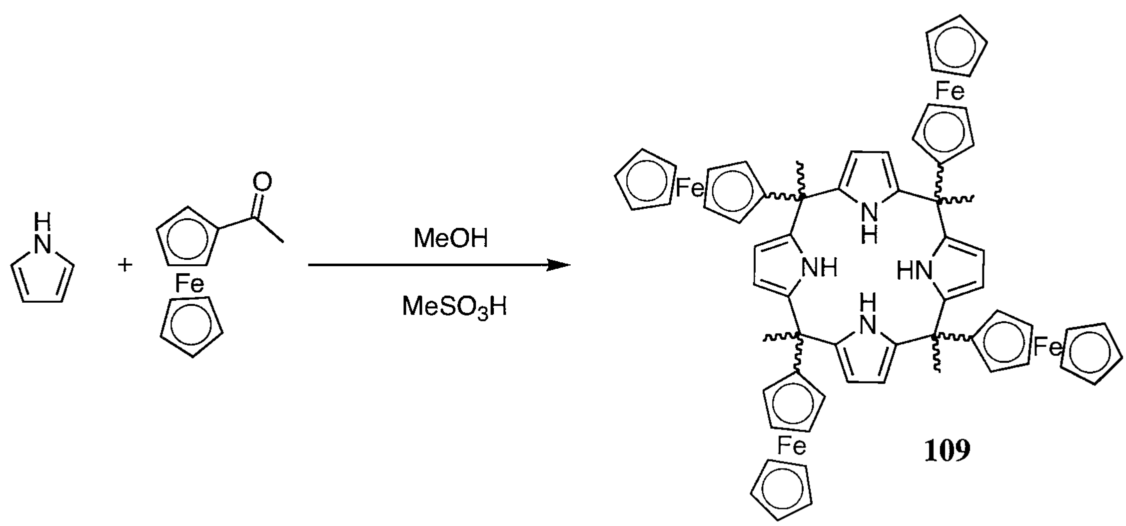

109

Scheme 2.2: The acid catalysed condensation of pyrrole with acetylferrocene, forming the tetra-ferrocene calixpyrrole **109**.

The reaction of acetylferrocene with pyrrole to form a macrocycle gives four isomeric products (αααα, αααβ, ααββ and αβαβ), these are shown in figure 2.3.

However, attempts to purify the reaction mixture and obtain a single isomer by column chromatography on silica gel, or preparative layer chromatography using silica on glass plates were unsuccessful in a variety of eluents. We sent a crude sample of **109** to the Sessler group at The University of Texas at Austin, and unfortunately their attempts to separate the mixture using high performance liquid chromatography were also unsuccessful. We then tried to separate the mixture using crystallisation techniques. This was successful and two isomers were obtained. Unfortunately this method yielded very small quantities of each isomer, and an insufficient amount to allow full characterisation of the compounds. We were therefore unable to study the anion receptor and/or electrochemical sensor capabilities of the tetraferrocene calix[4]pyrroles. Similarly attempts to form a singularly isomeric octa-ferrocene calixpyrrole species by condensing diferrocene-methanone with pyrrole was totally unsuccessful. No reaction between the starting materials was observed, even with prolonged reaction times of up to a week, heating at reflux or variation of the reaction catalyst (methanesulfonic acid, trifluoroacetic acid and boron trifluoride etherate catalysts were used).

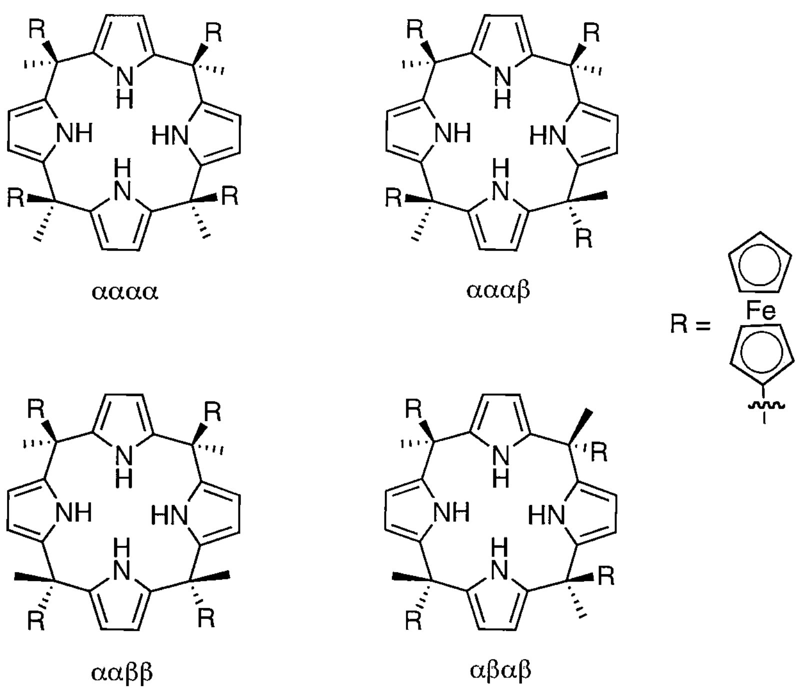

Figure 2.3: The four isomers of calixpyrrole **109** that are formed when pyrrole is condensed with acetylferrocene

Although we were unable to isolate a sufficient quantity of compound **109** to allow full characterisation and physical property analysis, we were able to crystallise two isomers of this receptor from dimethyl sulfoxide and dichloromethane solutions giving the $\alpha\alpha\alpha\alpha$ and $\alpha\alpha\beta\beta$ conformations respectively (Figure 2.4) (see Appendix for structural information). The calix[4]pyrrole skeleton of the $\alpha\alpha\alpha\alpha$ isomer shown in figure 2.4(a) adopts a 1,3-alternate conformation, while the $\alpha\alpha\beta\beta$ derivative shown in figure 2.4(b) has the four pyrrolic rings in a 1,2-alternate conformation.

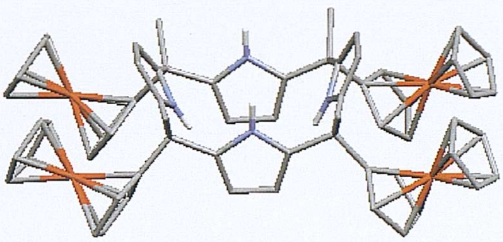

(a)

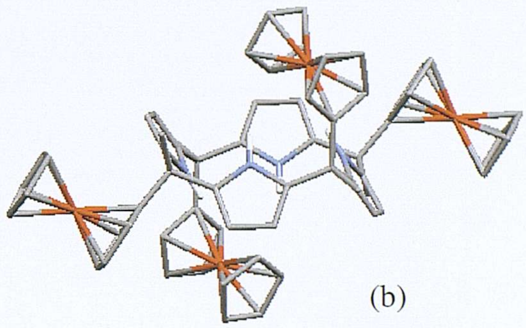

(b)

Figure 2.4: Compound **109** was crystallised from dimethyl sulfoxide (a) and dichloromethane (b) solutions. Solvent molecules have been removed for clarity.

We therefore decided to adopt a different approach and attempt to synthesise a mono-ferrocene calixpyrrole from a statistical condensation of starting reagents. Compound **110** was synthesised by the acid catalysed condensation of pyrrole with cyclohexanone and acetylferrocene in a 4:3:1 ratio (Scheme 2.3). The reagents were stirred in methanol under an inert atmosphere of nitrogen to give a mixture of condensation products, due to the presence of the two ketones and isomeric products thereof. After stirring overnight the solution was neutralised with triethylamine and the solvent removed *in vacuo*. The residue was separated by column chromatography on silica gel eluting with dichloromethane:hexane (2:1). The mono-ferrocene calix[4]pyrrole **110** was isolated as an orange powder in 30% yield.[120] Crystals of compound **110** were obtained by slow evaporation of an acetonitrile solution of the receptor.

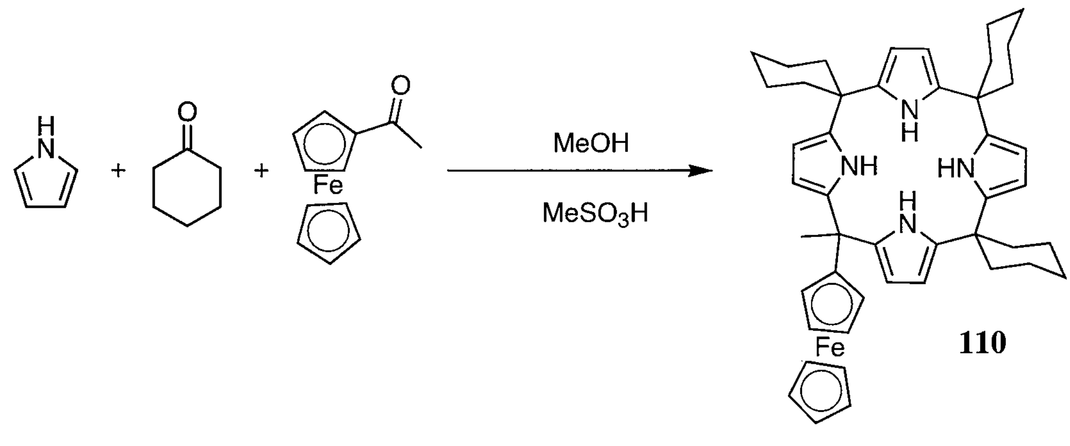

110

Scheme 2.3: Synthesis of mono-ferrocene calix[4]pyrrole **110**.

We wished to synthesise a bis-calixpyrrole with a calix[4]pyrrole macrocycle linked to both of the ferrocene cyclopentadienyl rings, forming a ferrocene bridged species. It is possible that such a receptor may bind anions in a 2:1 anion:receptor ratio or possibly in a 1:1 sandwich complex. This would be of interest because two anion co-ordination sites would be linked together by a ferrocene "reporter group", that could also enable electrochemical sensing of anionic species.

To accomplish this we co-condensed pyrrole with cyclohexanone and 1,1'-diacetylferrocene in a 8:6:1 ratio (Scheme 2.4). The reagents were stirred in methanol under an inert atmosphere of nitrogen to give a mixture of products. After stirring overnight the solution was neutralised with triethylamine and the solvent removed *in*

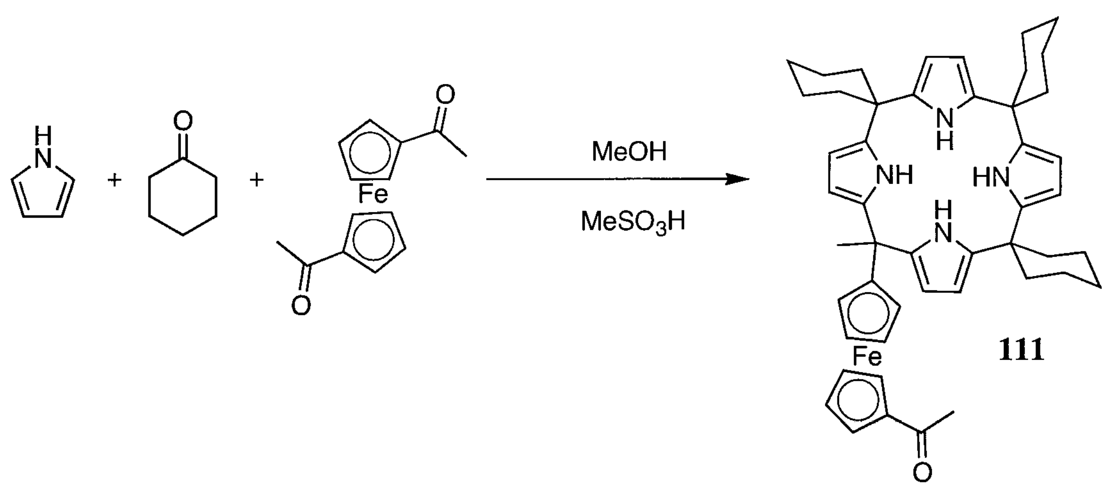

111

Scheme 2.4: Synthesis of mono-acetylferrocene calix[4]pyrrole **111**.

vacuo. Mass spectrometry analysis revealed that formation of the desired 1,1'-dicalixpyrroleferrocene product was not possible under our reaction conditions, but a mass corresponding to compound **111** was evident. The residue was separated by column chromatography on silica gel eluting with dichloromethane/methanol (99:1). This yielded an impure product that was further purified by preparative layer chromatography using the same solvent system to obtain compound **111** as an orange powder in 2% yield (the only isolable compound from the reaction mixture).

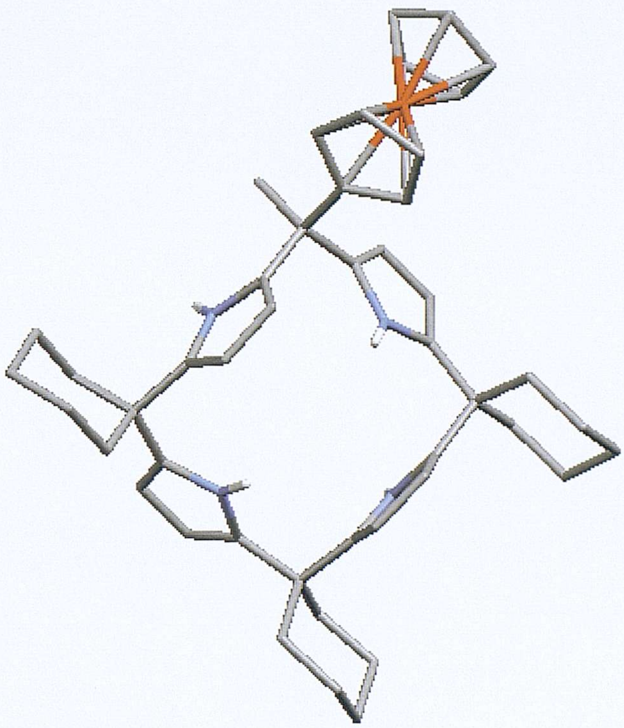

Figure 2.5: Crystal structure of compound **110**.

X-ray quality single crystals of **110** were obtained by slow evaporation of a acetonitrile solution of the macrocycle (Figure 2.5). As in the case of most other calix[4]pyrrole macrocycles, the uncomplexed receptor adopts a 1,3 alternate conformation in the solid state (see Appendix for structural information).

Single crystals of **111** were obtained by slow evaporation of a hexane/acetone (50:50) solution of the receptor. The crystal structure reveals the formation of hydrogen bonded cyclic dimers[121] (Figure 2.6). In the dimer, both of the receptors adopt a 1,3-alternate conformation, one of the pyrrolic NH groups of one calixpyrrole forms a hydrogen bond to a ferrocene acetyl group of an adjacent calixpyrrole and vice versa with N···O=C distances of 3.145(10)Å (see Appendix for structural information.

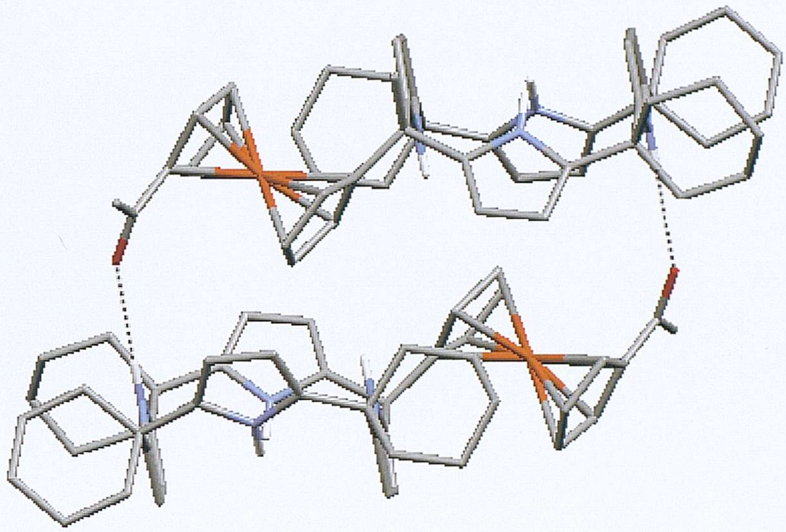

Figure 2.6: Crystal structure of compound **111** showing dimer formation in the solid state.

2.2.2 Co-ordination studies

2.2.2.1 Binding study results. Evidence for a direct co-ordination mechanism by CH···anion hydrogen bonds

The binding properties of receptors **110** and **111** have been investigated using ^{1}H NMR titration techniques in acetonitrile-d_3/dimethyl sulfoxide-d_6 (9:1) with the association constants being elucidated using EQNMR[118] software. The anions were added as their tetrabutylammonium salts because this counter cation is regarded as being relatively "innocent" (as it is not in great competition with the anion binding site).

10% Dimethyl sulfoxide was used for solubility reasons, because compound **110** readily crystallises from acetonitrile solution even at low concentrations, forming crystalline clusters. Addition of anionic solutions to the receptor during the titrations broadened the pyrrolic NH resonances, making them unsuitable for the calculation of the association constants. However, for both receptors **110** and **111**, a significant downfield shift was observed for one of the ferrocene CH resonances. This not only enabled calculation of the K_a values but also provided evidence for the formation of CH···anion hydrogen bonds in solution (Figure 2.7). Variable temperature (cold) ^{1}H and ^{19}F NMR experiments were conducted with **110** and tetrabutylammonium fluoride, to try to evaluate any coupling (upon binding) between the fluoride and the host pyrrolic NH groups. Unfortunately the peaks were too broad to provide any evidence for this process.

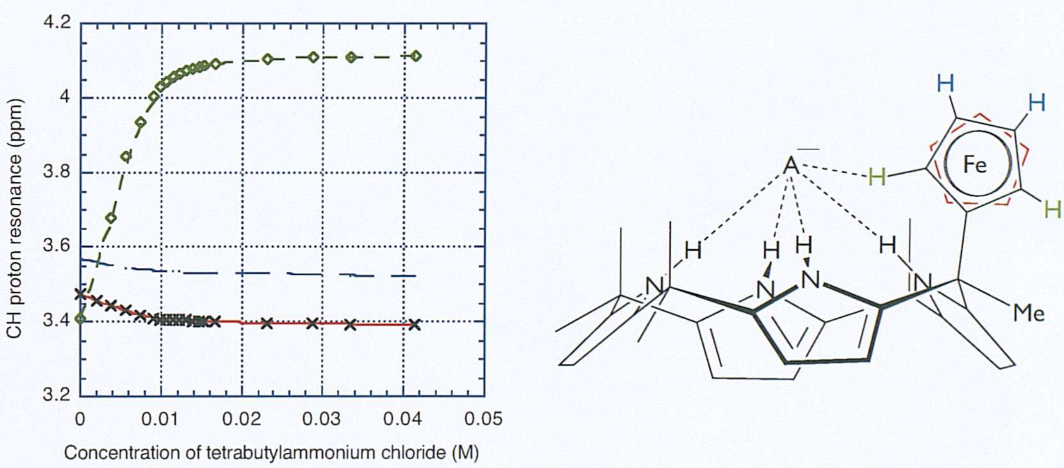

(a) (b)

Figure 2.7: A plot of the ferrocene CH resonance shifts of compound **110** upon addition of chloride anions (a). A schematic representation of the hydrogen bonding interactions that are believed to stabilise the anion, we believe this causes a distinctive shift of only one ferrocene proton (b).

Although titrations with tetrabutylammonium hydrogen sulfate were conducted, a stability constant was not determined. There was no shift in the ^{1}H NMR spectra of either **110** or **111** upon the addition of this anion, implying there was no interaction between the hosts and the anion. The results of the other titrations are summarised in table 2.1 revealing that compounds **110** and **111** co-ordinate anions such as fluoride, chloride and dihydrogen phosphate in this solvent system with all of the data fitting a 1:1 binding model. The values for dihydrogen phosphate should be treated with some caution as the ferrocene resonance was partly obscured during these titrations.

Anion	**110** $K_a (M^{-1})$	**111** $K_a (M^{-1})$
Fluoride	3375	#
Chloride	3190	3731
Bromide	50	47
Dihydrogen phosphate	304*	564*

Table 2.1: Stability constants for **110** and **111** with anionic substrates in deuterated acetonitrile/dimethyl sulfoxide (9:1) solution at 298K # A value was not obtained because of slow exchange * The CH resonance was partly obscured during the titration.

To create a standard for comparison, titrations with *meso*-octamethylcalixpyrrole **68** were conducted in the same solvent system with chloride and dihydrogen phosphate anions. The titrations were performed to give an insight into the binding affinities of compound **68** for anions in this solvent system. These particular anions were chosen because:- (a) we were unable to obtain an association constant for fluoride with compound **111**, (b) receptor **110** did not indicate selectivity for fluoride over chloride, (c) bromide was not used because both ferrocene appended receptors showed a weak affinity for this anion. In the titration of **68** with chloride the NH resonance broadened, however we were able to follow an upfield shift of the pyrrolic backbone resonance (although this doesn't indicate that this proton is involved in hydrogen bonding, there can only be one association constant) that gave an association constant $K_a = 13{,}997 \pm 430\ M^{-1}$, and in the case of dihydrogen phosphate $K_a = 7366 \pm 835\ M^{-1}$ errors of 3 and 11% respectively. This shows that anions such as chloride and dihydrogen phosphate were more strongly bound by **68**, indicating that the ferrocene group has a significant effect on the binding affinity. The possible addition of a weak CH hydrogen bond to aid co-ordination is clearly outweighed by what seems to be steric factors. The two ferrocene appended receptors have similar affinities for anions. The results suggest that the acetyl group has little effect on halide binding, but the presence of a hydrogen bond acceptor may account for the two-fold increase of the association constant observed for **111** compared to **110** when binding dihydrogen phosphate.

The titration of receptor **111** with fluoride revealed a slow exchange process with the formation of new ferrocene CH, pyrrolic NH and backbone CH resonances, the change was complete around the addition of one equivalent of fluoride (Figure 2.9).

In addition there was evidence of fluorine coupling to the pyrrole NH groups at room temperature. The two NH signals were split into doublets suggesting that they are coupled to one fluoride anion, the data is consistent with the formation of a 1:1 receptor/fluoride complex. This type of behaviour has been seen before in super-extended cavity calix[4]pyrrole systems.[79,80] ^{19}F NMR spectroscopy confirmed the coupling to the pyrrolic NH's although the splitting pattern was not clearly resolved. The signals in the proton spectrum are split into doublets with a coupling constant J = 32 Hz, this is consistent with the protons coupling to one fluorine atom. However, we are unable to quote coupling constants from the fluorine spectrum, as the observed signal probably consists of overlapping triplets arising from very similar coupling constants to the two inequivalent pyrrole NH sites of the receptor (Figure 2.8).

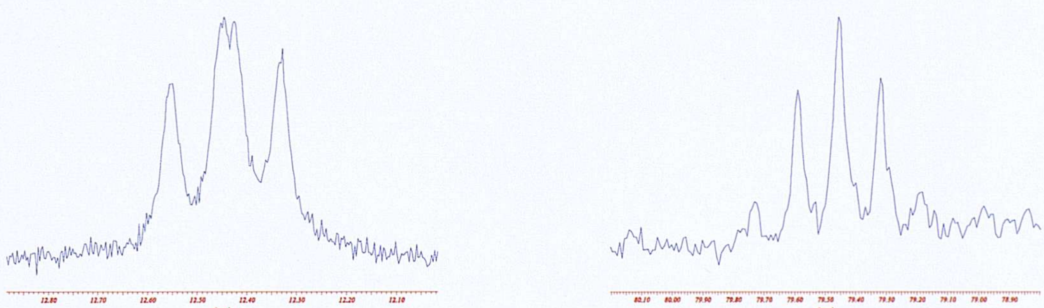

(a) ^{1}H NMR (b) ^{19}F NMR

Figure 2.8: The ^{1}H NMR recorded at 300 MHz (a) and ^{19}F NMR recorded at 282 MHz (b) spectra of **111** with four equivalents of fluoride, in acetonitrile-d_3/dimethyl sulfoxide-d_6 (9:1) solution on a 300 MHz spectrometer. This data suggests coupling between the four calixpyrrole NH and the bound fluoride anion.

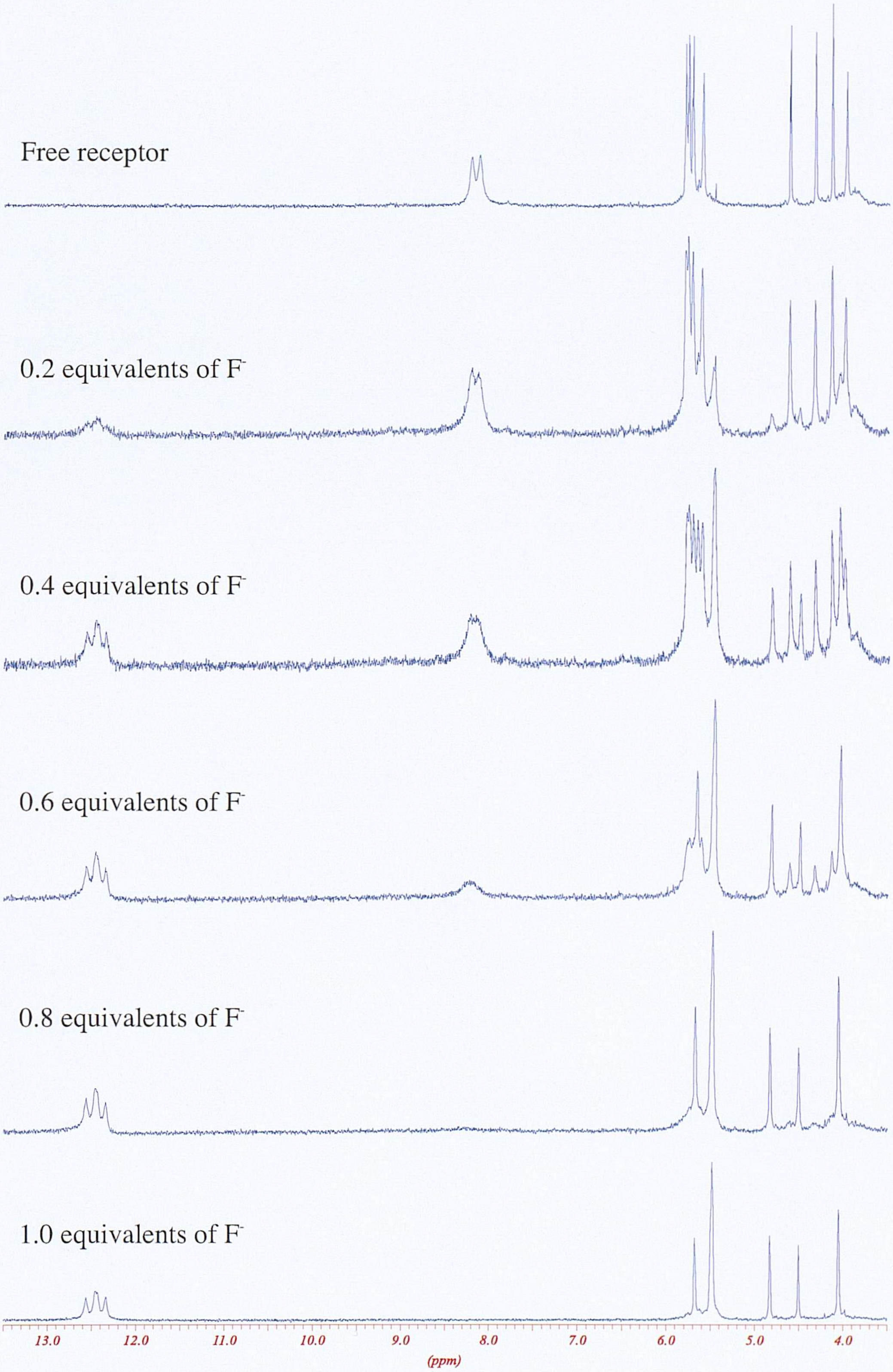

Figure 2.9: Proton NMR titration of calix[4]pyrrole **111** with tetrabutylammonium fluoride, revealing a slow kinetic complexation/decomplexation process.

2.2.2.2 Electrochemical results

The values in table 2.1 (perhaps non too surprisingly) indicate that the receptors have similar binding properties. For this reason electrochemical studies were only conducted with receptor **110** as it seemed fair to assume that the electrochemical properties would also be similar to that of **111**. The electrochemical experiments were conducted on compound **110** by R. Zimmerman of the Sessler group and Dr. P. Gale in Texas, however their findings are reported below.

The electrochemical properties were investigated using square wave (SWV) and cyclic voltammetric (CV) techniques. To maintain consistency (with ^1H NMR experiments) the electrochemical experiments were conducted in a acetonitrile/dimethyl sulfoxide (9:1) solvent mixture with tetrabutylammonium hexafluorophosphate (0.1M) as the supporting electrolyte. The working electrode used was a platinum disc, with a platinum gauze counter electrode and a silver/silver-chloride reference electrode separated from the electrochemical solution by a salt bridge. All of the voltammetric measurements were carried out under a dry argon atmosphere.

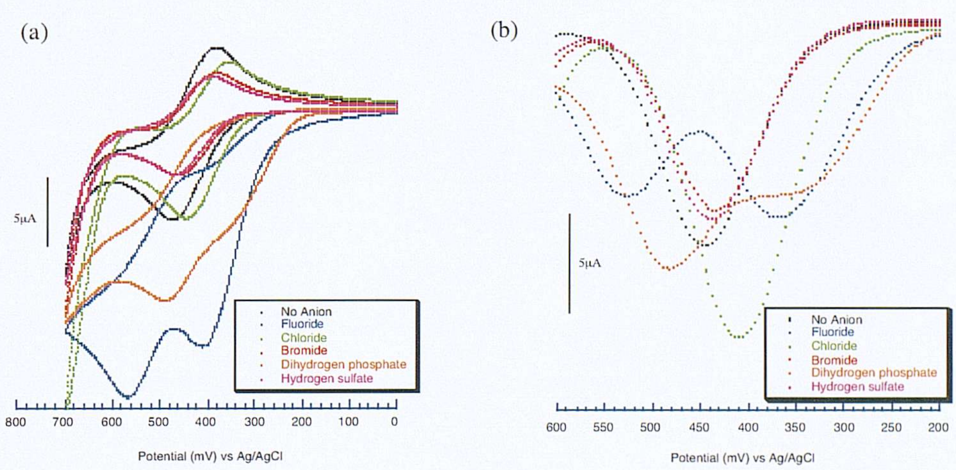

Figure 2.10: Cyclic (a) and square-wave (b) voltammograms of compound **110**

Square wave and cyclic voltammograms of a 5×10^{-4} M solution of receptor **110** in the absence and presence of anions were collected between 0 and 800 mV versus Ag/AgCl at 25°C (Figure 2.10). The observed half-wave potentials and cathodic shifts recorded from solutions containing **110** and three equivalents of various anionic guests are reported (Table 2.2).

Anion	$E_{1/2}$ (Fc/Fc$^+$) (mV)	Δ E (mV)
No anion	+ 444	n/a
Fluoride	+ 368	- 76
Chloride	+ 408	- 36
Bromide	+ 432	- 12
Dihydrogen phosphate	+ 350 *	- 100 *
Hydrogen sulfate	+ 436	<10

Table 2.2: The observed Fc/Fc$^+$ redox potentials for compound **110** with various anionic guests. The $E_{1/2}$ values were obtained from SWV and are versus Ag/AgCl. * The shift observed with dihydrogen phosphate is approximate as the voltammogram peak was not well defined.

The induced cathodic shift in the ferrocene/ferrocenium couple among the halides appears to be inversely proportional to the ionic radius, with fluoride producing the largest cathodic shift (76mV), followed by chloride (36mV) and bromide (12mV). Dihydrogen phosphate gave a shift of approximately 100mV, while hydrogen sulfate, perturbed the redox couple by less than 10mV. Attention should be drawn to the voltammograms for both fluoride and dihydrogen phosphate. The new feature that has appeared within the spectral window corresponds to the oxidation of the calix[4]pyrrole skeleton.

2.3 Pentapyrrolic calix[4]pyrrole

2.3.1 Introduction

The previous work on ferrocene substituted calixpyrroles revealed that one of the ferrocene cyclopentadienyl protons shifted significantly downfield in the presence of anions. This suggests that this proton may be involved in hydrogen bonding to the anionic guest. We therefore decided to synthesise a calix[4]pyrrole that contained a pyrrole group in a *meso*-position (Figure 2.11) in the hope that the pyrrolic NH group may form a stronger hydrogen bond to the bound species than the ferrocene CH, and hence form stronger complexes with anions when compared to *meso*-octamethylcalix[4]pyrrole **68**.

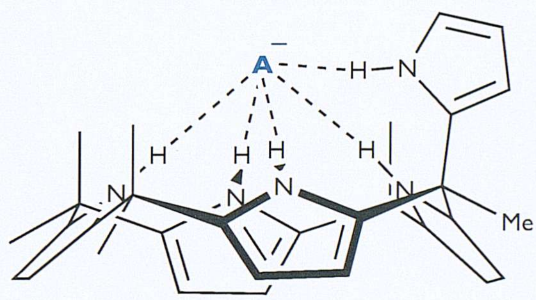

Figure 2.11: A schematic representation of a calix[4]pyrrole bearing a pyrrolic group at the *meso*-position, with the proposed hydrogen bond interactions that a pentapyrrolic calix[4]pyrrole may utilise in anion complexation.

The synthesis of compound **110** used readily accessible starting reagents, and then purification of the condensation products. However, in this case we were unable to obtain the desired calix[4]pyrrole in the same manner. In an analogous reaction we would have reacted 2-acetylpyrrole with pyrrole and cyclohexanone and purified the reaction mixture. But unfortunately the 2-acetylpyrrole is still free to react at the 5-

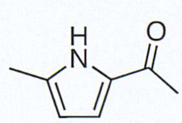

112

position and would greatly hinder this method of synthesis. We therefore needed a 2-acetylpyrrole that had a blocked 5-position to allow a controlled condensation of reactants, such as 2-acetyl-5-methyl-pyrrole[122,123] **112**.

We synthesised this compound by modification of a literature procedure[124] (see experimental section) and obtained **112** in 14% yield. The compound characterisation was in agreement with that previously reported in the literature.[125] However attempts to form a calix[4]pyrrole by co-condensing **112** with cyclohexanone and pyrrole in a 1:1:2 ratio respectively proved unsuccessful. It seemed that **112** was not as reactive as cyclohexanone resulting in no products containing the desired *meso*-pyrrole group. We then tried reacting **112** with dimethyldipyrromethane[126,127] (synthesised using literature methods), as this would prevent the formation of the *meso*-tetraspirocyclohexylcalix[4]pyrrole and hopefully give two isomers that could be separated by chromatographic techniques. Unfortunately no reaction at all occurred between the starting materials. This is presumably due to the pyrrole ring deactivating the ketone in **112**.

Tripyrrolylmethane subunits[128,129] have been used by Beer and co-workers to form cryptand type receptor molecules for neutral guests.[130] Our attempts to react **112** under more forcing conditions using pyrrole as the solvent using trifluoroacetic acid catalyst would not yield the corresponding tripyrrolylmethane. These failed reactions indicated to us that the carbonyl group of **112** was too electron rich and hence not sufficiently electrophillic to react with pyrrole. It has been shown in the literature that pentafluorobenzaldehyde (an electron deficient aryl aldehyde) reacts with pyrrole derivatives in the absence of any catalyst.[131,86] We therefore attempted to brominate **112** in the 3 and 4 positions using *N*-bromosuccinimide in tetrahydrofuran, the electron withdrawing bromine atoms were intended to increase the reactivity of the ketone, however we were unable to isolate any brominated pyrrole species.

2.3.2 Synthesis and characterisation

Lee and co-workers have reported the synthesis of 2-acetyl-3,4,5-bromopyrrole[132] **113** in 85% yield from 2-acetylpyrrole. This readily accessible compound was a suitable starting reagent because the 5-position is blocked by a bromine substituent allowing for a controlled condensation with pyrrole to form the trispyrrolylmethane, whilst this and additional bromine atoms withdraw electron density from the pyrrole

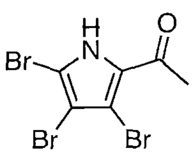

113

ring that in turn make the carbonyl group more electron deficient when compared to **112**. In addition the bromine substituents would serve to increase the acidity of the pyrrole NH group[64] so enhancing any putative NH···anion hydrogen bond interactions.

We tried to condense **113** directly with pyrrole (using methanesulfonic acid, trifluoroacetic acid and borontrifluoride etherate as reaction catalysts) in an attempt to form a pyrrolic analogue **114** of the extended cavity calix[4]pyrroles.[77,79] Negative electrospray mass spectrometry was used to probe the progress of the reaction. After two hours stirring at room temperature the formation of condensation products was evident e.g. **115**, **116** and **117** (Figure 2.12). A peak at 1364 Da/e corresponds to compound **117** (an oligomer containing four pyrrole, and three *meso*-pyrrole subunits) plus trifluoroacetic acid. However after longer reaction time periods (overnight) we were still unable to obtain the corresponding calix[4]pyrrole macrocycle. At extended reaction times of up to seventy-two hours it appeared that the products had degraded, also suggested by a darkening of the solution. Interestingly the satellite peaks are an equivalent mass distance away that correspond to bromine, the brominated pyrrole may be degrading creating free bromide ions. Our attempts to clip **117** together using a simple ketone such as cyclohexanone to form a macrocycle were also

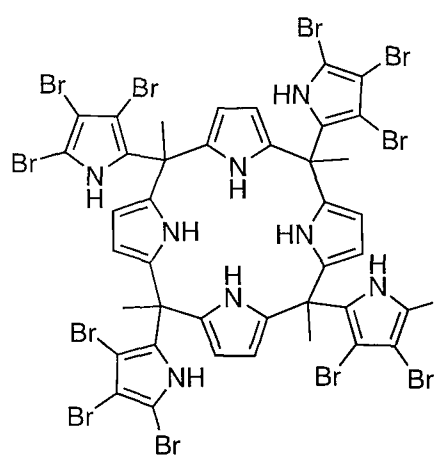

114

unsuccessful. This is probably due to steric interactions between the *meso*-substituents, as the pyrrolic ketone is clearly reacting with pyrrole under these conditions.

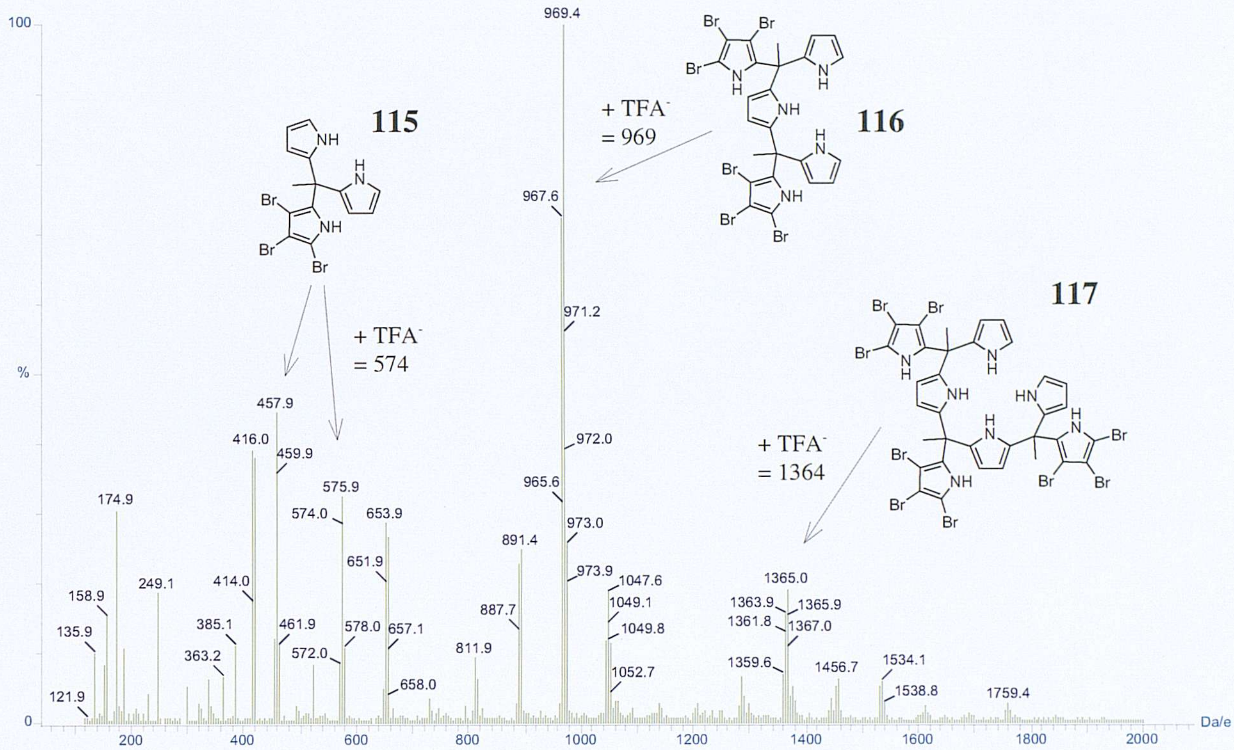

Figure 2.12: A negative electrospray mass spectrum of the reaction between pyrrole and **113** indicating the formation of oligomeric condensation products **115**, **116** and **117**.

We were successful in synthesising trispyrrolylmethane **115** from the 2-acetyl-3,4,5-bromopyrrole (Scheme 2.5). Pyrrole was used in large excess as co-solvent with methanol 1:2 ratio respectively and then heated to 80°C, methanesulfonic acid catalyst was added and the reaction stirred for half an hour prior to the work up procedure to give the final product in 27% yield. An analytically pure sample was obtained by column chromatography on silica gel eluting with dichloromethane. Crystals of **115** that were suitable for X-ray analysis were obtained from a chloroform solution of the receptor (Figure 2.13).

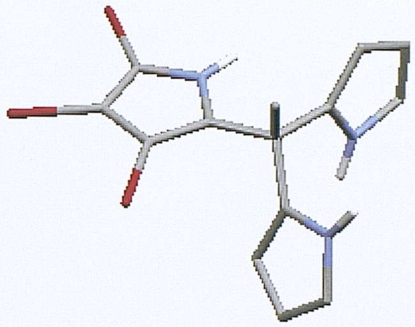

Figure 2.13: Crystal structure of compound **115**.

Colourless needles of compound **115**, suitable for X-ray crystallographic analysis, were obtained from slow evaporation of a chloroform solution of the receptor. The elucidation of this structure was useful in confirming the successful synthesis of the trispyrrolylmethane fragment **115**. This was an inspiring result because we believed the condensation of this fragment with acetone and pyrrole would be facile in comparison to the synthesis of **115**.

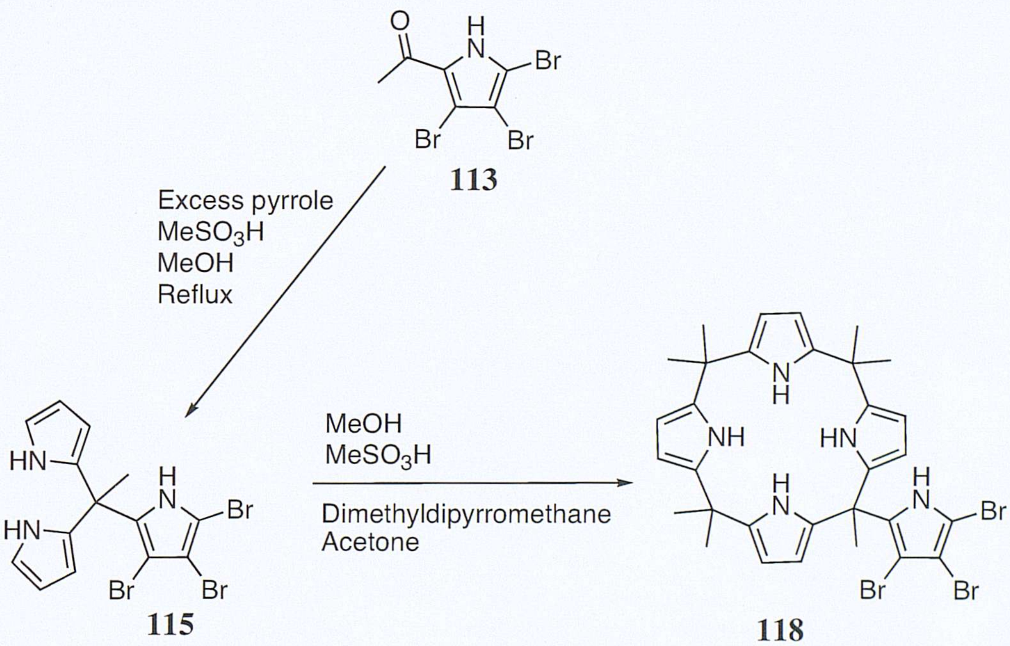

Scheme 2.5: Synthesis of a pentapyrrolic calix[4]pyrrole **118** using a tripyrrolylmethane intermediate **115**.

The methanesulfonic acid catalysed condensation of **115** with dimethyldipyrromethane and acetone in methanol (Scheme 2.5) gave pentapyrrolic calix[4]pyrrole[133] **118**. Purification of the crude product was achieved on silica gel eluting with dichloromethane, affording the mono-pyrrole pendant arm macrocycle in 14% overall yield. A sample of the reaction mixture was subjected to high resolution positive electrospray mass spectrometry analysis revealing a peak that corresponded to the expected value for $(M+H)^+$. The experimental value was at 714.0429 Da/e while the predicted peak for $C_{31}H_{35}Br_3N_5$ was 714.0436 (a 1.1 ppm error). Elemental bromine occurs as a mixture of isotopes, with ^{79}Br and ^{81}Br isotopes having natural abundances of 50.7 and 49.3% respectively. This creates an isotope pattern derived from the different mass combinations that can be obtained. The total number of combinations arising from three bromine atoms is eight; some of the combinations correspond to the same mass value giving different peak intensities in a ratio of 1:3:3:1, this allows us to predict a profile of the expected signal (Figure 2.14) the smaller satellite peaks arise from the ^{13}C isotope that occurs in 1.1% natural abundance (hydrogen and nitrogen isotopes have negligible contribution). This provides further evidence and in conjunction with other data gives proof for the successful synthesis of compound **118**.

Following this, we attempted to produce hexapyrrolic calix[4]pyrrole **119** that contained two pendant arm pyrrole groups on the same face of the macrocycle. In order to achieve this we tried co-condensing compound **115** with acetone using trifluoroacetic acid a reaction catalyst (this would produce two isomers). A sample of the reaction mixture was subjected to negative electrospray mass spectrometry, the spectrum revealed a peak at 1117 Da/e that corresponds to the expected value for $(M+TFA)^-$. Although this provided evidence for the formation of **119** we were unable to isolate a pure sample of this product. The formation of **118** was also evident in the reaction mixture as the predominant product. Even though very unlikely, it may be possible that some pyrrole

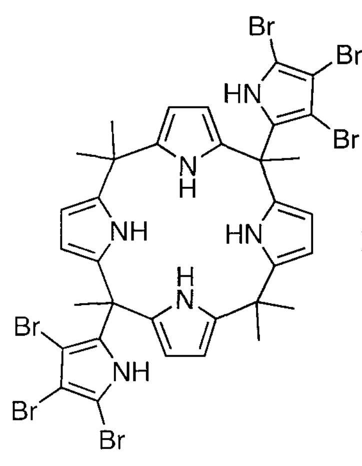

119

impurity was introduced to the reaction vessel. Compound **115** was purified before use and great care was taken to ensure that no unwanted pyrrole impurity was present. Negative electrospray mass spectrometry reveals a 2:1 ratio of **118** to **119**, and although it is possible that compound **119** doesn't ionise as easily as **118** the signal corresponding to **118** is sufficiently strong to support this idea (there was no indication a multiply charged **119** species). Sessler and co-workers have reported that even under mild conditions higher order calixpyrroles formed by the condensation reaction of pyrrole with acetone form a fast equilibrium in favour of the calix[4]pyrrole product,[65] indicating that bond cleavage and formation at the *meso*-position is possible.

Sessler and co-workers treated *meso*-octamethylcalix[4]pyrrole **68** with *N*-bromosuccinimide in tetrahydrofuran solution to obtain β-octabromo-*meso*-octamethylcalix[4]pyrrole **73** in 90% yield.[64] This receptor showed an enhanced affinity for anions over the parent macrocycle **68**. For this reason we reacted **118** under similar conditions using an excess of NBS to attempt to form a pentapyrrolic calix[4]pyrrole with fully brominated pyrrole subunits **120**. Negative electrospray mass spectrometry provided evidence supporting the formation of the fully brominated species (with some other partially substituted impurities). Peaks corresponding to both M^- and $(M+Cl)^-$, 1346 and 1381 Da/e respectively were observed. However, as with the other derivatives that we have attempted to synthesise, we were unable to obtain a pure sample.

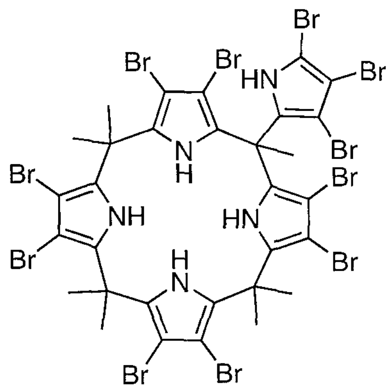

120

2.3.3 Co-ordination studies

The anion co-ordination chemistry of pentapyrrolic calix[4]pyrrole **118** was studied using ^{1}H NMR titration techniques. These experiments indicate a 1:1 receptor:anion stoichiometry of the complexes formed in solution, in addition to the association constants for the binding process.

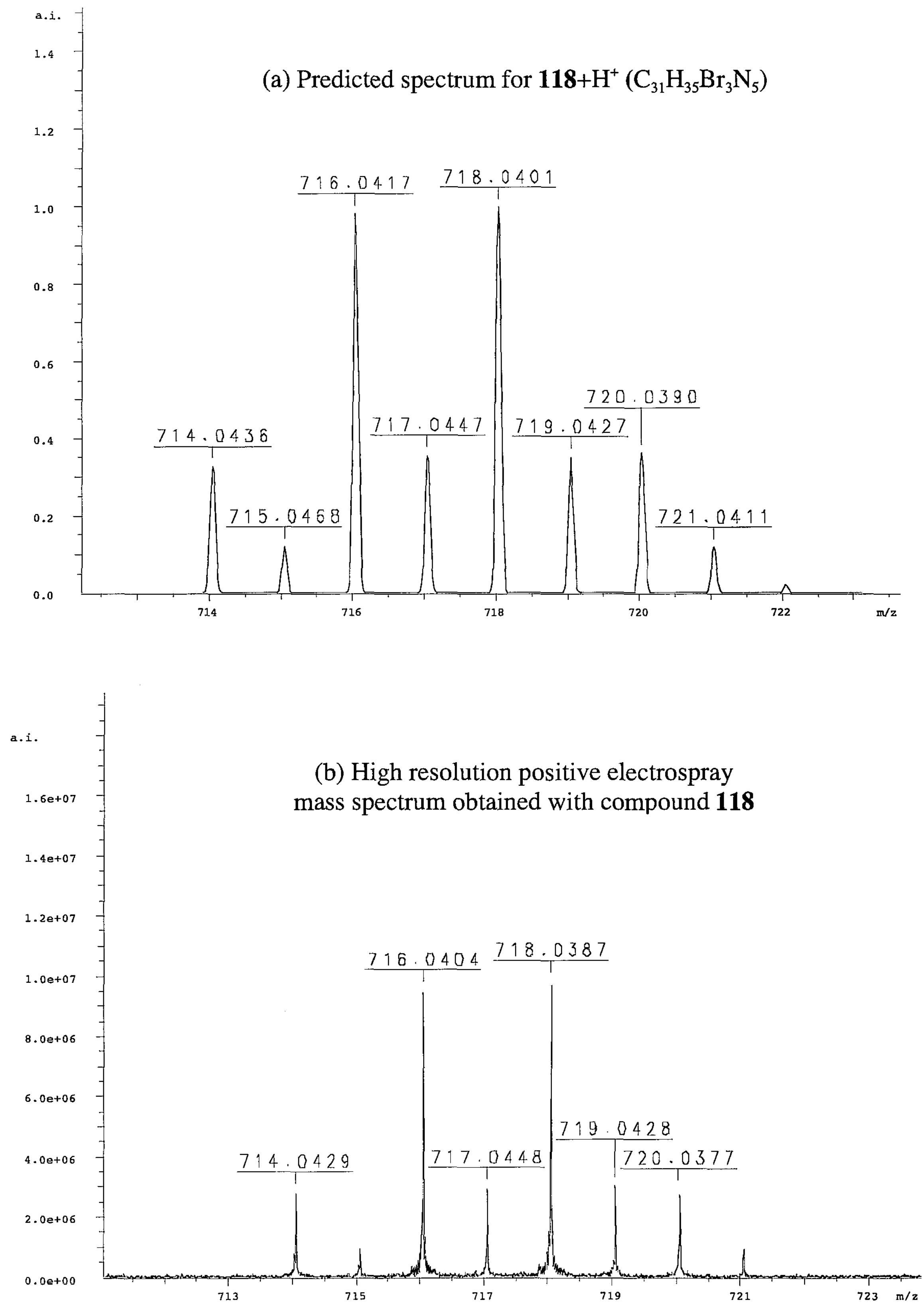

Figure 2.14: Predicted (a) and experimental (b) positive electrospray mass spectrometry for compound **118**. There is clearly a very good agreement between experimental data and theoretical prediction, confirming the presence of three bromine atoms.

2.3.3.1 Binding study results. High affinity and selectivity for carboxylates

We decided to conduct our titration experiments under the same conditions that were originally used to obtain the association constants of **68** with anions (i.e. in dichloromethane-d_2) in order to draw direct comparisons between the data. Therefore ^{1}H NMR titrations with compound **118** were conducted in dichloromethane-d_2 solution with anions added as their tetrabutylammonium salts, the results were compared to those formerly obtained for the parent macrocycle **68** (Table 2.3). The ^{1}H NMR spectrum of **118** shows three discrete pyrrole NH proton resonances; the pendant pyrrole NH (**a**) and two inequivalent calixpyrrole NH groups (**b** (upfield calixpyrrole NH) and **c** (down field calixpyrrole NH)). All three of the pyrrolic resonances were followed where possible during the titrations, the results obtained from each proton were consistent giving similar values for the association constant. All of the NH resonances of compound **118** broadened upon addition of tetrabutylammonium fluoride to a solution of the receptor, for this reason the association constant with this anion was not determined and hence not reported.

	68 K_a (M^{-1})	**118** K_a (M^{-1})		
Anion		**a**	**b**	**c**
Chloride	350*	740	1042	1031
Bromide	10*	36	27	27
Dihydrogen phosphate	97*	br.#	116	183
Hydrogen sulfate	<10*	28	26	15
Benzoate	196	br.#	> 10^4	> 10^4
Acetate	668	br.#	> 10^4	> 10^4

Table 2.3: The stability constants for *meso*-octamethylcalix[4]pyrrole **68** and pentapyrrolic calix[4]pyrrole **118** determined in dichloromethane solution at 298K. The letters **a, b** and **c** denote the three different pyrrolic sites present in compound **118**. * Data from reference 57. # The tribromopyrrole NH proton resonance broadened during the titration and could not be followed.

The data clearly shows the pentapyrrolic derivative **118** has an increased affinity for anions relative to the parent macrocycle **68**. The new receptor has a modest but notable increase in binding affinity for the halides, and tetrahedral anions such as dihydrogen phosphate or hydrogen sulfate with respect to **68**. The somewhat unexpected result was the two orders of magnitude increase in carboxylate binding shown by **118** for benzoate and acetate as compared to **68**. To illustrate the radical difference in complexation the standardized ^{1}H NMR titration curves of compounds **68** and **118** with benzoate are shown in figure 2.15.

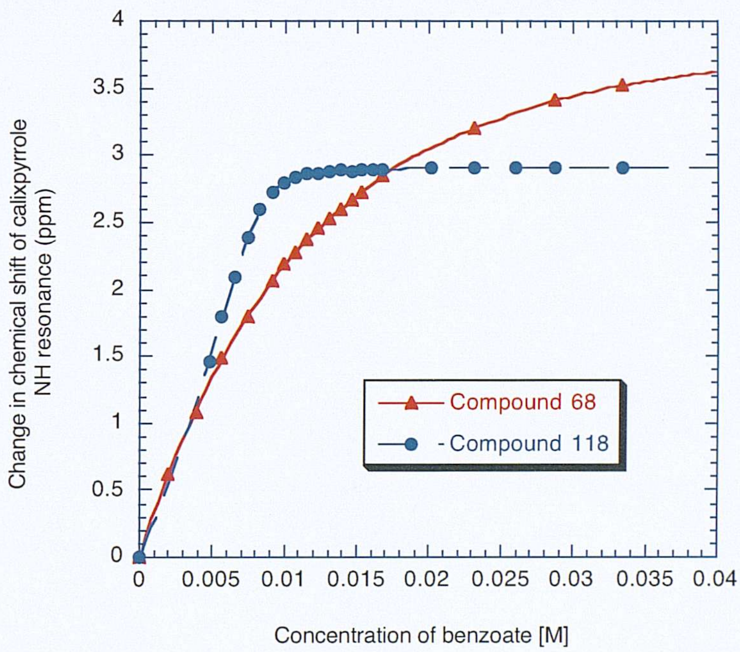

Figure 2.15: Standardized ^{1}H NMR titration plot of calix[4]pyrrole NH resonance for compounds **68** and **118** upon addition tetrabutylammonium benzoate in dichloromethane-d_2.

The titration profile with *meso*-octamethylcalixpyrrole **68** is a gradual curve with no plateau region at the end of the titration (typical of weak binding), while in contrast the profile seen with the new receptor **118** shows an almost linear shift in the resonance up to the addition of one equivalent of benzoate, after which a clearly defined plateau region is observed. In order to explain further it is important to point out that the binding of anions is a dynamic process in solution, the NMR resonance seen is an average of co-ordinated and non co-ordinated host species. If a guest is strongly bound then the host becomes essentially saturated and the average signal seen in the NMR spectrum will be weighted more to the co-ordinated host resonance. In the presence of excess guest species the host is already saturated and a plateau is seen as no further shift can be perturbed.

We questioned the unexpectedly high association constants obtained with both acetate and benzoate anions, there was a possibility that the tribromopyrrole ring of receptor **118** was being deprotonated that would render the values useless. Gale and co-workers have observed this deprotonation phenomenon with other pyrrole derivatives that have a chlorinated backbone. In dichloromethane-d_2 solution these compounds gave unusual titration profiles, although they gave elegant structures in the solid state.[67,68] Analysis of the titration curves for **118** with carboxylates reveal the plateau region is reached after the addition of one equivalent of the anion. If a deprotonation process was occurring in solution then after the addition of excess benzoate or acetate one would expect the species in solution to be identical. It would therefore be reasonable to expect the two calix[4]pyrrole NH protons from the separate titrations to resonate at identical chemical shifts. The NH resonances of receptor **118** upon addition of benzoate form plateau regions at 11.37 and 10.02 ppm, while the resonance shifts are complete at 11.15 and 10.47 ppm after addition of acetate. The non-recurrence of the values suggests that the species in solution are unique, and are hence the benzoate and acetate complexes respectively. Further evidence to suggest the formation of individual complexes was given by negative electrospray mass spectrometry. Acetonitrile solutions of **118** with three equivalents of tetrabutylammonium benzoate or acetate were ionised, the peaks (**118**+benzoate)$^-$ 834, and (**118**+acetate)$^-$ 774 Da/e that are concordant with the formation of the carboxylate complexes were observed.

2.3.3.2 Modelling studies

Molecular modelling was used to investigate the affinity displayed by compound **118** for carboxylates. The modelling work was conducted at the University of Southampton by Professor R. J. Whitby.

Using Spartan[134] a range of possible minimum energy conformations were generated. The program rejects any duplicates and non-favourable conformations using a molecular mechanics forcefield to leave the minimum energy structures. The data set was analysed with the semi-empirical methods AM1 and PM3, with both methods indicating that the acetate complex of **118** was more stable than the acetate complex of *meso*-octamethylcalixpyrrole **68** by 6.196 and 8.256 kcal/mol respectively. The AM1 minimum energy conformation reveals that acetate is bound by all five pyrrole NH bond donors. While a partial cone type conformation was calculated using PM3, forming only four hydrogen bonds from the receptor to the guest, with one pyrrole group pointing away from the bound anion (Figure 2.16). Interestingly the conformation found with PM3 is more stable than that found by AM1 by 2.096 kcal/mol. These preliminary modelling studies give an insight to the co-ordination properties of compound **118**, with both minimum energy structures indicating that the receptor employs a hydrogen bond from the pendant pyrrole arm to bind anions. The increased affinity for anions relative to **68** may be a direct result of introducing an extra hydrogen bond donor, or more subtle effects such as increased acidity of one pyrrole donor or the slightly different geometrical arrangement of donors within the calix[4]pyrrole may account for the improvement.

(a) (b)

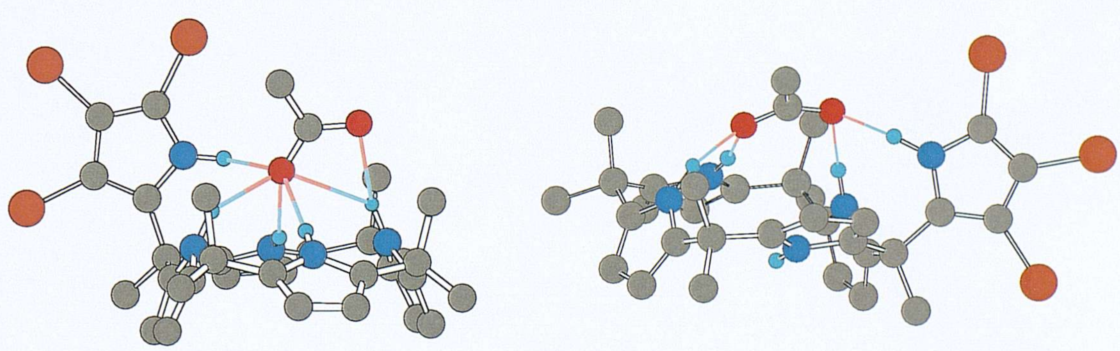

Figure 2.16: The lowest energy conformation of **118**-acetate found by AM1 (a) and PM3 (b) energy minimalisation methods.

2.4 Conclusion

Three calix[4]pyrrole derivatives have been synthesised that bear either a ferrocene (e.g. **110-111**) or pyrrolic (e.g. **118**) moiety at the *meso*-position. The anion co-ordination properties of these receptors have been investigated using ^{1}H NMR titration techniques with all of the receptor:anion complexes fitting a 1:1 binding model.

The NMR studies on the ferrocene derivatives were conducted in deuterated acetonitrile/dimethyl sulfoxide (9:1) solution revealing that these receptors can bind a variety of anions. Further investigation of the data provided support for a direct co-ordination mechanism involving a ferrocene cyclopentadienyl group forming a CH hydrogen bond to the bound anion.

Electrochemical studies using SWV and CV revealed compound **110** functions as an electrochemical sensor for anions, displaying cathodic shifts of up to 76 and 100 mV with fluoride and dihydrogen phosphate anions respectively.

We introduced a pyrrole group at the *meso*-position to form a pentapyrrolic calix[4]pyrrole, thus increasing the number of hydrogen bond donors without increasing the macrocycle ring size. This receptor showed an enhanced affinity for all anions studied, over the parent macrocycle, *meso*-octamethylcalix[4]pyrrole in dichloromethane-d_2 solution. The unexpected affinity of **118** for carboxylates could be explained by the receptor co-ordinating both atoms of the carboxylate anion simultaneously.

In conclusion, mono *meso*-substituted calixpyrroles can be used to electrochemically sense anions, in addition they have been shown to form very strong and selective complexes with carboxylate anions.

3. *Heterocyclic amide clefts*

3.1 Introduction

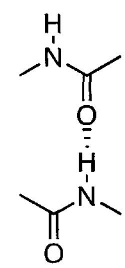

Figure 3.1: Amides can self-associate via hydrogen-bond formation.

The amide group has been incorporated into a diverse selection of anion receptors.[26] The presence of both a hydrogen bond donor and acceptor within the amide group can result in self-assembly processes occurring either in solution or in the solid state (Figure 3.1). The analogous thioamide functional group has been shown to form stronger hydrogen bonds than it's amide counterpart[27] and yet is a worse hydrogen bond acceptor,[27,135,136] lowering the probability of self association. We can therefore predict that thioamide receptors, when compared to their oxoamide derivatives, will form stronger complexes with anions. This is due to an enhanced NH acidity, attributed to the increased polarizability of the sulfur with a concomitant decrease in the NH bond energy (~10 kcal mol^{-1}).[137,138]

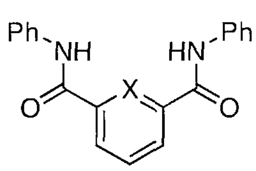

6 X = CH
121 X = N

In 1997 Crabtree and co-workers reported an acyclic cleft receptor **6**, the receptor employed two amide groups to co-ordinate anions. This simple receptor formed very strong complexes in organic solvent with the smaller halide anions.[29] Two years later[60] they reported that an analogous pyridine bis-amide derivative **121** displayed an increased selectivity for smaller anions. The pyridine based receptor contains a nitrogen lone pair in close proximity to the anion binding site. The lone pair introduces both steric and electrostatic repulsive interactions with the anion upon co-ordination with this effect being most pronounced for the larger anions. As previously mentioned in the introduction, Gale and co-workers have shown that 2,5-diamido-3,4-dichloropyrroles are deprotonated by basic anions such as fluoride and form unusual interlocked anionic dimers both in solution and in the solid state.[67]

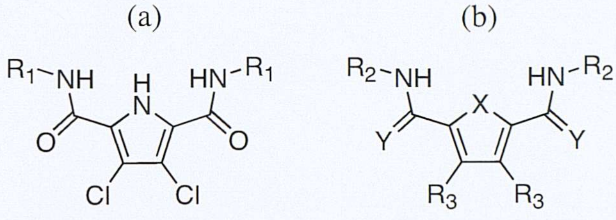

63 R_1 = n-Bu
64 R_1 = Ph

124 X = Y = O, R_2 = Bu, R_3 = Ph
125 X = Y = O, R_2 = R_3 = Ph
126 X = O, Y = S, R_2 = Bu, R_3 = Ph
127 X = O, Y = S, R_2 = R_3 = Ph
130 X = S, Y = O, R_2 = Bu, R_3 = H
131 X = S, Y = O, R_2 = Ph, R_3 = H
132 X = Y = S, R_2 = Bu, R_3 = H
133 X = Y = S, R_2 = Ph, R_3 = H

Figure 3.2: 2,5-Diamido-3,4-dichloropyrroles (a) can self assemble when deprotonated (see figure 1.12), generic structure of heterocyclic amide/thioamide derivatives (b) that will be synthesised to investigate their anion receptor and potential self-assembly properties.

We were interested in determining whether we could replicate the same self-assembly process using neutral building blocks. To achieve this goal we decided to synthesise a variety of heterocyclic 2,5-diamides and thioamide clefts (Figure 3.2). The introduction of a heteroatom may allow dimer formation through amide NH···heteroatom hydrogen bonds (Figure 3.3). The anion binding properties of these receptors was investigated using ^{1}H NMR titration techniques, with the possible self assembly process predominantly being investigated using X-ray crystallographic analysis.

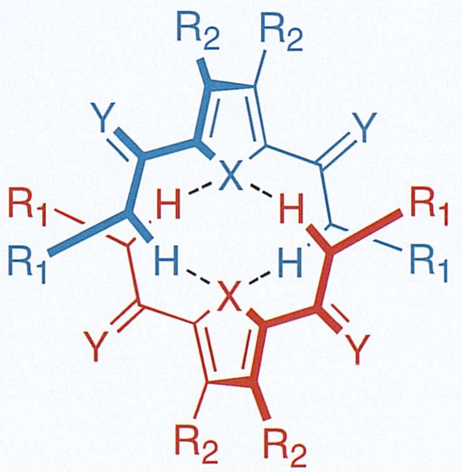

124 X = Y = O, R_1 = Bu, R_2 = Ph
125 X = Y = O, R_1 = R_2 = Ph
126 X = O, Y = S, R_1 = Bu, R_2 = Ph
127 X = O, Y = S, R_1 = R_2 = Ph
130 X = S, Y = O, R_1 = Bu, R_2 = H
131 X = S, Y = O, R_1 = Ph, R_2 = H
132 X = Y = S, R_1 = Bu, R_2 = H
133 X = Y = S, R_1 = Ph, R_2 = H

Figure 3.3: The proposed dimer complex that compounds **124-133** could potentially form in the solution phase and/or the solid state, via NH···heteroatom hydrogen bonds.

3.2 3,4-diphenyl-furan-2,5-diamide/dithioamide clefts.

3.2.1 Synthesis and characterisation

Two new furan diamide clefts **124** and **125**[139] have been synthesised (Scheme 3.1). 3,4-Diphenylfuran-2,5-dicarboxylic acid **122** was prepared following a literature procedure,[140] and was converted to the bis-acid chloride **123** by refluxing overnight in thionyl chloride. Reacting **123** with a slight excess of either *n*-butylamine or aniline in the presence of DMAP and triethylamine afforded the desired products **124** and **125** in 53 and 80% yields respectively.

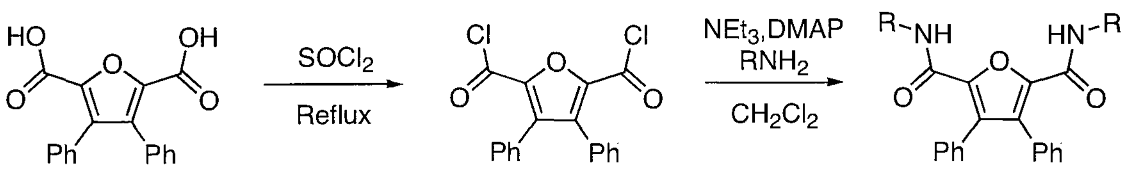

122 **123** **124** R = n-Bu
125 R = Ph

Scheme 3.1: The synthesis of furan-diamide receptors **124** and **125**.

The furan dithioamide clefts **126** and **127** have been prepared by converting the previously synthesised furan amide derivatives **124** and **125** (Scheme 3.2). The amide derivatives were dissolved in tetrahydrofuran solvent and refluxed with a slight excess of Lawessons reagent[141] (2,4-bis(4-methoxyphenyl)-1,3-dithia-2,4-diphosphetane-2,4-disulfide see scheme 3.2) for 24 hours. The resulting solids were purified using column chromatography on silica gel eluting with dichloromethane/methanol (98:2) solution. The products **126** and **127** were crystallised from acetonitrile solutions in 80 and 78% yield respectively.

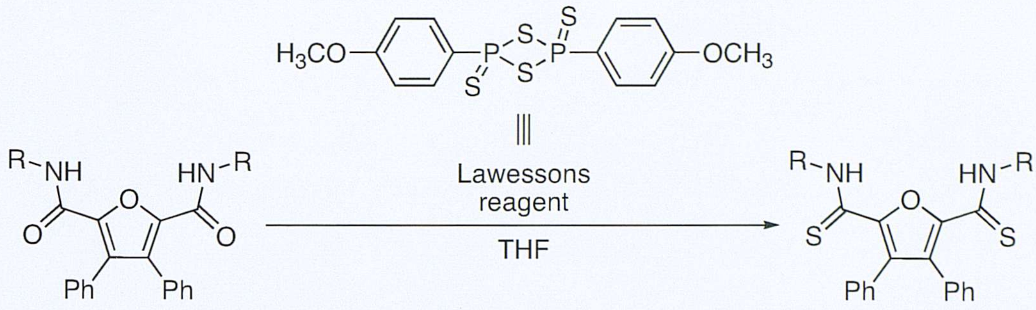

126 R = n-Bu
127 R = Ph

Scheme 3.2: Synthesis of compounds **126** and **127**.

We obtained crystals of the butylamide derivative **124** from two different solvent systems, elucidation of the structures revealed that they were polymorphs. The first crystal was collected from a diethyl-ether (Figure 3.4(a)) solution whilst the second crystallised from a mixture of ether:acetonitrile:dimethyl sulfoxide solvents in a 2:2:1 ratio (Figure 3.4(b)). Although both structures reveal the receptor assuming a cleft type conformation, the structure shown in figure 3.4(a) reveals the amide moieties deviate from the furan plane by 23.4 and 22.5° with the amide groups orientated to opposite sides of the central furan ring. Whilst the structure in figure 3.4(b) shows the amide groups pointing to the same side of the molecule with deviations of 19.2 and 17.9° from the furan plane. This variation between the structures has led to very different hydrogen bonding arrays in the extended crystal lattices (Figure 3.5).

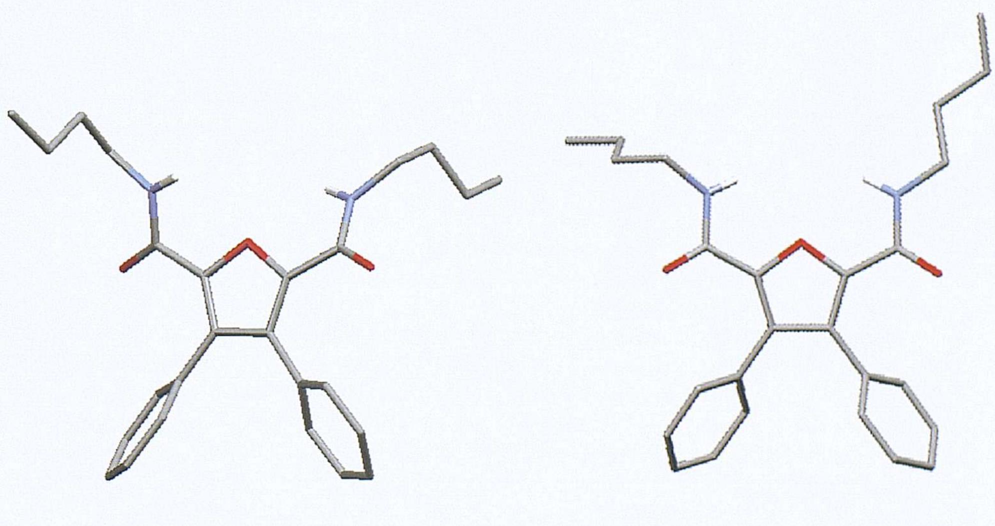

(a) (b)

Figure 3.4: The crystal structures of compound **124** obtained from diethylether (a) and ether:acetonitrile:dimethyl sulfoxide (2:2:1) (b) solutions.

In the case of the crystal obtained from ether (Figure 3.5(a)) the molecules form infinite chains along the a axis via NH···O hydrogen bond linkages with N···O distances of 2.953(1) (N2-O2) and 2.956(2)Å (N1-O3), the adjacent furan rings adopt alternating orientations. The other structure (Figure 3.5(b)) shows the receptor forming a helical chain along the c-axis, completing a rotational turn every 30.27Å. Each molecule forms two NH···O hydrogen bonds (N···O distances of 3.108(4) (N1-O3) and 3.090(3)Å (N2-O3)) to only one of the two carbonyl groups present on the next molecule, the helix is formed by the molecules rotating about a central axis by 60 degrees with every step along the chain (see Appendix for structural information).

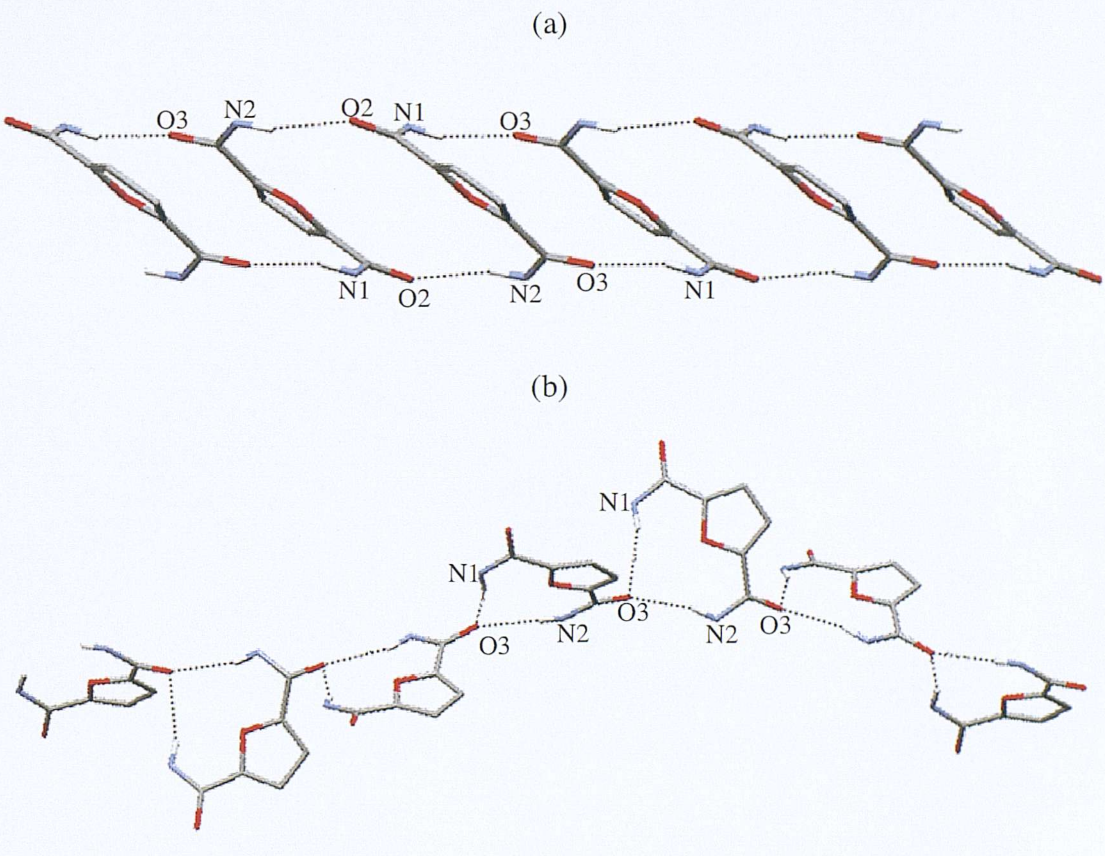

Figure 3.5: The crystal structures of compound **124** obtained from diethylether (a) and ether:acetonitrile:dimethyl sulfoxide (2:2:1) (b) solutions revealing different hydrogen bond arrays. Butyl chains, phenyl groups and hydrogen atoms not involved in hydrogen bonding have been removed for clarity.

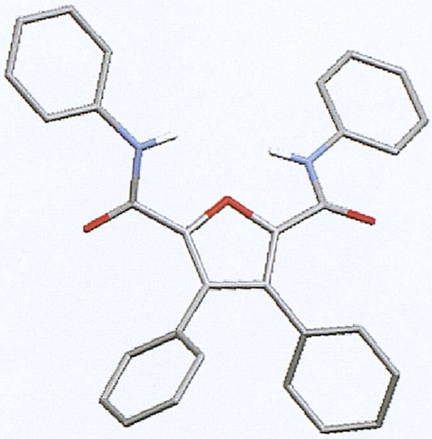

Figure 3.6: Crystal structure of Compound **125**

Crystals of compound **125** suitable for single crystal X-ray diffraction analysis were obtained by slow evaporation of an acetonitrile solution of the receptor. As seen previously for the butyl derivative, the free receptor adopts a cleft conformation in the solid state (Figure 3.6) the amide moieties point to opposite sides of the central furan ring, deviating from this ring plane by 26.8 and 20.6°. The hydrogen bond array shown in figure 3.7 is similar to that seen with **124** when crystallised from diethylether (Figure 3.5(a)). The molecules form chains along the a axis via NH···O hydrogen bond linkages, again the adjacent furan rings adopt alternating orientations. Except in this case there are two unique hydrogen bonds operating as independent pairs; the shorter pair (N···O, 3.008(2)Å (N2-O1)) link the molecules into centrosymmetric dimers and the longer pair (N···O, 3.248(2)Å (N1-O3)) connect the dimers into chains (see Appendix for structural information).

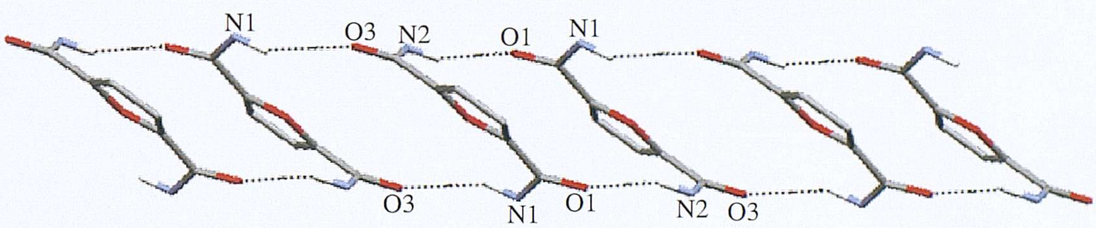

Figure 3.7: The hydrogen bonding array present in the solid state structure of compound **125**. Phenyl rings and hydrogen atoms not involved in hydrogen bonding have been removed for clarity.

Crystals of compounds **126** and **127** were both obtained by evaporation of acetonitrile solutions of the receptors. Compound **126** crystallised with the thioamide groups in an 'anti-anti' conformation while **127** adopted a cleft type conformation (Figure 3.8) (see Appendix for structural information).

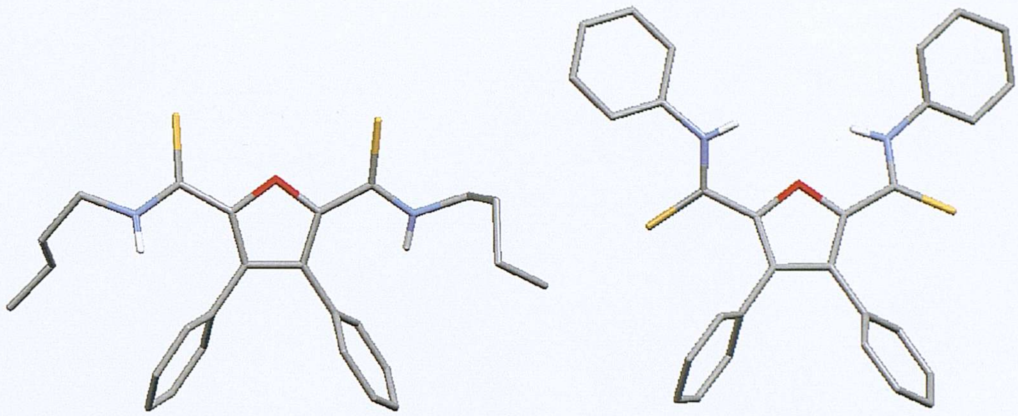

(a) (b)

Figure 3.8: The crystal structures of compounds **126** (a) and **127** (b). Some hydrogen atoms have been removed for clarity.

There was no hydrogen bonding observed in the extended structure of **126** presumably because the amide NH donors are unable to form hydrogen bonds due to the steric limitations introduced by the phenyl rings. However in the case of **127** the molecules form dimers (Figure 3.9) through two NH···S hydrogen bonds (N···S distance of 3.469(7)Å (N2-S1)) one from each receptor, the amide involved in this interaction shows a deviation from the furan plane of 18.0°. The other thioamide NH donor has a dihedral angle of 30.7° with the furan ring and is involved in hydrogen bonding to an acetonitrile molecule via NH···N hydrogen bonds (N···N distance of 3.063(5)Å (N1-N3)) (see Appendix for structural information).

The furan receptors have revealed interesting hydrogen bonding interactions in the solid state and for this reason we wished to discover whether any self association processes would occur in solution. Dilutions studies on compounds **124** and **125** were conducted in dimethyl sulfoxide-d_6/0.5% water solution, however, no perturbation of the amide resonances were observed. In dichloromethane-d_2 the amide NH resonance of the butyl derivative **124** shifts by 0.26 ppm (6.14 to 6.40 ppm) in a concentration range of 2 to 56 mM. Elaboration of the dilution curve using software provided by Professor C. A. Hunter[142] (NMRDILL_Dimer) showed that the compound appears to dimerise in solution albeit weakly with a dimerisation constant of only 1.7 M^{-1}.

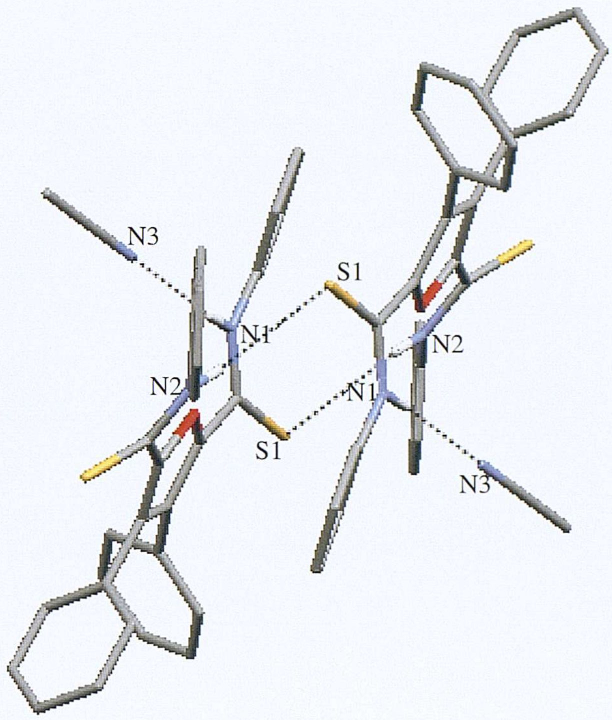

Figure 3.9: The 2:2 complex formed between **127** and acetonitrile in the solid state.

3.2.2 Binding study results. Selectivity for fluoride

Anion binding studies of the receptors **124**-**127** were carried out in dimethyl sulfoxide-d_6/0.5% water solution with the results summarised in table 3.1. Titrations with hydrogen sulfate and bromide anions were conducted but the data has been omitted as no binding was observed. Some evidence for hydrogen sulfate binding was shown by receptors **125** and **126** although the values were below 20 M^{-1} with very large errors. The results reveal that the both of the oxoamide derivatives are selective for fluoride, this is in contradistinction to the previously reported 2,5-diamidopyrroles that showed selectivity for oxo-anions.[61] The selectivity for oxo-anions by the pyrrolic systems **59** and **60** is believed to be due to the formation of three hydrogen bonds to the anion.[63] The substitution of pyrrole for the furan heterocycle at the core of the receptor has replaced an NH bond donor for an oxygen atom. The introduction of oxygen has not only reduced the number of hydrogen bond donors but may have also introduced a repulsive electrostatic effect upon anion binding. It seems reasonable to assume that larger anions would feel this repulsive effect more greatly and hence have a larger effect on binding than for their smaller counterparts.

	Association constants K_a (M^{-1})			
Anion	Receptor **124**	Receptor **125**	Receptor **126**	Receptor **127**
Fluoride	557	1140	*	*
Chloride	14	47	23	20
Dihydrogen phosphate	46	78	176	*
Benzoate	28	49	68	*

Table 3.1: Calculated association constants for compounds **124** - **127** (using NH resonance NMR shifts) in dimethyl sulfoxide-d_6/0.5% water solution at 298K. Anions added as their tetrabutylammonium salts. * Resonance broadened during titration.

The thioamide **126** shows an improvement in anion binding when compared to analogous oxoamide **124**. This receptor binds chloride, benzoate and dihydrogen phosphate anions more strongly, with the latter having the most notable improvement in binding affinity with an increase from 46 to 176 M^{-1}. The slight enhancement in anion binding is presumably a direct result of the increased acidity of the thioamide NH hydrogen bond donor, thus forming stronger complexes with anions. The increased acidity of the thioamide can also account for the broadening of the amide resonance seen in titrations with compound **127**.

3.3 Thiophene based receptors

3.3.1 Thiophene-2,5-diamide/thioamide clefts

3.3.1.1 Synthesis and characterisation

Two new thiophene-diamide clefts **130** and **131** have been synthesised[143] (Scheme 3.3). The commercially available thiophene-2,5-dicarboxylic acid **128** was converted to the bis-acid chloride **129** by refluxing overnight in thionyl chloride. Reacting **129** with a slight excess of either *n*-butylamine or aniline in the presence of DMAP and triethylamine, precipitated white solids that were washed with water and dichloromethane to afford the pure compounds **130** and **131** in 76 and 77% yields respectively.

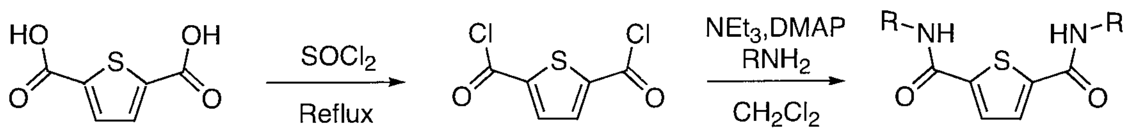

128 **129** **130** R = n-Bu
131 R = Ph

Scheme 3.3: Synthesis of compounds **130** and **131**.

The thiophene dithioamide clefts **132** and **133** have been prepared by converting the previously synthesised thiophene amide derivatives **130** and **131** (Scheme 3.4). The diamide cleft **130** was dissolved in tetrahydrofuran solvent and refluxed with 1.3 equivalents of Lawessons reagent for 24 hours, purification was achieved by crystallisation from dichloromethane solution yielding compound **132** in 84% yield. The diphenylamide **131** needed more forcing conditions to convert it to the thioamide analogue **133** requiring 4.3 equivalents of Lawessons reagent and refluxing for 72 hours. Removal of the solvent *in vacuo* gave a crude solid that was purified by precipitation from hot acetonitrile solution affording the product in 74% yield.

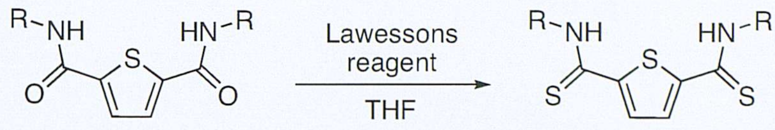

132 R = n-Bu
133 R = Ph

Scheme 3.4: Synthesis of compounds **132** and **133**

Crystals of compound **130** were obtained from a methanol solution of the receptor by slow evaporation of the solvent. The crystal structure reveals four independent molecules in the asymmetric unit, with each one adopting an 'anti-anti' conformation (Figure 3.11). The receptor forms layers of hydrogen bonded sheets that alternate their direction and are perpendicular to the c axis. Each sheet contains two of the four independent molecules. The hydrogen bonds are formed between the amide NH and a carbonyl group of an adjacent molecule, all the amide groups involved in hydrogen bonding have N···O distances within the range of 2.839(9) (N5-O2) – 2.950(10) Å (N8-O3) (see Appendix for structure information).

Crystals of compound **131** were obtained from a dimethyl sulfoxide solution of the receptor. In this case the receptor adopts a similar conformation to that of **130** but crystallised with two molecules of hydrogen bonded solvent (Figure 3.10) (see Appendix for structural information).

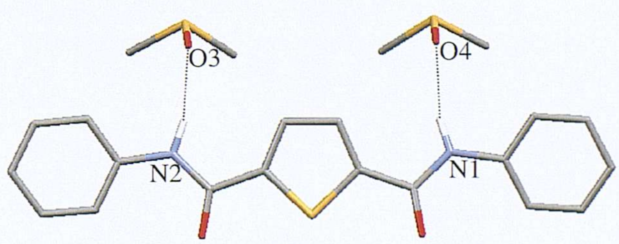

Figure 3.10: Crystal structure of compound **131** with N···O distances of 2.945(2) (N1-O4) and 2.907(2)Å (N2-O3). Hydrogens not involved in hydrogen bonding interactions have been removed for clarity.

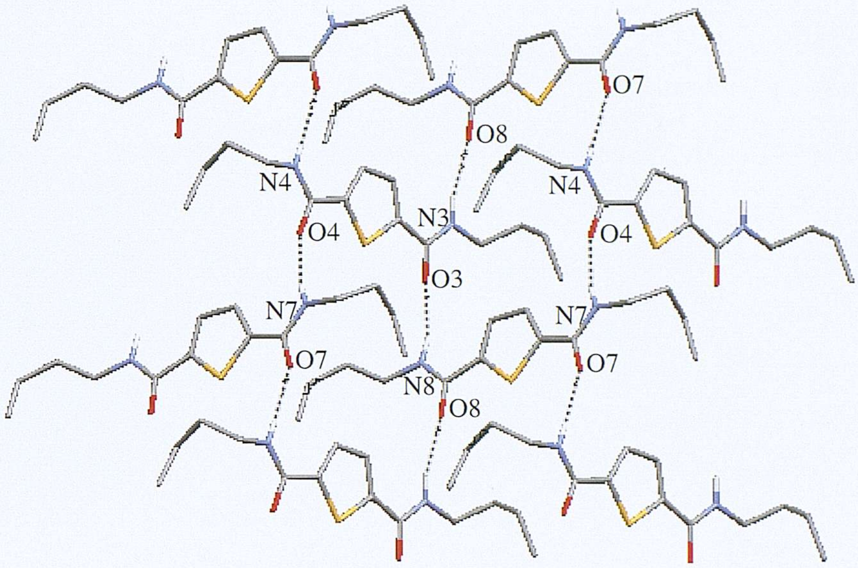

(a) Hydrogen bonded sheet *a* runs North-South in the ab plane

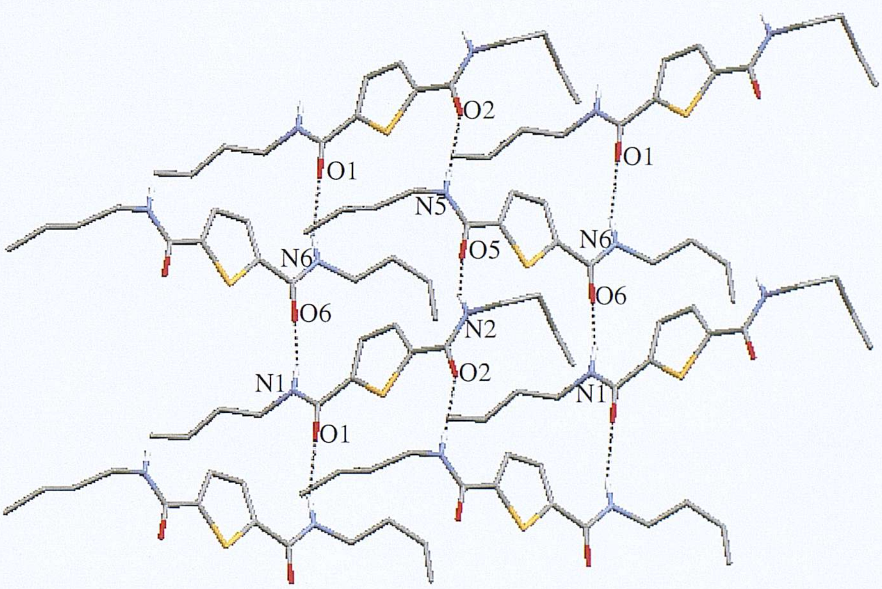

(b) Hydrogen bonded sheet *b* runs East-West in the ab plane

Figure 3.11: Compound **130** packs in alternating hydrogen bonded sheets. North-South in the ab plane (a) East-West in the ab plane (b) with an average N···O distance of 2.879(9)Å. Hydrogens not involved in hydrogen bonding interactions have been removed for clarity.

Although crystals of **132** were obtained from both dichloromethane and dimethyl sulfoxide solutions of the receptor, they were of insufficient quality to determine the structure. However crystallisation of **133** was achieved from a dimethyl sulfoxide solution of the receptor with the structure shown in figure 3.12. As seen with the amide derivative **131**, the thioamide analogue **133** adopts an 'anti-anti' conformation with two hydrogen bonded dimethyl sulfoxide molecules. One of the molecules is complexed by a single NH···O interaction (N···O distance 2.768(5)Å) while the other has both NH···O (N···O distance 2.868(6)Å) and NH···S (N···S distance 3.643(4)Å) hydrogen bonds (see Appendix for structural information). The shorter NH···O hydrogen bond lengths observed with **133** compared to those seen with **131** are consistent with the formation of stronger hydrogen bonds (in the solid state).

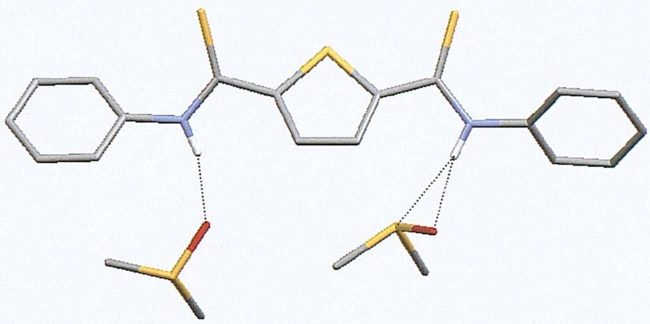

Figure 3.12: The crystal structure of compound **133** co-ordinating two molecules of dimethyl sulfoxide. Hydrogens not involved in hydrogen bonding interactions have been removed for clarity.

3.3.1.2 Binding studies. A colorimetric sensor for fluoride?

The association constants were obtained for compounds **130** to **133** with a variety of anionic guests (added as their tetrabutylammonium salts) in dimethyl sulfoxide-d_6/0.5% water solution using NMR titration techniques. The amide NH resonance was perturbed upon addition of anions and the data fitted using a 1:1 binding model. There were no significant shifts in the ^{1}H NMR titrations of bromide or hydrogen sulfate anions indicating that these guests are weakly bound, if at all by compounds **130-133**, under the experimental conditions.

	Association constants K_a (M^{-1})			
Anion	Receptor **130**	Receptor **131**	Receptor **132**	Receptor **133**
Fluoride	*	*	*	*
Chloride	<10	<10	<10	11
Dihydrogen phosphate	13	48	45	*
Benzoate	<10	23	24	*

Table 3.2: Calculated association constants for compounds **130** – **133** (using NH resonance NMR shifts) in dimethyl sulfoxide-d_6/0.5% water solution at 298K. Anions added as their tetrabutylammonium salts. * Resonance broadened during titration.

The results summarised in table 3.2 indicate that the thiophene receptors bind dihydrogen phosphate more strongly than chloride, bromide, hydrogen sulfate and benzoate anions. The butylthioamide **132** binds both dihydrogen phosphate and benzoate anions more strongly than its similar oxoamide **130**, in both cases the binding has more than doubled. The NH resonance for compound **133** broadened upon addition of both dihydrogen phosphate and benzoate anions, it was possible to follow the thiophene CH resonance although accurate values for the association constant were not obtained. Interestingly with these anions the thiophene proton of **133** observed an upfield shift, yet with all the other anions and receptors studied a downfield shift was observed in the ^1H NMR spectrum. The downfield shifting thiophene CH resonance allowed calculation of association constants that were in agreement with those obtained following the amide resonance.

The NH proton resonance broadened upon addition of tetrabutylammonium fluoride to solutions of the thiophene receptors **130-133**, while the thiophene CH protons remained sharp allowing them to be followed throughout the titrations. Using this method compound **130** could be fitted using a simple 1:1 host:guest binding model giving an association constant of 82 M^{-1}, while the data collected for **131-133** suggested that multiple equilibria processes were occurring in solution. The titration plots of chemical shift (of the thiophene resonance) against concentration of fluoride contained characteristic profiles that would not allow simple 1:1 or 2:1

fluoride:receptor binding models to be applied. In the case of compound **131** the thiophene resonance undergoes an initial downfield shift of around 0.3 ppm followed by a upfield shift after the addition around 1.3 equivalents of fluoride (Figure 3.13). It is quite possible that the receptor is forming both 1:1 and 2:1 complexes in solution although as yet we have been unable to fit the data using standard methods.

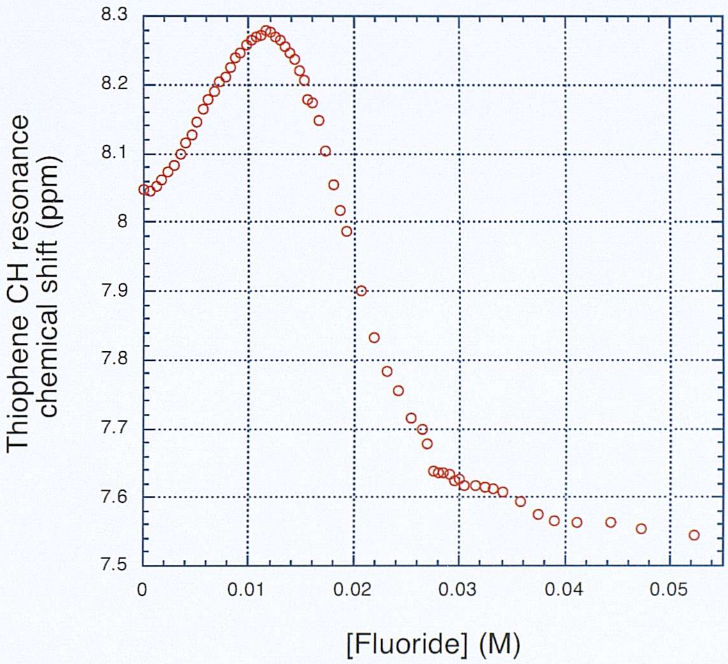

Figure 3.13: ^{1}H NMR titration curve of compound **131** with tetrabutylammonium fluoride in dimethyl sulfoxide-d_6/0.5% water solution following the thiophene CH resonance shift.

To study the species formed by **131** and fluoride in solution, we tried using Job's method of continuous variation to establish the stoichiometry of the complex.[119,144] Although the "Job plot" (Figure 3.14) shows a maximum corresponding to formation of a 1:1 species in solution, the profile also suggests that other processes may be simultaneously occurring (at lower molar ratios). For this reason we are unable to report the exclusive stoichiometry of binding.

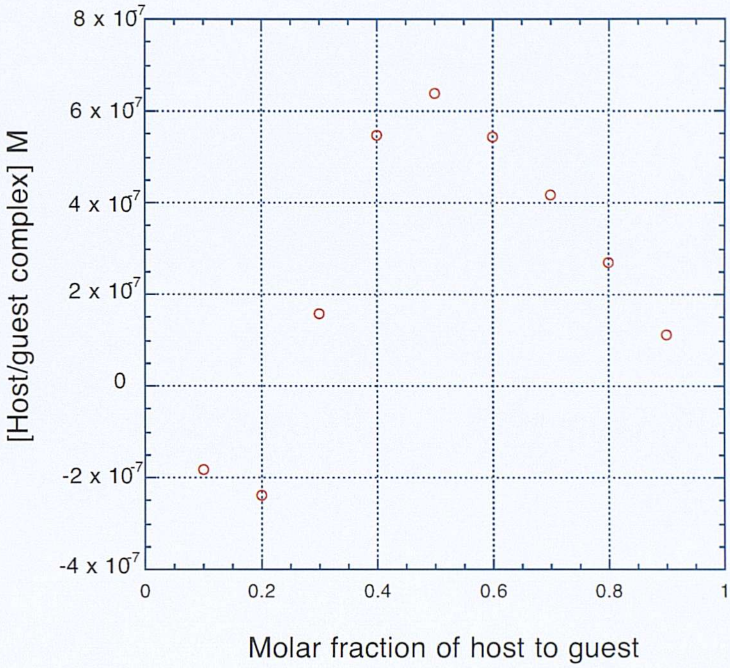

Figure 3.14: Job plot analysis of the **131**/fluoride system in dimethyl sulfoxide-d_6/0.5% water solution.

Addition of fluoride (and hydroxide, not shown) to compound **131** induces a dramatic colourless to yellow colour change (Figure 3.15), a much weaker yellow colour is observed upon addition of benzoate and dihydrogen phosphate anions. The thioamide derivative **133** is orange when in solution, addition of these anions makes the solution a paler yellow colour although the effect is not as noticeable, while the butyl derivatives **130** and **132** show no colour change at all. There are previous reports in the literature that observe a colour change upon addition of anions to aromatic compounds that contain hydrogen bond donors.[145] Inspired by this unexpected colour change we attempted to gain solution phase complexation information by UV/Vis titration. Unfortunately numerous attempts to obtain association constants or solution phase information by this method were unsuccessful. The absorbance spectrum of compound **131** with and without fluoride is shown in figure 3.16. The spectra of the free receptor shows a single peak at 317 nm, when the receptor is in the presence of ten equivalents of fluoride this peak disappears and two new peaks form at 286 nm and 371 nm.

Free receptor　F^-　Cl^-　Br^-　HSO_4^-　benzoate　$H_2PO_4^-$

Figure 3.15: Solutions of compound **131** (2mM) with 10 equivalents of tetrabutylammonium anion salt in dimethyl sulfoxide/0.5% water.

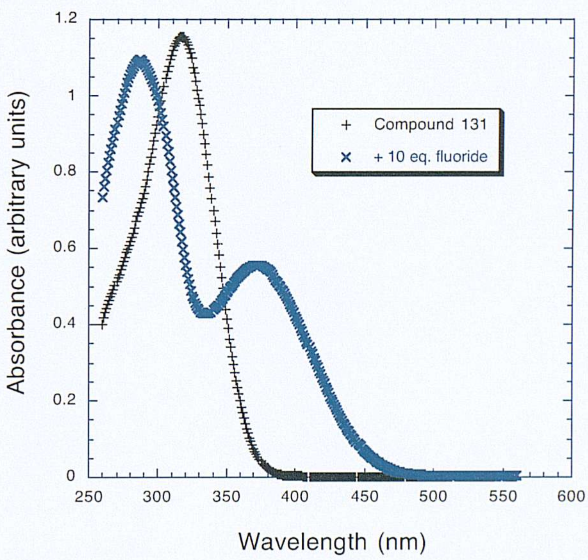

Figure 3.16: UV/Vis spectra of compound **131** (0.05mM) in dimethyl sulfoxide/0.5% water in the absence (black) and presence of 10 equivalents of fluoride (blue).

Crystals of the fluoride complex of **131** suitable for single crystal X-ray analysis were obtained by slow evaporation of a dichloromethane solution of the receptor in the presence of an excess of tetrabutylammonium fluoride. The 2:2 cyclic receptor:fluoride complex contains both NH···F^- (with N···F distances of 2.5903(16) (N1-F1) and 2.6187(16)Å (N2-F1) and N-H···F^- angles of 157.3 and 168.4°

respectively) and CH···F$^-$ (with C···F distances of 3.13(4) (C9-F1) and 3.05(4)Å (C10-F1) and C-H···F$^-$ angles of 140.6 and 148.5° respectively) hydrogen bonds in the solid state shown in figure 3.17 (see Appendix for structure information).

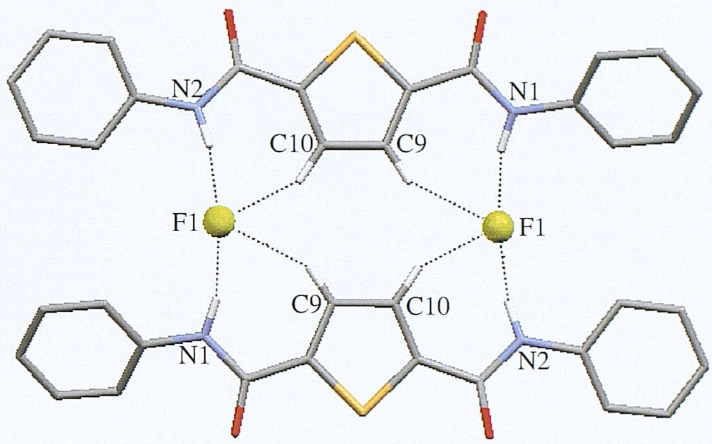

Figure 3.17: Crystal structure of the complex formed between **131** and fluoride. Tetrabutylammonium counter cations and non-acidic hydrogens have been omitted for clarity.

The crystal structure revealed that in the solid state fluoride is bound by **131** in a 2:2 complex, containing CH hydrogen bonds from the thiophene backbone to the fluoride anion indicating that these protons are acidic. As previously mentioned the thiophene proton resonance could be followed in the titrations of compounds **130-133** and apart from a couple of instances (compound **133** with benzoate and dihydrogen phosphate) a downfield shift of this resonance was observed, consistent with hydrogen bond formation in solution. We therefore decided to synthesise thiophene receptors that could utilise this hydrogen bond donor in conjunction with the both amide groups by producing 2,4-diamidothiophenes. Only the 2,4 diamidothiophenes will be synthesised, because the 2,5-thioamide derivatives of both thiophene and furan receptors have neither shown a large increase in affinity for anions over the corresponding amide, or provided the desired interlocked dimer motif in the solid state.

3.3.2 Thiophene-2,4-diamide clefts

3.3.2.1 Synthesis and characterisation

Two thiophene-2,4-diamide clefts **138** and **139** have been synthesised[143] in accordance to scheme 3.5. The commercially available 2,4-dibromothiophene **134** was reacted with copper-cyanide to form 2,4-dicyanothiophene **135** using an adapted literature preparation.[146] Following another literature method[147] this compound was converted to the thiophenedicarboxylic acid **136** by refluxing in concentrated hydrochloric acid for 6 hours. As previously described for the thiophene-2,5-diamide clefts, the final compounds were synthesised by conversion of the dicarboxylic acid to the bis-acid chloride **137** and then coupling to either *n*-butylamine or aniline to give **138** and **139** in 46 and 59% yields respectively.

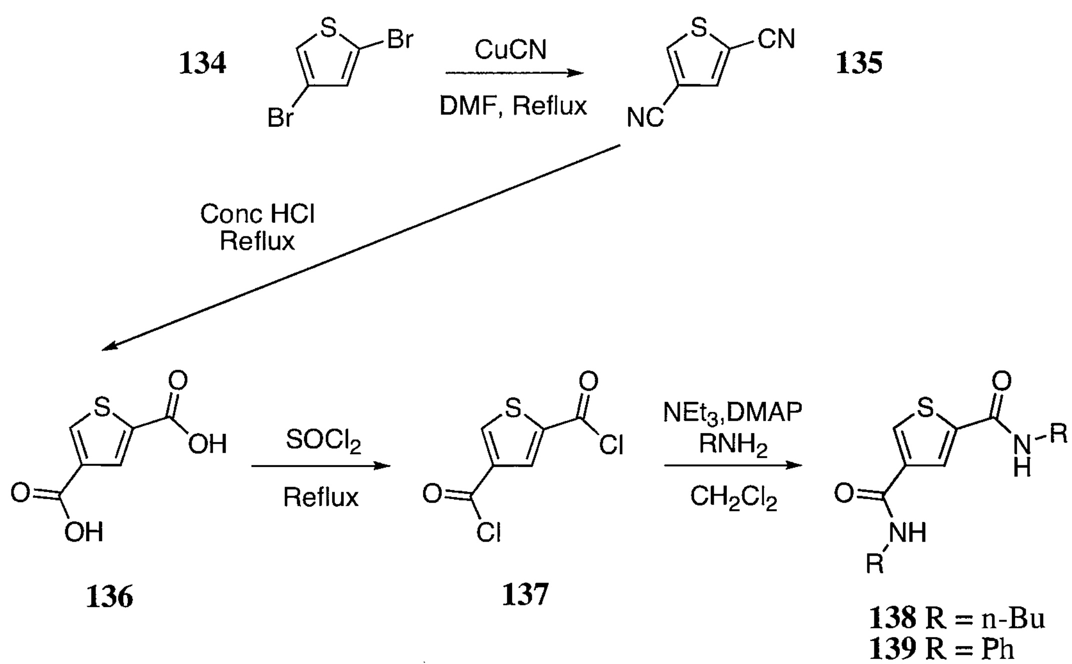

Scheme 3.5: Synthesis of compounds **138** and **139**.

Crystals of compound **139** were obtained from a dimethyl sulfoxide solution of the receptor (Figure 3.18). The structure is disordered with a carbon and sulfur atom sharing the same site. The side arms are in the 'anti-anti' conformation and there is no evidence to suggest hydrogen bond formation in the solid state (see Appendix for structural information).

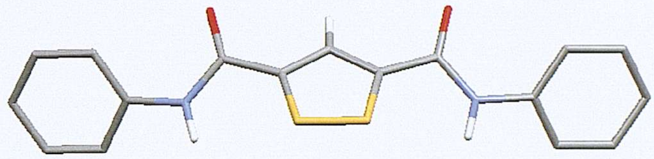

Figure 3.18: Crystal structure of compound **139**, some hydrogen atoms have been omitted for clarity.

3.3.2.2 Binding studies reveals high selectivity for oxo-anions

To form a consistent data set the ^{1}H NMR titrations were carried out in dimethyl sulfoxide-d_6/0.5% water solution. Receptors **138** and **139** do not contain a C_2 symmetry axis through the sulphur atom which causes both the amide and thiophene protons present to be inequivalent and seen as independent peaks in the proton NMR spectrum. In most cases it was possible to follow all four of the proton shifts, with each producing association constants that were in good agreement with each other. The association constants obtained from the amide resonances are summarised (Table 3.3), these results show similar trends to those previously seen for the 2,5 substituted compounds. The phenylamide receptor **139** forms stronger complexes with anions than does the butyl receptor **138** with both binding dihydrogen phosphate more strongly than benzoate, chloride, bromide and hydrogen sulfate. However there is a much higher affinity and selectivity shown for dihydrogen phosphate by the 2,4-diamido derivatives, with **139** showing an association constant K_a of 1508 M^{-1}, which over 100 times greater than that obtained with **130**. Again broadening of the NH resonances upon addition of tetrabutylammonium fluoride was observed, but the thiophene protons could be followed throughout the titrations. The *n*-butyl functionalised derivative **138** gave data that could be fitted using a 1:1 binding model, an association constant of 203 M^{-1} was calculated using the most upfield thiophene resonance. Interestingly this value is nearly three times larger than that obtained for the fluoride binding by the pyrrole 2,5-diphenylamide receptor **60** in the same solvent system. As with compound **131** the titration profiles obtained with **139** and fluoride were complicated (Figure 3.19) and we have been unable to fit the data using standard procedures. Addition of basic anions to solutions of **139** revealed a colourless to yellow colour change analogous to that seen for **131**.

	Association constants K_a (M^{-1})			
Anion	Receptor **138** [a]	Receptor **138** [b]	Receptor **139** [a]	Receptor **139** [b]
Fluoride	*	*	*	*
Chloride	<10	<10	<10	<10
Dihydrogen phosphate	156	159	1508	1625
Benzoate	36	37	173	169

Table 3.3: Calculated association constants for compounds **138** - **139** (using NH resonance NMR shifts) in dimethyl sulfoxide-d_6/0.5% water solution at 298K. Anions added as their tetrabutylammonium salts. [a] Calculated using most upfield amide resonance, [b] Calculated using most downfield amide resonance. * Resonance broadened during titration.

The titration curve of the upfield thiophene CH is shown in figure 3.19(a), an initial downfield shift is followed by an upfield shift, with a further downfield shift seen at higher concentrations of fluoride before reaching a plateau region. This indicates that there are multiple processes occurring in solution, and although the downfield CH profile (Figure 3.19(b)) is not as complicated we have still not been able to obtain an adequate fit using NMR fitting techniques.

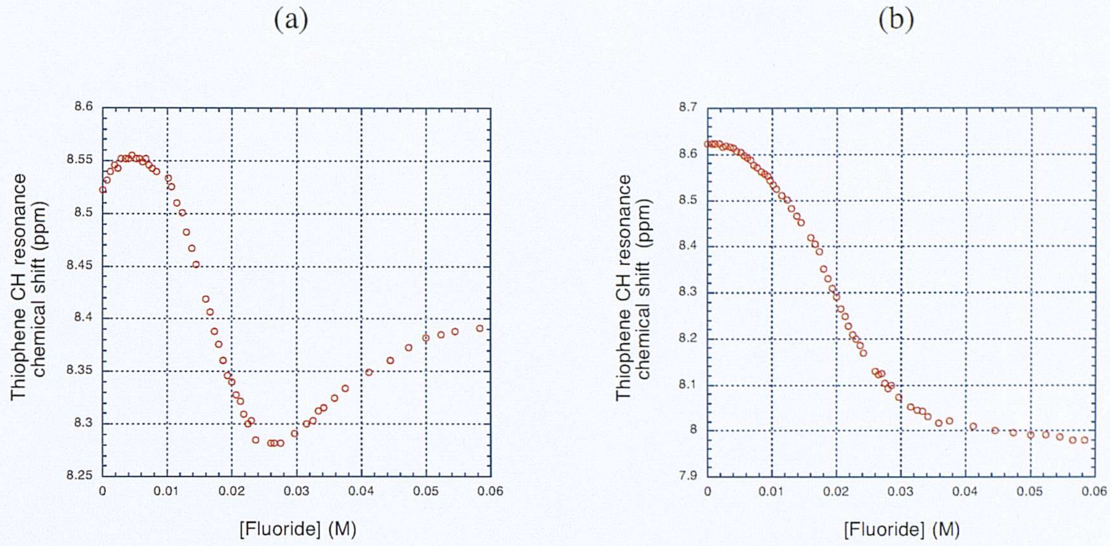

Figure 3.19: Plots of the observed shifts seen for the thiophene resonances of compound **139**, most upfield resonance (a) and downfield resonance (b).

Dilution studies were performed on compound **139** in dimethyl sulfoxide-d_6/0.5% water and showed no evidence of self association in solution. Over the concentration range 0.5×10^{-4} – 7.1×10^{-2} M, no significant shifts in the proton NMR of either the amide or thiophene resonances were observed.

Compounds **138** and **139** show a higher affinity for anions than receptors **130** and **131**, presumably due to the absence of the sulfur atom between the amide groups. The largest improvement in binding was shown for the dihydrogen phosphate anion, e.g. 2,5-diamido receptor **131** binds dihydrogen phosphate with $K_a = 48\ M^{-1}$ while the 2,4-diamido derivative **139** has an association constant $K_a = 1508\ M^{-1}$. The latter value is comparable to that seen for the pyrrole 2,5-diamide receptor **60** with dihydrogen phosphate ($K_a = 1450\ M^{-1}$) in the same solvent system. The selectivity of the pyrrole based receptor **60** for oxo-anions was attributed to the ability of the receptor to form three hydrogen bonds to the guest species.[62,63] This suggested that in addition to removing the sulfur-anion repulsion interaction, the thiophene CH hydrogen was indeed involved in anion binding. In order to investigate this hypothesis we decided to synthesise thiophene-2-phenylamide **142** and thiophene-3,4-diphenyl-2,5-diphenylamide **145**.

3.3.3 Investigating the anion co-ordination by thiophene-amides.

3.3.3.1 Synthesis and characterisation

The commercially available thiophene-2-carboxylic acid **140** was refluxed overnight in thionyl chloride to give the acid chloride derivative **141**. This was then reacted with aniline in the presence of triethylamine and DMAP, the final product **142** was isolated in 65% yield as an off white solid (Scheme 3.6).

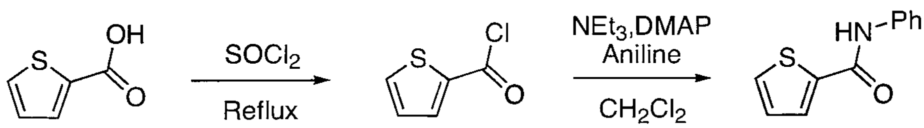

140 **141** **142**

Scheme 3.6: Synthesis of compound **142**.

3,4-Diphenylthiophene-2,5-dicarboxylic acid **143** was prepared following a literature synthesis,[140] which was converted to the bis-acid chloride **144** by refluxing overnight in thionyl chloride. Compound **145** was prepared by reacting the bis-acid chloride with a slight excess of aniline in the presence of DMAP and triethylamine. Crystallisation from hot acetonitrile led to the desired compound in 58% yield (Scheme 3.7).

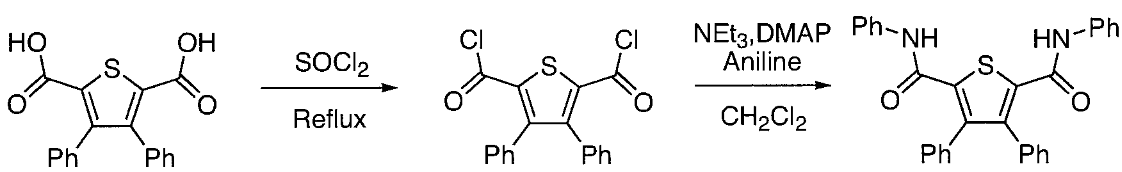

143 **144** **145**

Scheme 3.7: Synthesis of compound **145**.

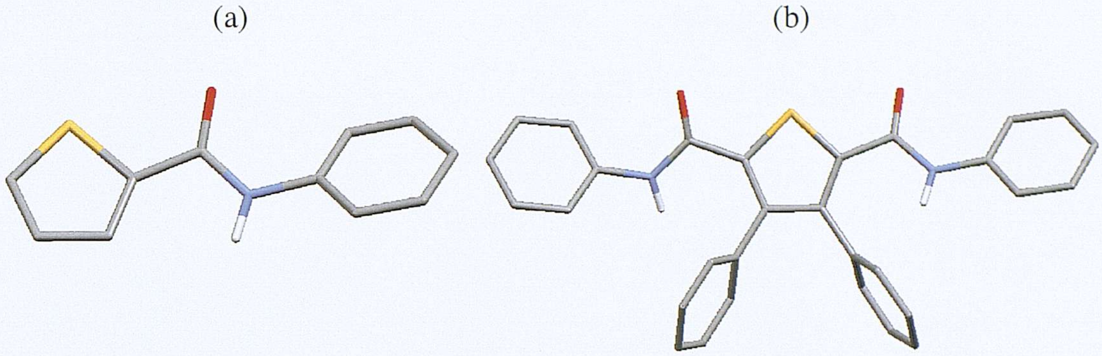

Figure 3.20: Crystal structures of compounds **142** (a) and **145** (b). Some hydrogens have been omitted for clarity.

Compound **142** was crystallised from a dimethyl sulfoxide solution of the receptor with the free receptor adopting a pseudo 'anti' conformation (Figure 3.20(a)). The molecules form chains along the a axis via formation of hydrogen bonds between an amide NH and a carbonyl group of an adjacent molecule (Figure 3.21(a)). The alternating molecules are nearly orthogonal to each other (Figure 3.21(b)), but there is no rotation of the molecules down the chain to form a helix (see Appendix for structural information).

Crystals of compound **145** suitable for single crystal x-ray diffraction were obtained from an acetonitrile solution of the receptor. The receptor adopts an 'anti-anti' conformation with no hydrogen bond formation to either bound solvent or other molecules (Figure 3.20(b)) (see Appendix for structural information).

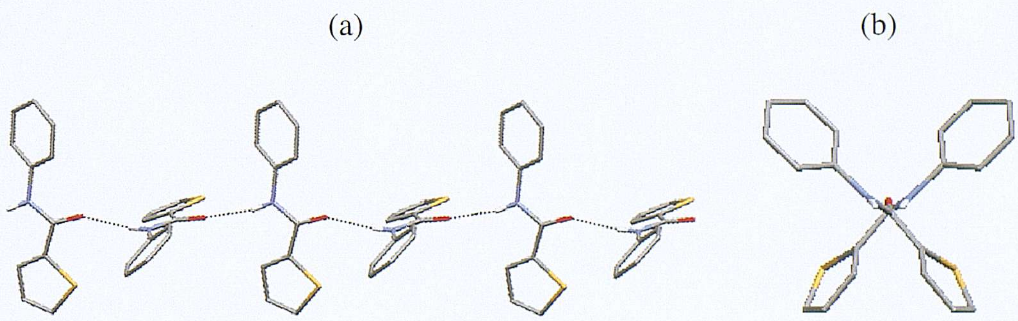

Figure 3.21: Compound **142** packs in infinite chains along the a axis (N···O distance 2.891(4)Å) (a) an end on view of the chain (b). Hydrogens not involved in hydrogen bonding interactions have been removed for clarity.

3.3.3.2 Binding studies; further evidence to suggest that a thiophene CH can be used for anion co-ordination

The ^{1}H NMR titrations for compounds **142** and **145** were performed in identical solvent conditions used for the preceding compounds (dimethyl sulfoxide-d_6/0.5% water). Again the amide NH resonances were followed to calculate the association constants for a variety of anions. Upon the addition of chloride, bromide and hydrogen sulfate anions to these receptors no meaningful shifts in the proton resonances were observed. It is reasonable to assume that there is no interaction between the receptors with these anions under the conditions used. Addition of fluoride to the receptors broadened the NH resonance, not allowing the calculation of the association constant. However, as previously seen for other thiophene phenylamide derivatives, a colourless to yellow colour change was observed upon addition of this anion to **145**, while the effect was less pronounced in the case of receptor **142**. We attempted to follow other proton resonances present in the receptors, however we have been unable to fit any of the data using standard NMR procedures (Figure 3.22).

(a) (b)

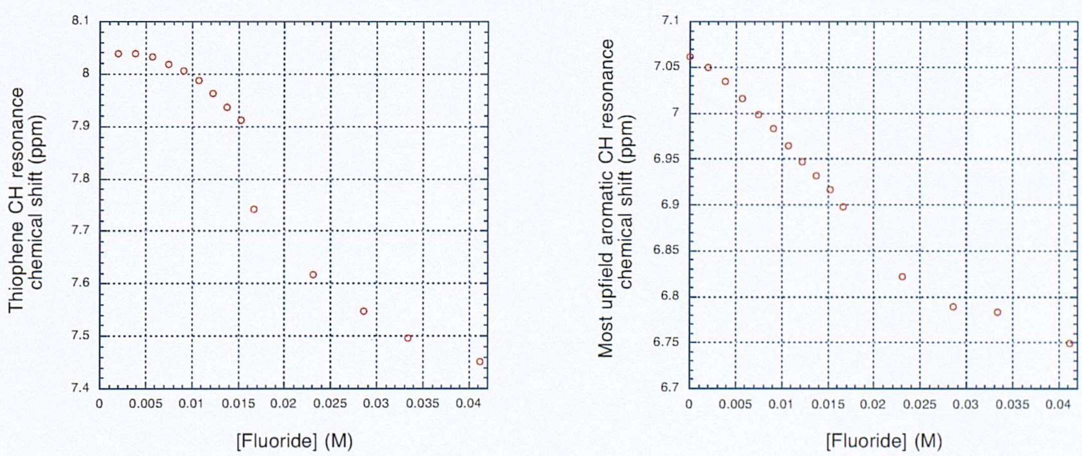

Figure 3.22: Plots of the observed shifts seen for the most downfield thiophene resonance of compound **142** (a) and the most upfield aromatic resonance of compound **145** (b) upon addition of tetrabutylammonium fluoride.

Although we have been unable to fit the data collected from the titrations of **142** and **145** with fluoride (Figure 3.22), comparison with the plots previously shown for both **131** and **139** (Figures 3.13 and 3.19 respectively) reveals there is no initial downfield shift. Unfortunately we cannot account for this odd behaviour with fluoride other than it is likely that the irregularities arise from multiple equilibria in solution.

We were however successful in obtaining association constants for both receptors with dihydrogen phosphate and benzoate anions, (Table 3.4) using 1:1 binding models. As seen for all the thiophene based receptors in this chapter a higher affinity was displayed by both **142** and **145** for dihydrogen phosphate over benzoate.

	Association constants K_a (M^{-1})	
Anion	Receptor **142**	Receptor **145**
Fluoride	*	*
Dihydrogen phosphate	21	97
Benzoate	10	10

Table 3.4: Calculated association constants for compounds **142** and **145** (using NH resonance NMR shifts) in dimethyl sulfoxide-d_6/0.5% water solution at 298K. Anions added as their tetrabutylammonium salts. * Resonance broadened during titration.

Schneider and co-workers conducted a systematical investigation of anion complexation by open-chain hosts in deuterated chloroform solution,[148] that included mono-amide receptor **146**. They showed that this receptor bound a variety of anionic guests through amide NH hydrogen bonds, with the largest affinity shown for dihydrogen phosphate $K_a = 26\ M^{-1}$ in this solvent system. Compound **146** employs a single amide NH group to form anion complexes, it would be fair to assume that in more polar conditions i.e. in dimethyl sulfoxide solution, that the association constant would be reduced compared to that in chloroform-d_1 due to the solvent competing for hydrogen bond formation.

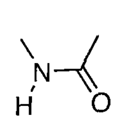

146

Jeong and co-workers wanted to investigate the significance of CH···O hydrogen bonds in polar solvents.[149] They studied the benzoate complexation of receptor **147** in dimethyl sulfoxide-d_6 solution, ^{1}H NMR titration results gave an association constant $K_a = 16\ M^{-1}$ for the formation of the benzoate complex (Figure 3.23) involving amide NH and CH hydrogen bonds. This is nearly identical to the experimental value elucidated between **142** and benzoate in dimethyl sulfoxide-d_6 /0.5% water solution ($K_a = 10\ M^{-1}$), implying that the thiophene receptor **142** employs both an amide NH and a thiophene CH in anion co-ordination. The difference between the affinity is minimally small, accountable perhaps by our addition of 0.5% water, or the slightly better geometric arrangement of donors in **147**.

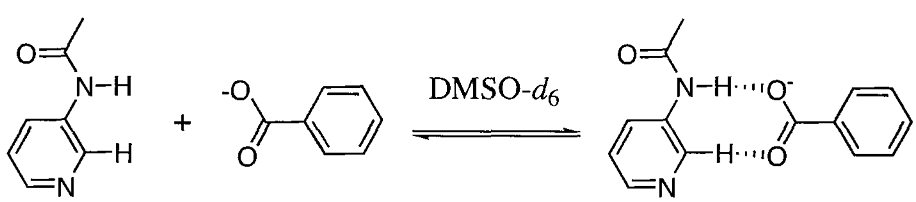

147

Figure 3.23: The complex formation between compound **147** and benzoate in dimethyl sulfoxide-d_6 solution that is believed to use both CH and NH hydrogen bonds.

Further evidence to suggest CH···anion hydrogen bond formation in solution is shown in figure 3.24. The plot (Figure 3.24(a)) shows standardised chemical shifts for the amidic NH (in black) and the three thiophene CH protons (green, blue and red) upon addition of dihydrogen phosphate to a solution of **142**. In the case of the amide NH a downfield shift is observed and an association constant $K_a = 21\ M^{-1}$ can be calculated. In addition one of the thiophene CH resonances also shifts downfield while the other two are perturbed slightly upfield. Calculation of the association constant using the downfield shifted thiophene resonance gives a value in excellent agreement with that obtained using the amide with $K_a = 24\ M^{-1}$. The same effect is seen upon addition of benzoate anions to a solution of receptor **142**.

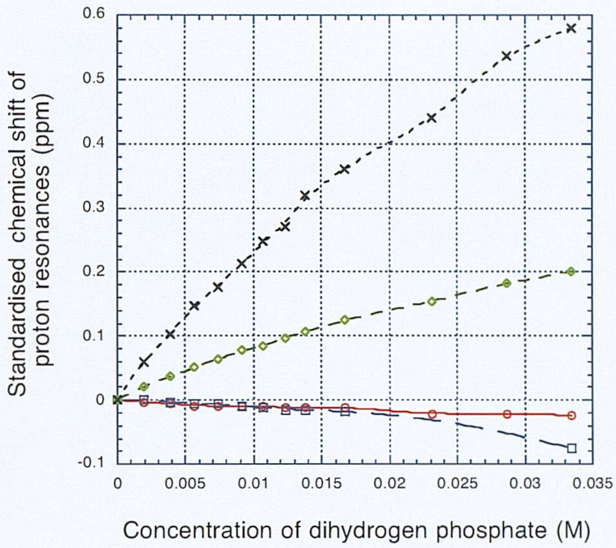

(a)

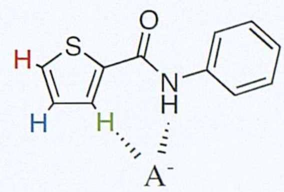

(b)

Figure 3.24: A standardised plot of the observed shifts seen for the thiophene and amide resonances of compound **142** upon addition of tetrabutylammonium dihydrogen phosphate (a). A schematic representation of the hydrogen bonds employed by **142** when binding anions (b).

It should be noted that compound **145** binds dihydrogen phosphate marginally better than the similar compound **131**, this could be due to the phenyl groups on the thiophene backbone of **145** forcing the molecule to adopt a cleft conformation in solution (although solid state analysis suggests not). Receptor **145** is unable to form hydrogen bonds from the thiophene backbone because of the phenyl rings and so can only employ hydrogen bonds from the amide groups. The protonated dihydrogen phosphate anion may be able to form a weak hydrogen bond to the thiophene sulfur atom, while in comparison the non-protonated benzoate does not reveal a significant change in binding between the two receptors.

3.4 Conclusions

A variety of heterocyclic based amide and thioamide receptors have been synthesised (**124-127, 130-133, 138-139, 142, 145**) with their affinity for anions in polar solvent media being investigated by ^{1}H NMR titration techniques. The central heteroatom has been shown to alter the selectivity and binding affinities displayed by the receptors.

The furan based host species (e.g. **124-125**) revealed up to a 40-fold selectivity for fluoride (Compound **124**) over other putative anionic guests. It is believed that the oxygen atom within the central ring promotes this selectivity because larger anionic guests are effected more by the presence of the oxygen lone pairs. The strategy of converting the amide groups to thioamides was successful with stronger complexes being formed.

When the heteroatom was exchanged for sulfur, compounds **130-131** bound anions less strongly than the furan based receptors suggesting this was a direct consequence of incorporating the larger sulfur atom. The thioamide derivatives **132** and **133** showed a marginal improvement in anion binding relative to the corresponding amide species. Unusual titration curves were obtained upon addition of fluoride anions to all of the phenylamide receptors. This indicated multiple equilibria in solution, which was also suggested by Job plot analysis. Thiophene 2,4-diamides have been shown to be selective receptors for dihydrogen phosphate in solution, while we have also shown that **131** can function as an anion receptor in the solid state. There is evidence to suggest that compound **142** uses both CH and NH hydrogen bonds in anion co-ordination, this helps to support the very high selectivity shown for dihydrogen phosphate by **139** through the formation of three hydrogen bonds. Thiophene phenylamides reveal a colourless to yellow colour change upon addition of basic anions, with fluoride and hydroxide inducing the strongest colour, this could allow colorimetric sensing of basic anions in solution.

4. *Ferrocene appended pyrrole amide clefts*

4.1 Introduction

In 2000 Gale and co-workers reported the synthesis and anion binding properties of compound **148**.[150] They attached electron withdrawing chromium-tricarbonyl groups to a 'Crabtree-type' amide cleft[29] that would serve to activate the anion co-ordinating ability of the amide NH groups, by making them more acidic. The compound proved to be a highly selective receptor for chloride ($K_a > 10^4$ M^{-1}) over other putative anionic guests in acetonitrile-d_3 solution.

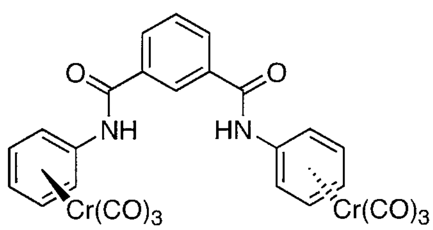

148

Crabtree and co-workers have synthesised ferrocene appended cleft type receptors **101-103** based upon the isophthalamide derivative **5**.[101] These receptors did not display large shifts in the ferrocene redox couple upon addition of anions. For example, addition of one equivalent of tetrabutylammonium chloride to compound **103** gave a cathodic shift of –20 mV, and **101** displayed a very weak negative shift of < 5mV with the same anion.

In 2001 Gale and co-workers reported that simple 2,5-diamidopyrrole receptors were effective oxo-anion binding agents,[61] and that chlorinated derivatives such as **63** and **64** sufficiently increased the acidity of the pyrrole NH to allow it to become deprotonated.[67,68] Continuing their studies, they introduced electron withdrawing groups to the phenylamide rings to produce nitro-aromatic receptors such as compound **149**.[151] This receptor behaved as a highly selective optical sensor for fluoride, observing a colourless to dark blue colour change in acetonitrile solution when in the presence of this anion.

There are relatively few examples of electrochemical sensors for anions based upon pyrrole, however examples such as **95-98** or **110** are included within this thesis. The latter, a mono *meso*-ferrocene calixpyrrole, we believe may electrochemically sense anions via a direct co-ordination pathway, such that a ferrocene CH proton is involved in the anion binding process.

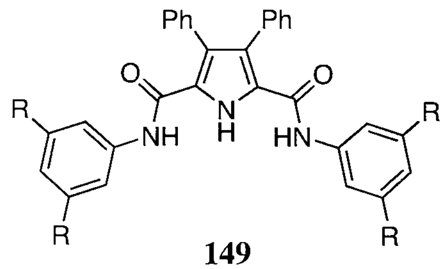

149

R = NO_2

We therefore decided to synthesise a series of mono- and bis- ferrocene appended diamido-pyrrole cleft species, whereby the ferrocene 'reporter group' is linked to the anion binding site (pyrrole-amide cleft) by either a conjugated (**153** and **161**) or non-conjugated (**152** and **160**) bond. This will enable us to study the effects of the through-bond mechanism for anion recognition by these systems. The anion binding affinities will be investigated using ^{1}H NMR titration techniques, while the electrochemical properties in the absence and presence of anions will be studied by cyclic voltammetry using a platinum microdisc working electrode.[152]

4.2 Synthesis and characterisation

Four new ferrocene appended pyrrole amide clefts **152-153** and **160-161** that bear either one or two ferrocene moieties have been synthesised. The bis-ferrocene species **152** and **153**[153] were prepared according to scheme 4.1. 3,4-Diphenyl-1*H*-pyrrole-2,5-dicarboxylic acid[154] **150** (crystal structure information for this compound can be found in the appendix) was refluxed with an excess of thionyl chloride overnight in order to obtain 3,4-diphenyl-1*H*-pyrrole-2,5-dicarbonyl dichloride **151**. The bis-acid chloride was then dissolved in dry dichloromethane solution with 2.2 equivalents of either ferrocenemethylamine[155] or ferrocenylamine[101,156] in the presence of triethylamine and DMAP and left to stir overnight under an inert atmosphere of nitrogen. The organic solvent was removed and the residue dried before being purified using chromatographic techniques on silica gel (preparative layer or column chromatography respectively), eluting with dichloromethane/methanol-2% solution, yielded the pure compounds **152** and **153** in 31 and 13% yields respectively.

150

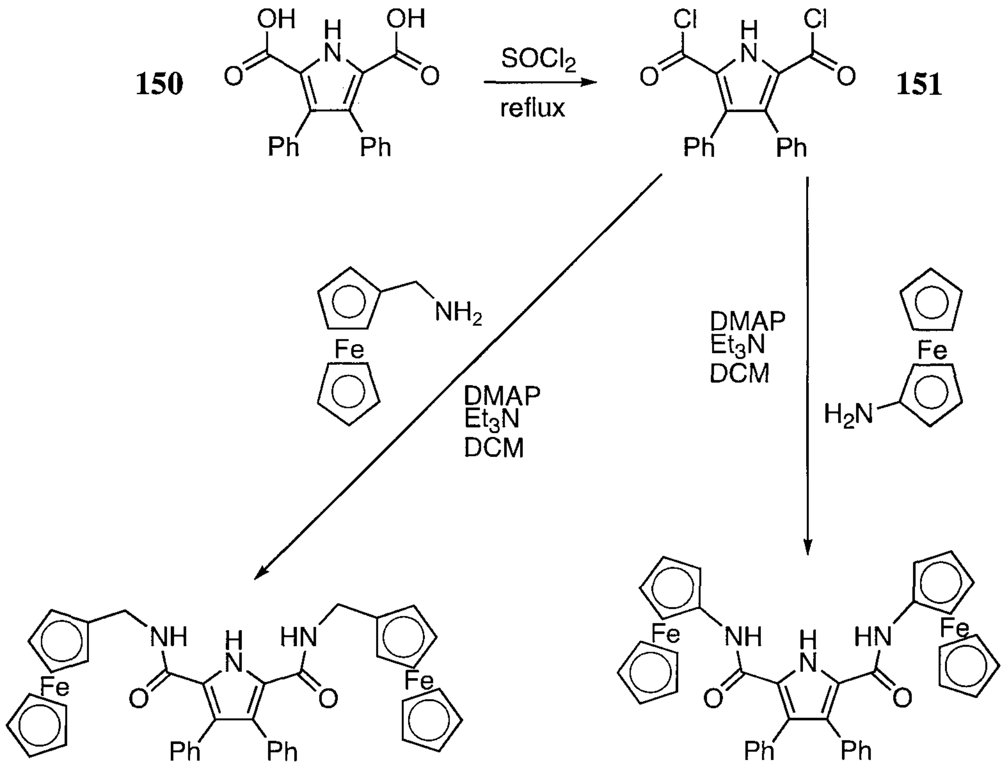

151

152 **153**

Scheme 4.1: Synthesis of receptors **152** and **153**.

The mono-ferrocene substituted pyrrole clefts **160** and **161**[157] were synthesised in accordance with scheme 4.2. 3,4-Diphenyl-pyrrole-1*H*-2,5-dicarboxylic acid di-methyl ester **154**[154] was mono-de-esterified in aqueous methanol solution using one equivalent of potassium hydroxide and precipitated using concentrated hydrochloric acid giving the mono-acid mono-ester pyrrole **155** (crystal structure information on both of these compounds can be found in the appendix). Compound **155** was dissolved in dimethylformamide and then coupled to either ferrocenemethylamine or ferrocenylamine, using one equivalent of benzotriazol-1-yloxytripyrrolidino-phosphonium hexafluorophosphate (pyBOP) and triethylamine in the presence of a catalytic quantity of 1-hydroxybenzotriazole hydrate (HOBt). After stirring in the dark for 72 hours under an inert atmosphere the solvent was removed, the corresponding residues were purified by column chromatography on silica gel eluting with dichloromethane/methanol-2% solution to yield the mono-esters **156** and **157** in 69 and 79% yields respectively. These in turn were subsequently de-esterified in aqueous methanol to afford the corresponding mono-acid monoferroceneamides **158** and **159** in 48 and 49% yields respectively. The mono- acid monoferroceneamides were then coupled to aniline (using the same method as previously described) to give the desired products **160** and **161** in 14 and 38% yields respectively.

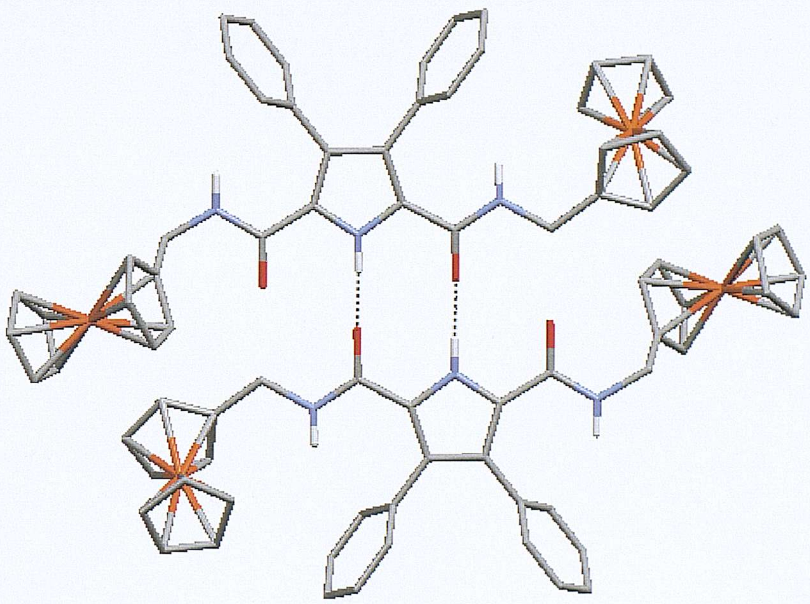

Figure 4.1: Crystal structure of compound **152**.

Compound **152** was crystallised by slow evaporation of solvent from a dichloromethane solution of the receptor. The molecules dimerise in the solid state (Figure 4.1) via NH···O hydrogen bonds (N···O distance 2.961(3) Å) (see Appendix for structural information).

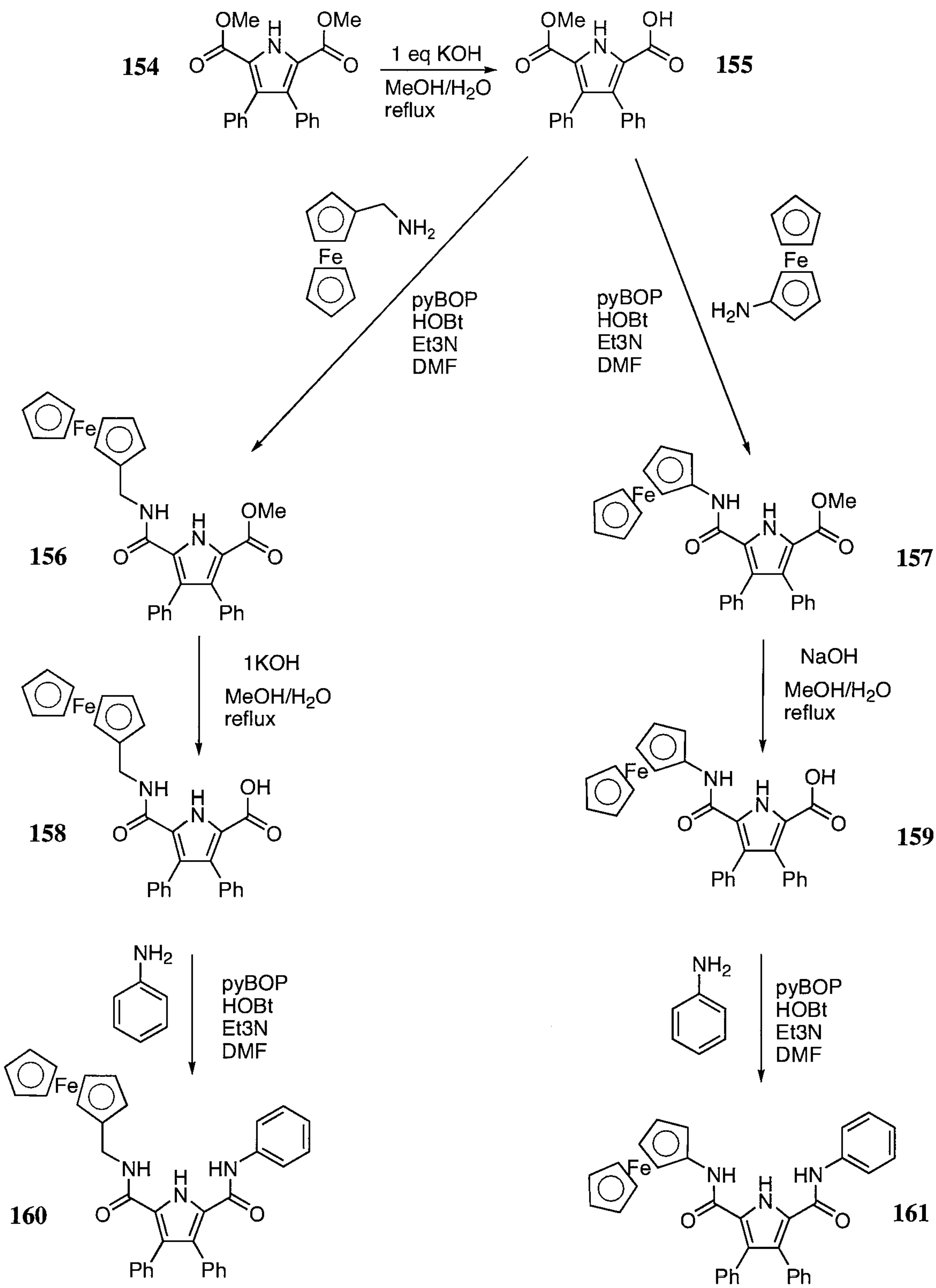

Scheme 4.1: Synthesis of receptors **160** and **161**.

Receptor **153** also forms dimers in the solid state (Figure 4.2), X-ray crystallographic analysis of single crystals collected from a dichloromethane/diethyl ether (50:50) solution of the receptor reveals NH···O and CH···O hydrogen bonds (N···O distances 2.795(4) and 3.020(3) Å, C···O distance 3.2245(5) Å) (see Appendix for structural information).

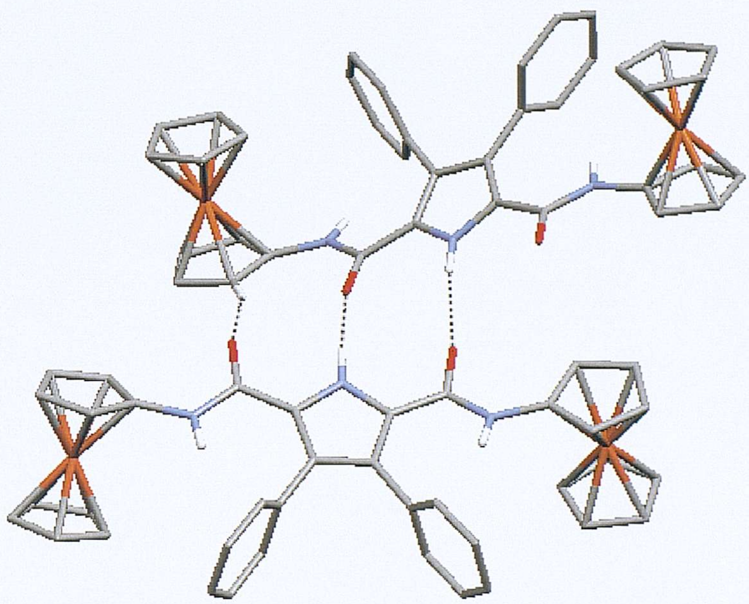

Figure 4.2: Crystal structure of compound **153**.

Crystallisation of compound **156** was achieved by slow evaporation of a dichloromethane/methanol (2:1) solution of the receptor. The molecules form infinite chains along the *b* glide plane via NH···O hydrogen bonds (N···O distance 2.906(5) Å) shown in figure 4.3 (See Appendix for structural information).

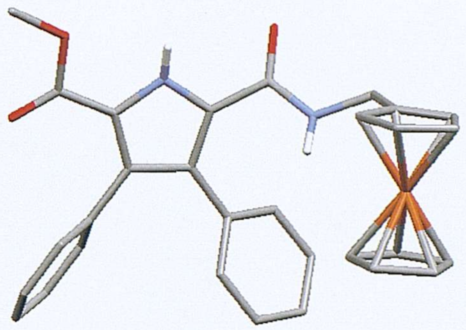

(a)

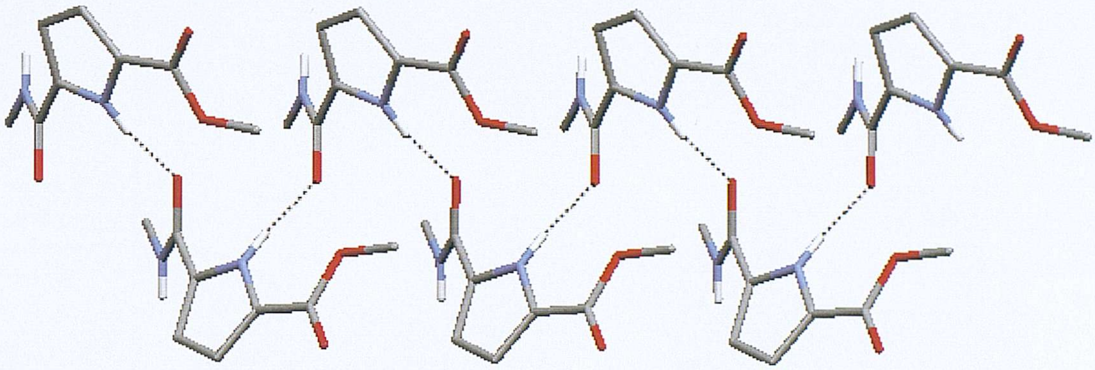

(b)

Figure 4.3: Crystal structure of compound **156** (a) and packing diagram showing the hydrogen bonds that form the infinite chains along the *b* glide plane (b) (phenyl and ferrocenyl groups omitted for clarity).

Receptor **157** crystallised from a diethyl ether/dichloromethane (4:1) solution, the compound forms centrosymmetric dimers (Figure 4.4) via CH···O hydrogen bonds (C···O distance 3.432(6) Å) from a ferrocene CH to the amide carbonyl oxygen (See Appendix for structural information).

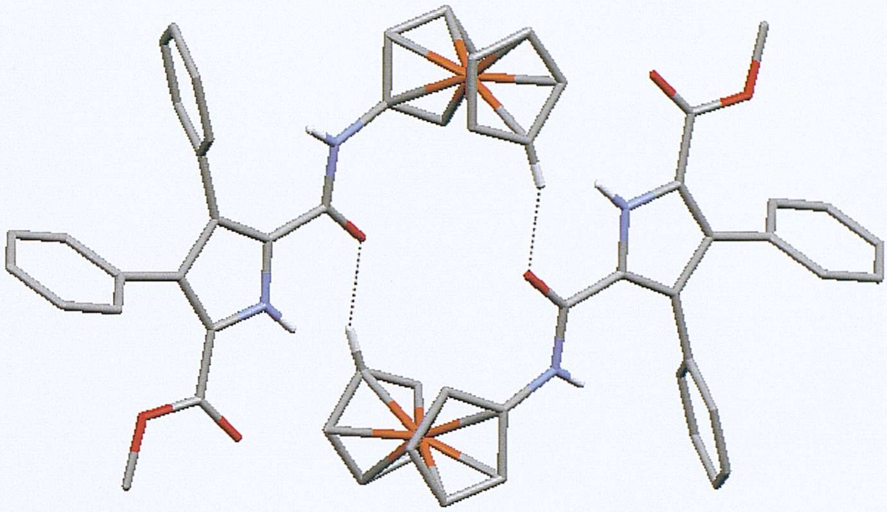

Figure 4.4: Crystal structure of compound **157**.

Compound **158** was crystallised from a benzene solution of the receptor forming centrosymmetric dimers via OH···O hydrogen bonds with an O···O distance of 2.605(3) Å as shown in figure 4.5 (See Appendix for structural information). Similarly receptor **159** also forms dimers through the carboxylic acid groups via OH···O hydrogen bonds with an O···O distance of 2.648(4) Å (Figure 4.6).

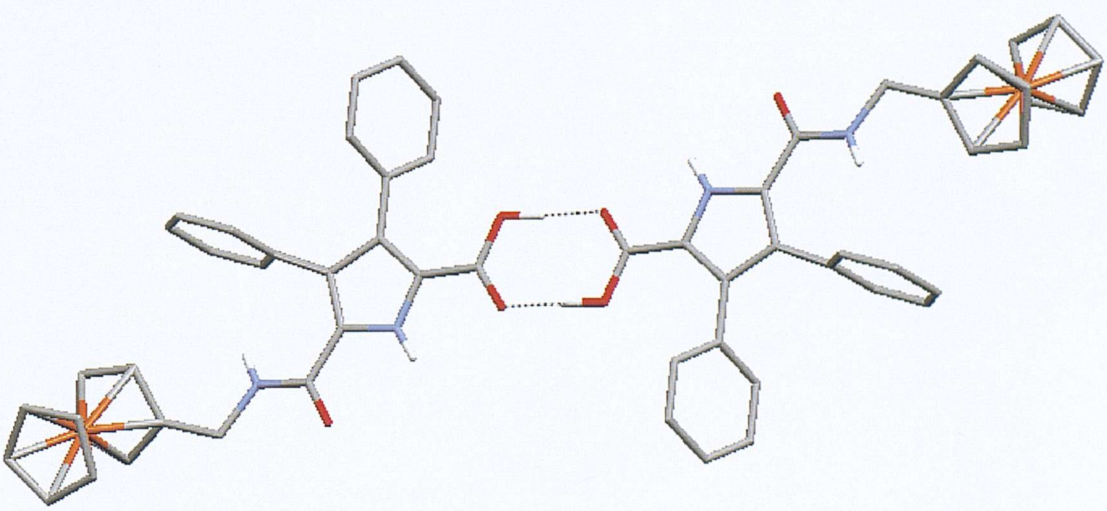

Figure 4.5: The crystal structure of compound **158** (Benzene and certain hydrogens have been removed for clarity).

In this case the pyrrolic nitrogen co-ordinates a chloroform molecule via a single NH···Cl interaction with an N···Cl distance of 3.431(6) Å (see Appendix for structural information).

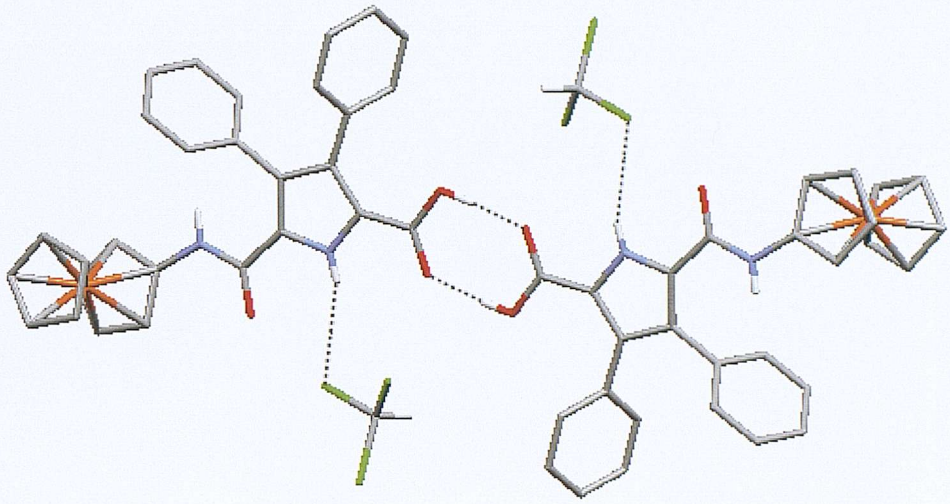

Figure 4.6: The crystal structure of compound **159**.

The crystal structure of compound **160** was elucidated from single crystals obtained from an acetonitrile/dichloromethane (2:1) solution of the receptor, again reveals the presence of dimer formation in the solid state. Two unique dimers can be found within the structure (Figure 4.7), each dimer forms part of a non-hydrogen bonded layer parallel to the *ac* plane, these layers pack alternately throughout the structure along the *b* axis. Both of the centrosymmetric dimer sets are formed via NH···O and additional CH···O hydrogen bonds from the methylene spacer group (see Appendix for structural information).

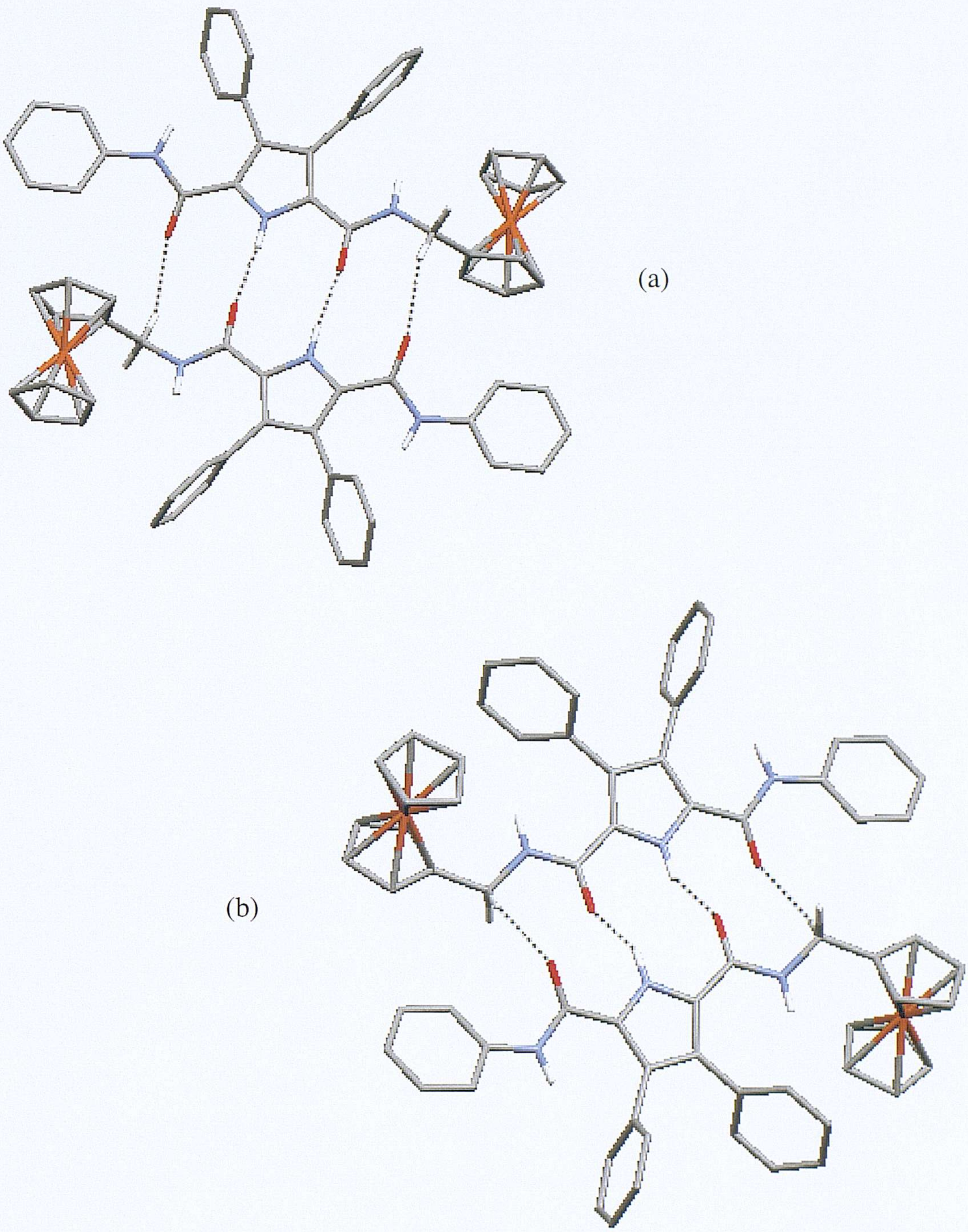

(a)

(b)

Figure 4.7: The crystal structure of compound **160** reveals two distinct dimers via NH···O and CH···O hydrogen bonds the first (a) has an N···O distance of 2.843(4) Å and C···O distance 3.354(5) Å, while the second (b) reveals an N···O distance of 2.900(4) Å and C···O distance 3.473(5) Å.

Finally X-ray quality crystals of compound **161** were obtained from a methanol/dichloromethane solution of the receptor, but unlike the previously shown examples, does not form dimers or chains but instead forms two hydrogen bonds to a molecule of methanol (Figure 4.8). The methanol is bound via NH···O (N···O distance 2.930(6) Å) and OH···O hydrogen bonds (O···O distance 2.696(6) Å) (see Appendix for structural information).

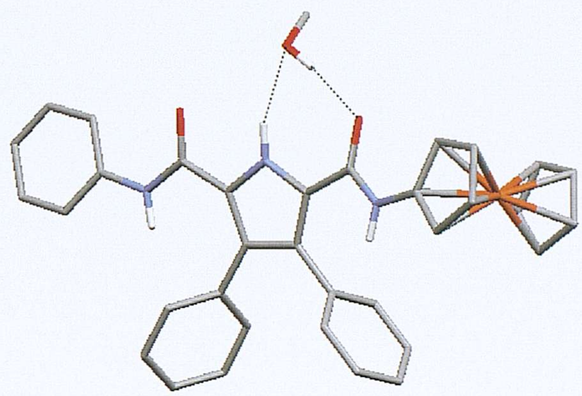

Figure 4.8: Crystal structure of compound **161**.

4.3 Binding study results

The anion binding properties of receptors **152**, **153**, **160** and **161** were investigated using proton NMR titration techniques,[118,119] in deuterated dichloromethane solution (due to solubility problems in other solvents). The association constants were calculated using the amide NH resonances as the pyrrolic NH broadened in some instances. All of the receptors gave weak association constants with bromide (K_a values all < 20 M^{-1}) and these results are not tabulated, the values obtained with the other anionic guests studied are summarised in table 4.1. All of the experimental data was fitted using a 1:1 receptor:anion binding model using the EQNMR[118] computer program. Comparison of the results show the conjugated receptors **153** and **161** have predominantly higher affinities for anions than do their non-conjugated counterparts

152 and **160** respectively. All of the receptors bind fluoride quite strongly, however the electrochemistry results reported later in this chapter have led us to treat this data with an element of caution. Compound **152** is generally the worst receptor binding all of the anions (except fluoride) with association constants less than 50 M^{-1}, this is presumably due to the rotationally free ferrocene groups blocking the binding site. The other remaining receptors show a degree of selectivity for benzoate anions with compound **153** binding this anion the strongest with an association constant $K_a = 1827$ M^{-1}. Compounds **153** and **161** in addition, show a notable affinity for dihydrogen phosphate, matching the previously seen oxo-anion selectivity of the 2,5-diamidopyrrole clefts.[61]

	Association constants K_a M^{-1}			
Anion	**152**	**153**	**160**	**161**
Fluoride	170	704	1518	1582
Chloride	< 20	68	< 20	54
Dihydrogen phosphate	44	143	35	296
Hydrogen sulfate	47	76	69	47
Benzoate	34	1827	213	807

Table 4.1: Calculated association constants for compounds **152**, **153**, **160** and **161** (using the amide NH resonance NMR shift) in dichloromethane-d_2 solution at 298K. the anions were added as their tetrabutylammonium salts.

Addition of anions to solutions of compounds **153** and **161** significantly perturbs one of the ferrocene CH resonances, while this shift is not observed for any of the ferrocene protons in the non-conjugated receptors **152** and **160**. By way of example the standardised ferrocene resonance shifts of compound **153** upon addition of tetrabutylammonium chloride have been plotted against the concentration of chloride (Figure 4.9). The green line corresponds to the unsubstituted cyclopentadienyl ring while the blue and red lines are the two proton sites present on the substituted ring (α and β respectively). The corresponding association constants can be calculated; in the cases of the lower cyclopentadienyl ring and β protons the values are in poor agreement, while an association constant $K_a = 69\ M^{-1}$ can be calculated using the α proton (blue line). This is identical to the value obtained with the amide resonance (within the error margins). This shift may be due to the formation of a CH···anion hydrogen bond,[120] but may also be due to the presence of the conjugated pathway between the binding site and ferrocene group.[158] The latter case is more likely, certainly in-light of the previously reported calixpyrroles **110** and **111** where only one ferrocene proton experienced a downfield shift.

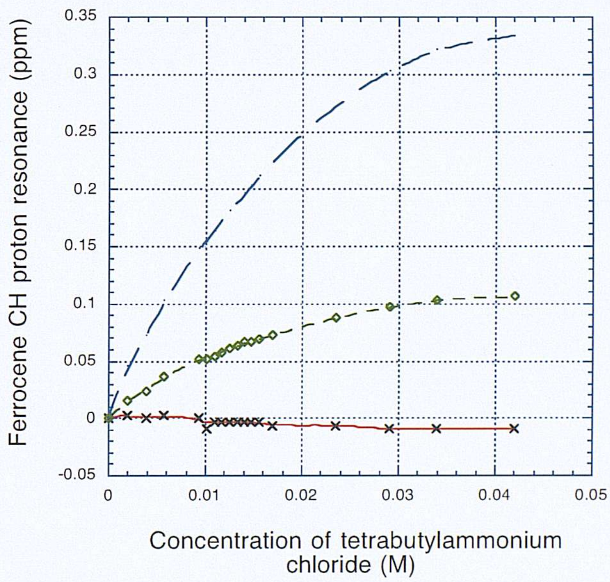

Figure 4.9: A plot showing the relative shifts (in ppm) of the three independent ferrocene proton resonances (NMR) present in compound **153** upon addition of tetrabutylammonium chloride. Green line - unsubstituted cyclopentadienyl ring, blue line - α proton and red line - β proton.

Dilution studies were performed and showed no evidence of self association in solution. For example in the case of compound **153**, over the concentration range 2.6 x 10^{-4} to 3.5 x 10^{-2} M no significant shift in the ^1H NMR proton resonances was observed.

4.4 Electrochemical properties

4.4.1 Introduction

The steady state electrochemical properties of receptors **152, 153, 160** and **161** in the presence and absence of anionic guests were studied by voltammetric techniques (recording the electrode current while sweeping the electrode potential) using a platinum microdisc as the working electrode. This work was conducted as a collaboration at the University of Southampton with Dr. Guy Denuault, whose knowledge and equipment were integral in obtaining the following results.

Microelectrodes are defined as an electrode bearing at least one dimension in the range of 0.1 to 50 μm. This characteristic dimension gives microelectrodes their unique properties of increased rate of mass transport, the decreased dependence upon the need for a conducting medium and faster response times. The experimental timescale has dramatic effects on the data collected, this is due to the type of diffusion layer formed at the tip of the electrode.[152] At fast scan rates the electrode is analogous to a plane and responds like a conventional larger electrode producing a transient voltammogram. While at slower scan rates spherical diffusion is prevalent, allowing a steady state voltammogram to be recorded. The physical size of the electrode allows electrochemical information to be obtained from very small solution volumes, while still functioning effectively at low concentrations.

The current involved when using microelectrodes is very small (a few nA), this causes a dramatic reduction in ohmic drop meaning that a counter electrode is not necessary. Therefore experiments were conducted using only two electrodes; the microelectrode as the working electrode (where the electrochemical reaction occurs) and a reference electrode that provides a stable and fixed potential so that the drop in potential between the electrode and solution is precisely defined when a voltage is applied.

4.4.2 Electrochemical results

The electrochemical properties of **152**, **153**, **160** and **161** were investigated using steady state cyclic voltammetry in bench grade dichloromethane solvent, with 0.1M tetrabutylammonium tetrafluoroborate as the supporting electrolyte, and the receptors at 0.5 mM. The experiments were conducted at room temperature, performed using a two electrode set-up with a scan rate of 20 mV s^{-1}. The working electrode used was a 25μm platinum microdisc, whilst the counter-reference electrode was a silver wire in 0.1M silver nitrate in dry acetonitrile solution. Argon gas was bubbled through the solution to purge the cell and remove oxygen although when recording a voltammogram the flow was turned off as the blanket formed was found to be sufficient. This also eliminated any additional convection of reactant to the electrode.

Very similar oxidation potentials were obtained from the free receptors **152** and **160** with corresponding half-wave potentials of 0.182 and 0.170 V. The conjugated receptors **153** and **161** were more easily oxidised than **152** and **160** but their half-wave potentials are significantly different ($E_{1/2}$ = 0.080 and 0.058 V respectively). A typical steady state cyclic voltammogram is shown in figure 4.10 (recorded with compound **152**). There are clearly defined plateau regions at the start and end of the scan with a smooth steadily rising mid-section, the return scan closely tracks the forward scan showing little hysteresis. The limiting current is the value corresponding to the difference between the lower and upper plateau regions.

If the electron transfer is fast compared with other processes (such as diffusion) then the reaction is said to be electrochemically reversible. This information can be obtained from the cyclic voltammogram by a simple analysis. The Tomes criterion (at 25°C) for a reversible one electron wave is $\Delta E = E_{3/4} - E_{1/4} = 56.5/n$ mV, where $E_{3/4}$ and $E_{1/4}$ are the corresponding potentials at 3/4 and 1/4 of the limiting current value, and n is the number of electrons involved in the electron transfer process.

Performing this analysis on the cyclic voltammograms, indicates that the oxidation process in all cases is reversible with ΔE = 55, 48, 55 and 63 mV respectively. Interestingly the limiting currents show a direct correlation to the number of ferrocene groups present in the receptors with values of 4.4, 3.7, 2.0 and 1.8 nA respectively. In

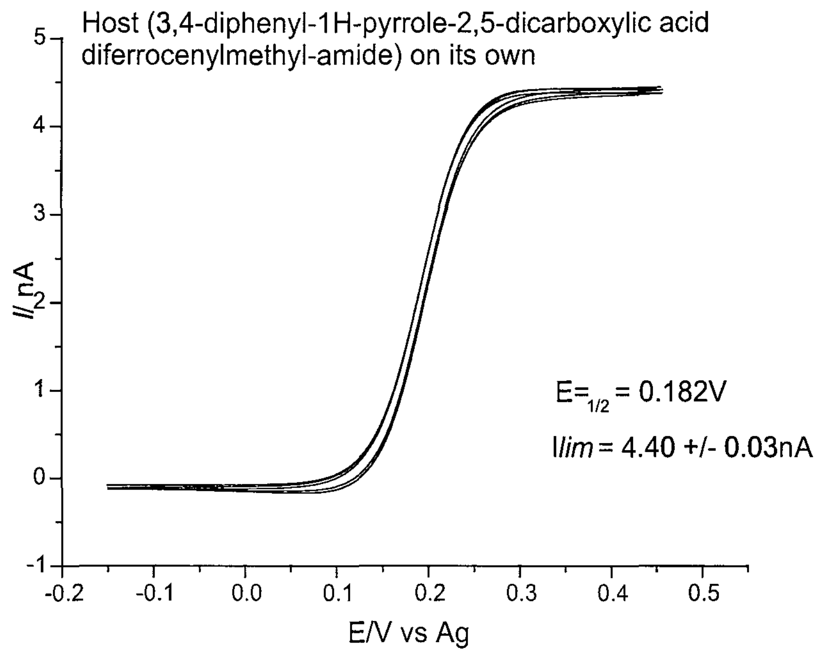

Figure 4.10: A microelectrode cyclic voltammogram of compound **152** in dichloromethane solution.

the cases of **152** and **153** this suggests that a simultaneous oxidation of both ferrocene moieties is occurring i.e. the ligands are undergoing a two electron oxidation in one single step, which is also supported by the presence of only one wave.

The voltammetric responses obtained with compounds **152** and **160** are nearly identical (except for the doubling of the limiting current), while contrastingly the responses of **153** and **161** are appreciably different. It would appear that the methylene spacer present in the non-conjugated receptors insulates the ferrocene reporter groups, and subsequently are unaffected by the rest of the molecule yielding similar voltammetric responses. Yet in the cases bearing a conjugated link the redox activity of the ferrocene groups is clearly affected by the rest of the molecule.

To investigate to electrochemical recognition properties of the receptors we recorded cyclic voltammograms of the receptors in the presence of three equivalents of various anionic guests (added as their tetrabutylammonium salts), the results are reported in table 4.2. With some anions the product of the electrochemical reaction passivates the electrode, this has detrimental effects to the shape of the voltammetric wave. When in the presence of dihydrogen phosphate all of the receptors exhibit a substantial hysteresis between the forward and reverse scans, the voltammograms do not reach the expected plateaus and evaluation of the half-wave potential becomes more difficult. To be sure that the half-wave potentials reported were reproducible we had to ensure that the electrode surface was free of any residue that may inhibit the electrochemical reaction. In order to obtain a clean electrode surface, a potential ramp was employed that held the electrode at large negative potentials for a few seconds prior to collecting the voltammogram. This pre-treatment proved successful in removing the passivating material, without the need for polishing the electrode between scans. However, when new solutions were introduced to the electrochemical cell the electrode was carefully cleaned polished using 0.3 μm alumina on a polishing microcloth.

	Shift (ΔE) in Fc/Fc^+ redox couple (mV)			
Anion	**152**	**153**	**160**	**161**
Fluoride	- 131	- 123 & - 255#	- 55	- 28 & - 232#
Chloride	- 76	- 53	- 30	- 26
Bromide	0	- 12	0	+ 7
Dihydrogen phosphate	*	*	- 130*	- 248*
Hydrogen sulfate	*	- 37	- 3	- 29
Benzoate	- 60	- 122	- 80	- 150

Table 4.2: The observed shift in the Fc/Fc^+ redox couples of the receptors in the presence of various anionic guests in dichloromethane solution. # Two waves are observed. * The voltammetric wave is seriously distorted as the product of the electrochemical reaction passivates the electrode.

The results show that all of the receptor:anion complexes observe a negative shift of the ferrocene/ferrocenium couple with respect to the wave seen for the free receptors, except in the case of bromide where the electrochemical response was negligible if any when considering a ±10 mV experimental error. Considering only the halides, fluoride produces the largest cathodic shifts. These results however should be treated with a degree of caution as compounds **153** and **161** uniquely have two waves that we believe may be caused by deprotonation of the hosts by this anion. Addition of benzoate produces large shifts of up to – 122 and – 150 mV with the same receptors, this not only reflects the affinity shown by the receptors for this anion but also the presence of a conjugated pathway between the binding site and the ferrocene reporter groups. Although mentioned in the introduction, it is worth re-iterating that the electrochemical shifts measure the interaction of the anionic guest with the oxidised receptor while NMR titrations measure the affinity shown for the guest by the neutral host. An anion that gives a large binding constant will not necessarily correspond to a large shift of the redox couple and vice versa. These independent data sets are related by the association constant of the oxidised receptor for the anion through the scheme of one square (Scheme 4.3).[159] Comparison of data collected for compounds **103** and **153** illustrates this point. The Crabtree receptor **103** binds chloride in dichloromethane-d_2 solution with an association constant K_a = 9500 M^{-1} while compound **153** has a small value K_a = 68 M^{-1}, yet the shifts of the ferrocene redox couples in dichloromethane were - 20 and - 53 mV respectively (although there are slight experimental differences[101,157] it is reasonable to compare the redox shift magnitudes as the half-wave potentials should still shift by the same amount within experimental error).

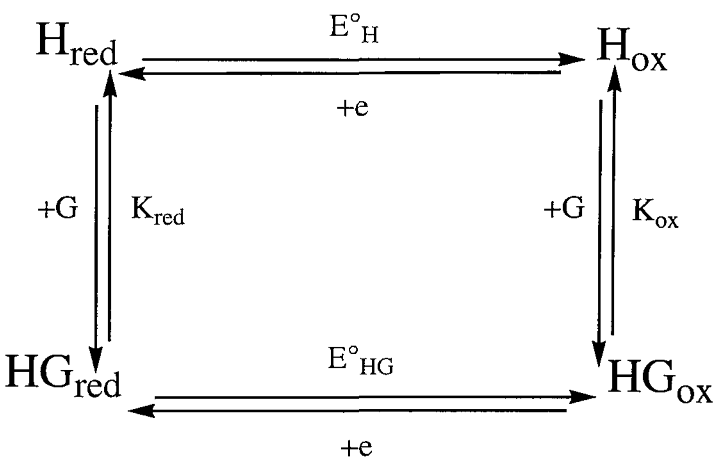

Scheme 4.3: The scheme of one square linking guest binding and electron transfer. Where H corresponds to the host, G the guest and HG the complex formed between the two species. The subscripts "ox" and "red" indicate that the molecules or parameters are in oxidised or reduced states, E° is the formal potential of electron transfer and K is the association constant.

4.5 Conclusions

A series of ferrocene appended pyrrole-amide clefts have been synthesised (**152-153** and **160-161**) and their anion co-ordination properties investigated by ^1H NMR titration techniques in deuterated dichloromethane solvent. The studies revealed that these receptors were able to form complexes with a variety of anions, whilst maintaining the oxo-anion selectivity previously shown by other 2,5-diamidopyrrole clefts.[61,62]

The ferrocene appended pyrrole-amide clefts were shown to successfully function as electrochemical anion sensors, although the electrochemistry of some systems revealed complications. Distorted voltammetric waves were caused by the passivation of the electrode in the case of dihydrogen phosphate, and strange two wave behaviour was observed with fluoride that we believe may be due to deprotonation of the pyrrolic NH group. With this in mind the strong binding of fluoride by the neutral receptors should be treated with a degree of caution.

The large negative shifts of the ferrocene/ferrocenium redox couple observed upon addition of benzoate anions to solutions of **153** and **161** can be attributed to complex formation with this anion and the following facile oxidation of the complex.

5. *Experimental*

5.1 Solvent and reagent pre-treatment

Where necessary solvents were purified prior to use. Dichloromethane was distilled over calcium hydride. Tetrahydrofuran and diethyl-ether were distilled from sodium using benzophenone as an indicator. Anhydrous acetonitrile (water <0.003%) was purchased from Fisher. Anhydrous methanol was bought from Aldrich (99.8%) as was anhydrous dimethylformamide (99.8%). Pyrrole was dried over NaOH, fractionally distilled under reduced pressure from sodium, and stored under nitrogen in refrigerator. Triethylamine was distilled from KOH and stored under nitrogen in the presence of an excess of KOH pellets. Thionyl chloride was distilled from 10% (w/w) triphenyl phosphite and stored under nitrogen. Commercial grade reagents have been used without further purification. Reagents prepared in accordance with literature are so referenced. All of the syntheses have been performed under an inert atmosphere of nitrogen. Tetrabutylammonium salts of the anions used during ^{1}H NMR titrations have been thoroughly dried overnight under high vacuum.

5.2 Instrumental methods

NMR data were recorded on Bruker AM300, AC300 and DPX400 spectrometers. The spectra were referenced[160,161] internally using the residual protio-solvent (^{1}H), the signals of the solvent (^{13}C), or hexafluorobenzene (^{19}F) and chemical shifts reported in ppm. Low resolution mass spectra were recorded on a Micromass Platform single quadrupole mass spectrometer, whereas high resolution mass spectra were recorded on a VG 70-250-SE normal geometry double focusing mass spectrometer by the mass spectrometry service at the University of Southampton. Elemental analyses were carried out at the University of Strathclyde and by Medac Ltd. Ultra-violet/Visible spectra were recorded on a Unicam UV1 spectrometer. Melting points were recorded in open capillaries on a Gallenkamp melting point apparatus and are uncorrected.

5.3 Synthesis

5.3.1 Synthesis included in chapter 2

5,10,15-Trispirocyclohexyl-20-methyl-20-ferrocenyl-calix[4]pyrrole (110): Pyrrole (2g, 30mmol), acetylferrocene (1.7g, 7.5mmol), cyclohexanone (2.2g, 22mmol) and 5 drops of methanesulfonic acid were stirred in methanol (100ml) overnight under nitrogen. Triethylamine was added to neutralise the green solution. The methanol solvent was removed *in vacuo* and the resulting crude residue dried under high vacuum. The residue was separated by column chromatography on silica gel eluting with dichloromethane:hexane (2:1). Further purification was achieved by crystallisation from an acetonitrile solution (0.15g, 30%). ^{1}H NMR (CD_3CN, 300 MHz) δ 1.42 (br. m, 18H, CH_2), 1.90-2.05 (br. m, 15H, CH_2 and CH_3), 3.93 (s, 2H, FcH), 4.02 (s, 5H, FcH), 4.12 (s, 2H, FcH), 5.68 (m, 2H, $CH_{pyrrole}$), 5.82 (m, 6H, $CH_{pyrrole}$), 7.38 (s, 2H, NH), 7.43 (s, 2H, NH). ^{13}C NMR (DMSO-d_6, 75 MHz) δ 22.09, 22.33, 25.79, 26.17, 33.55, 34.19, 36.01, 38.13, 66.39, 66.93, 68.40, 99.34, 101.87, 102.28, 102.83, 103.45, 104.63, 135.42, 136.62, 137.62, 138.06. MS (ES^+) 718 (M^+). HRMS (ES^+) 718 (M^+), $\Delta = 1.3$ ppm. Anal. calcd. for $C_{46}FeH_{54}N_4$: C, 76.88; H, 7.79; N, 7.52. Found: C, 76.77; H, 7.59; N, 7.75. Mp: 128°C.

5,10,15-Trispirocyclohexyl-20-methyl-20-acetylferrocenyl-calix[4]pyrrole (111): Pyrrole (4.97g, 74mmol), 1,1'-diacetylferrocene (2.5g, 9.3mmol), cyclohexanone (5.45g, 56mmol) and 5 drops of methanesulfonic acid were stirred in methanol (200ml) overnight under nitrogen. Triethylamine was added to neutralise the green solution. The methanol solvent was removed *in vacuo* and the resulting crude residue was dried under high vacuum. The residue was separated by column chromatography on silica gel eluting with dichloromethane/methanol (99:1). This yielded an impure product that was further purified by preparative layer chromatography using the same solvent system to obtain the pure compound as an orange powder (0.13g, 2%). Crystallisation was achieved by slow evaporation from hexane/acetone (50:50) solution. ^{1}H NMR (CD_3CN, 300 MHz) δ 1.27 (s, 3H, CH_3), 1.42-1.49 (br. m, 18H, CH_2), 2.06-2.22 (br. m, 15H, CH_2 and CH_3), 3.98 (s, 2H, FcH), 4.16 (s, 2H, FcH), 4.33 (s, 2H, FcH), 4.63 (s, 2H, FcH), 5.64 (br. s, 2H, $CH_{pyrrole}$), 5.82 (br. s, 6H, $CH_{pyrrole}$), 7.41 (br. s, 4H, NH). ^{13}C NMR (DMSO-d_6, 75 MHz) δ 23.41, 23.45, 23.65, 26.74, 26.81, 26.98, 28.06, 35.96, 36.12, 40.37, 69.30, 70.27, 70.95, 74.13, 80.38, 100.61, 104.00, 104.29, 104.47, 105.82, 137.01, 137.10, 137.60, 18.00, 202.21. MS (ES$^+$) 761 (M+H$^+$). HRMS (ES$^+$) 760 (M$^+$), Δ = 2.0 ppm. Anal. calcd. for $C_{48}H_{56}FeN_4O$ + 0.29 CH_2Cl_2 : C, 73.87; H, 7.26; N, 7.14. Found: C, 74.10; H, 6.87; N, 7.34. Mp: 124°C.

2-acetyl-5-methylpyrrole (112): This synthesis is based upon that used for ethyl 5-methylpyrrole-2-carboxylate.[124] 2,4-pentanedione (20g, 0.2mol) was dissolved in acetic acid (75ml) and magnetically stirred. An aqueous solution (50ml) of sodium nitrite (16.6g, 0.24mol) was added dropwise over an icebath. After complete addition the reaction mixture was left to stir overnight at room temperature. 3-Oxobutylaldehyde-dimethylacetyl (26.8g, 0.2mol) was added to the solution followed by careful portion-wise addition of zinc powder (28.6g, 0.43mol). The reaction mixture was heated to reflux at 120°C for 10 minutes before being allowed to cool to 50°C. The suspension was then poured onto a slurry of ice (500ml) and magnetically stirred for 2 hours. The aqueous layer was extracted using diethylether (5x200ml) before the organic solvent was removed *in vacuo* to leave a dark orange residue. Di-*n*-butyl ether (150ml) was added to the residue and then removed *in vacuo* to remove any excess acetic acid. The crude product was purified by column chromatography on silica gel eluting with dichloromethane-2% methanol solution to give the pure product as a yellow solid. (3.55g, 14%). ^{1}H NMR ($CDCl_3$, 300MHz) δ 2.33 (s, 3H, CH_3), 2.39 (s, 3H, CH_3), 5.98 (s, 1H, CH), 6.83 (s, 1H, CH), 9.79. (s, 1H, NH). In agreement with literature[125]

Tribrominated - tripyrrolylmethane derivative (115): 2-Acetyl-3,4,5-tribromopyrrole[132] (2.5g, 7.3mmol) and pyrrole (75ml, 1.07mol) were stirred in dry methanol (150ml) under nitrogen. The solution was degassed for 15 minutes and the solution heated to 80°C. Methanesulfonic acid (200μl) was added and the solution heated for 30 minutes. After cooling, 0.1M sodium hydroxide solution in water (200ml) was added. Brine (150ml) was added to the aqueous solution which was then extracted with dichloromethane (5x150ml). The organic solution was washed with brine (4x75ml) then dried with magnesium sulphate and the organic solvent removed *in vacuo*. The resulting dark solution was dried under high vacuum using an in-line trap to remove the last of the remaining pyrrole:methanol solution giving a dark viscous oil. Acetone (20ml) and hexane (30ml) were added to the oil and stirred. A red solution formed suspending a dark oil, upon settling the solution was decanted and further extraction/decantation of the remaining suspension with hexane (5x100ml) gave further red solution. The hexane solution was filtered and the solvent removed *in vacuo* giving a red oil. Dichloromethane (10ml) was added to the red oil and hexane (60ml) to precipitate the product as an off white solid (0.9g, 27%). Analytically pure material was obtained by column chromatography eluting with dichloromethane on silica giving the product as a white solid. The product was crystallised from chloroform as colourless needles. ^{1}H NMR ($CDCl_3$, 400MHz) δ 2.09 (s, 3H, CH_3), 6.14 (m, 2H, CH), 6.26 (m, 2H, CH), 6.73 (m, 2H, CH), 7.87 (s, 2H, NH), 7.91. (s, 1H, NH). ^{13}C NMR ($CDCl_3$, 100MHz) δ 26.12, 41.85, 97.09, 97.21, 103.74, 106.66, 109.31, 117.81, 133.46, 134.74. MS (ES^-) 458 $(M-H)^-$, 494 $(M+Cl^-)$, 572 $(M+TFA^-)$. HRMS (ES^-) 458 $(M-H)^-$, Δ = 9.5 ppm. Anal. calcd. for $C_{14}H_{12}Br_3N_3$: C, 36.40, H, 2.62, N, 9.09. Found: C, 36.21, H, 2.50, N, 8.96. Mp: decomp >75°C.

5,10,15-hexamethyl-20-methyl-20-(3,4,5-tribromo)pyrrolyl-calix[4]pyrrole (118): In this step, compound **115** was used crude as a red oil without further purification from the previous procedure and it was assumed that the reaction had gone to completion in an ideal yield. Compound **115**, dimethyldipyrromethane[126,127] (2.5g, 14mmol) and acetone (1.25g, 21mmol) were magnetically stirred in dry methanol (600ml) under nitrogen and degassed for 15 minutes. Methanesulfonic acid (200μl) was added and the reaction mixture stirred overnight. Triethylamine was added to neutralise the acid. The solution was filtered to remove *meso*-octamethylcalixpyrrole. The methanol was evaporated down to leave 100ml, to this water (100ml) and brine (100ml) were added to the solution. The aqueous phase was extracted with dichloromethane (5x100ml) and the organic layer dried with magnesium sulphate. The organic solvent was evaporated. Hexane (3x200ml) was added to the dark oil forming a red solution and dark solid that was removed by filtration. The organic solvent was removed *in vacuo*. Methanol (50ml) was added to the resulting red solid, the off white solid was removed by filtration (*meso*-octamethylcalixpyrrole). The solvent was removed in vacuo yielding 2g of crude product. The solid was purified by column chromatography eluting with dichloromethane on silica giving the product as a white/pink solid (0.72g, 14% $_{\text{overall yield from 2-acetyl-3,4,5-tribromopyrrole}}$). ^{1}H NMR ($CD_2Cl_2$, 400MHz) δ 1.50 (s, 3H, CH_3), 1.51 (s, 6H, CH_3), 1.53 (s, 3H, CH_3), 1.56 (s, 6H, CH_3), 1.92 (s, 3H, CH_3), 5.89 (m, 6H, CH), 6.00 (m, 2H, CH), 7.14 (s, 2H, NH), 7.22 (s, 2H, NH), 7.74. (s, 1H, NH). ^{13}C NMR (CD_2Cl_2, 100MHz) δ 25.67, 28.24, 28.48, 29.39, 30.37, 35.92, 42.35, 97.40, 97.54, 103.60, 103.90, 105.60, 107.31, 132.86, 136.03, 138.64, 139.28, 139.38, 140.50. Anal. calcd. for $C_{31}H_{34}Br_3N_5$ + $0.33CH_2Cl_2$ requires C, 50.54, H, 4.69, N, 9.40. Found: C, 50.41, H, 4.63, N, 9.34. MS (ES^-) 748 ($M+Cl^-$), 826 ($M+TFA^-$). HRMS (ES^+) 714 ($M+H^+$), Δ = 1.1 ppm. Mp: decomp >95°C.

5.3.2 Synthesis included in chapter 3

3,4-Diphenyl-furan-2,5-dicarboxylic acid dibutyl-amide (124): 3,4-Diphenyl-furan-2,5-dicarboxylic acid[140] (2.0g, 4.8mmol) was suspended in freshly distilled thionyl chloride (50ml) and heated at reflux overnight. The excess thionyl chloride was removed *in vacuo* and the resulting solid dried under high vacuum for 2 hours. The resulting 3,4-Diphenyl-furan-2,5-dicarbonyl dichloride was dissolved in dry dichloromethane (80ml). Triethylamine (2.0g, 19.8mmol), DMAP (catalytic quantity) and n-butylamine (1.00g, 13.6mmol) were added whilst the solution was stirred under a nitrogen atmosphere. The reaction mixture was stirred overnight and the organic solution was then washed with water (4x100ml), dried with magnesium sulphate and the dichloromethane removed *in vacuo*. The yellow oily residue was purified by column chromatography on silica eluting with dichloromethane-2% methanol giving the desired compound (1.07g, 53%). The product was crystallised from diethyl-ether (200ml) and also from a solution of diethyl-ether:acetonitrile:dimethyl sulfoxide (2:2:1) giving polymorphic structures. ^{1}H NMR ($CDCl_3$, 300MHz) 0.88 (t, J = 7.29 Hz, 6H, CH_3), 1.24 (m, 4H, CH_2), 1.43 (m, 4H, CH_2), 3.32 (m, 4H, CH_2), 6.28 (t, 2H, J = 5.49 Hz, NH), 7.18–7.30 (m, 10H, Ar). ^{13}C NMR ($CDCl_3$, 100MHz) δ 13.76, 20.09, 31.47, 39.14, 128.39, 128.46, 130.25, 130.35, 131.09, 142.52, 158.26. MS (ES^+) 520 ($M+Et_3NH^+$), 837 ($2M+H^+$). HRMS (ES^+) 859 ($2M+Na^+$), Δ = 0.4 ppm. Anal. calcd. for $C_{26}H_{30}N_2O_3$ + 0.33 MeOH : C, 73.69; H, 7.36; N, 6.53. Found: C, 73.79; H, 7.16; N, 6.51. Mp: 144°C.

3,4-Diphenyl-furan-2,5-dicarboxylic acid diphenyl-amide (125): 3,4-Diphenyl-furan-2,5-dicarboxylic acid[140] (2.0g, 4.8mmol) was suspended in freshly distilled thionyl chloride and heated at reflux overnight. The excess thionyl chloride was removed *in vacuo* and the resulting solid dried under high vacuum for 2 hours. The resulting 3,4-diphenyl-furan-2,5-dicarbonyl dichloride was dissolved in dry dichloromethane (80ml). Triethylamine (2.0g, 19.8mmol), DMAP (catalytic quantity) and aniline (1.27g, 13.6mmol) were added whilst the solution was stirred under a nitrogen atmosphere. The reaction mixture was stirred overnight and the organic solution was then washed with water (4x100ml), dried with magnesium sulphate and the dichloromethane removed *in vacuo*. The product was recrystallised from acetonitrile (200ml) affording the final product in yield as a white powder (1.77g, 80%). ^{1}H NMR (DMSO-d_6, 300MHz) δ 7.13 – 7.72 (m, 20H, Ar), 10.38 (s, 2H, NH). ^{13}C NMR (DMSO-d_6, 100MHz) δ 120.83, 124.34, 127.49, 127.68, 128.79, 130.02, 130.29, 132.21, 137.84, 141.45, 155.67. MS (ES$^+$) 560 (M+Et$_3$NH$^+$), 917 (2M + H$^+$). HRMS (ES$^+$) 939 (2M + Na$^+$), Δ = 2.8 ppm. Anal. calcd. for $C_{30}H_{22}N_2O_3$ + H_2O requires C, 75.61; H, 5.08; N, 5.88. Found: C, 75.82; H, 5.11; N, 5.69. Mp: 278°C.

3,4-Diphenyl-furan-2,5-dicarboxylic acid dibutyl-thioamide (126): 3,4-Diphenyl-furan-2,5-dicarboxylic acid dibutyl-amide[139] **(124)** (0.7g, 1.7mmol) was suspended in freshly distilled tetrahydrofuran (100ml), Lawessons reagent (1.75g, 4.3mmol) was added and the solution heated at reflux for 24 hours. The solvent was removed *in vacuo* and the resulting solid suspended in dichloromethane (50ml). The organic layer was washed with water (3x20ml), dried with magnesium sulphate and the dichloromethane removed *in vacuo*. The resultant solid was purified using column chromatography on silica gel eluting with dichloromethane-2% methanol solution. The product was crystallised from acetonitrile as yellow needles (0.60g, 80%). ^{1}H NMR (CD_2Cl_2, 400MHz) δ 0.86 (t, 6H, J = 7.00 Hz, CH$_3$), 1.18 (m, 4H, CH$_2$), 1.44 (m, 4H, CH$_2$), 3.53 (m, 4H, CH$_2$), 7.17 – 7.31 (m, 10H, Ar), 7.60 (s, 2H, NH). ^{13}C NMR (CD_2Cl_2, 100MHz) δ 14.20, 20.80, 30.53, 45.71, 129.14, 129.28, 130.04, 130.91, 131.69, 146.49, 183.49. MS (ES$^+$) 451 (M+H$^+$), 473 (M+Na$^+$) 923 (2M+Na$^+$). HRMS (ES$^+$) 473 (M+Na$^+$), Δ = 2.5 ppm. Anal. calcd. for $C_{26}H_{30}N_2OS_2$: C, 69.29; H, 6.71; N, 6.22. Found: C, 68.93, H, 6.67, N, 6.23. Mp: 184-185°C.

3,4-Diphenyl-furan-2,5-dicarboxylic acid diphenyl-thioamide (127): 3,4-Diphenyl-furan-2,5-dicarboxylic acid diphenyl-amide[139] **(125)** (0.77g, 1.7mmol) was suspended in freshly distilled tetrahydrofuran (100ml), Lawessons reagent (1.75g, 4.3mmol) was added and the solution heated at reflux for 24 hours. The solvent was removed *in vacuo* and the resulting solid suspended in dichloromethane (50ml). The organic layer was washed with water (3x20ml), dried with magnesium sulphate and the dichloromethane removed *in vacuo*. The resultant solid was purified using column chromatography on silica gel eluting with dichloromethane-2% methanol solution.

The product was crystallised from acetonitrile as red prisms and needles (0.64g, 78%). ^{1}H NMR (CD_2Cl_2, 400MHz) δ 7.25 – 7.55 (m, 20H, Ar), 9.37 (s, 2H, NH). ^{13}C NMR (CD_2Cl_2, 100MHz) δ 124.05, 127.54, 129.37, 129.41, 129.53, 131.02, 131.49, 138.89, 142.85, 147.16, 181.57. MS (ES$^+$) 491 (M+H$^+$), 1002 (2M+Na$^+$). HRMS (ES$^+$) 513 (M+Na$^+$), Δ = 2.3 ppm. Anal. calcd. for $C_{30}H_{22}N_2OS_2$ + MeCN : C, 72.29; H, 4.74; N, 7.90. Found: C, 71.91 H, 4.58, N, 7.84. Mp: 204-206°C.

Thiophene-2,5-dicarboxylic acid dibutyl-amide (130): Thiophene-2,5-dicarboxylic acid (3g, 17mmol) was suspended in freshly distilled thionyl chloride (100ml) and heated at reflux overnight. The excess thionyl chloride was removed *in vacuo* and the resulting solid dried under high vacuum for 2 hours. The thiophene-2,5-dicarbonyl dichloride was dissolved in dry dichloromethane (100ml). The solution was stirred under a nitrogen atmosphere and triethylamine (5.48g, 54.2mmol), DMAP (catalytic quantity) and n-butylamine (2.7g, 36.9mmol) were added. Upon addition of n-butylamine the solution was effervescent forming a solid, however the reaction was left stirring overnight. The solid was collected by filtration and washed with water (3 x 30ml) then with dichloromethane (2x15ml). A white material resulted affording the final product (3.8g, 77%). Further purification was achieved by crystallisation from methanol. ^{1}H NMR (DMSO-d_6, 300MHz) δ 0.89 (t, 6H, J = 7.29 Hz, CH_3), 1.31 (m, 4H, CH_2), 1.48 (m, 4H, CH_2), 3.21 (m, 4H, CH_2), 7.68 (s, 2H, CH), 8.56 (t, 2H, J = 5.46 Hz, NH). ^{13}C NMR (DMSO-d_6, 100MHz) δ 13.66, 19.60, 31.16, 38.81, 127.82, 143.17, 160.54. MS (ES$^+$) 283 (M+H$^+$), 461(M+2DMSO+Na$^+$). HRMS (ES$^+$) 587 (2M + Na$^+$), Δ = 0.4 ppm. Anal. calcd. for $C_{14}H_{22}N_2O_2S$: C, 59.54; H, 7.85; N, 9.92. Found: C, 59.69; H, 8.01; N, 9.59. Mp: decomp >225°C.

Thiophene-2,5-dicarboxylic acid diphenyl-amide (131): Thiophene-2,5-dicarboxylic acid (3g, 17mmol) was suspended in freshly distilled thionyl chloride (100ml) and heated at reflux overnight. The excess thionyl chloride was removed *in vacuo* and the resulting solid dried under high vacuum for 2 hours. The thiophene-2,5-dicarbonyl dichloride was dissolved in dry dichloromethane (100ml). The solution was stirred under a nitrogen atmosphere and triethylamine (5.48g, 54.2mmol), DMAP (catalytic quantity) and aniline (3.44g, 36.9mmol) were added. Upon addition of aniline the solution was effervescent forming a solid, however the reaction was left stirring overnight. The solid was collected by filtration and washed with water (3x30ml) then with dichloromethane (2x15ml) affording the final product as a white powder (4.3g, 76%). Further purification was achieved by crystallisation from dimethyl sulfoxide. ^{1}H NMR (DMSO-d_6, 300MHz) δ 7.13 (t, 2H, J = 7.26 Hz, Ar), 7.38 (t, 4H, J = 7.29 Hz, Ar), 7.74 (d, 4H, J = 7.29 Hz, Ar), 8.05 (s, 2H, CH), 10.40 (s, 2H, NH). ^{13}C NMR (DMSO-d_6, 100MHz) δ 120.52, 124.13, 128.77, 129.29, 138.41, 143.92, 159.36. MS (ES$^+$) 323 (M+H$^+$), 501(M+2DMSO+Na$^+$). HRMS (ES$^+$) 667 (2M + Na$^+$), Δ = 0.4 ppm. Anal. calcd. for $C_{18}H_{14}N_2O_2S$: C, 67.06; H, 4.38; N, 8.69. Found: C, 67.15; H, 4.58; N, 8.51. Mp: decomp >300°C.

Thiophene-2,5-dicarboxylic acid dibutyl-thioamide (132): Thiophene-2,5-dicarboxylic acid dibutyl-amide[143] **(130)** (1g, 3.5mmol) was suspended in freshly distilled tetrahydrofuran (200ml), Lawessons reagent (3.68g, 9.1mmol) was added and the solution heated at reflux for 24 hours. The solvent was removed *in vacuo* and the resulting solid suspended in dichloromethane (100ml). The organic layer was washed with water (3x20ml) dried with magnesium sulphate and the dichloromethane removed *in vacuo*. The product was obtained as a yellow solid, further purification was achieved by crystallisation of yellow needles from a dichloromethane solution. (0.93g, 84%) ^{1}H NMR (DMSO-d_6, 400MHz) δ 0.91 (t, 6H, J = 7.04 Hz, CH_3), 1.35 (m, 4H, CH_2), 1.64 (m, 4H, CH_2), 3.66 (m, 4H, CH_2), 7.62 (s, 2H, CH), 10.21 (t, 2H, J = 5.00 Hz, NH). ^{13}C NMR (DMSO-d_6, 100MHz) δ 13.67, 19.72, 29.37, 45.55, 124.34, 151.30, 185.87. MS (ES$^+$) 315 (M+H$^+$), 337 (M+Na$^+$), 651 (2M+Na$^+$). HRMS (ES$^+$) 315 (M+H$^+$), Δ = 1.8 ppm. Anal. calcd. for $C_{14}H_{22}N_2S_3$: C, 53.46, H, 7.05, N, 8.90. Found: C, 53.24, H, 7.03, N, 8.64. Mp: 166-168°C.

Thiophene-2,5-dicarboxylic acid diphenyl-thioamide (133): Thiophene-2,5-dicarboxylic acid diphenyl-amide[143] **(131)** (0.67g, 2.1mmol) was suspended in freshly distilled tetrahydrofuran (200ml), Lawessons reagent (4.4g, 18.2mmol) was added and the solution refluxed for 72 hours. The solvent was removed *in vacuo* and the resulting solid suspended in dichloromethane (100ml). The organic layer was washed with water (3x20ml) dried with magnesium sulfate and the dichloromethane removed *in vacuo*. The solid was purified by precipitation from hot acetonitrile (150ml) the product was obtained as an orange solid (0.55g, 74%). Further purification was achieved by crystallisation from a dimethyl sulfoxide solution. ^{1}H NMR (DMSO-d_6, 300MHz) δ 7.28 – 7.71 (m, 10H, Ar), 7.88 (s, 2H, CH), 11.70 (s, 2H, NH). ^{13}C NMR (DMSO-d_6, 75MHz) δ 124.98, 125.17, 126.68, 128.64, 139.26, 153.28, 186.01. MS (ES$^-$) 353 (M-H)$^-$, 707 (2M-H)$^-$. HRMS (ES$^-$) 353 (M-H)$^-$, Δ = 2.6 ppm. Anal. calcd. for $C_{18}H_{14}N_2S_3$ requires C, 60.99, H, 3.98, N, 7.90. Found: C, 60.86, H, 3.99, N, 8.08. Mp: 357-359°C.

Thiophene-2,4-dicarboxylic acid dibutyl-amide (138): Thiophene-2,4-dicarboxylic acid[146,147] (0.45g, 2.6mmol) was suspended in freshly distilled thionyl chloride (30ml) and refluxed overnight. The excess thionyl chloride was removed *in vacuo* and the resulting solid dried under high vacuum for a couple of hours. The thiophene-2,4-dicarbonyl dichloride was dissolved in dry dichloromethane (20ml) and stirred under a nitrogen atmosphere. To the solution triethylamine (0.81g, 8mmol), DMAP (catalytic quantity) and n-butylamine (0.41g, 5.5mmol) were added. After stirring overnight triethylammoniumhydrochloride was removed by filtration and the organic solution washed with brine (2x50ml). The dichloromethane solvent was removed *in vacuo* leaving an oil. The oil was triturated in ether (50ml) to precipitate a solid that was collected by filtration. The dark solid was dissolved in dichloromethane (20ml), ether (100ml) was added to precipitate the product as a beige solid (0.34g, 46%). ^{1}H NMR (DMSO-d_6, 300MHz) δ 0.89 (t, J = 6.36 Hz, 6H, CH_3), 1.32 (m, 4H, CH_2), 1.49 (m, 4H, CH_2), 3.21 (m, 4H, CH_2), 8.09 (s, 1H, CH), 8.24 (s, 1H, CH), 8.34 (t, J = 6.39 Hz, 1H, NH), 8.59 (t, J = 5.46 Hz, 1H, NH). ^{13}C NMR (DMSO-d_6, 100MHz) δ 13.63, 13.66, 19.54, 19.59, 31.08, 31.21, 38.53, 38.74, 127.65, 131.03, 138.31, 140.29, 160.62, 161.67. MS (ES$^+$) 283 (M+H$^+$), 565(2M+H$^+$). HRMS (ES$^+$) 587 (2M + Na$^+$), Δ = 1.2 ppm. Anal. calcd. for $C_{14}H_{22}N_2O_2S$ + 0.125 CH_2Cl_2 : C, 57.90; H, 7.65; N, 9.56. Found: C, 57.95; H, 7.55; N, 9.43. Mp: 113-115°C.

Thiophene-2,4-dicarboxylic acid diphenyl-amide (139): Thiophene-2,4-dicarboxylic acid[146,147] (0.45g, 2.6mmol) was suspended in freshly distilled thionyl chloride (30ml) and refluxed overnight. The excess thionyl chloride was removed *in vacuo* and the resulting solid dried under high vacuum for a couple of hours. The thiophene-2,4-dicarbonyl dichloride was dissolved in dry dichloromethane (20ml) and stirred under a nitrogen atmosphere. To the solution triethylamine (0.81g, 8mmol), DMAP (catalytic quantity) and aniline (0.51 g, 5.5mmol) were added. Although a white solid precipitated almost instantaneously upon addition of aniline the solution was stirred overnight. The solid was collected by filtration and washed with water (2x10ml) then with dichloromethane (2x15ml) affording the desired product as a white powder (0.49g, 59%). Crystallisation was achieved by slow evaporation from a dimethyl sulfoxide solution. ^{1}H NMR (DMSO-d_6, 300MHz) δ 7.11 (m, 2H, Ar), 7.37 (m, 4H, Ar), 7.75 (m, 4H, Ar), 8.53 (s, 1H, CH), 8.63 (s, 1H, CH), 10.26 (s, 1H, NH), 10.46 (s, 1H, NH). ^{13}C NMR (DMSO-d_6, 100MHz) δ 120.27, 120.32, 123.74, 123.86, 128.67, 128.69, 129.13, 133.69, 138.22, 138.61, 138.81, 140.45, 159.45, 160.51. MS (ES$^-$) 341 (M+F$^-$), 435 (M+TFA$^-$). HRMS (ES$^+$) 667 (2M + Na$^+$), Δ = 2.6 ppm. Anal. calcd. for $C_{18}H_{14}N_2O_2S$ + 0.05 CH_2Cl_2 requires C, 66.37; H, 4.35; N, 8.58. Found: C, 66.40; H, 4.27; N, 8.66. Mp: 233-235°C.

Thiophene-2-carboxylic acid phenyl-amide (142): Thiophene-2-carboxylic acid (3g, 23mmol) was suspended in freshly distilled thionyl chloride (50ml) and refluxed overnight. The excess thionyl chloride was removed *in vacuo* and the resulting solid dried under high vacuum for 2 hours. The thiophene-2-carbonyl chloride was dissolved in dry dichloromethane (50ml). The solution was stirred under a nitrogen atmosphere and triethylamine (4g, 40mmol), DMAP (catalytic quantity) and aniline (2.79g, 30mmol) were added. Upon addition of aniline the solution was effervescent, however the reaction was left stirring overnight. The solution was washed with water (2x50ml). The organic layer was dried with magnesium sulphate and then filtered before removing the solvent *in vacuo* until a solid precipitated. To the slurry diethylether (40ml) was added and the suspension filtered. The solid was washed with dichloromethane (2x10ml) then with ether (2x10ml). An off white material resulted affording the final product (3.02g, 65%). Further purification was achieved by crystallisation from a dimethyl sulfoxide solution. ^{1}H NMR (MeCN-d_3, 400MHz) δ 7.12 – 7.79 (m, 8H, Ar overlapping signals), 8.69 (s, 1H, NH). ^{13}C NMR ($CDCl_3$, 100MHz) δ 120.34, 124.78, 127.96, 128.60, 129.26, 130.86, 137.74, 139.42, 160.03. MS (ES$^-$) 238 (M+Cl$^-$), 316(M+TFA$^-$). HRMS (ES$^+$) 204 (M+H$^+$), Δ = 0.4 ppm. Anal. calcd. for $C_{11}H_9NOS$: C, 65.00; H, 4.46; N, 6.89. Found: C, 64.86; H, 4.41; N, 6.89. Mp: 131-133°C.

3,4-Diphenyl-thiophene-2,5-dicarboxylic acid diphenyl-amide (145): 3,4-Diphenyl-thiophene-2,5-dicarboxylic acid[140] (2.5g, 7.7mmol) was suspended in freshly distilled thionyl chloride and refluxed overnight. The excess thionyl chloride was removed *in vacuo* and the resulting solid dried under high vacuum for a couple of hours. The 3,4-diphenyl-thiophene-2,5-dicarbonyl dichloride was dissolved in dry dichloromethane (120ml) under a nitrogen atmosphere. To the solution triethylamine (1.5g, 15mmol), DMAP (catalytic quantity) and aniline (0.93g, 10mmol) were added and stirred overnight. The organic solution was washed with brine (4x50ml) dried with magnesium sulfate and the dichloromethane solvent removed *in vacuo*. Acetonitrile (60ml) was added leaving an undissolved solid that was collected by filtration and washed with cold acetonitrile (2x20ml) affording the final product as a beige powder. Further purification was achieved by crystallisation from hot acetonitrile (2.14g, 58%). ^{1}H NMR (DMSO-d_6, 300MHz) δ 7.04 – 7.39 (m, 20H, Ar), 9.70 (s, 2H, NH). ^{13}C NMR (DMSO-d_6,100MHz) δ 119.66, 124.10, 127.85, 128.05, 128.73, 129.88, 134.00, 135.40, 138.10, 142.01, 160.09. MS (ES$^-$) 509 (M+Cl$^-$), 587 (M+TFA$^-$). HRMS (ES$^+$) 475 (M+H$^+$), Δ = 1.3 ppm. Anal. calcd. for $C_{30}H_{22}N_2O_2S$ + 0.03 MeCN : C, 75.88; H, 4.68; N, 5.98. Found: C, 75.42; H, 4.53; N, 5.89. Mp: 234-236°C.

5.3.3 Synthesis included in chapter 4

3,4-Diphenyl-1*H*-pyrrole-2,5-dicarboxylic acid diferrocenylmethyl-amide (152): 3,4-Diphenyl-1H-pyrrole-2,5-dicarboxylic acid[154] (1g, 3.2mmol) was refluxed in thionyl chloride (0.84g, 7.2 mmol) overnight, the excess thionyl chloride was removed *in vacuo*. The resulting 3,4-diphenyl-1H-pyrrole-2,5-dicarbonyl dichloride (1.2g, 3.2mmol) was dissolved in dry dichloromethane (50ml). The solution was stirred under a nitrogen atmosphere and triethylamine (0.711g, 7mmol), DMAP (catalytic quantity) and ferrocenemethylamine[155] (1.51 g, 7mmol) were added. The reaction mixture was stirred overnight under a nitrogen atmosphere. The dichloromethane solvent was removed *in vacuo* and the residue dissolved in acetonitrile (50ml). The resultant precipitate was filtered, washed with acetonitrile (3x15ml) and water (3x15ml) and dried under high vacuum for two hours. The precipitate was purified by preparative layer chromatography on silica plates eluted with dichloromethane/methanol 2% affording the final product as an orange powder (0.69g, 31%). Crystallisation was achieved by slow evaporation from dichloromethane solution. ^{1}H NMR (CD_2Cl_2, 300MHz) δ 3.89 (s, 4H, FcH), 3.96 (s, 10H, FcH), 4.04 (s, 4H, FcH), 4.10 (d, 4H, J = 5.46 Hz, CH_2), 5.75 (br. s, 2H, NH_{amide}), 7.21-7.31 (m, 10H, Ar), 10.21 (s, 1H, $NH_{pyrrole}$). ^{13}C NMR ($CDCl_3$, 100MHz) δ (ppm): 38.92, 67.48, 68.01, 68.60, 84.85, 123.99, 125.88, 128.17, 129.03, 130.96, 133.38, 159.99. MS (ES^+) 701 (M^+). HRMS 701 (M^+), Δ = 2.0 ppm. Anal. calcd. for $C_{40}H_{35}Fe_2N_3O_2$ + 0.5 CH_2Cl_2 : C, 65.39; H, 4.88; N, 5.65. Found: C, 65.59; H, 4.88; N, 5.47. Mp: decomp >200°C.

3,4-Diphenyl-1*H*-pyrrole-2,5-dicarboxylic acid bis-ferrocenylamide (153): 3,4-Diphenyl-1H-pyrrole-2,5-dicarboxylic acid[154] (0.74g, 2.4mmol) was refluxed in thionyl chloride (0.63g, 5.4mmol) overnight, the excess thionyl chloride was removed *in vacuo*. The resulting 3,4-diphenyl-1H-pyrrole-2,5-dicarbonyl dichloride (0.83g, 2.4mmol) was dissolved in dry dichloromethane (50ml). The solution was stirred under a nitrogen atmosphere and triethylamine (0.487g, 4.8mmol), DMAP (catalytic quantity) and ferrocenylamine[101,156] (0.9g, 4.8mmol) were added. The reaction mixture was stirred overnight under a nitrogen atmosphere. The dichloromethane solvent was removed *in vacuo*, acetonitrile (80ml) was added to the residue and then filtered. Water (100ml) was added to the solution separating the product from solution as an oil. The oil was dissolved in acetone, dried with magnesium sulphate, filtered and the organic solvent removed *in vacuo*. Further purification by column chromatography on silica gel eluted with dichloromethane:methanol (98:2) afforded the final product as an orange powder (0.21g, 13%). Crystallisation was achieved by slow evaporation from dichloromethane solution. ^{1}H NMR ($CDCl_3$, 300MHz) δ 3.95 (t, 4H, J = 1.5 Hz, FcH), 4.02 (m, 10H, FcH), 4.32 (t, 4H, J = 1.98 Hz, FcH), 6.69 (s, 2H, NH_{amide}), 7.36-7.49 (m, 10H, Ar), 10.29 (s, 1H, $NH_{pyrrole}$). ^{13}C NMR ($CDCl_3$, 75MHz) δ 62.27, 65.04, 69.26, 93.09, 124.48, 126.13, 128.69, 129.29, 131.00, 133.30, 158.39. MS (ES^+) 673 (M^+). HRMS 673 (M^+), Δ = 0.4 ppm. Anal. calcd. for $C_{38}H_{31}Fe_2N_3O_2$ + 1.2 CH_2Cl_2

requires C, 60.73; H, 4.34; N, 5.42. Found: C, 61.11; H, 4.11; N, 5.32. Mp: decomp >200°C.

3,4-Diphenyl-1H-pyrrole-2,5-dicarboxylic acid monomethyl ester (155): 3,4-Diphenyl-1H-pyrrole-2,5-dicarboxylic acid dimethyl ester[154] **(154)** (4g, 11.9mmol) was suspended in methanol (200ml). The suspension was magnetically stirred and heated to reflux to form a solution. Potassium hydroxide (0.67g, 11.9mmol) was added in water (50ml). After refluxing overnight, the solution was left to cool to room temperature. The solution was acidified to pH 1 using concentrated hydrochloric acid, forming a white precipitate. This was removed by filtration and washed with water (3x50ml). The white solid was dissolved in ether, and the aqueous layer that formed was removed. The organic layer was dried with magnesium sulphate, filtered and then the solvent removed *in vacuo*. The product was obtained as a white powder (3g, 78%). Crystallisation was achieved from slow evaporation of dichloromethane:methanol (1:1) solution, and also from a solution of ethylacetate:acetone (3:1) giving polymorphic structures. ^{1}H NMR (DMSO-d_6, 400MHz) δ 3.64 (s, 3H, CH_3), 7.02-7.18 (m, 10H, Ar), 12.15 (s, 1H, NH), 12.45 (s, 1H, OH). ^{13}C NMR (DMSO-d_6, 100MHz) δ 51.26, 121.10, 121.68, 122.87, 126.39, 126.49, 126.58, 127.09, 127.11, 127.16, 129.83, 130.34, 130.40, 130.53, 130.66, 133.29, 133.46, 133.68, 160.30, 161.34. MS (ES^-) 320 $(M-H)^-$, 641 $(2M-H)^-$. HRMS (ES^+) 344 ($M+Na^+$), $\Delta = 0.5$ ppm. Anal. calcd. for $C_{19}H_{15}NO_4 + 0.33\ H_2O$: C, 69.72; H, 4.82; N, 4.28. Found: C, 69.82; H, 4.70; N, 4.22. Mp: decomp >220°C.

5-(Ferrocenylmethyl-carbamoyl)-3,4-diphenyl-1*H*-pyrrole-2-carboxylic acid methyl ester (156): 3,4-Diphenyl-1H-pyrrole-2,5-dicarboxylic acid monomethyl ester[157] **(155)** (1.49g, 4.7mmol), ferrocenemethylamine (1g, 4.7mmol) were magnetically stirred under a nitrogen atmosphere in dimethylformamide (50ml). Benzotriazol-1-yloxytripyrrolidinophosphonium hexafluorophosphate (2.45g, 4.7mmol), triethylamine (0.47g, 4.7mmol) and a catalytic quantity of 1-hydroxybenzotriazole hydrate were added and the solution stirred in the dark. After 72 hours the solvent was removed under high vacuum. Acetonitrile (50ml) was added and a precipitate formed. The orange solid was collected by filtration and washed with acetonitrile (3x15ml). Column chromatography on silica gel eluting with dichloromethane-2% methanol isolated the compound (1.66g, 69%). Further purification was achieved through crystallisation, by slow evaporation of dichloromethane:methanol (2:1) solution of the product. ^{1}H NMR ($CDCl_3$, 300MHz) δ 3.79 (s, 3H, CH_3), 3.89 (s, 2H, FcH), 3.97 (s, 5H, FcH), 4.05 (s, 2H, FcH), 4.17 (d, 2H, J = 5.49Hz, CH_2), 5.90 (s, 1H, NH_{amide}), 7.11-7.33 (m, 10H, Ar), 10.12 (s, 1H, $NH_{pyrrole}$). ^{13}C NMR (CD_2Cl_2, 100MHz) δ 39.46, 52.18, 68.02, 68.64, 69.24, 85.25, 120.77, 125.93, 126.58, 127.61, 128.01, 128.91, 129.70, 131.46, 131.70, 132.10, 134.04, 134.12, 160.22, 161.34. MS (ES$^+$) 518 (M$^+$). HRMS (ES$^+$) 518 (M$^+$), Δ = 2.0 ppm. Anal. calcd. for $C_{30}H_{26}FeN_2O_3$: C, 69.51; H, 5.06; N, 5.40. Found C, 69.06; H, 4.81; N, 5.12. Mp: decomp >190°C.

5-(Ferrocenylmethyl-carbamoyl)-3,4-diphenyl-1H-pyrrole-2-carboxylic acid (158): 5-(ferrocenylmethyl-carbamoyl)-3,4-diphenyl-1H-pyrrole-2-carboxylic acid methyl ester[157] **(156)** (1.2g, 2.3mmol) was suspended in methanol (75ml) and heated to reflux under a nitrogen atmosphere. Potassium hydroxide (0.13g, 2.3mmol) was added in water (20ml). After refluxing overnight the solution was left to cool on an ice-bath. Hydrochloric acid was added to the solution until it reached pH 1 and the resulting solid collected by filtration. The solid was dissolved in chloroform (100ml) and the aqueous layer that formed from residual water in the solid separated. The organic layer was dried with magnesium sulphate and then filtered before the solvent was removed *in vacuo*. Triturating in acetonitrile (200ml) left a yellow solid that was collected by filtration affording the product (0.36g). The remaining acetonitrile solution was reduced *in vacuo*, and the resulting solid was purified by column chromatography on silica gel eluting with dichloromethane-2% methanol. This gave a second crop of material (0.2g) giving a total yield of (0.56g, 48%). Crystallisation was achieved by slow evaporation of a benzene solution. ^{1}H NMR ($CDCl_3$, 300MHz) δ 3.87 (d, 2H, J = 1.83 Hz, FcH), 3.96 (s, 5H, FcH), 4.04 (d, 2H, J = 1.83 Hz, FcH), 4.14 (d, 2H, J = 5.46 Hz, CH_2), 5.91 (t, 1H, J = 5.46 Hz, NH_{amide}), 7.12-7.31 (m, 10H, Ar), 10.41 (s, 1H, pyrrole NH). ^{13}C NMR (DMSO-d_6, 100MHz) δ 37.87, 48.57, 67.34, 67.91, 68.31, 85.35, 121.57, 124.84, 126.02, 126.23, 126.90, 127.36, 129.08, 130.64, 130.76, 134.34, 159.48, 162.28. MS (ES$^+$) 504 (M$^+$), 527 (M+Na$^+$). HRMS: (ES$^+$) 504 (M$^+$), Δ = 0.9 ppm. Anal. calcd. for $C_{29}H_{24}FeN_2O_3$ + 0.56 CH_2Cl_2 : C, 64.36; H, 4.59; N, 5.08. Found: C, 64.18; H, 4.50; N, 5.12. Mp: decomp >120°C.

3,4-Diphenyl-1*H*-pyrrole-2,5-dicarboxylic acid 2-ferrocenylmethyl-amide 5-phenylamide (160): 5-(Ferrocenylmethyl-carbamoyl)-3,4-diphenyl-1H-pyrrole-2-carboxylic acid[157] **(158)** (0.45g, 0.9mmol) and aniline (0.083g, 0.9mmol) were magnetically stirred under nitrogen in dimethylformamide (30ml). Benzotriazol-1-yloxytripyrrolidinophosphonium hexafluorophosphate (0.494g, 0.95mmol), triethylamine (0.09g, 0.9mmol) and a catalytic quantity of 1-hydroxybenzotriazole hydrate were added and the flask stirred in the dark. After 72 hours the solvent was removed under high vacuum. Acetonitrile (50ml) was added and a precipitate formed. The orange solid was collected by filtration and washed with acetonitrile (3x15ml). The solid was purified by column chromatography on silica gel eluting with dichloromethane-2% methanol. Crystallisation was achieved by slow evaporation of an acetonitrile:dichloromethane (2:1) solution yielding the pure product (0.07g, 14%). ^{1}H NMR (CD_2Cl_2, 300MHz) δ 3.88 (s, 2H, FcH), 3.95 (s, 5H, FcH), 4.04 (s, 2H, FcH), 4.13 (d, 2H, *J* = 5.46, CH_2), 5.80 (s, 1H, $NH_{methylferrocene\ amide}$), 7.00-7.43 (m, 16H, Ar and NH), 10.31 (s, 1H, $NH_{pyrrole}$). ^{13}C NMR (DMSO-d_6, 100MHz) δ 38.17, 67.60, 67.68, 68.53, 85.34, 119.58, 123.65, 124.39, 124.62, 126.47, 126.77, 127.23, 127.76, 128.04, 128.28, 128.90, 130.73, 130.83, 134.02, 134.12, 138.89, 158.75, 159.88. MS (ES$^+$) 579 (M$^+$). HRMS (ES$^+$) 579 (M$^+$), Δ = 1.1 ppm. Anal. calcd. for $C_{35}H_{29}FeN_3O_2$ + 0.16 CH_2Cl_2 requires C, 71.35; H, 4.99; N, 7.10. Found: C, 71.28; H, 4.94; N, 7.06. Mp: decomp >190°C.

5-(Ferrocenyl-carbamoyl)-3,4-diphenyl-1*H*-pyrrole-2-carboxylic acid methyl ester (157): 3,4-Diphenyl-1H-pyrrole-2,5-dicarboxylic acid monomethyl ester[157] **(155)** (1.76g, 5.5mmol), ferrocenylamine (1.1g, 5.5mmol) were magnetically stirred under nitrogen in dimethylformamide (50ml). Benzotriazol-1-yloxytripyrrolidinophosphonium hexafluorophosphate (2.86g, 5.5mmol), triethylamine (0.55g, 5.5mmol) and a catalytic quantity of 1-hydroxybenzotriazole hydrate were added and the flask stirred in the dark. After 72 hours the solvent was removed under high vacuum. The resultant oil was purified using flash column chromatography on silica gel eluting with dichloromethane-2% methanol. After drying under high vacuum the product was obtained as a foam (2.49g, 79%). Crystallisation was achieved by slow evaporation of an ether:dichloromethane (4:1) solution. ^{1}H NMR ($CDCl_3$, 300MHz) δ 3.79 (s, 3H, CH_3), 3.96 (s, 2H, FcH), 4.02 (s, 5H, FcH), 4.31 (s, 2H, FcH), 6.75 (s, 1H, NH_{amide}), 7.21-7.46 (m, 10H, Ar), 10.08 (s, 1H, pyrrole NH). ^{13}C NMR ($CDCl_3$, 75MHz) δ 29.82, 51.81, 62.24, 65.11, 69.30, 120.32, 127.19, 127.54, 127.64, 127.72, 127.93, 128.67, 128.95, 129.30, 130.68, 130.82, 131.14, 131.71, 132.88, 133.43, 158.28, 160.84. MS (ES^+) 504 (M^+). HRMS (ES^+) 504 (M^+), Δ = 1.5 ppm. Anal. calcd. for $C_{29}H_{24}FeN_2O_3$: C, 69.06; H, 4.80; N, 5.55. Found: C, 69.18; H, 4.64; N, 6.12. Mp: decomp >190°C.

5-(Ferrocenyl-carbamoyl)-3,4-diphenyl-1*H*-pyrrole-2-carboxylic acid (159): 5-(ferrocenyl-carbamoyl)-3,4-diphenyl-1*H*-pyrrole-2-carboxylic acid methyl ester[157] **(157)** (2.4g, 4.8mmol) was dissolved in methanol (125ml), and heated to reflux under a nitrogen atmosphere. Sodium hydroxide (6g, 0.15mol) was added in water (120ml). The solution was kept at 95 °C for 2 hours then left to cool. Hydrochloric acid was added to the solution until it reached pH 1 forming a precipitate. The solid was collected by filtration and dissolved in dichloromethane (200ml) and the resulting aqueous layer separated. The organic layer was dried with magnesium sulphate and then filtered before the solvent was removed *in vacuo* and the product dried under high vacuum (1.15g, 49%). Crystallization was achieved by slow evaporation of a chloroform:dichloromethane (1:1) solution. ^1H NMR ($CDCl_3$, 300MHz) δ 3.98 (s, 2H, FcH), 4.03 (s, 5H, FcH), 4.31 (s, 2H, FcH), 6.82 (s, 1H, NH_{amide}), 7.22-7.48 (m, 10H, Ar), 10.37 (s, 1H, OH), 10.82 (s, 1H, $NH_{pyrrole}$). ^{13}C NMR ($CDCl_3$, 100MHz) δ 62.26, 65.15, 69.32, 120.43, 125.84, 126.87, 127.23, 127.59, 127.91, 128.33, 128.67, 129.29, 130.70, 131.14, 131.12, 132.49, 132.71, 133.29, 158.56, 164.52. MS (ES^+) 490 (M^+). HRMS (ES^+) 490 (M^+), Δ = 0.5 ppm. Anal. calcd. for $C_{28}H_{22}FeN_2O_3$ + 0.33 CH_2Cl_2 : C, 65.61; H, 4.41; N, 5.40. Found: C, 65.36; H, 4.67; N, 5.28. Mp: decomp >170°C.

3,4-Diphenyl-1*H*-pyrrole-2,5-dicarboxylic acid 2-ferrocenylamide 5-phenylamide (161): 5-(ferrocenyl-carbamoyl)-3,4-diphenyl-1*H*-pyrrole-2-carboxylic acid[157] **(159)** (0.8g, 1.6mmol) and aniline (0.15g, 1.6mmol) were magnetically stirred under nitrogen in dimethylformamide (50ml). Benzotriazol-1-yloxytripyrrolidinophosphonium hexafluorophosphate (0.85g, 1.6mmol), triethylamine (0.17g, 1.6mmol) and a catalytic quantity of 1-hydroxybenzotriazole hydrate were added and the flask stirred in the dark. After 72 hours the solvent was removed under high vacuum. The residue was dissolved in acetonitrile (50ml) to which water (50ml) was added. The solution was separated with dichloromethane (6x50ml) and the organic layer dried over magnesium sulphate before removing the solvent *in vacuo*. The resultant oil was purified using column chromatography on silica gel eluting with dichloromethane-2% methanol. Crystallization was achieved from a methanol:dichloromethane (95:5) solution, giving the desired compound (0.35g, 38%). ^{1}H NMR ($CDCl_3$, 300MHz) δ 3.97 (s, 2H, FcH), 4.04 (s, 5H, FcH), 4.33 (s, 2H, FcH), 6.72 (s, 1H, $NH_{ferrocenyl\ amide}$), 7.05-7.48 (m, 16H, Ar and NH_{amide}), 10.37 (s, 1H, $NH_{pyrrole}$). ^{13}C NMR (CD_2Cl_2, 100MHz) δ 53.52, 62.25, 65.02, 69.23, 92.98, 119.31, 124.25, 124.46, 124.79, 126.13, 126.41, 128.36, 128.69, 128.76, 129.10, 129.26, 130.96, 131.12, 133.00, 133.19, 137.59, 158.01, 158.32. MS (ES^+) 565 (M^+), 1153 ($2M+Na^+$). HRMS (ES^+) 566 ($M+H^+$), Δ = 2.2 ppm. Anal. calcd. for $C_{34}H_{27}FeN_3O_2$ + 0.33 CH_2Cl_2 : C, 69.45; H, 4.70; N, 7.08. Found: C, 69.36; H, 5.07; N, 7.00. Mp: decomp >190°C.

5.4 General method used for an NMR titration

All the ^{1}H NMR titration experiments were performed on a Bruker AM300 NMR spectrometer. The anions were added as their tetrabutylammonium salts and would be dried under high vacuum overnight without heating. The receptor would be made up as a 0.01 M solution in a cooled yet previously oven dried NMR tube (5mm), the top would be sealed using a suba-seal rubber septum which was secured using laboratory film. The anion would be made up as a 0.1 M solution in a separate vial, the lid was made airtight so that the concentration would not change through the evaporation of solvent. These solutions can be made quite simply; (1) for the receptor, molecular mass of the receptor/200 gives the required mass in mg to be dissolved in 500 μl of the chosen solvent. (2) for the anion, molecular mass of the salt/10 gives the required mass in mg to be dissolved in 1ml of the same solvent. Small aliquots of the anionic guest would be introduced via syringe addition to the NMR tube after which a proton NMR spectrum of the receptor:anion solution would be recorded. The chemical shift of proton resonances believed to be involved in hydrogen bonding were recorded and the resulting data subsequently processed using the EQNMR[118] program to calculate both the association constant and corresponding errors. The titration would be repeated if the error was estimated to be > 15%.

5.5 Electrochemistry experimental details

5.5.1 For experiments included in chapter 2

Although the electrochemistry experiments from this chapter were performed by R. Zimmerman and Dr. P. Gale, the experimental details have been included for completeness. The electrochemical measurements were performed under dry argon using a Bioanalytic Systems Inc. (BAS) CV-50W Version 2 MF 9093 Voltammetric Analyzer. The voltammograms were recorded at room temperature, using a 1.6 mm diameter platinum disk working electrode and a platinum gauze counter electrode. A silver/silver chloride couple, separated from the bulk solution by means of a porous Vycor plug, was used as the reference electrode. A solution of acetonitrile/dimethyl sulfoxide (9:1) containing 0.5 mM ferrocene calix[4]pyrrole compound, 1.5 mM tetrabutylamonium salt of the anion of interest and 0.1 M tetrabutylammonium hexafluorophosphate supporting electrolyte were purged with argon between recordings and kept under an argon blanket during recordings. The cyclic voltammograms were recorded using a scan rate of 100 mV s^{-1}.

5.5.2 For experiments included in chapter 4

The experiments were conducted inside a Faraday cage, with this and all electronic equipment earthed to minimise electronic noise. The steady state voltammograms were recorded at room temperature, using a scan rate of 20 mV s^{-1}, with a 25 μm diameter platinum microdisc electrode that was prepared following literature methods.[152] A silver wire located in a separate compartment with 0.1 M silver nitrate solution (dry acetonitrile) was used as the counter-reference electrode. The potential was controlled using a HiTek PPR1 waveform generator and the current measured using a homemade current follower. The voltammograms were carried out and recorded on a computer fitted with an Advantek PCL-818L data acquisition card, running a University of Southampton electrochemistry data-acquisition program.[162] When new solutions were introduced to the electrochemical cell (three neck pear shaped flask) the microdisc was cleaned using 0.3 μm alumina on a polishing microcloth. Before each voltammogram the electrode was held at - 2.5 V for 12 seconds then at - 0.175 V for 12 seconds. We found that this pre-treatment was essential to record reproducible voltammograms. Dichloromethane solutions containing 0.5 mM ferrocene compound, 1.5 mM tetrabutylamonium salt of the anion of interest and 0.1 M tetrabutylammonium tetrafluoroborate supporting electrolyte were purged with argon between recordings and kept under an argon blanket during recordings. To ensure that the measurements were reproducible a series of voltammograms were recorded for each solution.

Conclusion

This thesis reports work on the synthesis of neutral organic molecules that are able to bind and/or sense various anions through hydrogen bond formation. These anion receptors/sensors displayed strong and selective binding towards specific anionic substrates, in concordance with the projects initial aims.

The *meso*-substituted calix[4]pyrrole derivatives (Chapter 2) yielded interesting results. The ferrocene appended receptors **110-111** showed a downfield shift (NMR) of a ferrocene CH resonance that suggested a direct coordination mechanism may operate between the bound anion and the redox-active group. While the pentapyrrolic calix[4]pyrrole species **118** exhibited a high affinity for carboxylates. Calix[4]pyrroles typically show a strong affinity for spherical anions such as fluoride and chloride, this result illustrates how synthetic modification of a receptor binding site can dramatically alter the observed anion selectivity. It is thought that the selectivity of **118** arises from interaction of the receptor with both oxygen atoms of the carboxylate anion. A similar effect may explain the large cathodic shift (100 mV) of the redox couple of compound **110** in the presence of dihydrogen phosphate.

The ferrocene appended pyrrole amide clefts (Chapter 4) **153** and **161** revealed large cathodic shifts of 122 and 150 mV respectively upon the addition of benzoate. These receptors could electrochemically differentiate benzoate, from the other oxo-anions, hydrogen sulfate (37 and 29 mV respectively) and dihydrogen phosphate (distorted wave). Differently to **110**, it is thought that the binding process is relayed to the reporter groups in these receptors via a through-bond mechanism. The neutral receptors displayed selectivity for oxo-anions in deuterated dichloromethane solution.

The introduction of the heteroatom between the two amide groups of the structurally analogous furan and thiophene amide clefts (Chapter 3) revealed a dramatic change in selectivity. The oxo-anion selectivity seen for the pyrrole derivatives, was exchanged for fluoride in the case of the furan derivatives **124-127** yet maintained in the case of the thiophene derivatives **130-133** (although it was weak binding). A crystal structure revealed the formation of a thiophene CH···anion hydrogen bond in the solid state. New derivatives **138** and **139** were synthesised to utilise this hydrogen bond donor, this was proved successful with a significant increase in dihydrogen phosphate binding. This was believed to be due to the formation of three hydrogen bonds from the host to the guest in a manner analogous to that of the pyrrole amide clefts.

Finally in conclusion, a selection of relatively simple anion receptors/sensors have been synthesised from readily available starting reagents in good yield. They have been shown to function as selective anion receptors/sensors in various solvent media (including mixtures). The full synthesis and characterisation details of these compounds can be found in the experimental chapter 5, and where appropriate the crystallographic data may be found in the appendix.

Appendix: Crystal data

A.1 Introduction

The crystal structures reported in this thesis were solved by the EPSRC Crystallographic Service at the University of Southampton. The refinement of the structures and the fractional co-ordinates are reported here for the sake of completeness and so that the structures may be regenerated from the text of this thesis if necessary.

Some of the crystal structures have been deposited onto the CCDC database, the corresponding numbers are listed below. The crystal pictures throughout this thesis were generated using the free Mercury software version 1.1.1 available at www.ccdc.ac.uk.

110 -164777, **124** - 229150 and 229151, **125** - 195420, **126** - 229144, **127** - 229149, **130** - 209227, **131** - 209225, **133** - 229145, **131:F** - 209226, **139** - 229148, **142** - 229146, **145** - 229147, **153** – 184544, **156** - 189978, **157** - 189977, **159** - 189979, **160** - 189976, **161** - 189980.

A.2 Crystal data

5,10,15,20-tetramethyl-5,10,15,20-tetraferrocenyl-calix[4]pyrrole (αααα isomer)

Identification code	**(109) Crystallised from DMSO**	
Empirical formula	$C_{72}H_{84}Fe_4N_4O_4S_4$	
Formula weight	1421.07	
Temperature	150(2) K	
Wavelength	0.71073 Å	
Crystal system	Monoclinic	
Space group	*C2/c*	
Unit cell dimensions	a = 28.2703(5) Å	
	b = 15.1700(4) Å	β = 112.92°
	c = 33.6410(8) Å	
Volume	13287.8(5) Å^3	
Z	8	
Density (calculated)	1.421 Mg / m^3	
Absorption coefficient	1.034 mm^{-1}	
F(000)	5952	
Crystal	Colourless block	
Crystal size	0.05 × 0.05 × 0.05 mm^3	
θ range for data collection	2.99 – 23.26°	
Index ranges	$-31 \leq h \leq 30$, $-16 \leq k \leq 16$, $-37 \leq l \leq 37$	
Reflections collected	30555	
Independent reflections	9504 [R_{int} = 0.1019]	
Completeness to θ = 23.26°	99.6 %	
Max. and min. transmission	0.9501 and 0.9501	
Refinement method	Full-matrix least-squares on F^2	
Data / restraints / parameters	9504 / 69 / 804	
Goodness-of-fit on F^2	1.084	
Final R indices [$F^2 > 2\sigma(F^2)$]	$R1$ = 0.1011, $wR2$ = 0.2802	
R indices (all data)	$R1$ = 0.1707, $wR2$ = 0.3287	
Extinction coefficient	0.00000(6)	
Largest diff. peak and hole	2.864 and –1.720 e Å^{-3}	

Table A.1: Structure and refinement data.

Atom	x	y	z	U_{eq}	$S.o.f.$
Fe1	737(1)	5788(1)	1308(1)	28(1)	1
Fe2	1960(1)	5162(1)	276(1)	26(1)	1
Fe3	3068(1)	−1606(1)	1516(1)	28(1)	1
Fe4	1712(1)	−1000(1)	2557(1)	38(1)	1
C1	1271(5)	5696(8)	1923(4)	40(3)	1
C2	964(4)	4932(7)	1811(3)	27(3)	1
C3	1021(4)	4534(7)	1448(3)	28(3)	1
C4	1355(4)	5054(7)	1343(3)	29(3)	1
C5	1508(4)	5787(7)	1629(4)	33(3)	1
C6	−32(5)	6013(9)	1108(4)	48(4)	1
C7	80(4)	5797(8)	750(4)	39(3)	1
C8	435(5)	6435(8)	724(4)	40(3)	1
C9	535(5)	7020(8)	1072(4)	47(3)	1
C10	248(5)	6770(8)	1306(4)	47(3)	1
C11	2300(4)	4424(7)	816(3)	29(3)	1
C12	2150(4)	3865(7)	445(3)	25(3)	1
C13	2414(4)	4176(7)	193(3)	30(3)	1
C14	2721(4)	4921(8)	399(3)	32(3)	1
C15	2645(4)	5060(7)	784(3)	33(3)	1
C16	1546(4)	6164(7)	384(4)	31(3)	1
C17	1225(4)	5473(8)	171(3)	33(3)	1
C18	1262(4)	5327(7)	−229(3)	31(3)	1
C19	1618(5)	5945(8)	−261(4)	39(3)	1
C20	1789(5)	6459(8)	123(4)	43(3)	1
C21	2825(5)	−613(7)	1805(3)	31(3)	1
C22	3365(4)	−807(7)	2044(4)	33(3)	1
C23	3617(4)	−666(7)	1771(4)	37(3)	1
C24	3268(4)	−384(7)	1362(3)	26(3)	1
C25	2765(4)	−358(7)	1382(3)	27(3)	1
C26	2741(5)	−2762(8)	1591(4)	40(3)	1
C27	3281(6)	−2845(8)	1735(4)	51(4)	1
C28	3408(5)	−2687(8)	1378(5)	50(4)	1
C29	2954(6)	−2471(8)	1028(4)	54(4)	1
C30	2540(5)	−2517(7)	1165(4)	39(3)	1
C31	1795(4)	−115(7)	3036(3)	34(3)	1
C32	1357(4)	90(7)	2660(3)	32(3)	1
C33	1512(4)	257(7)	2305(3)	23(2)	1
C34	2055(5)	105(7)	2476(3)	32(3)	1
C35	2230(5)	−114(8)	2931(3)	39(3)	1
C36	1569(7)	−2169(9)	2770(5)	67(4)	1
C37	2026(6)	−2218(9)	2754(5)	60(4)	1
C38	2063(8)	−2027(11)	2394(6)	92(5)	1
C39	1603(8)	−1937(9)	2105(5)	77(5)	1
C40	1205(7)	−1973(10)	2287(7)	105(6)	1
C42	788(4)	3643(7)	1259(3)	21(2)	1
C43	862(4)	3486(7)	831(3)	21(2)	1
C44	557(4)	3574(7)	409(3)	29(3)	1
C45	851(4)	3378(7)	161(3)	27(3)	1
C46	1339(4)	3202(6)	436(3)	21(2)	1

Table A.2: Continued overleaf

C47	1825(4)	3039(7)	366(3)	22(2)	1
C48	2151(4)	2338(7)	686(3)	23(3)	1
C49	2576(4)	2402(8)	1051(4)	38(3)	1
C50	2697(4)	1555(7)	1239(3)	28(3)	1
C51	2345(4)	989(7)	979(3)	22(2)	1
C52	2277(4)	1(7)	1029(3)	23(2)	1
C53	1818(4)	-150(7)	1150(3)	22(2)	1
C54	1428(4)	-732(7)	1014(3)	30(3)	1
C55	1108(4)	-570(7)	1244(3)	29(3)	1
C56	1324(4)	113(7)	1517(3)	21(2)	1
C57	1174(4)	559(7)	1862(3)	24(3)	1
C58	1241(4)	1544(7)	1837(3)	18(2)	1
C59	1638(4)	2062(7)	2092(3)	28(3)	1
C60	1528(4)	2943(7)	1918(3)	29(3)	1
C61	1071(4)	2911(7)	1571(3)	22(2)	1
C62	198(4)	3604(8)	1165(4)	36(3)	1
C63	1676(4)	2727(7)	-99(3)	29(3)	1
C64	2186(4)	-476(7)	587(3)	26(3)	1
C65	603(4)	322(7)	1759(3)	31(3)	1
N1	1348(3)	3263(5)	855(2)	22(2)	1
N2	2008(3)	1461(5)	646(3)	22(2)	1
N3	1752(3)	369(5)	1450(2)	20(2)	1
N4	901(3)	2070(5)	1528(3)	22(2)	1
O3	5000	6191(9)	2500	111(7)	1
S3	4839(3)	7106(6)	2323(2)	70(2)	0.50
C70	4630(6)	7664(8)	2651(5)	71(5)	1
O4	0	4639(9)	2500	151(10)	1
S4	0(4)	5561(6)	2334(3)	81(3)	0.50
C71	535(6)	6083(10)	2632(6)	107(7)	1
O1	9651(4)	-1271(7)	1437(4)	123(5)	1
S1	9260(3)	-1916(6)	1166(3)	209(4)	1
C66	9118(9)	-2598(13)	1512(7)	251(16)	1
C67	8653(5)	-1300(12)	1007(6)	148(9)	1
O2	9809(3)	1418(5)	911(2)	57(3)	1
S2	9313(2)	1893(3)	733(2)	122(3)	1
C68	8809(5)	1171(10)	568(6)	154(9)	1
C69	9248(7)	2125(13)	172(4)	152(9)	1
O5	1119(2)	676(5)	-42(2)	33(2)	1
S5	623(1)	523(2)	4(1)	34(1)	1
C72	172(4)	1182(9)	-370(3)	54(4)	1
C73	659(4)	1177(7)	473(3)	37(3)	1

Table A.2: Atomic coordinates [$\times 10^4$], equivalent isotropic displacement parameters [$Å^2 \times 10^3$] and site occupancy factors. U_{eq} is defined as one third of the trace of the orthogonalized U^{ij} tensor.

5,10,15,20-tetramethyl-5,10,15,20-tetraferrocenyl-calix[4]pyrrole (ααββ isomer)

Identification code	**(109) Crystallised from DCM**	
Empirical formula	$C_{65}H_{60}Fe_4N_4 . 2CH_2Cl_2$	
Formula weight	1278.41	
Temperature	150(2) K	
Wavelength	0.71073 Å	
Crystal system	Monoclinic	
Space group	$P2_1/c$	
Unit cell dimensions	a = 15.0277(9) Å	
	b = 9.4698(5) Å	β = 93.413(2)°
	c = 19.2400(12) Å	
Volume	2733.2(3) $Å^3$	
Z	2	
Density (calculated)	1.553 Mg / m^3	
Absorption coefficient	1.284 mm^{-1}	
F(000)	1320	
Crystal	Orange block	
Crystal size	0.03 × 0.03 × 0.02 mm^3	
θ range for data collection	3.02 – 23.25°	
Index ranges	$-16 \le h \le 16$, $-10 \le k \le 10$, $-21 \le l \le 21$	
Reflections collected	32520	
Independent reflections	3915 [R_{int} = 0.2585]	
Completeness to θ = 23.25°	99.8 %	
Max. and min. transmission	0.9810 and 0.9625	
Refinement method	Full-matrix least-squares on F^2	
Data / restraints / parameters	3915 / 0 / 353	
Goodness-of-fit on F^2	0.959	
Final R indices [$F^2 > 2\sigma(F^2)$]	$R1$ = 0.0617, $wR2$ = 0.1205	
R indices (all data)	$R1$ = 0.1529, $wR2$ = 0.1544	
Extinction coefficient	0.0016(3)	
Largest diff. peak and hole	0.690 and –0.796 e $Å^{-3}$	

Table A.3: Structure and refinement data.

Atom	x	y	z	U_{eq}	*S.o.f.*
C1	969(6)	2019(7)	4150(4)	39(2)	1
C2	1899(6)	2209(7)	4150(4)	42(2)	1
C3	2107(6)	2699(7)	3480(4)	46(2)	1
C4	1298(6)	2784(7)	3068(4)	39(2)	1
C5	594(6)	2354(7)	3481(4)	34(2)	1
C6	2223(5)	-1068(7)	3499(4)	33(2)	1
C7	2432(6)	-361(7)	2885(4)	41(2)	1
C8	1637(6)	-218(7)	2476(4)	38(2)	1
C9	939(5)	-854(7)	2818(4)	32(2)	1
C10	1306(6)	-1392(8)	3469(4)	35(2)	1
C11	845(5)	-2414(7)	3937(3)	26(2)	1
C12	968(5)	-3898(7)	3631(4)	35(2)	1
C13	1241(5)	-2401(7)	4677(3)	29(2)	1
C14	1391(6)	-3461(8)	5136(4)	44(2)	1
C15	1718(5)	-2873(8)	5784(4)	43(2)	1
C16	1776(5)	-1461(7)	5695(4)	29(2)	1
C17	2065(5)	-305(8)	6213(4)	35(2)	1
C18	1999(5)	-874(8)	6957(4)	41(2)	1
C19	3006(5)	208(8)	6109(4)	36(2)	1
C20	3497(5)	101(8)	5504(4)	37(2)	1
C21	4296(6)	876(8)	5612(4)	47(2)	1
C22	4306(6)	1492(8)	6286(4)	46(2)	1
C23	3520(5)	1060(8)	6587(4)	45(2)	1
C24	4306(7)	-1996(11)	7174(5)	67(3)	1
C25	4162(7)	-2784(10)	6566(6)	66(3)	1
C26	4867(8)	-2499(10)	6140(6)	74(3)	1
C27	5468(7)	-1576(11)	6490(6)	70(3)	1
C28	5114(7)	-1259(11)	7141(5)	71(3)	1
C29	-145(5)	-2166(7)	3938(3)	28(2)	1
C30	-825(6)	-3101(8)	4027(3)	36(2)	1
C31	-1632(5)	-2364(8)	3996(4)	34(2)	1
C32	1455(5)	979(8)	6109(4)	36(2)	1
C33	6509(10)	830(14)	311(6)	146(6)	1
N1	1481(4)	-1160(6)	5019(3)	31(2)	1
N2	-554(4)	-852(6)	3872(3)	33(2)	1
Fe1	1514(1)	772(1)	3390(1)	32(1)	1
Fe2	4244(1)	-663(1)	6349(1)	45(1)	1
Cl1	6290(2)	-681(3)	-216(1)	72(1)	1
Cl2	6205(2)	757(4)	1106(2)	125(1)	1

Table A.4: Atomic coordinates [$\times 10^4$], equivalent isotropic displacement parameters [$Å^2 \times 10^3$] and site occupancy factors. U_{eq} is defined as one third of the trace of the orthogonalized U^{ij} tensor.

5,10,15-Trispirocyclohexyl-20-methyl-20-ferrocenyl-calix[4]pyrrole

Identification code	**(110)**	
Empirical formula	$C_{52}H_{63}FeN_7$	
Formula weight	841.94	
Temperature	150(2) K	
Wavelength	0.71073 Å	
Crystal system	Monoclinic	
Space group	$P2_1/c$	
Unit cell dimensions	a = 12.8096(6) Å	
	b = 15.8408(3) Å	β = 102.931(3)°
	c = 22.9401(6) Å	
Volume	4536.8(3) $Å^3$	
Z	4	
Density (calculated)	1.233 Mg / m^3	
Absorption coefficient	0.376 mm^{-1}	
F(000)	1800	
Crystal	Yellow prism	
Crystal size	0.40 × 0.10 × 0.10 mm^3	
θ range for data collection	2.99 – 23.25°	
Index ranges	$-14 \leq h \leq 14$, $-17 \leq k \leq 17$, $-25 \leq l \leq 25$	
Reflections collected	20690	
Independent reflections	6485 [R_{int} = 0.1249]	
Completeness to θ = 23.25°	99.4 %	
Max. and min. transmission	0.9634 and 0.8642	
Refinement method	Full-matrix least-squares on F^2	
Data / restraints / parameters	6485 / 93 / 563	
Goodness-of-fit on F^2	0.908	
Final R indices [$F^2 > 2\sigma(F^2)$]	$R1$ = 0.0878, $wR2$ = 0.2292	
R indices (all data)	$R1$ = 0.1597, $wR2$ = 0.2850	
Extinction coefficient	0.0001(6)	
Largest diff. peak and hole	1.115 and –0.827 e $Å^{-3}$	

Table A.5: Structure and refinement data.

Atom	x	y	z	U_{eq}	$S.o.f.$
C47	5775(9)	5407(8)	278(6)	143(6)	1
C48	6581(9)	6004(8)	568(6)	113(5)	1
N5	7406(13)	6277(7)	839(6)	231(9)	1
C49	9382(12)	3525(7)	1520(12)	264(11)	1
C50	9283(14)	4409(9)	1359(6)	240(12)	1
N6	9150(30)	5145(9)	1393(12)	385(16)	1
C51A	615(6)	8387(5)	7210(4)	62(2)	0.50
C52A	341(14)	7513(6)	7068(8)	91(9)	0.50
N7A	−100(19)	6910(9)	6830(10)	162(10)	0.50
C51B	615(6)	8387(5)	7210(4)	62(2)	0.50
C52B	−194(9)	7830(7)	6872(6)	37(4)	0.50
N7B	−1011(8)	7583(7)	6575(5)	60(4)	0.50
Fe1	1317(1)	487(1)	1198(1)	37(1)	1
N2	5978(4)	3253(3)	226(2)	31(1)	1
N4	2745(4)	1374(3)	−912(2)	34(1)	1
N1	3773(4)	2110(3)	538(2)	31(1)	1
N3	5134(4)	2276(3)	−1207(2)	31(1)	1
C46	2774(5)	978(4)	−376(3)	27(2)	1
C1	2115(5)	597(4)	510(3)	32(2)	1
C11	2113(5)	1295(4)	48(3)	30(2)	1
C44	4001(5)	406(4)	−819(3)	38(2)	1
C43	3495(5)	1022(4)	−1187(3)	38(2)	1
C15	3192(5)	3262(4)	901(3)	38(2)	1
C45	3549(5)	374(4)	−316(3)	36(2)	1
C27	6604(5)	3281(4)	−743(3)	32(2)	1
C26	6553(5)	2888(4)	−150(3)	31(2)	1
C36	4259(5)	2207(4)	−1668(3)	36(2)	1
C25	6884(5)	2121(4)	100(3)	32(2)	1
C28	6774(5)	4248(4)	−706(3)	38(2)	1
C16	4105(5)	2828(4)	862(3)	33(2)	1
C37	3668(5)	1360(4)	−1775(3)	42(2)	1
C33	5578(5)	3081(4)	−1193(3)	30(2)	1
C5	2836(6)	490(5)	1066(3)	48(2)	1
C3	1720(6)	−652(4)	915(4)	47(2)	1
C17	5276(5)	2945(4)	1146(3)	35(2)	1
C29	7849(5)	4488(4)	−305(3)	41(2)	1
C31	8647(5)	3147(4)	−593(4)	44(2)	1
C23	5935(5)	2734(4)	698(3)	31(2)	1
C32	7559(5)	2899(4)	−976(3)	35(2)	1
C13	2670(5)	2070(4)	376(3)	32(2)	1
C24	6505(5)	2028(4)	623(3)	33(2)	1
C12	975(5)	1525(4)	−277(3)	36(2)	1
C2	1415(5)	−116(4)	421(3)	40(2)	1
C10	−225(6)	650(5)	1270(4)	53(2)	1
C14	2302(5)	2787(4)	594(3)	36(2)	1

Table A.6: Continued overleaf

C18	5575(6)	2357(5)	1700(3)	47(2)	1
C30	8771(6)	4108(4)	−538(4)	46(2)	1
C6	384(8)	273(5)	1797(5)	68(3)	1
C34	4956(5)	3503(4)	−1656(3)	39(2)	1
C20	6863(7)	3409(6)	2270(4)	72(3)	1
C35	4129(5)	2963(4)	−1950(3)	42(2)	1
C19	6687(6)	2497(5)	2074(4)	59(2)	1
C4	2594(6)	−284(5)	1315(4)	54(2)	1
C7	1215(7)	830(7)	2033(4)	68(3)	1
C22	5458(6)	3883(4)	1362(4)	48(2)	1
C42	2602(6)	1492(6)	−2253(3)	66(3)	1
C21	6599(6)	4017(5)	1734(5)	71(3)	1
C38	4380(7)	737(4)	−2039(4)	57(2)	1
C9	238(8)	1427(5)	1210(4)	64(3)	1
C39	3852(9)	−101(5)	−2240(5)	82(3)	1
C8	1103(8)	1535(5)	1672(5)	68(3)	1
C41	2076(9)	631(7)	−2444(4)	100(4)	1
C40	2795(11)	57(7)	−2700(5)	110(5)	1

Table A.6: Atomic coordinates [$\times 10^4$], equivalent isotropic displacement parameters [$\text{Å}^2 \times 10^3$] and site occupancy factors. U_{eq} is defined as one third of the trace of the orthogonalized U^{ij} tensor.

5,10,15-Trispirocyclohexyl-20-methyl-20-acetylferrocenyl-calix[4]pyrrole

Identification code	**(111)**	
Empirical formula	$C_{54}H_{70}FeN_4O$	
Formula weight	846.99	
Temperature	120(2) K	
Wavelength	0.71073 Å	
Crystal system	Triclinic	
Space group	P-1	
Unit cell dimensions	a = 11.1835(9) Å	α = 99.772(4)°
	b = 13.6433(10) Å	β = 93.331(4)°
	c = 16.335(2) Å	γ = 111.569(5)°
Volume	2264.4(4) Å^3	
Z	2	
Density (calculated)	1.242 Mg / m^3	
Absorption coefficient	0.377 mm^{-1}	
F(000)	912	
CrystalOrange Block		
Crystal size	0.10 × 0.04 × 0.03 mm^3	
θ range for data collection	3.03 - 25.02°	
Index ranges	$-13 \le h \le 13, -16 \le k \le 15, -17 \le l \le 19$	
Reflections collected	13668	
Independent reflections	7390 [R_{int} = 0.2296]	
Completeness to θ = 25.02°	92.2 %	
Max. and min. transmission	0.9888 and 0.9633	
Refinement method	Full-matrix least-squares on F^2	
Data / restraints / parameters	7390 / 0 / 543	
Goodness-of-fit on F^2	0.884	
Final R indices [$F^2 > 2\sigma(F^2)$]	$R1$ = 0.0961, $wR2$ = 0.1229	
R indices (all data)	$R1$ = 0.3345, $wR2$ = 0.1829	
Extinction coefficient	0.0018(4)	
Largest diff. peak and hole	0.482 and -0.358 e Å^{-3}	

Table A.7: Structure and refinement data.

Atom	x	y	z	U_{eq}	$S.o.f.$
Fe1	601(1)	1393(1)	2218(1)	38(1)	1
N1	1053(6)	2786(6)	−2789(4)	29(2)	1
N2	3838(6)	2755(6)	−1657(5)	37(2)	1
N3	2323(7)	2240(6)	46(4)	34(2)	1
N4	−180(6)	2668(5)	−860(4)	28(2)	1
O1	90(6)	−365(5)	3744(4)	46(2)	1
C1	326(9)	3316(8)	−2378(6)	34(2)	1
C2	1137(9)	4312(8)	−2024(6)	36(2)	1
C3	2403(8)	4437(7)	−2219(5)	34(2)	1
C4	2321(9)	3490(8)	−2688(5)	32(2)	1
C5	3339(9)	3145(8)	−3052(5)	35(2)	1
C6	2872(8)	2470(8)	−3966(6)	43(3)	1
C7	2608(9)	3137(8)	−4561(6)	46(3)	1
C8	3819(9)	4125(8)	−4583(6)	50(3)	1
C9	4333(9)	4801(8)	−3712(6)	44(3)	1
C10	4565(9)	4157(8)	−3086(5)	38(3)	1
C11	3734(8)	2480(8)	−2522(6)	35(2)	1
C12	4112(8)	1658(8)	−2686(6)	39(3)	1
C13	4444(8)	1403(8)	−1926(6)	43(3)	1
C14	4273(9)	2104(8)	−1295(6)	39(3)	1
C15	4471(8)	2231(7)	−352(6)	32(2)	1
C16	5917(8)	2905(7)	−17(5)	35(2)	1
C17	6272(8)	2930(8)	908(6)	46(3)	1
C18	5888(9)	1781(7)	1066(5)	39(3)	1
C19	4462(8)	1138(8)	777(5)	39(3)	1
C20	4134(8)	1101(7)	−143(5)	36(2)	1
C21	3627(9)	2775(8)	63(6)	34(2)	1
C22	3928(9)	3803(8)	517(5)	41(3)	1
C23	2762(8)	3849(7)	787(5)	34(2)	1
C24	1776(9)	2868(8)	490(5)	34(2)	1
C25	358(9)	2477(8)	606(6)	36(2)	1
C26	−50(8)	1553(8)	1063(5)	35(3)	1
C27	388(9)	689(8)	995(5)	38(3)	1
C28	−334(9)	−55(8)	1466(6)	39(3)	1
C29	−1254(9)	324(9)	1813(6)	46(3)	1
C30	−1068(8)	1298(8)	1567(5)	41(3)	1
C31	964(9)	2360(8)	3362(5)	40(3)	1
C32	1952(9)	2847(8)	2874(6)	44(3)	1
C33	2534(9)	2118(8)	2644(6)	42(3)	1
C34	1954(8)	1203(8)	2971(6)	40(3)	1
C35	977(9)	1333(8)	3427(5)	31(2)	1
C36	48(9)	531(9)	3794(6)	41(3)	1
C37	−956(9)	786(8)	4259(6)	49(3)	1
C38	82(8)	3426(7)	1087(5)	39(3)	1
C39	−467(8)	2096(8)	−229(6)	31(2)	1

Table A.8: Continued overleaf

C40	−1631(8)	1287(7)	−513(6)	32(2)	1
C41	−2051(8)	1313(8)	−1348(5)	35(2)	1
C42	−1145(9)	2182(7)	−1537(5)	29(2)	1
C43	−1070(9)	2733(8)	−2290(5)	34(2)	1
C44	−1747(8)	3547(7)	−2129(6)	34(2)	1
C45	−1856(8)	4049(7)	−2880(5)	38(3)	1
C46	−2522(9)	3199(8)	−3649(6)	42(3)	1
C47	−1884(8)	2392(7)	−3842(5)	36(2)	1
C48	−1807(8)	1882(7)	−3088(5)	33(2)	1
C49	5195(19)	1390(30)	3574(16)	320(20)	1
C50	5037(15)	1011(14)	4241(9)	130(7)	1
C51	5025(16)	228(16)	4682(11)	192(11)	1
C52	8243(11)	3517(10)	3293(7)	79(4)	1
C53	8669(10)	4457(9)	4021(6)	58(3)	1
C54	9804(10)	4550(8)	4617(5)	51(3)	1

Table A.8: Atomic coordinates [x 10^4], equivalent isotropic displacement parameters [$Å^2$ x 10^3] and site occupancy factors. U_{eq} is defined as one third of the trace of the orthogonalized U^{ij} tensor.

Tribrominated - tripyrrolylmethane derivative

Identification code	**(115)**	
Empirical formula	$C_{14}H_{12}Br_3N_3$	
Formula weight	462.00	
Temperature	120(2) K	
Wavelength	0.71073 Å	
Crystal system	Monoclinic	
Space group	$P2_1/c$	
Unit cell dimensions	a = 17.13(4) Å	
	b = 10.965(8) Å	β = 114.25(7)°
	c = 17.450(15) Å	
Volume	2989(7) $Å^3$	
Z	8	
Density (calculated)	2.053 Mg / m^3	
Absorption coefficient	8.090 mm^{-1}	
F(000)	1776	
Crystal	Colourless Needle	
Crystal size	0.10 × 0.03 × 0.03 mm^3	
θ range for data collection	4.90 - 25.03°	
Index ranges	$-19 \le h \le 20$, $-13 \le k \le 13$, $-19 \le l \le 19$	
Reflections collected	13791	
Independent reflections	3468 [R_{int} = 0.0742]	
Completeness to θ = 25.03°	65.7 %	
Absorption correction	Semi–empirical from equivalents	
Max. and min. transmission	0.7934 and 0.4984	
Refinement method	Full-matrix least-squares on F^2	
Data / restraints / parameters	3468 / 0 / 364	
Goodness-of-fit on F^2	1.043	
Final R indices [$F^2 > 2\sigma(F^2)$]	$R1$ = 0.0480, $wR2$ = 0.0952	
R indices (all data)	$R1$ = 0.0915, $wR2$ = 0.1081	
Extinction coefficient	0.00032(17)	
Largest diff. peak and hole	0.626 and –0.835 e $Å^{-3}$	

Table A.9: Structure and refinement data.

Atom	x	y	z	U_{eq}	$S.o.f.$
Br1	925(1)	−940(1)	−380(1)	44(1)	1
Br2	917(1)	−3881(1)	602(1)	39(1)	1
Br3	1353(1)	−3237(1)	2750(1)	30(1)	1
N1	1236(4)	−354(6)	1292(4)	18(2)	1
N2	2206(5)	−175(7)	4356(5)	44(2)	1
N3	2358(4)	1743(5)	2742(4)	21(2)	1
C1	1090(5)	−1256(8)	712(5)	27(2)	1
C2	1107(5)	−2338(7)	1109(5)	21(2)	1
C3	1272(5)	−2060(6)	1943(5)	17(2)	1
C4	1348(5)	−818(7)	2051(5)	20(2)	1
C5	1436(5)	−10(7)	2781(5)	20(2)	1
C6	584(5)	−138(7)	2881(5)	27(2)	1
C7	2169(5)	−438(7)	3573(5)	22(2)	1
C8	2911(8)	−689(10)	4948(7)	59(3)	1
C9	3319(6)	−1300(8)	4569(7)	51(3)	1
C10	2863(5)	−1129(7)	3669(6)	30(2)	1
C11	1563(5)	1300(7)	2602(5)	17(2)	1
C12	990(6)	2245(7)	2283(5)	24(2)	1
C13	1467(6)	3274(7)	2250(5)	24(2)	1
C14	2294(7)	2944(7)	2522(5)	25(2)	1
Br4	3217(1)	−785(1)	1502(1)	48(1)	1
Br5	5311(1)	−863(1)	3146(1)	33(1)	1
Br6	6632(1)	1161(1)	2531(1)	32(1)	1
N4	4986(4)	1328(5)	1199(4)	20(2)	1
N5	1970(4)	1852(6)	−695(4)	22(2)	1
N6	3897(4)	3235(6)	−348(4)	23(2)	1
C15	5454(5)	865(7)	1968(5)	20(2)	1
C16	4955(5)	109(7)	2190(5)	23(2)	1
C17	4135(5)	145(7)	1521(5)	20(2)	1
C18	4157(5)	880(6)	916(5)	17(2)	1
C19	3509(5)	1157(6)	16(5)	18(2)	1
C20	3283(5)	−59(7)	−463(5)	26(2)	1
C21	2711(5)	1734(7)	31(5)	22(2)	1
C22	2546(6)	2195(8)	677(6)	32(2)	1
C23	1673(6)	2586(8)	332(5)	29(2)	1
C24	1357(5)	2349(7)	−516(5)	25(2)	1
C25	3918(5)	2007(6)	−409(5)	19(2)	1
C26	4364(5)	1731(7)	−870(5)	21(2)	1
C27	4616(5)	2847(7)	−1118(5)	29(2)	1
C28	4315(5)	3761(7)	−785(5)	25(2)	1

Table A.10: Atomic coordinates [↔10^4], equivalent isotropic displacement parameters [$Å^2$ ↔10^3] and site occupancy factors. U_{eq} is defined as one third of the trace of the orthogonalized U^{ij} tensor.

3,4-Diphenyl-furan-2,5-dicarboxylic acid dibutyl-amide

Identification code	**(124) Crystallised from Ether**	
Empirical formula	$C_{26}H_{30}N_2O_3$	
Formula weight	418.52	
Temperature	120(2) K	
Wavelength	0.71073 Å	
Crystal system	Triclinic	
Space group	P–1	
Unit cell dimensions	a = 8.5528(2) Å	α = 99.7980(10)°
	b = 11.6747(3) Å	β = 96.3680(10)°
	c = 11.9030(3) Å	γ = 100.7530(10)°
Volume	1138.07(5) $Å^3$	
Z	2	
Density (calculated)	1.221 Mg / m^3	
Absorption coefficient	0.080 mm^{-1}	
F(000)	448	
Crystal	Rod; colourless	
Crystal size	0.18 × 0.04 × 0.03 mm^3	
θ range for data collection	3.22 – 27.49°	
Index ranges	$-10 \le h \le 11, -15 \le k \le 15, -15 \le l \le 15$	
Reflections collected	20647	
Independent reflections	5177 [R_{int} = 0.0447]	
Completeness to θ = 27.49°	99.1 %	
Absorption correction	Semi–empirical from equivalents	
Max. and min. transmission	0.9976 and 0.9858	
Refinement method	Full-matrix least-squares on F^2	
Data / restraints / parameters	5177 / 0 / 291	
Goodness-of-fit on F^2	1.026	
Final R indices [$F^2 > 2\sigma(F^2)$]	$R1$ = 0.0453, $wR2$ = 0.1030	
R indices (all data)	$R1$ = 0.0693, $wR2$ = 0.1131	
Extinction coefficient	0.022(3)	
Largest diff. peak and hole	0.302 and –0.219 e $Å^{-3}$	

Table A.11: Structure and refinement data.

Atom	x	y	z	U_{eq}	$S.o.f.$
C1	1900(2)	1260(1)	6002(1)	18(1)	1
C2	2539(2)	1770(1)	7121(1)	18(1)	1
C3	3793(2)	1152(1)	7430(1)	18(1)	1
C4	3801(2)	311(1)	6485(1)	18(1)	1
C5	2156(2)	2826(1)	7825(1)	19(1)	1
C6	3399(2)	3792(1)	8357(1)	24(1)	1
C7	3043(2)	4831(1)	8926(1)	29(1)	1
C8	1460(2)	4911(1)	8983(1)	30(1)	1
C9	226(2)	3946(1)	8494(1)	28(1)	1
C10	576(2)	2906(1)	7919(1)	23(1)	1
C11	4801(2)	1374(1)	8573(1)	19(1)	1
C12	4080(2)	1364(1)	9570(1)	23(1)	1
C13	5017(2)	1553(1)	10639(1)	28(1)	1
C14	6675(2)	1781(1)	10728(1)	28(1)	1
C15	7403(2)	1803(1)	9746(1)	29(1)	1
C16	6472(2)	1595(1)	8672(1)	24(1)	1
C17	720(2)	1515(1)	5110(1)	19(1)	1
C18	−41(2)	1289(1)	3007(1)	25(1)	1
C19	919(2)	1888(1)	2182(1)	27(1)	1
C20	1556(2)	3215(1)	2612(1)	34(1)	1
C21	2526(2)	3800(2)	1791(2)	42(1)	1
C22	4678(2)	-663(1)	6222(1)	19(1)	1
C23	4598(2)	-2578(1)	4956(1)	25(1)	1
C24	3423(2)	-3761(1)	4806(1)	26(1)	1
C25	2877(2)	-4034(1)	5925(1)	34(1)	1
C26	1947(2)	-5298(1)	5791(2)	36(1)	1
N1	994(1)	1182(1)	4026(1)	21(1)	1
N2	3896(1)	-1569(1)	5382(1)	22(1)	1
O1	2656(1)	367(1)	5604(1)	18(1)	1
O2	-396(1)	1988(1)	5377(1)	23(1)	1
O3	6031(1)	-603(1)	6751(1)	24(1)	1

Table A.12: Atomic coordinates [↔10[4]], equivalent isotropic displacement parameters [Å[2] ↔10[3]] and site occupancy factors. U_{eq} is defined as one third of the trace of the orthogonalized U^{ij} tensor.

3,4-Diphenyl-furan-2,5-dicarboxylic acid dibutyl-amide

Identification code	**(124) Crystallised from Ether:MeCN:DMSO (2:2:1)**	
Empirical formula	$C_{26}H_{30}N_2O_3$	
Formula weight	418.52	
Temperature	120(2) K	
Wavelength	0.71073 Å	
Crystal system	Hexagonal	
Space group	$P6_5$	
Unit cell dimensions	a = 11.4137(3) Å	$\alpha = 90°$
	b = 11.4137(3) Å	$\beta = 90°$
	c = 30.2650(10) Å	$\gamma = 120°$
Volume	3414.48(17) $Å^3$	
Z	6	
Density (calculated)	1.221 Mg / m^3	
Absorption coefficient	0.080 mm^{-1}	
F(000)	1344	
Crystal	Prism; colourless	
Crystal size	0.24 × 0.10 × 0.07 mm^3	
θ range for data collection	3.39 - 27.08°	
Index ranges	$-11 \le h \le 14$, $-14 \le k \le 12$, $-38 \le l \le 34$	
Reflections collected	16128	
Independent reflections	4869 [R_{int} = 0.0784]	
Completeness to θ = 27.08°	99.5 %	
Absorption correction	Semi–empirical from equivalents	
Max. and min. transmission	0.9944 and 0.9811	
Refinement method	Full-matrix least-squares on F^2	
Data / restraints / parameters	4869 / 1 / 302	
Goodness-of-fit on F^2	0.979	
Final R indices [$F^2 > 2\sigma(F^2)$]	$R1$ = 0.0563, $wR2$ = 0.1122	
R indices (all data)	$R1$ = 0.1302, $wR2$ = 0.1369	
Absolute structure parameter	-0.9(15)	
Extinction coefficient	0.0062(12)	
Largest diff. peak and hole	0.224 and –0.198 e $Å^{-3}$	

Table A.13: Structure and refinement data.

Atom	*x*	*y*	*z*	U_{eq}	*S.o.f.*
C1	5330(3)	8204(4)	210(1)	45(1)	1
C2	4880(3)	8095(4)	–213(1)	46(1)	1
C3	6030(3)	8414(3)	–492(1)	39(1)	1
C4	7080(3)	8689(3)	–217(1)	35(1)	1
C5	3532(4)	7815(4)	–372(1)	50(1)	1
C6	3485(4)	8751(5)	–661(1)	63(1)	1
C7	2217(6)	8525(6)	–809(1)	76(2)	1
C8	1048(5)	7395(7)	–674(2)	87(2)	1
C9	1111(4)	6474(6)	–399(2)	77(1)	1
C10	2341(4)	6669(4)	–245(1)	58(1)	1
C11	6031(3)	8358(4)	–982(1)	42(1)	1
C12	5135(4)	7177(4)	–1198(1)	49(1)	1
C13	5134(4)	7096(5)	–1652(1)	67(1)	1
C14	5998(5)	8205(6)	–1900(1)	71(1)	1
C15	6869(5)	9384(5)	–1691(1)	70(1)	1
C16	6905(4)	9474(4)	–1232(1)	56(1)	1
C17	4685(3)	7899(4)	653(1)	50(1)	1
C18	5110(3)	7958(3)	1444(1)	38(1)	1
C19	4303(3)	8523(3)	1659(1)	44(1)	1
C20	5083(4)	10024(4)	1729(1)	65(1)	1
C21	4251(7)	10566(6)	1963(2)	114(2)	1
C22	8464(3)	8947(3)	–284(1)	31(1)	1
C23	10671(3)	9692(4)	49(1)	55(1)	1
C24	11417(4)	10295(6)	459(1)	72(1)	1
C25	12848(4)	10483(7)	449(2)	99(2)	1
C26	13492(7)	10615(9)	849(2)	67(3)	0.526(10)
C26'	12976(8)	9525(9)	569(3)	53(3)	0.474(10)
N1	5547(3)	8423(3)	994(1)	39(1)	1
N2	9280(2)	9425(3)	63(1)	37(1)	1
O1	6674(2)	8596(2)	215(1)	38(1)	1
O2	3462(3)	7164(4)	700(1)	82(1)	1
O3	8803(2)	8688(2)	–642(1)	39(1)	1

Table A.14: Atomic coordinates [↔10^4], equivalent isotropic displacement parameters [$Å^2$ ↔10^3] and site occupancy factors. U_{eq} is defined as one third of the trace of the orthogonalized U^{ij} tensor.

3,4-Diphenyl-furan-2,5-dicarboxylic acid diphenyl-amide (MeCN complex)

Identification code	**(125)·MeCN**	
Empirical formula	$C_{30}H_{22}N_2O_3 . CH_3CN$	
Formula weight	499.55	
Temperature	120(2) K	
Wavelength	0.71073 Å	
Crystal system	Monoclinic	
Space group	$P2_1/n$	
Unit cell dimensions	a = 8.8334(2) Å	
	b = 15.6053(4) Å	β = 102.4470(10)°
	c = 19.0971(7) Å	
Volume	2570.62(13) $Å^3$	
Z	4	
Density (calculated)	1.291 Mg / m^3	
Absorption coefficient	0.084 mm^{-1}	
F(000)	1048	
CrystalColourless Block		
Crystal size	0.20 × 0.07 × 0.07 mm^3	
θ range for data collection	3.10 – 25.02°	
Index ranges	$-10 \le h \le 10$, $-18 \le k \le 18$, $-22 \le l \le 22$	
Reflections collected	8697	
Independent reflections	4541 [R_{int} = 0.0390]	
Completeness to θ = 25.02°	99.7 %	
Absorption correction	Semi–empirical from equivalents	
Max. and min. transmission	0.9941 and 0.9834	
Refinement method	Full-matrix least-squares on F^2	
Data / restraints / parameters	4541 / 0 / 344	
Goodness-of-fit on F^2	0.965	
Final R indices [$F^2 > 2\sigma(F^2)$]	$R1$ = 0.0435, $wR2$ = 0.0987	
R indices (all data)	$R1$ = 0.0763, $wR2$ = 0.1127	
Largest diff. peak and hole	0.209 and –0.256 e $Å^{-3}$	

Table A.15: Structure and refinement data.

Atom	x	y	z	U_{eq}	$S.o.f.$
N1	6031(2)	6190(1)	408(1)	23(1)	1
N2	8873(2)	4081(1)	−613(1)	22(1)	1
O1	4535(1)	5559(1)	1109(1)	25(1)	1
O2	7596(1)	4747(1)	391(1)	21(1)	1
O3	10892(1)	3563(1)	245(1)	26(1)	1
C1	4414(2)	7361(1)	718(1)	28(1)	1
C2	3855(2)	8193(1)	586(1)	34(1)	1
C3	4235(2)	8680(1)	46(1)	34(1)	1
C4	5190(2)	8338(1)	−371(1)	32(1)	1
C5	5739(2)	7506(1)	−252(1)	27(1)	1
C6	5353(2)	7016(1)	292(1)	23(1)	1
C7	5654(2)	5549(1)	820(1)	20(1)	1
C8	6731(2)	4811(1)	906(1)	19(1)	1
C9	7183(2)	4204(1)	1426(1)	19(1)	1
C10	8435(2)	3738(1)	1223(1)	19(1)	1
C11	8634(2)	4088(1)	595(1)	19(1)	1
C12	9588(2)	3878(1)	66(1)	21(1)	1
C13	9463(2)	3991(1)	−1243(1)	21(1)	1
C14	8913(2)	4563(1)	−1797(1)	22(1)	1
C15	9383(2)	4497(1)	−2440(1)	26(1)	1
C16	10425(2)	3864(1)	−2529(1)	29(1)	1
C17	10971(2)	3295(1)	−1978(1)	29(1)	1
C18	10488(2)	3348(1)	−1337(1)	25(1)	1
C19	6635(2)	4098(1)	2104(1)	20(1)	1
C20	5062(2)	4071(1)	2115(1)	25(1)	1
C21	4589(2)	4023(1)	2761(1)	29(1)	1
C22	5672(2)	3998(1)	3398(1)	33(1)	1
C23	7242(2)	3996(1)	3398(1)	32(1)	1
C24	7718(2)	4043(1)	2754(1)	25(1)	1
C25	9243(2)	2987(1)	1607(1)	20(1)	1
C26	8380(2)	2292(1)	1761(1)	27(1)	1
C27	9105(2)	1582(1)	2119(1)	32(1)	1
C28	10690(2)	1565(1)	2340(1)	30(1)	1
C29	11573(2)	2250(1)	2199(1)	31(1)	1
C30	10857(2)	2957(1)	1830(1)	26(1)	1
C32	284(3)	1408(1)	391(1)	43(1)	1
C33	1252(2)	664(1)	615(1)	32(1)	1
N3	2004(2)	76(1)	789(1)	47(1)	1

Table A.16: Atomic coordinates [x 10^4], equivalent isotropic displacement parameters [$Å^2$ x 10^3] and site occupancy factors. U_{eq} is defined as one third of the trace of the orthogonalized U^{ij} tensor.

3,4-Diphenyl-furan-2,5-dicarboxylic acid dibutyl-thioamide

Identification code	**(126)**	
Empirical formula	$C_{26}H_{30}N_2OS_2$	
Formula weight	450.64	
Temperature	120(2) K	
Wavelength	0.71069 Å	
Crystal system	Monoclinic	
Space group	$P2_1/c$	
Unit cell dimensions	a = 8.699(5) Å	
	b = 14.163(5) Å	β = 91.566(5)°
	c = 19.438(5) Å	
Volume	2393.9(17) $Å^3$	
Z	4	
Density (calculated)	1.250 Mg / m^3	
Absorption coefficient	0.243 mm^{-1}	
F(000)	960	
Crystal	Yellow Rod	
Crystal size	0.40 × 0.15 × 0.15 mm^3	
θ range for data collection	4.96 – 25.02°	
Index ranges	$-9 \leq h \leq 10$, $-16 \leq k \leq 16$, $-23 \leq l \leq 23$	
Reflections collected	21486	
Independent reflections	21498 [R_{int} = 0.0000]	
Completeness to θ = 25.02°	97.1 %	
Absorption correction	Semi–empirical from equivalents	
Max. and min. transmission	0.9645 and 0.9091	
Refinement method	Full-matrix least-squares on F^2	
Data / restraints / parameters	21498 / 2 / 291	
Goodness-of-fit on F^2	1.057	
Final R indices [$F^2 > 2\sigma(F^2)$]	$R1$ = 0.0682, $wR2$ = 0.2055	
R indices (all data)	$R1$ = 0.0804, $wR2$ = 0.2201	
Extinction coefficient	0.0047(13)	
Largest diff. peak and hole	0.479 and –0.493 e $Å^{-3}$	

Table A.17: Structure and refinement data.

Atom	*x*	*y*	*z*	U_{eq}	*S.o.f.*
S1	1115(1)	6428(1)	6029(1)	19(1)	1
S2	3779(1)	3283(1)	5891(1)	19(1)	1
N1	189(2)	7002(2)	4793(1)	19(1)	1
N2	5059(2)	3111(2)	4680(1)	18(1)	1
O1	2495(2)	4951(1)	5186(1)	15(1)	1
C1	387(3)	9696(2)	3641(2)	44(1)	1
C2	700(3)	8922(2)	4169(2)	32(1)	1
C3	−755(3)	8585(2)	4509(1)	23(1)	1
C4	−485(3)	7856(2)	5069(1)	19(1)	1
C5	951(2)	6359(2)	5173(1)	14(1)	1
C6	1726(2)	5606(2)	4791(1)	14(1)	1
C7	2004(2)	5465(2)	4108(1)	13(1)	1
C8	3057(2)	4687(2)	4081(1)	13(1)	1
C9	3304(2)	4390(2)	4749(1)	14(1)	1
C10	4096(2)	3583(2)	5076(1)	16(1)	1
C11	5890(3)	2259(2)	4890(1)	23(1)	1
C12	4927(3)	1370(2)	4827(2)	31(1)	1
C13A	4310(30)	1170(30)	4050(14)	56(2)	0.50
C14A	5748(18)	766(8)	3730(6)	83(4)	0.50
C13B	4360(30)	1140(30)	4157(13)	56(2)	0.50
C14B	5279(18)	1191(8)	3502(6)	83(4)	0.50
C15	1340(2)	5967(2)	3498(1)	14(1)	1
C16	2265(3)	6489(2)	3070(1)	20(1)	1
C17	1627(3)	6944(2)	2498(1)	24(1)	1
C18	60(3)	6874(2)	2337(1)	23(1)	1
C19	−863(3)	6358(2)	2764(1)	20(1)	1
C20	−236(2)	5900(2)	3342(1)	16(1)	1
C21	3691(2)	4302(2)	3438(1)	15(1)	1
C22	2734(3)	3824(2)	2965(1)	19(1)	1
C23	3317(3)	3465(2)	2361(1)	25(1)	1
C24	4859(3)	3595(2)	2219(1)	22(1)	1
C25	5812(3)	4069(2)	2685(1)	22(1)	1
C26	5241(3)	4428(2)	3293(1)	18(1)	1

Table A.18: Atomic coordinates [$\leftrightarrow 10^{4}$], equivalent isotropic displacement parameters [$Å^2 \leftrightarrow 10^{3}$] and site occupancy factors. U_{eq} is defined as one third of the trace of the orthogonalized U^{ij} tensor.

3,4-Diphenyl-furan-2,5-dicarboxylic acid diphenyl-thioamide

Identification code	**(127)**	
Empirical formula	$C_{32}H_{25}N_3OS_2$	
Formula weight	531.67	
Temperature	120(2) K	
Wavelength	0.71073 Å	
Crystal system	Triclinic	
Space group	P–1	
Unit cell dimensions	a = 10.1937(2) Å	α = 64.5590(10)°
	b = 11.9696(2) Å	β = 89.3040(10)°
	c = 13.4313(3) Å	γ = 66.6820(10)°
Volume	1334.16(5) Å^3	
Z	2	
Density (calculated)	1.323 Mg / m^3	
Absorption coefficient	0.231 mm^{-1}	
$F(000)$	556	
Crystal	Prism; orange	
Crystal size	0.32 × 0.21 × 0.18 mm^3	
θ range for data collection	3.05 - 27.50°	
Index ranges	$-13 \le h \le 13$, $-15 \le k \le 15$, $-17 \le l \le 17$	
Reflections collected	24851	
Independent reflections	6103 [R_{int} = 0.0757]	
Completeness to θ = 27.50°	99.4 %	
Absorption correction	Semi–empirical from equivalents	
Max. and min. transmission	0.9597 and 0.9298	
Refinement method	Full-matrix least-squares on F^2	
Data / restraints / parameters	6103 / 0 / 353	
Goodness-of-fit on F^2	1.013	
Final R indices [$F^2 > 2\sigma(F^2)$]	$R1$ = 0.0383, $wR2$ = 0.0950	
R indices (all data)	$R1$ = 0.0530, $wR2$ = 0.1035	
Extinction coefficient	0.0101(16)	
Largest diff. peak and hole	0.282 and –0.318 e Å^{-3}	

Table A.19: Structure and refinement data.

Atom	x	y	z	U_{eq}	$S.o.f.$
C31	1221(2)	10604(2)	5559(2)	39(1)	1
C32	2392(2)	9410(2)	6450(1)	25(1)	1
N3	3304(2)	8485(2)	7147(1)	33(1)	1
C1	6241(2)	3720(1)	7827(1)	18(1)	1
C2	5785(1)	4538(1)	8337(1)	17(1)	1
C3	3813(2)	4905(1)	7351(1)	18(1)	1
C4	4958(2)	3950(1)	7189(1)	18(1)	1
C5	7755(2)	2806(2)	7878(1)	21(1)	1
C6	8657(2)	3358(2)	7291(2)	30(1)	1
C7	10089(2)	2513(2)	7353(2)	43(1)	1
C8	10620(2)	1115(2)	7995(2)	45(1)	1
C9	9729(2)	550(2)	8564(2)	43(1)	1
C10	8291(2)	1389(2)	8505(1)	32(1)	1
C11	4953(2)	3225(2)	6535(1)	20(1)	1
C12	5803(2)	3241(2)	5720(1)	24(1)	1
C13	5800(2)	2555(2)	5109(1)	30(1)	1
C14	4961(2)	1847(2)	5314(2)	33(1)	1
C15	4130(2)	1812(2)	6135(2)	34(1)	1
C16	4122(2)	2496(2)	6746(2)	27(1)	1
C17	6516(2)	4770(1)	9110(1)	17(1)	1
C18	6287(2)	6644(1)	9558(1)	18(1)	1
C19	5186(2)	7632(2)	9750(1)	21(1)	1
C20	5541(2)	8314(2)	10230(2)	28(1)	1
C21	6980(2)	8034(2)	10501(1)	28(1)	1
C22	8070(2)	7054(2)	10307(1)	24(1)	1
C23	7732(2)	6355(2)	9830(1)	21(1)	1
C24	2237(2)	5612(1)	6948(1)	19(1)	1
C25	−29(2)	6944(2)	7389(1)	19(1)	1
C26	−579(2)	8162(2)	7461(1)	22(1)	1
C27	−2070(2)	8899(2)	7307(1)	26(1)	1
C28	−3004(2)	8424(2)	7075(1)	28(1)	1
C29	−2445(2)	7199(2)	7023(1)	27(1)	1
C30	−960(2)	6445(2)	7188(1)	23(1)	1
N1	5847(1)	6038(1)	9003(1)	18(1)	1
N2	1502(1)	6201(1)	7561(1)	19(1)	1
O1	4308(1)	5280(1)	8048(1)	17(1)	1
S1	7997(1)	3485(1)	10038(1)	22(1)	1
S2	1518(1)	5696(1)	5803(1)	27(1)	1

Table A.20: Atomic coordinates [$\leftrightarrow 10^4$], equivalent isotropic displacement parameters [$Å^2 \leftrightarrow 10^3$] and site occupancy factors. U_{eq} is defined as one third of the trace of the orthogonalized U^{ij} tensor.

Thiophene-2,5-dicarboxylic acid dibutyl-amide

Identification code	**(130)**	
Empirical formula	$C_{14}H_{22}N_2O_2S$	
Formula weight	282.40	
Temperature	120(2) K	
Wavelength	0.71069 Å	
Crystal system	Triclinic	
Space group	P1	
Unit cell dimensions	a = 9.750(5) Å	α = 87.570(5)°
	b = 9.970(5) Å	β = 87.549(5)°
	c = 15.582(5) Å	γ = 84.233(5)°
Volume	1504.5(12) Å^3	
Z	4	
Density (calculated)	1.247 Mg / m^3	
Absorption coefficient	0.216 mm^{-1}	
$F(000)$	608	
Crystal	Colourless Block	
Crystal size	0.15 × 0.10 × 0.06 mm^3	
θ range for data collection	3.01 – 25.03°	
Index ranges	$-11 \leq h \leq 11$, $-11 \leq k \leq 11$, $-18 \leq l \leq 18$	
Reflections collected	11960	
Independent reflections	9238 [R_{int} = 0.0680]	
Completeness to θ = 25.03°	96.8 %	
Absorption correction	Semi–empirical from equivalents	
Max. and min. transmission	0.9872 and 0.9684	
Refinement method	Full-matrix least-squares on F^2	
Data / restraints / parameters	9238 / 3 / 693	
Goodness-of-fit on F^2	0.943	
Final R indices [$F^2 > 2\sigma(F^2)$]	$R1$ = 0.0864, $wR2$ = 0.2258	
R indices (all data)	$R1$ = 0.1342, $wR2$ = 0.2544	
Absolute structure parameter	0.06(14)	
Largest diff. peak and hole	0.560 and –0.381 e Å^{-3}	

Table A.21: Structure and refinement data.

Atom	x	y	z	U_{eq}	$S.o.f.$
C43	18447(11)	−2970(10)	1819(7)	48(3)	1
C1	2588(10)	10401(10)	7012(6)	41(2)	1
C29	7635(11)	15689(10)	4157(7)	48(3)	1
C15	13809(12)	1414(10)	−782(8)	57(3)	1
C42	8621(11)	885(11)	7172(8)	52(3)	1
C28	398(12)	2219(10)	1908(8)	56(3)	1
C14	3189(11)	−3381(13)	4258(8)	60(3)	1
C56	5280(20)	−3633(18)	−999(13)	122(7)	1
C2	2310(11)	9134(10)	7509(7)	44(2)	1
C3	1790(9)	8110(9)	6947(6)	34(2)	1
C4	1706(10)	6711(9)	7424(6)	37(2)	1
C5	2322(9)	4891(8)	6418(6)	33(2)	1
C6	1821(8)	3818(8)	5894(6)	27(2)	1
C7	492(8)	3534(9)	5766(6)	33(2)	1
C8	506(9)	2480(9)	5200(6)	37(2)	1
C9	1773(7)	1933(8)	4940(6)	29(2)	1
C10	2207(9)	856(8)	4321(6)	31(2)	1
C11	1469(10)	−859(9)	3403(6)	39(2)	1
C12	919(9)	−2132(9)	3754(7)	38(2)	1
C13	1692(12)	−2813(11)	4517(8)	56(3)	1
C30	7275(10)	14474(9)	3660(6)	38(2)	1
C31	6793(8)	13397(9)	4269(7)	35(2)	1
C32	6594(10)	12082(9)	3804(6)	36(2)	1
C33	7185(9)	10170(9)	4796(6)	35(2)	1
C34	6727(7)	9022(8)	5329(6)	28(2)	1
C35	5460(8)	8604(9)	5470(6)	33(2)	1
C36	5483(8)	7432(8)	6002(6)	33(2)	1
C37	6770(8)	6982(8)	6250(6)	29(2)	1
C38	7276(8)	5775(9)	6803(6)	36(2)	1
C39	6753(10)	3583(9)	7458(7)	43(2)	1
C40	6396(12)	2372(10)	6969(8)	53(3)	1
C41	7059(9)	1072(10)	7372(8)	46(3)	1
N1	1345(7)	5673(7)	6841(5)	31(2)	1
N2	1217(7)	217(7)	4023(5)	37(2)	1
N5	6246(7)	10984(7)	4381(5)	31(2)	1
N6	6343(7)	4889(7)	6992(5)	38(2)	1
O1	3567(5)	4967(6)	6454(4)	37(2)	1
O2	3452(5)	559(6)	4147(4)	37(2)	1
O5	8455(6)	10346(6)	4718(4)	36(2)	1
O6	8485(5)	5637(6)	7030(4)	36(2)	1
S1	3031(2)	2856(2)	5308(2)	32(1)	1
S3	7986(2)	7999(2)	5854(2)	32(1)	1
C16	13094(11)	2781(10)	−538(7)	47(3)	1
C17	12331(9)	3566(10)	−1252(7)	41(2)	1
C18	11021(9)	3010(10)	−1490(7)	40(2)	1

Table A.22: Continued overleaf

C19	9058(9)	2431(8)	-538(6)	29(2)	1
C20	7955(8)	2933(9)	105(7)	35(2)	1
C21	7617(10)	4179(8)	397(7)	37(2)	1
C22	6451(10)	4251(8)	978(7)	41(2)	1
C23	5938(8)	3044(8)	1078(6)	29(2)	1
C24	4730(9)	2658(8)	1637(6)	32(2)	1
C25	2970(10)	3356(9)	2738(6)	37(2)	1
C26	1571(10)	4141(8)	2561(7)	41(2)	1
C27	896(11)	3632(11)	1794(8)	55(3)	1
C44	17934(11)	-1465(9)	1698(7)	45(3)	1
C45	17169(9)	-890(10)	2515(7)	39(2)	1
C46	15863(8)	-1547(9)	2769(6)	32(2)	1
C47	14202(8)	-2370(8)	1842(6)	29(2)	1
C48	13128(9)	-1986(9)	1202(6)	33(2)	1
C49	12556(9)	-754(8)	911(6)	34(2)	1
C50	11431(9)	-813(9)	337(7)	40(2)	1
C51	11235(9)	-2098(9)	208(6)	32(2)	1
C52	10147(8)	-2657(9)	-307(6)	33(2)	1
C53	8138(10)	-2135(10)	-1180(7)	44(3)	1
C54	6747(11)	-1869(14)	-678(9)	63(3)	1
C55	5524(15)	-2340(17)	-1097(10)	89(5)	1
N3	9909(7)	3331(7)	-820(5)	34(2)	1
N4	3993(8)	3616(8)	2089(5)	36(2)	1
N7	14830(8)	-1353(7)	2115(5)	37(2)	1
N8	9295(8)	-1753(8)	-714(5)	41(2)	1
O3	9168(6)	1217(6)	-721(4)	39(2)	1
O4	4437(6)	1480(6)	1658(5)	42(2)	1
O7	14491(6)	-3550(6)	2056(4)	40(2)	1
O8	10113(7)	-3877(6)	-323(4)	41(2)	1
S2	6827(2)	1808(2)	492(2)	37(1)	1
S4	12289(2)	-3252(2)	792(2)	41(1)	1

Table A.22: Atomic coordinates [$\leftrightarrow 10^4$], equivalent isotropic displacement parameters [$Å^2 \leftrightarrow 10^3$] and site occupancy factors. U_{eq} is defined as one third of the trace of the orthogonalized U^{ij} tensor.

Thiophene-2,5-dicarboxylic acid diphenyl-amide (DMSO complex)

Identification code	**(131)·2(DMSO)**
Empirical formula	$C_{22}H_{26}N_2O_4S_3$
	$C_{18}H_{14}N_2O_2S \cdot 2C_2H_6S$
Formula weight	478.63
Temperature	120(2) K
Wavelength	0.71073 Å
Crystal system	Monoclinic
Space group	$P2_1/n$
Unit cell dimensions	$a = 8.5976(2)$ Å
	$b = 28.2287(6)$ Å $\beta = 99.4300(10)°$
	$c = 9.5512(2)$ Å
Volume	2286.74(9) $Å^3$
Z	4
Density (calculated)	1.390 Mg / m^3
Absorption coefficient	0.356 mm^{-1}
F(000)	1008
Crystal	Colourless Prism
Crystal size	0.20 × 0.10 × 0.06 mm^3
θ range for data collection	2.96 – 25.02°
Index ranges	$-10 \le h \le 10$, $-33 \le k \le 31$, $-11 \le l \le 11$
Reflections collected	6736
Independent reflections	4003 [$R_{int} = 0.0283$]
Completeness to $\theta = 25.02°$	99.1 %
Absorption correction	Semi–empirical from equivalents
Max. and min. transmission	0.9790 and 0.9322
Refinement method	Full-matrix least-squares on F^2
Data / restraints / parameters	4003 / 0 / 285
Goodness-of-fit on F^2	1.035
Final R indices [$F^2 > 2\sigma(F^2)$]	$R1 = 0.0369$, $wR2 = 0.0841$
R indices (all data)	$R1 = 0.0591$, $wR2 = 0.0919$
Extinction coefficient	0.0014(5)
Largest diff. peak and hole	0.243 and –0.343 e $Å^{-3}$

Table A.23: Structure and refinement data.

Atom	*x*	*y*	*z*	U_{eq}	*S.o.f.*
N1	4439(2)	932(1)	614(2)	22(1)	1
N2	4712(2)	−1234(1)	4558(2)	21(1)	1
O1	6770(2)	896(1)	2141(2)	31(1)	1
O2	6988(2)	−823(1)	5257(2)	31(1)	1
S1	6281(1)	4(1)	3492(1)	24(1)	1
C1	5709(3)	1712(1)	467(2)	28(1)	1
C2	5816(3)	2121(1)	−304(2)	33(1)	1
C3	4851(3)	2199(1)	−1569(2)	32(1)	1
C4	3746(3)	1860(1)	−2094(2)	29(1)	1
C5	3633(2)	1447(1)	−1353(2)	24(1)	1
C6	4627(2)	1369(1)	−72(2)	21(1)	1
C7	5498(2)	720(1)	1611(2)	22(1)	1
C8	5069(2)	244(1)	2061(2)	20(1)	1
C9	3869(2)	−60(1)	1547(2)	20(1)	1
C10	3922(2)	−483(1)	2325(2)	21(1)	1
C11	5159(2)	−498(1)	3420(2)	19(1)	1
C12	5701(2)	−866(1)	4493(2)	21(1)	1
C13	5027(2)	−1653(1)	5362(2)	19(1)	1
C14	4037(2)	−2033(1)	4994(2)	24(1)	1
C15	4287(3)	−2456(1)	5721(2)	28(1)	1
C16	5539(3)	−2506(1)	6813(2)	29(1)	1
C17	6511(3)	−2124(1)	7181(2)	29(1)	1
C18	6273(2)	−1699(1)	6481(2)	25(1)	1
S3	9833(1)	709(1)	109(1)	22(1)	1
O4	11253(2)	593(1)	−565(1)	26(1)	1
C21	9918(3)	1326(1)	475(2)	29(1)	1
C22	10253(3)	498(1)	1886(2)	26(1)	1
S2	9902(1)	1214(1)	−3725(1)	23(1)	1
O3	8489(2)	1325(1)	−3030(2)	25(1)	1
C19	9525(3)	1471(1)	−5456(2)	31(1)	1
C20	9716(3)	611(1)	−4234(2)	31(1)	1

Table A.24: Atomic coordinates [↔10^4], equivalent isotropic displacement parameters [$Å^2$ ↔10^3] and site occupancy factors. U_{eq} is defined as one third of the trace of the orthogonalized U^{ij} tensor.

Thiophene-2,5-dicarboxylic acid diphenyl-thioamide

Identification code	**(133)**	
Empirical formula	$C_{22}H_{26}N_2O_2S_5$	
Formula weight	510.75	
Temperature	121(2) K	
Wavelength	0.71073 Å	
Crystal system	Triclinic	
Space group	$P1$	
Unit cell dimensions	a = 5.1621(3) Å	α = 70.293(2)°
	b = 9.5482(4) Å	β = 85.521(2)°
	c = 13.2970(7) Å	γ = 86.786(4)°
Volume	614.81(5) Å^3	
Z	1	
Density (calculated)	1.379 Mg / m^3	
Absorption coefficient	0.493 mm^{-1}	
F(000)	268	
Crystal	Orange Lath	
Crystal size	0.60 × 0.15 × 0.03 mm^3	
θ range for data collection	3.21 - 25.02°	
Index ranges	$-6 \le h \le 6$, $-11 \le k \le 11$, $-15 \le l \le 15$	
Reflections collected	5652	
Independent reflections	3891 [R_{int} = 0.0371]	
Completeness to θ = 25.02°	96.6 %	
Absorption correction	Semi–empirical from equivalents	
Max. and min. transmission	0.9854 and 0.7562	
Refinement method	Full-matrix least-squares on F^2	
Data / restraints / parameters	3891 / 3 / 284	
Goodness-of-fit on F^2	1.196	
Final R indices [$F^2 > 2\sigma(F^2)$]	$R1$ = 0.0508, $wR2$ = 0.1338	
R indices (all data)	$R1$ = 0.0533, $wR2$ = 0.1404	
Absolute structure parameter	-0.04(11)	
Largest diff. peak and hole	1.773 and –0.497 e Å^{-3}	

Table A.25: Structure and refinement data.

Atom	x	y	z	U_{eq}	$S.o.f.$
C1	3181(11)	6715(6)	4346(4)	23(1)	1
C2	1735(11)	7275(6)	3431(4)	24(1)	1
C3	2292(11)	8654(7)	2691(4)	29(1)	1
C4	4254(11)	9470(6)	2846(4)	28(1)	1
C5	5700(11)	8921(6)	3743(4)	25(1)	1
C6	5107(10)	7529(5)	4499(4)	20(1)	1
C7	7614(9)	5712(5)	5913(4)	14(1)	1
C8	9124(10)	5602(5)	6830(4)	15(1)	1
C9	10615(10)	6691(5)	6953(4)	19(1)	1
C10	12033(12)	6165(5)	7889(4)	23(1)	1
C11	11592(9)	4707(5)	8453(4)	16(1)	1
C12	12764(10)	3766(5)	9453(4)	18(1)	1
C13	14867(10)	4012(5)	11005(4)	16(1)	1
C14	14110(11)	4566(6)	11814(4)	23(1)	1
C15	15514(13)	4134(7)	12745(5)	36(2)	1
C16	17674(12)	3191(7)	12826(5)	32(1)	1
C17	18463(12)	2673(6)	11980(5)	30(1)	1
C18	17061(10)	3082(5)	11078(4)	20(1)	1
C19	11961(16)	1015(9)	5144(7)	57(2)	1
C20	13338(15)	1436(8)	6907(5)	41(2)	1
C21	17529(15)	−937(9)	8777(5)	48(2)	1
C22	17155(13)	−1880(8)	10901(5)	40(2)	1
N1	6552(8)	7059(4)	5445(3)	15(1)	1
N2	13482(8)	4555(4)	10051(3)	17(1)	1
S1	7504(2)	4229(1)	5515(1)	25(1)	1
S2	9512(2)	3935(1)	7854(1)	17(1)	1
S3	13026(2)	1920(1)	9758(1)	22(1)	1
S4	14852(3)	940(2)	5814(1)	31(1)	1
S5	18453(3)	−2548(1)	9852(1)	28(1)	1
O1	15754(9)	−646(4)	6278(3)	34(1)	1
O2	21437(8)	−2519(5)	9865(3)	32(1)	1

Table A.26: Atomic coordinates [↔10^{4}], equivalent isotropic displacement parameters [Å^{2} ↔10^{3}] and site occupancy factors. U_{eq} is defined as one third of the trace of the orthogonalized U^{ij} tensor.

Thiophene-2,5-dicarboxylic acid diphenyl-amide (Fluoride complex)

Identification code	**[(131)·F⁻]·TBA⁺**	
Empirical formula	$C_{34}H_{50}FN_3O_2S$	
Formula weight	583.83	
Temperature	120(2) K	
Wavelength	0.71073 Å	
Crystal system	Monoclinic	
Space group	*P*21/*c*	
Unit cell dimensions	a = 9.5551(2) Å	
	b = 17.7042(3) Å	β = 93.8900(10)°
	c = 19.3409(5) Å	
Volume	3264.27(12) Å^3	
Z	4	
Density (calculated)	1.188 Mg / m^3	
Absorption coefficient	0.138 mm^{-1}	
F(000)	1264	
Crystal	Colourless Block	
Crystal size	0.40 × 0.30 × 0.10 mm^3	
θ range for data collection	3.10 – 25.02°	
Index ranges	$-11 \le h \le 11$, $-21 \le k \le 21$, $-23 \le l \le 22$	
Reflections collected	11226	
Independent reflections	5740 [R_{int} = 0.0289]	
Completeness to θ = 25.02°	99.7 %	
Absorption correction	Semi–empirical from equivalents	
Max. and min. transmission	0.9863 and 0.9467	
Refinement method	Full-matrix least-squares on F^2	
Data / restraints / parameters	5740 / 0 / 375	
Goodness-of-fit on F^2	1.038	
Final *R* indices [$F^2 > 2\sigma(F^2)$]	$R1$ = 0.0398, $wR2$ = 0.1044	
R indices (all data)	$R1$ = 0.0502, $wR2$ = 0.1106	
Extinction coefficient	0.0052(11)	
Largest diff. peak and hole	0.201 and –0.271 e Å^{-3}	

Table A.27: Structure and refinement data.

Atom	x	y	z	U_{eq}	$S.o.f.$
F1	1258(1)	6669(1)	64(1)	25(1)	1
S1	2519(1)	4489(1)	1827(1)	18(1)	1
O1	1360(1)	3007(1)	2099(1)	27(1)	1
O2	4313(1)	5814(1)	1943(1)	22(1)	1
N1	-32(1)	2865(1)	1094(1)	18(1)	1
N2	3158(1)	6534(1)	1098(1)	18(1)	1
C1	-1220(2)	1728(1)	722(1)	24(1)	1
C2	-1959(2)	1077(1)	853(1)	32(1)	1
C3	-2227(2)	887(1)	1526(1)	34(1)	1
C4	-1749(2)	1350(1)	2063(1)	30(1)	1
C5	-1000(2)	2006(1)	1943(1)	23(1)	1
C6	-731(2)	2195(1)	1263(1)	18(1)	1
C7	906(2)	3237(1)	1523(1)	19(1)	1
C8	1382(2)	3984(1)	1274(1)	18(1)	1
C9	1042(2)	4369(1)	672(1)	19(1)	1
C10	1685(2)	5084(1)	659(1)	19(1)	1
C11	2512(2)	5233(1)	1251(1)	17(1)	1
C12	3410(2)	5890(1)	1456(1)	17(1)	1
C13	3932(2)	7215(1)	1193(1)	18(1)	1
C14	4695(2)	7404(1)	1810(1)	23(1)	1
C15	5435(2)	8080(1)	1853(1)	27(1)	1
C16	5402(2)	8576(1)	1301(1)	28(1)	1
C17	4620(2)	8394(1)	692(1)	27(1)	1
C18	3886(2)	7719(1)	638(1)	22(1)	1
N3	2149(1)	5037(1)	-2501(1)	17(1)	1
C19	1386(2)	4517(1)	-2024(1)	19(1)	1
C20	2293(2)	4027(1)	-1531(1)	25(1)	1
C21	1370(2)	3481(1)	-1164(1)	26(1)	1
C22	2164(2)	3026(1)	-601(1)	27(1)	1
C23	3232(2)	5522(1)	-2094(1)	19(1)	1
C24	2645(2)	6058(1)	-1578(1)	25(1)	1
C25	3828(2)	6435(1)	-1135(1)	36(1)	1
C26	4534(2)	5921(2)	-596(1)	45(1)	1
C27	2960(2)	4581(1)	-3010(1)	20(1)	1
C28	2087(2)	4035(1)	-3467(1)	32(1)	1
C29	2938(2)	3693(1)	-4029(1)	33(1)	1
C30	4099(2)	3175(1)	-3752(1)	35(1)	1
C31	1014(2)	5517(1)	-2873(1)	20(1)	1
C32	1504(2)	6082(1)	-3395(1)	25(1)	1
C33	245(2)	6510(1)	-3733(1)	26(1)	1
C34	-712(2)	6016(1)	-4204(1)	38(1)	1

Table A.28: Atomic coordinates [$\times 10^4$], equivalent isotropic displacement parameters [Å^2 $\times 10^3$] and site occupancy factors. U_{eq} is defined as one third of the trace of the orthogonalized U^{ij} tensor.

Thiophene-2,4-dicarboxylic acid diphenyl-amide

Identification code	**(139)**	
Empirical formula	$C_{18}H_{14}N_2O_2S$	
Formula weight	322.37	
Temperature	120(2) K	
Wavelength	0.71073 Å	
Crystal system	Orthorhombic	
Space group	*Pbcm*	
Unit cell dimensions	a = 5.1983(2) Å	α = 90°
	b = 7.8605(3) Å	β = 90°
	c = 35.409(2) Å	γ = 90°
Volume	1446.86(11) Å^3	
Z	4	
Density (calculated)	1.480 Mg / m^3	
Absorption coefficient	0.236 mm^{-1}	
F(000)	672	
Crystal	Plate; colourless	
Crystal size	0.30 × 0.16 × 0.04 mm^3	
θ range for data collection	3.45 – 27.46°	
Index ranges	$-6 \le h \le 6$, $-8 \le k \le 10$, $-45 \le l \le 43$	
Reflections collected	4436	
Independent reflections	1451 [R_{int} = 0.0565]	
Completeness to θ = 27.46°	86.1 %	
Absorption correction	Semi–empirical from equivalents	
Max. and min. transmission	0.9906 and 0.9327	
Refinement method	Full-matrix least-squares on F^2	
Data / restraints / parameters	1451 / 7 / 111	
Goodness-of-fit on F^2	1.040	
Final R indices [$F^2 > 2\sigma(F^2)$]	$R1$ = 0.0544, $wR2$ = 0.1392	
R indices (all data)	$R1$ = 0.0757, $wR2$ = 0.1535	
Extinction coefficient	0.006(3)	
Largest diff. peak and hole	0.404 and –0.505 e Å^{-3}	

Table A.29: Structure and refinement data.

Atom	*x*	*y*	*z*	U_{eq}	*S.o.f.*
C1	2673(5)	3339(3)	3854(1)	16(1)	1
C2	652(5)	2762(3)	4076(1)	18(1)	1
C3	545(5)	3233(4)	4456(1)	19(1)	1
C4	2430(5)	4277(3)	4612(1)	20(1)	1
C5	4449(5)	4845(4)	4387(1)	21(1)	1
C6	4578(5)	4388(3)	4009(1)	19(1)	1
C7	1002(5)	2679(3)	3216(1)	18(1)	1
C8	1843(5)	2215(4)	2828(1)	18(1)	1
C9	577(7)	2740(5)	2500	17(1)	1
N1	2952(4)	2859(3)	3469(1)	17(1)	1
O1	−1279(4)	2919(3)	3293(1)	29(1)	1
S1	4442(2)	1096(2)	2731(1)	23(1)	0.50
C10	4442(2)	1096(2)	2731(1)	23(1)	0.50

Table A.30: Atomic coordinates [$\leftrightarrow 10^4$], equivalent isotropic displacement parameters [$Å^2 \leftrightarrow 10^3$] and site occupancy factors. U_{eq} is defined as one third of the trace of the orthogonalized U^{ij} tensor.

Thiophene-2-carboxylic acid phenyl-amide

Identification code	**(142)**
Empirical formula	$C_{11}H_9NOS$
Formula weight	203.25
Temperature	120(2) K
Wavelength	0.71073 Å
Crystal system	Orthorhombic
Space group	$Pna2_1$
Unit cell dimensions	a = 9.9803(10) Å
	b = 16.7614(18) Å
	c = 5.6223(3) Å
Volume	940.52(15) $Å^3$
Z	4
Density (calculated)	1.435 Mg / m^3
Absorption coefficient	0.305 mm^{-1}
F(000)	424
Crystal	Colourless Blade
Crystal size	0.60 × 0.15 × 0.10 mm^3
θ range for data collection	3.17 - 25.02°
Index ranges	$-11 \le h \le 11, -18 \le k \le 19, -5 \le l \le 6$
Reflections collected	4765
Independent reflections	1553 [R_{int} = 0.0533]
Completeness to θ = 25.02°	99.7 %
Absorption correction	Semi–empirical from equivalents
Max. and min. transmission	0.9702 and 0.8384
Refinement method	Full-matrix least-squares on F^2
Data / restraints / parameters	1553 / 1 / 131
Goodness-of-fit on F^2	1.063
Final R indices [$F^2 > 2\sigma(F^2)$]	$R1$ = 0.0430, $wR2$ = 0.1065
R indices (all data)	$R1$ = 0.0535, $wR2$ = 0.1123
Absolute structure parameter	-0.02(14)
Largest diff. peak and hole	0.418 and –0.294 e $Å^{-3}$

Table A.31: Structure and refinement data.

Atom	*x*	*y*	*z*	U_{eq}	*S.o.f.*
C1	4369(4)	4043(2)	8783(7)	30(1)	1
C2	3147(4)	3685(2)	8758(7)	29(1)	1
C3	2995(3)	3143(2)	6823(7)	25(1)	1
C4	4120(3)	3097(2)	5455(6)	26(1)	1
C5	4511(4)	2549(2)	3535(6)	26(1)	1
C6	3656(3)	1489(2)	891(6)	22(1)	1
C7	4556(3)	1546(2)	−921(7)	26(1)	1
C8	4635(3)	962(2)	−2547(6)	21(1)	1
C9	3794(3)	286(2)	−2486(7)	27(1)	1
C10	2875(3)	230(2)	−639(7)	27(1)	1
C11	2799(3)	824(2)	1063(5)	21(1)	1
N1	3497(3)	2113(2)	2645(5)	23(1)	1
O1	5683(2)	2486(2)	2879(5)	33(1)	1
S1	5378(1)	3718(1)	6547(2)	33(1)	1

Table A.32: Atomic coordinates [↔10^4], equivalent isotropic displacement parameters [$Å^2$ ↔10^3] and site occupancy factors. U_{eq} is defined as one third of the trace of the orthogonalized U^{ij} tensor.

3,4-Diphenyl-thiophene-2,5-dicarboxylic acid diphenyl-amide

Identification code	**(145)**	
Empirical formula	$C_{30}H_{22}N_2O_2S$	
Formula weight	474.56	
Temperature	120(2) K	
Wavelength	0.71073 Å	
Crystal system	Triclinic	
Space group	*P*-1	
Unit cell dimensions	a = 9.47580(10) Å	α = 97.4930(10)°
	b = 9.74920(10) Å	β = 90.7210(10)°
	c = 26.1353(4) Å	γ = 92.9810(10)°
Volume	2390.10(5) Å^3	
Z	4 (2 molecules)	
Density (calculated)	1.319 Mg / m^3	
Absorption coefficient	0.167 mm^{-1}	
F(000)	992	
Crystal	Colourless Block (Cut from needle)	
Crystal size	0.20 × 0.15 × 0.08 mm^3	
θ range for data collection	2.95 - 25.03°	
Index ranges	$-11 \leq h \leq 11$, $-11 \leq k \leq 11$, $-31 \leq l \leq 31$	
Reflections collected	16236	
Independent reflections	8365 [R_{int} = 0.0359]	
Completeness to θ = 25.03°	98.9 %	
Absorption correction	Semi–empirical from equivalents	
Max. and min. transmission	0.9868 and 0.9675	
Refinement method	Full-matrix least-squares on F^2	
Data / restraints / parameters	8365 / 0 / 631	
Goodness-of-fit on F^2	0.883	
Final R indices [$F^2 > 2\sigma(F^2)$]	$R1$ = 0.0414, $wR2$ = 0.0983	
R indices (all data)	$R1$ = 0.0546, $wR2$ = 0.1081	
Largest diff. peak and hole	0.202 and –0.274 e Å^{-3}	

Table A.33: Structure and refinement data.

Atom	x	y	z	U_{eq}	$S.o.f.$
S1	8511(1)	8076(1)	384(1)	22(1)	1
O1	7467(2)	9063(2)	−539(1)	30(1)	1
O2	8432(2)	7067(2)	1376(1)	30(1)	1
N1	9493(2)	8975(2)	−1003(1)	26(1)	1
N2	10671(2)	6311(2)	1400(1)	25(1)	1
C1	10180(2)	9651(2)	−1810(1)	29(1)	1
C2	9880(2)	10103(2)	−2279(1)	33(1)	1
C3	8515(2)	10373(2)	−2408(1)	32(1)	1
C4	7446(2)	10164(2)	−2071(1)	29(1)	1
C5	7717(2)	9694(2)	−1602(1)	26(1)	1
C6	9101(2)	9450(2)	−1471(1)	22(1)	1
C7	8714(2)	8792(2)	−585(1)	22(1)	1
C8	9469(2)	8217(2)	−162(1)	22(1)	1
C9	10809(2)	7731(2)	−128(1)	21(1)	1
C10	11055(2)	7239(2)	356(1)	21(1)	1
C11	9893(2)	7357(2)	669(1)	22(1)	1
C12	9592(2)	6918(2)	1185(1)	22(1)	1
C13	10641(2)	5632(2)	1849(1)	25(1)	1
C14	11496(2)	4515(2)	1856(1)	32(1)	1
C15	11573(3)	3848(2)	2292(1)	40(1)	1
C16	10798(3)	4287(3)	2719(1)	43(1)	1
C17	9928(2)	5378(3)	2709(1)	40(1)	1
C18	9838(2)	6060(2)	2273(1)	32(1)	1
C19	11887(2)	7646(2)	−540(1)	21(1)	1
C20	11720(2)	6632(2)	−971(1)	27(1)	1
C21	12714(2)	6540(2)	−1355(1)	33(1)	1
C22	13890(2)	7446(2)	−1313(1)	34(1)	1
C23	14074(2)	8453(2)	−888(1)	34(1)	1
C24	13081(2)	8556(2)	−502(1)	26(1)	1
C25	12418(2)	6644(2)	481(1)	22(1)	1
C26	13559(2)	7501(2)	688(1)	28(1)	1
C27	14810(2)	6936(3)	813(1)	37(1)	1
C28	14932(3)	5522(3)	727(1)	41(1)	1
C29	13808(3)	4660(2)	516(1)	39(1)	1
C30	12558(2)	5221(2)	391(1)	30(1)	1
S2	6328(1)	8304(1)	5110(1)	22(1)	1
O3	6889(2)	6754(2)	4118(1)	34(1)	1
O4	6842(1)	9959(1)	6104(1)	27(1)	1
N3	4765(2)	5528(2)	3985(1)	26(1)	1
N4	4581(2)	10516(2)	6276(1)	25(1)	1
C31	4160(2)	3352(2)	3479(1)	27(1)	1
C32	4372(2)	2334(2)	3068(1)	31(1)	1
C33	5458(2)	2512(2)	2730(1)	33(1)	1
C34	6319(2)	3716(2)	2800(1)	31(1)	1
C35	6118(2)	4749(2)	3210(1)	27(1)	1

Table A.34: Continued overleaf

C36	5044(2)	4553(2)	3554(1)	24(1)	1
C37	5675(2)	6511(2)	4244(1)	24(1)	1
C38	5099(2)	7299(2)	4718(1)	22(1)	1
C39	3754(2)	7368(2)	4914(1)	20(1)	1
C40	3721(2)	8263(2)	5392(1)	20(1)	1
C41	5053(2)	8841(2)	5541(1)	20(1)	1
C42	5571(2)	9819(2)	6000(1)	21(1)	1
C43	4786(2)	11371(2)	6758(1)	23(1)	1
C44	3702(2)	11367(2)	7111(1)	32(1)	1
C45	3835(3)	12196(2)	7586(1)	36(1)	1
C46	5049(2)	13031(2)	7704(1)	35(1)	1
C47	6116(2)	13044(2)	7350(1)	31(1)	1
C48	5999(2)	12217(2)	6874(1)	26(1)	1
C49	2456(2)	6615(2)	4665(1)	21(1)	1
C50	1611(2)	7271(2)	4343(1)	25(1)	1
C51	396(2)	6601(2)	4113(1)	33(1)	1
C52	46(2)	5248(2)	4185(1)	35(1)	1
C53	887(2)	4575(2)	4496(1)	33(1)	1
C54	2082(2)	5261(2)	4744(1)	27(1)	1
C55	2422(2)	8464(2)	5700(1)	20(1)	1
C56	1298(2)	9161(2)	5526(1)	24(1)	1
C57	92(2)	9338(2)	5822(1)	28(1)	1
C58	6(2)	8839(2)	6295(1)	28(1)	1
C59	1121(2)	8157(2)	6470(1)	28(1)	1
C60	2317(2)	7960(2)	6174(1)	24(1)	1

Table A.34: Atomic coordinates [$\leftrightarrow 10^4$], equivalent isotropic displacement parameters [$Å^2 \leftrightarrow 10^3$] and site occupancy factors. U_{eq} is defined as one third of the trace of the orthogonalized U^{ij} tensor.

3,4-Diphenyl-1H-pyrrole-2,5-dicarboxylic aeid

Identification code	**(150)**	
Empirical formula	$C_{20}H_{21}NO_6$	
Formula weight	371.38	
Temperature	120(2) K	
Wavelength	0.71073 Å	
Crystal system	Triclinic	
Space group	$P-1$	
Unit cell dimensions	$a = 9.0469(2)$ Å	$\alpha = 70.8480(10)°$
	$b = 9.2755(2)$ Å	$\beta = 70.0030(10)°$
	$c = 12.5890(4)$ Å	$\gamma = 72.970(2)°$
Volume	918.14(4) $Å^3$	
Z	2	
Density (calculated)	1.343 Mg / m^3	
Absorption coefficient	0.100 mm^{-1}	
F(000)	392	
Crystal	Needle; colourless	
Crystal size	0.28 × 0.04 × 0.03 mm^3	
θ range for data collection	3.04 – 27.50°	
Index ranges	$-10 \le h \le 11$, $-11 \le k \le 12$, $-16 \le l \le 16$	
Reflections collected	12223	
Independent reflections	4048 [$R_{int} = 0.0580$]	
Completeness to $\theta = 27.50°$	95.9 %	
Absorption correction	Semi–empirical from equivalents	
Max. and min. transmission	0.9970 and 0.9726	
Refinement method	Full-matrix least-squares on F^2	
Data / restraints / parameters	4048 / 0 / 255	
Goodness-of-fit on F^2	1.030	
Final R indices [$F^2 > 2\sigma(F^2)$]	$R1 = 0.0436$, $wR2 = 0.0992$	
R indices (all data)	$R1 = 0.0638$, $wR2 = 0.1085$	
Extinction coefficient	0.023(3)	
Largest diff. peak and hole	0.232 and –0.217 e $Å^{-3}$	

Table A.35: Structure and refinement data.

Atom	*x*	*y*	*z*	U_{eq}	*S.o.f.*
C19	3627(2)	7336(2)	−324(2)	34(1)	1
O5	4565(1)	7979(1)	50(1)	27(1)	1
C20	1486(2)	3923(2)	10651(1)	35(1)	1
O6	2594(1)	4049(1)	9519(1)	38(1)	1
C1	3324(2)	8941(2)	3801(1)	17(1)	1
C2	2703(2)	10051(2)	4448(1)	17(1)	1
C3	2498(2)	9220(2)	5643(1)	17(1)	1
C4	3034(2)	7640(2)	5668(1)	17(1)	1
C5	3645(2)	9144(2)	2549(1)	18(1)	1
C6	3181(2)	6201(2)	6607(1)	18(1)	1
C7	2297(2)	11768(2)	4012(1)	18(1)	1
C8	3497(2)	12620(2)	3341(1)	21(1)	1
C9	3108(2)	14234(2)	2980(1)	24(1)	1
C10	1526(2)	15015(2)	3260(1)	24(1)	1
C11	323(2)	14184(2)	3916(1)	24(1)	1
C12	711(2)	12571(2)	4299(1)	21(1)	1
C13	1860(2)	9963(2)	6631(1)	18(1)	1
C14	449(2)	9666(2)	7502(1)	20(1)	1
C15	−137(2)	10383(2)	8413(1)	24(1)	1
C16	670(2)	11410(2)	8468(1)	26(1)	1
C17	2051(2)	11742(2)	7596(1)	25(1)	1
C18	2632(2)	11026(2)	6681(1)	21(1)	1
N1	3517(1)	7495(1)	4549(1)	16(1)	1
O1	3933(1)	7826(1)	2261(1)	24(1)	1
O2	3628(1)	10419(1)	1844(1)	24(1)	1
O3	3794(1)	4930(1)	6410(1)	23(1)	1
O4	2568(1)	6446(1)	7666(1)	24(1)	1

Table A.36: Atomic coordinates [$\leftrightarrow 10^{4}$], equivalent isotropic displacement parameters [$Å^{2} \leftrightarrow 10^{3}$] and site occupancy factors. U_{eq} is defined as one third of the trace of the orthogonalized U^{ij} tensor.

3,4-Diphenyl-1*H*-pyrrole-2,5-dicarboxylic acid diferrocenylmethyl-amide

Identification code	**(152)**	
Empirical formula	$C_{40}H_{35}Fe_2N_3O_2$	
Formula weight	701.41	
Temperature	120(2) K	
Wavelength	0.71073 Å	
Crystal system	Monoclinic	
Space group	C2/c	
Unit cell dimensions	a = 16.1333(5) Å	
	b = 10.3709(3) Å	β = 97.9820(10)°
	c = 37.6445(12) Å	
Volume	6237.5(3) Å^3	
Z	8	
Density (calculated)	1.494 Mg / m^3	
Absorption coefficient	0.973 mm^{-1}	
F(000)	2912	
Crystal	Yellow Plate	
Crystal size	0.15 × 0.10 × 0.03 mm^3	
θ range for data collection	2.91 – 25.03°	
Index ranges	$-19 \le h \le 18$, $-10 \le k \le 12$, $-42 \le l \le 44$	
Reflections collected	11432	
Independent reflections	5096 [R_{int} = 0.0706]	
Completeness to θ = 25.03°	92.2 %	
Max. and min. transmission	0.9714 and 0.8678	
Refinement method	Full-matrix least-squares on F^2	
Data / restraints / parameters	5096 / 0 / 424	
Goodness-of-fit on F^2	0.984	
Final R indices [$F^2 > 2\sigma(F^2)$]	$R1$ = 0.0474, $wR2$ = 0.0817	
R indices (all data)	$R1$ = 0.0929, $wR2$ = 0.0938	
Largest diff. peak and hole	0.472 and –0.434 e Å^{-3}	

Table A.37: Structure and refinement data.

Atom	x	y	z	U_{eq}	*S.o.f.*
Fe1	3334(1)	3360(1)	2249(1)	17(1)	1
Fe2	4781(1)	1121(1)	−1430(1)	17(1)	1
N1	4432(2)	4046(3)	1251(1)	15(1)	1
N2	3800(2)	2691(3)	366(1)	13(1)	1
N3	4127(2)	1421(3)	−503(1)	15(1)	1
O1	3206(1)	3266(3)	979(1)	24(1)	1
O2	2984(1)	1550(2)	−224(1)	18(1)	1
C1	2342(3)	4485(4)	2318(1)	29(1)	1
C2	2502(3)	3626(4)	2602(1)	28(1)	1
C3	3318(3)	3839(4)	2773(1)	34(1)	1
C4	3656(3)	4848(5)	2592(1)	42(1)	1
C5	3058(3)	5243(4)	2310(1)	40(1)	1
C6	3947(2)	1644(4)	2217(1)	19(1)	1
C7	3141(2)	1582(4)	2013(1)	20(1)	1
C8	3088(2)	2571(3)	1751(1)	14(1)	1
C9	3860(2)	3259(3)	1790(1)	13(1)	1
C10	4390(2)	2673(3)	2077(1)	18(1)	1
C11	4065(2)	4396(3)	1573(1)	17(1)	1
C12	3946(2)	3515(3)	969(1)	14(1)	1
C13	4323(2)	3222(3)	640(1)	12(1)	1
C14	5111(2)	3348(3)	531(1)	11(1)	1
C15	5045(2)	2824(3)	180(1)	12(1)	1
C16	4220(2)	2428(3)	85(1)	13(1)	1
C17	3733(2)	1782(3)	−228(1)	14(1)	1
C18	3657(2)	682(4)	−795(1)	20(1)	1
C19	4158(2)	188(3)	−1069(1)	14(1)	1
C20	3799(2)	−105(3)	−1424(1)	17(1)	1
C21	4423(2)	−685(3)	−1604(1)	19(1)	1
C22	5169(2)	−744(3)	−1359(1)	19(1)	1
C23	5014(2)	−214(3)	−1028(1)	17(1)	1
C24	4372(3)	2832(5)	−1644(2)	75(2)	1
C25	4880(4)	2244(5)	−1863(1)	54(2)	1
C26	5650(3)	2080(4)	−1672(1)	37(1)	1
C27	5651(3)	2535(5)	−1333(1)	53(2)	1
C28	4850(5)	3008(5)	−1309(2)	75(2)	1
C29	5877(2)	3878(3)	744(1)	12(1)	1
C30	6230(2)	5027(3)	640(1)	17(1)	1
C31	6946(2)	5534(4)	837(1)	22(1)	1
C32	7316(2)	4915(4)	1144(1)	24(1)	1
C33	6974(2)	3786(4)	1250(1)	23(1)	1
C34	6261(2)	3273(4)	1052(1)	17(1)	1
C35	5731(2)	2675(3)	−41(1)	14(1)	1
C36	6055(2)	3718(4)	−210(1)	16(1)	1
C37	6707(2)	3551(4)	−410(1)	20(1)	1
C38	7033(2)	2331(4)	−452(1)	21(1)	1

Table A.38: Continued overleaf

C39	6723(2)	1291(4)	−286(1)	23(1)	1
C40	6077(2)	1459(4)	−85(1)	18(1)	1

Table A.38: Atomic coordinates [$\times 10^4$], equivalent isotropic displacement parameters [$Å^2 \times 10^3$] and site occupancy factors. U_{eq} is defined as one third of the trace of the orthogonalized U^{ij} tensor.

3,4-Diphenyl-1*H*-pyrrole-2,5-dicarboxylic acid bis-ferrocenylamide

Identification code	**(153)**	
Empirical formula	$C_{38}H_{31}Fe_2N_3O_2$	
Formula weight	673.36	
Temperature	120(2) K	
Wavelength	0.71073 Å	
Crystal system	Triclinic	
Space group	P-1	
Unit cell dimensions	a = 12.7602(3) Å	α = 87.7210(10)°
	b = 14.1906(4) Å	β = 83.1370(10)°
	c = 17.3431(5) Å	γ = 75.782(2)°
Volume	3022.22(14) $Å^3$	
Z	4	
Density (calculated)	1.480 Mg / m^3	
Absorption coefficient	1.001 mm^{-1}	
F(000)	1392	
CrystalRed prism		
Crystal size	0.15 × 0.10 × 0.03 mm^3	
θ range for data collection	2.96 – 25.03°	
Index ranges	$-15 \le h \le 15$, $-16 \le k \le 16$, $-20 \le l \le 20$	
Reflections collected	36068	
Independent reflections	10432 [R_{int} = 0.0867]	
Completeness to θ = 25.03°	97.7 %	
Max. and min. transmission	0.9706 and 0.8644	
Refinement method	Full-matrix least-squares on F^2	
Data / restraints / parameters	10432 / 360 / 909	
Goodness-of-fit on F^2	0.955	
Final R indices [$F^2 > 2\sigma(F^2)$]	$R1$ = 0.0456, $wR2$ = 0.0862	
R indices (all data)	$R1$ = 0.0968, $wR2$ = 0.1016	
Largest diff. peak and hole	0.325 and –0.380 e $Å^{-3}$	

Table A.39: Structure and refinement data.

Atom	x	y	z	U_{eq}	$S.o.f.$
N1	8812(2)	9901(2)	10003(1)	20(1)	1
N2	9200(2)	8864(2)	8084(1)	20(1)	1
N3	8939(2)	9233(2)	6042(1)	22(1)	1
O1	9555(2)	8347(2)	9613(1)	26(1)	1
O2	9436(2)	7799(2)	6692(1)	44(1)	1
Fe1	7337(1)	9708(1)	11483(1)	25(1)	1
C1	8747(2)	9756(2)	10811(2)	19(1)	1
C2	8434(3)	10551(2)	11341(2)	26(1)	1
C3	8396(3)	10150(2)	12098(2)	28(1)	1
C4	8668(3)	9123(2)	12040(2)	24(1)	1
C5	8892(3)	8880(2)	11239(2)	22(1)	1
C6	6264(3)	9684(4)	10712(2)	48(1)	1
C7	5899(3)	10516(4)	11162(3)	56(1)	1
C8	5765(3)	10218(4)	11954(3)	56(1)	1
C9	6049(3)	9197(4)	11981(2)	46(1)	1
C10	6355(3)	8858(3)	11202(2)	43(1)	1
C11	9116(3)	9193(2)	9459(2)	20(1)	1
C12	8828(2)	9513(2)	8675(2)	18(1)	1
C13	8126(2)	10327(2)	8387(2)	18(1)	1
C14	7480(3)	11204(2)	8823(2)	20(1)	1
C15	7965(3)	11906(2)	9059(2)	28(1)	1
C16	7357(3)	12683(3)	9497(2)	36(1)	1
C17	6267(3)	12779(3)	9696(2)	36(1)	1
C18	5755(3)	12105(2)	9451(2)	32(1)	1
C19	6359(3)	11322(2)	9014(2)	24(1)	1
C20	8090(2)	10152(2)	7597(2)	19(1)	1
C21	7398(3)	10794(2)	7059(2)	20(1)	1
C22	6480(3)	10556(3)	6849(2)	26(1)	1
C23	5858(3)	11123(3)	6319(2)	31(1)	1
C24	6140(3)	11936(3)	6005(2)	35(1)	1
C25	7053(3)	12185(3)	6205(2)	34(1)	1
C26	7671(3)	11628(2)	6739(2)	25(1)	1
C27	8773(3)	9239(2)	7422(2)	20(1)	1
C28	9076(3)	8683(3)	6698(2)	22(1)	1
Fe2	8143(1)	8668(1)	4525(1)	24(1)	1
C29	9179(3)	8914(2)	5271(2)	23(1)	1
C30	9543(3)	7951(2)	4983(2)	24(1)	1
C31	9726(3)	8027(2)	4162(2)	26(1)	1
C32	9483(3)	9022(2)	3947(2)	26(1)	1
C33	9125(3)	9574(2)	4634(2)	24(1)	1
C34	6682(3)	8695(3)	5158(2)	35(1)	1
C35	7027(3)	7843(3)	4701(2)	38(1)	1
C36	7147(3)	8139(3)	3918(2)	34(1)	1
C37	6879(3)	9159(3)	3883(2)	32(1)	1
C38	6588(3)	9510(3)	4652(2)	33(1)	1
N4	530(2)	5141(2)	1470(2)	24(1)	1

Table A.40: Continued overleaf

N5	896(2)	6272(2)	−434(1)	19(1)	1
O3	−401(2)	6563(2)	980(1)	29(1)	1
O4	1053(2)	7347(2)	−1827(1)	26(1)	1
Fe3	697(1)	5111(1)	3249(1)	30(1)	1
C39	−13(3)	5206(2)	2233(2)	24(1)	1
C40	−197(3)	4408(2)	2693(2)	32(1)	1
C41	−763(3)	4771(3)	3413(2)	38(1)	1
C42	−914(3)	5791(3)	3403(2)	37(1)	1
C43	−441(3)	6068(2)	2673(2)	28(1)	1
C44	2331(3)	4705(3)	2979(2)	50(1)	1
C45	1992(3)	4051(3)	3532(2)	49(1)	1
C46	1479(3)	4587(3)	4198(2)	50(1)	1
C47	1506(3)	5561(3)	4059(2)	47(1)	1
C48	2025(3)	5647(3)	3301(2)	49(1)	1
C49	327(3)	5814(2)	901(2)	19(1)	1
C50	1051(2)	5607(2)	163(2)	17(1)	1
C51	1960(2)	4870(2)	−67(2)	19(1)	1
C52	2489(3)	4023(2)	397(2)	21(1)	1
C53	2178(3)	3156(3)	426(2)	30(1)	1
C54	2676(3)	2391(3)	884(2)	44(1)	1
C55	3502(3)	2476(3)	1294(2)	42(1)	1
C56	3856(3)	3317(3)	1238(2)	45(1)	1
C57	3344(3)	4088(3)	799(2)	37(1)	1
C58	2360(3)	5101(2)	−825(2)	21(1)	1
C59	3320(3)	4508(2)	−1307(2)	22(1)	1
C60	4338(3)	4682(3)	−1296(2)	33(1)	1
C61	5225(3)	4173(3)	−1773(2)	47(1)	1
C62	5097(4)	3487(3)	−2262(2)	50(1)	1
C63	4093(3)	3308(3)	−2288(2)	45(1)	1
C64	3207(3)	3808(2)	−1805(2)	32(1)	1
C65	1683(3)	5980(2)	−1043(2)	22(1)	1
C66	1708(3)	6590(3)	−1742(2)	34(1)	1
N6A	2287(4)	6077(4)	−2372(3)	20(1)	0.50
Fe4A	3605(1)	7024(1)	−3637(1)	24(1)	0.50
C67A	2407(5)	6422(4)	−3140(3)	20(2)	0.50
C68A	1949(8)	7345(6)	−3455(4)	20(3)	0.50
C69A	2295(5)	7329(4)	−4262(3)	28(2)	0.50
C70A	2971(5)	6395(4)	−4442(3)	25(2)	0.50
C71A	3025(5)	5829(4)	−3752(3)	24(2)	0.50
C72A	4305(7)	7444(7)	−2785(4)	49(3)	0.50
C73A	4133(7)	8195(6)	−3344(5)	61(3)	0.50
C74A	4702(7)	7832(6)	−4047(5)	54(3)	0.50
C75A	5238(6)	6858(5)	−3942(4)	41(2)	0.50
C76A	5000(6)	6598(6)	−3150(5)	64(3)	0.50
N6B	2777(5)	6425(4)	−2203(3)	25(1)	0.50
Fe4B	3811(1)	6394(1)	−3913(1)	24(1)	0.50

Table A.40: Continued overleaf

C67B	3033(5)	6963(4)	−2877(3)	22(2)	0.50
C68B	4017(5)	7263(6)	−3067(4)	35(2)	0.50
C69B	3956(6)	7785(5)	−3775(4)	34(2)	0.50
C70B	2933(5)	7812(5)	−4020(4)	30(2)	0.50
C71B	2355(6)	7310(7)	−3466(5)	26(4)	0.50
C72B	4369(6)	5750(5)	−4971(4)	45(2)	0.50
C73B	3558(5)	5326(5)	−4583(4)	41(2)	0.50
C74B	3903(5)	4926(5)	−3879(4)	35(2)	0.50
C75B	4932(5)	5091(5)	−3826(4)	42(2)	0.50
C76B	5224(5)	5611(5)	−4495(4)	50(2)	0.50

Table A.40: Atomic coordinates [↔10^4], equivalent isotropic displacement parameters [$Å^2$ ↔10^3] and site occupancy factors. U_{eq} is defined as one third of the trace of the orthogonalized U^{ij} tensor.

3,4-Diphenyl-1H-pyrrole-2,5-dicarboxylic acid dimethyl ester

Identification code	**(154)**	
Empirical formula	$C_{20}H_{17}NO_4$	
Formula weight	335.35	
Temperature	120(2) K	
Wavelength	0.71073 Å	
Crystal system	Monoclinic	
Space group	*C*2/*c*	
Unit cell dimensions	a = 11.7128(4) Å	α = 90°
	b = 18.6419(6) Å	β = 100.669(2)°
	c = 15.7091(5) Å	γ = 90°
Volume	3370.77(19) Å^3	
Z	8	
Density (calculated)	1.322 Mg / m^3	
Absorption coefficient	0.093 mm^{-1}	
F(000)	1408	
Crystal	Needle; colourless	
Crystal size	0.26 × 0.03 × 0.02 mm^3	
θ range for data collection	3.09 – 27.43°	
Index ranges	$-15 \le h \le 15$, $-24 \le k \le 24$, $-20 \le l \le 20$	
Reflections collected	23433	
Independent reflections	3837 [R_{int} = 0.0986]	
Completeness to θ = 27.43°	99.4 %	
Absorption correction	Semi–empirical from equivalents	
Max. and min. transmission	0.9982 and 0.9763	
Refinement method	Full-matrix least-squares on F^2	
Data / restraints / parameters	3837 / 0 / 233	
Goodness-of-fit on F^2	0.970	
Final R indices [$F^2 > 2\sigma(F^2)$]	$R1$ = 0.0505, $wR2$ = 0.1099	
R indices (all data)	$R1$ = 0.1017, $wR2$ = 0.1313	
Extinction coefficient	0.0011(3)	
Largest diff. peak and hole	0.247 and –0.220 e Å^{-3}	

Table A.41: Structure and refinement data.

Atom	*x*	*y*	*z*	U_{eq}	*S.o.f.*
C1	3155(2)	3687(1)	1145(1)	22(1)	1
C2	2363(2)	3713(1)	367(1)	20(1)	1
C3	2992(2)	3902(1)	–286(1)	21(1)	1
C4	4152(2)	3982(1)	117(1)	22(1)	1
C5	3021(2)	3544(1)	2039(1)	26(1)	1
C6	1754(2)	3180(1)	2956(1)	38(1)	1
C7	5232(2)	4114(1)	–201(1)	23(1)	1
C8	6102(2)	4364(1)	–1398(1)	36(1)	1
C9	1090(2)	3577(1)	239(1)	20(1)	1
C10	333(2)	4109(1)	415(1)	23(1)	1
C11	–853(2)	3983(1)	289(1)	27(1)	1
C12	–1297(2)	3326(1)	–9(1)	27(1)	1
C13	–555(2)	2791(1)	–185(1)	28(1)	1
C14	632(2)	2916(1)	–61(1)	26(1)	1
C15	2467(2)	3989(1)	–1220(1)	22(1)	1
C16	2021(2)	3388(1)	–1697(1)	28(1)	1
C17	1432(2)	3465(1)	–2544(1)	32(1)	1
C18	1271(2)	4134(1)	–2917(1)	29(1)	1
C19	1733(2)	4732(1)	–2453(1)	28(1)	1
C20	2336(2)	4659(1)	–1609(1)	25(1)	1
N1	4231(1)	3849(1)	984(1)	23(1)	1
O1	3783(1)	3614(1)	2657(1)	52(1)	1
O2	1958(1)	3320(1)	2089(1)	29(1)	1
O3	6183(1)	4071(1)	256(1)	30(1)	1
O4	5057(1)	4272(1)	–1041(1)	33(1)	1

Table A.42: Atomic coordinates [$\times 10^4$], equivalent isotropic displacement parameters [$Å^2 \times 10^3$] and site occupancy factors. U_{eq} is defined as one third of the trace of the orthogonalized U^{ij} tensor.

3,4-Diphenyl-1H-pyrrole-2,5-dicarboxylic acid monomethyl ester

Identification code	**(155) crystallised from Ethyl acetate:Acetone (3:1)**	
Empirical formula	$C_{38}H_{30}N_2O_8$	
Formula weight	642.64	
Temperature	120(2) K	
Wavelength	0.71069 Å	
Crystal system	Monoclinic	
Space group	$P2_1$	
Unit cell dimensions	a = 6.181(5) Å	
	b = 29.082(5) Å	β = 94.244(5)°
	c = 8.658(5) Å	
Volume	1552.1(16) Å^3	
Z	2	
Density (calculated)	1.375 Mg / m^3	
Absorption coefficient	0.097 mm^{-1}	
F(000)	672	
CrystalColourless Needle		
Crystal size	0.15 × 0.04 × 0.03 mm^3	
θ range for data collection	3.16 – 23.25°	
Index ranges	$-6 \le h \le 6$, $-30 \le k \le 31$, $0 \le l \le 9$	
Reflections collected	3205	
Independent reflections	3205 [R_{int} = 0.0000]	
Completeness to θ = 23.25°	91.1 %	
Absorption correction	Semi–empirical from equivalents	
Max. and min. transmission	0.9971 and 0.9856	
Refinement method	Full-matrix least-squares on F^2	
Data / restraints / parameters	3205 / 293 / 435	
Goodness-of-fit on F^2	0.956	
Final R indices [$F^2 > 2\sigma(F^2)$]	$R1$ = 0.0756, $wR2$ = 0.1514	
R indices (all data)	$R1$ = 0.1497, $wR2$ = 0.2016	
Absolute structure parameter	not reliably determined	
Largest diff. peak and hole	0.279 and –0.246 e Å^{-3}	

Table A.43: Structure and refinement data.

Atom	x	y	z	U_{eq}	$S.o.f.$
C1	-40(20)	4409(5)	15605(16)	78(5)	1
C2	1130(20)	4289(5)	13138(17)	59(4)	1
C3	2490(20)	4458(4)	11882(16)	52(3)	1
C4	3780(20)	4827(5)	11787(15)	62(4)	1
C5	4859(19)	4785(4)	10378(14)	49(3)	1
C6	4100(20)	4382(4)	9738(14)	47(4)	1
C7	4430(20)	4157(5)	8259(16)	59(4)	1
C8	4140(20)	5208(4)	12987(15)	47(3)	1
C9	2240(20)	5483(4)	13190(14)	47(3)	1
C10	2490(20)	5794(4)	14512(15)	65(4)	1
C11	4370(20)	5817(5)	15484(14)	59(4)	1
C12	6130(20)	5572(5)	15269(14)	64(4)	1
C13	6020(20)	5253(4)	13936(15)	54(4)	1
C14	6510(20)	5112(5)	9916(14)	53(4)	1
C15	6150(20)	5590(4)	9926(12)	51(3)	1
C16	7760(20)	5917(5)	9503(13)	56(4)	1
C17	9570(30)	5739(6)	8950(14)	68(4)	1
C18	9940(20)	5284(5)	8892(16)	67(4)	1
C19	8430(20)	4966(4)	9343(14)	59(4)	1
C20	9123(18)	3152(5)	-2822(14)	59(4)	1
C21	7807(19)	3331(5)	-482(14)	49(4)	1
C22	6340(20)	3147(4)	727(14)	56(4)	1
C23	5080(20)	2769(4)	888(14)	47(3)	1
C24	4050(20)	2839(4)	2302(16)	58(4)	1
C25	4820(17)	3243(4)	2942(16)	51(4)	1
C26	4660(20)	3496(4)	4378(15)	46(3)	1
C27	4860(20)	2384(4)	-169(13)	44(3)	1
C28	6422(17)	2085(4)	-497(16)	56(4)	1
C29	6090(20)	1712(4)	-1492(16)	59(4)	1
C30	4170(30)	1681(5)	-2287(17)	71(5)	1
C31	2550(30)	1970(5)	-1998(17)	83(5)	1
C32	2800(20)	2320(5)	-1018(15)	63(4)	1
C33	2420(20)	2531(5)	2896(13)	50(3)	1
C34	2830(20)	2065(5)	3028(15)	63(4)	1
C35	1350(20)	1772(4)	3567(13)	45(3)	1
C36	-710(20)	1933(4)	3934(14)	52(4)	1
C37	-1060(20)	2397(4)	3867(13)	50(3)	1
C38	461(19)	2694(5)	3303(14)	53(4)	1
N1	2716(16)	4179(3)	10648(12)	51(3)	1
N2	6277(14)	3440(3)	1963(12)	46(3)	1
O1	173(15)	3934(3)	13003(9)	64(3)	1
O2	1289(13)	4577(3)	14376(10)	60(2)	1
O3	3762(13)	3760(3)	8021(9)	55(2)	1
O4	5364(14)	4393(3)	7194(11)	65(3)	1
O5	8737(12)	3694(3)	-445(9)	57(3)	1

Table A.44: Continued overleaf

O6	7818(12)	3017(3)	−1579(11)	58(2)	1
O7	5358(12)	3884(2)	4617(8)	43(2)	1
O8	3685(12)	3248(3)	5435(9)	55(2)	1

Table A.44: Atomic coordinates [$\leftrightarrow 10^4$], equivalent isotropic displacement parameters [$Å^2 \leftrightarrow 10^3$] and site occupancy factors. U_{eq} is defined as one third of the trace of the orthogonalized U^{ij} tensor.

3,4-Diphenyl-1H-pyrrole-2,5-dicarboxylic acid monomethyl ester

Identification code	**(155) crystallised from MeOH:DCM**	
Empirical formula	$C_{19}H_{15}NO_4$	
Formula weight	321.32	
Temperature	293(2) K	
Wavelength	0.71073 Å	
Crystal system	Triclinic	
Space group	P-1	
Unit cell dimensions	a = 6.3170(4) Å	α = 91.990(2)°
	b = 8.6640(6) Å	β = 101.033(2)°
	c = 14.7592(12) Å	γ = 94.166(5)°
Volume	789.78(10) Å^3	
Z	2	
Density (calculated)	1.351 Mg / m^3	
Absorption coefficient	0.096 mm^{-1}	
F(000)	336	
Crystal	Colourless Plate	
Crystal size	0.2 x 0.1 x 0.02 mm^3	
θ range for data collection	3.30 – 23.25°	
Index ranges	$-7 \le h \le 5$, $-9 \le k \le 9$, $-16 \le l \le 16$	
Reflections collected	6739	
Independent reflections	2259 [R_{int} = 0.0759]	
Completeness to θ = 23.25°	99.6 %	
Absorption correction	Semi–empirical from equivalents	
Refinement method	Full-matrix least-squares on F^2	
Data / restraints / parameters	2259 / 0 / 221	
Goodness-of-fit on F^2	0.965	
Final R indices [$F^2 > 2\sigma(F^2)$]	$R1$ = 0.1685, $wR2$ = 0.4571	
R indices (all data)	$R1$ = 0.1887, $wR2$ = 0.4694	
Extinction coefficient	0.023(14)	
Largest diff. peak and hole	0.983 and –0.573 e Å^{-3}	

Table A.45: Structure and refinement data.

Atom	x	y	z	U_{eq}	$S.o.f.$
N1	3548(18)	−607(12)	5756(8)	29(3)	1
O1	4085(14)	−3323(10)	4878(7)	31(2)	1
O2	6332(15)	−4014(11)	6144(7)	36(3)	1
O3	836(16)	1769(11)	5239(7)	36(3)	1
O4	2424(15)	3150(11)	6517(6)	34(2)	1
C1	5150(20)	−2995(14)	5683(10)	29(3)	1
C2	5060(20)	−1495(15)	6124(9)	26(3)	1
C3	6303(19)	−766(14)	6940(9)	21(3)	1
C4	5367(19)	697(13)	7022(8)	21(3)	1
C5	3645(19)	726(13)	6276(9)	23(3)	1
C6	2170(20)	1919(15)	5967(9)	28(3)	1
C7	1090(20)	4383(15)	6257(11)	36(4)	1
C8	8210(20)	−1239(14)	7589(9)	27(3)	1
C9	8190(30)	−1187(16)	8541(11)	39(4)	1
C10	10060(30)	−1571(16)	9135(10)	38(4)	1
C11	11820(20)	−2051(17)	8818(11)	41(4)	1
C12	11780(20)	−2118(15)	7874(10)	35(3)	1
C13	9980(20)	−1735(15)	7263(10)	30(3)	1
C14	6130(20)	1930(15)	7760(9)	28(3)	1
C15	8130(20)	2675(15)	7848(11)	37(4)	1
C16	8820(30)	3919(18)	8492(10)	44(4)	1
C17	7470(30)	4376(16)	9049(10)	40(4)	1
C18	5470(30)	3615(19)	8989(11)	43(4)	1
C19	4790(20)	2369(17)	8347(9)	35(3)	1

Table A.46: Atomic coordinates [↔10^4], equivalent isotropic displacement parameters [$Å^2$ ↔10^3] and site occupancy factors. U_{eq} is defined as one third of the trace of the orthogonalized U^{ij} tensor.

5-(Ferrocenylmethyl-carbamoyl)-3,4-diphenyl-1*H*-pyrrole-2-carboxylic acid methyl ester

Identification code	**(156)**	
Empirical formula	$C_{30}H_{26}FeN_2O_3$	
Formula weight	518.38	
Temperature	120(2) K	
Wavelength	0.71073 Å	
Crystal system	Orthorhombic	
Space group	*Pbca*	
Unit cell dimensions	a = 6.0816(4) Å	α = 90°
	b = 24.8503(16) Å	β = 90°
	c = 31.120(3) Å	γ = 90°
Volume	4703.2(6) $Å^3$	
Z	8	
Density (calculated)	1.464 Mg / m^3	
Absorption coefficient	0.678 mm^{-1}	
F(000)	2160	
Crystal	Needle; yellow	
Crystal size	0.20 × 0.03 × 0.03 mm^3	
θ range for data collection	3.09 – 26.00°	
Index ranges	$-6 \le h \le 6$, $-28 \le k \le 27$, $-38 \le l \le 28$	
Reflections collected	10713	
Independent reflections	3464 [R_{int} = 0.0691]	
Completeness to θ = 26.00°	74.8 %	
Absorption correction	Semi–empirical from equivalents	
Max. and min. transmission	0.9799 and 0.8763	
Refinement method	Full-matrix least-squares on F^2	
Data / restraints / parameters	3464 / 0 / 335	
Goodness-of-fit on F^2	0.986	
Final R indices [$F^2 > 2\sigma(F^2)$]	$R1$ = 0.0573, $wR2$ = 0.1046	
R indices (all data)	$R1$ = 0.1185, $wR2$ = 0.1243	
Extinction coefficient	0.00047(15)	
Largest diff. peak and hole	0.522 and –0.473 e $Å^{-3}$	

Table A.47: Structure and refinement data.

Atom	x	y	z	U_{eq}	$S.o.f.$
C1	7206(9)	4360(2)	798(2)	38(1)	1
C2	5928(9)	3907(2)	897(2)	39(1)	1
C3	3851(8)	4091(2)	1038(2)	32(1)	1
C4	3854(8)	4654(2)	1026(1)	27(1)	1
C5	5933(8)	4818(2)	874(2)	32(1)	1
C6	5492(8)	4596(2)	2040(1)	25(1)	1
C7	7324(8)	4892(2)	1897(2)	29(1)	1
C8	8997(8)	4526(2)	1788(2)	29(1)	1
C9	8208(7)	4002(2)	1865(1)	23(1)	1
C10	6020(7)	4041(2)	2021(1)	19(1)	1
C11	4539(7)	3581(2)	2151(1)	24(1)	1
C12	5653(7)	2629(2)	2108(2)	22(1)	1
C13	6340(7)	2198(2)	1811(2)	20(1)	1
C14	5750(7)	2045(2)	1394(2)	22(1)	1
C15	7205(7)	1612(2)	1273(2)	22(1)	1
C16	8612(7)	1535(2)	1615(2)	23(1)	1
C17	4042(7)	2300(2)	1122(1)	21(1)	1
C18	2058(7)	2477(2)	1293(2)	28(1)	1
C19	530(8)	2752(2)	1039(2)	29(1)	1
C20	984(8)	2852(2)	612(2)	35(1)	1
C21	2953(8)	2680(2)	435(2)	32(1)	1
C22	4459(8)	2409(2)	687(2)	29(1)	1
C23	7170(8)	1323(2)	856(2)	22(1)	1
C24	8990(8)	1340(2)	584(2)	27(1)	1
C25	8938(8)	1074(2)	194(2)	32(1)	1
C26	7117(9)	786(2)	70(2)	33(1)	1
C27	5287(8)	769(2)	338(2)	32(1)	1
C28	5321(8)	1036(2)	726(2)	27(1)	1
C29	10512(7)	1178(2)	1656(2)	23(1)	1
C30	13520(7)	941(2)	2092(2)	31(1)	1
N1	5122(7)	3095(2)	1917(1)	25(1)	1
N2	8036(7)	1881(2)	1935(1)	23(1)	1
O1	5658(4)	2561(1)	2501(1)	25(1)	1
O2	11066(5)	844(1)	1398(1)	30(1)	1
O3	11592(5)	1270(1)	2030(1)	29(1)	1
Fe1	6269(1)	4382(1)	1427(1)	25(1)	1

Table A.48: Atomic coordinates [$\times 10^4$], equivalent isotropic displacement parameters [$Å^2 \times 10^3$] and site occupancy factors. U_{eq} is defined as one third of the trace of the orthogonalized U^{ij} tensor.

5-(Ferrocenyl-carbamoyl)-3,4-diphenyl-1*H*-pyrrole-2-carboxylic acid methyl ester

Identification code	**(157)**	
Empirical formula	$C_{29}H_{24}FeN_2O_3$	
Formula weight	504.35	
Temperature	120(2) K	
Wavelength	0.71073 Å	
Crystal system	Triclinic	
Space group	*P*–1	
Unit cell dimensions	a = 10.4568(4) Å	α = 61.172(2)°
	b = 11.6216(5) Å	β = 70.776(2)°
	c = 11.7872(6) Å	γ = 67.863(2)°
Volume	1143.03(9) $Å^3$	
Z	2	
Density (calculated)	1.465 Mg / m^3	
Absorption coefficient	0.696 mm^{-1}	
F(000)	524	
Crystal	Plate; orange	
Crystal size	0.14 × 0.10 × 0.02 mm^3	
θ range for data collection	2.07 – 27.50°	
Index ranges	$-13 \le h \le 13$, $-15 \le k \le 14$, $-15 \le l \le 15$	
Reflections collected	16609	
Independent reflections	5111 [R_{int} = 0.0439]	
Completeness to θ = 27.50°	97.6 %	
Absorption correction	Semi–empirical from equivalents	
Max. and min. transmission	0.9862 and 0.9089	
Refinement method	Full-matrix least-squares on F^2	
Data / restraints / parameters	5111 / 0 / 326	
Goodness-of-fit on F^2	1.040	
Final R indices [$F^2 > 2\sigma(F^2)$]	$R1$ = 0.0435, $wR2$ = 0.0963	
R indices (all data)	$R1$ = 0.0651, $wR2$ = 0.1048	
Extinction coefficient	0.0016(9)	
Largest diff. peak and hole	0.461 and –0.505 e $Å^{-3}$	

Table A.49: Structure and refinement data.

Atom	x	y	z	U_{eq}	*S.o.f.*
C1	912(2)	1130(2)	1853(2)	27(1)	1
C2	1112(2)	571(2)	956(2)	28(1)	1
C3	37(2)	1355(2)	192(2)	28(1)	1
C4	−830(2)	2391(2)	628(2)	26(1)	1
C5	−289(2)	2254(2)	1657(2)	24(1)	1
C6	1752(2)	4283(2)	−628(2)	22(1)	1
C7	1239(2)	4340(2)	−1636(2)	24(1)	1
C8	2108(2)	3234(2)	−1976(2)	26(1)	1
C9	3143(2)	2481(2)	−1171(2)	24(1)	1
C10	2937(2)	3143(2)	−358(2)	20(1)	1
C11	5001(2)	1856(2)	724(2)	21(1)	1
C12	5629(2)	1646(2)	1787(2)	19(1)	1
C13	5318(2)	2267(2)	2636(2)	19(1)	1
C14	6317(2)	1507(2)	3488(2)	19(1)	1
C15	7199(2)	451(2)	3124(2)	19(1)	1
C16	8445(2)	−650(2)	3557(2)	19(1)	1
C17	10139(2)	−1616(2)	4901(2)	26(1)	1
C18	4125(2)	3440(2)	2733(2)	20(1)	1
C19	4074(2)	4764(2)	1799(2)	23(1)	1
C20	2945(3)	5840(2)	1915(2)	27(1)	1
C21	1861(3)	5607(2)	2983(3)	31(1)	1
C22	1914(3)	4299(3)	3939(3)	36(1)	1
C23	3036(2)	3221(2)	3811(2)	31(1)	1
C24	6333(2)	1839(2)	4542(2)	20(1)	1
C25	6451(2)	3121(2)	4237(2)	23(1)	1
C26	6377(2)	3471(2)	5233(2)	27(1)	1
C27	6185(2)	2556(2)	6533(2)	27(1)	1
C28	6083(2)	1283(2)	6842(2)	26(1)	1
C29	6155(2)	922(2)	5859(2)	23(1)	1
N1	3738(2)	2790(2)	576(2)	22(1)	1
N2	6766(2)	559(2)	2097(2)	19(1)	1
O1	5606(2)	1204(2)	47(2)	28(1)	1
O2	9007(2)	−1517(2)	3129(2)	25(1)	1
O3	8872(2)	−587(2)	4473(1)	22(1)	1
Fe1	1192(1)	2547(1)	−38(1)	20(1)	1

Table A.50: Atomic coordinates [↔10^4], equivalent isotropic displacement parameters [$Å^2$ ↔10^3] and site occupancy factors. U_{eq} is defined as one third of the trace of the orthogonalized U^{ij} tensor.

5-(Ferrocenylmethyl-carbamoyl)-3,4-diphenyl-1H-pyrrole-2-carboxylic acid

Identification code	**(158)**	
Empirical formula	$C_{32}H_{27}FeN_2O_3$	
Formula weight	543.41	
Temperature	120(2) K	
Wavelength	0.71073 Å	
Crystal system	Triclinic	
Space group	$P-1$	
Unit cell dimensions	a = 8.6796(3) Å	α = 98.9590(10)°
	b = 11.1346(4) Å	β = 103.3050(10)°
	c = 14.2857(6) Å	γ = 109.105(2)°
Volume	1228.83(8) Å^3	
Z	2	
Density (calculated)	1.469 Mg / m^3	
Absorption coefficient	0.653 mm^{-1}	
F(000)	566	
Crystal	Needle; yellow	
Crystal size	0.16 × 0.01 × 0.01 mm^3	
θ range for data collection	3.03 - 27.40°	
Index ranges	$-11 \le h \le 11$, $-14 \le k \le 14$, $-18 \le l \le 18$	
Reflections collected	18282	
Independent reflections	5495 [R_{int} = 0.1334]	
Completeness to θ = 27.40°	98.4 %	
Absorption correction	Semi–empirical from equivalents	
Max. and min. transmission	0.9935 and 0.9027	
Refinement method	Full-matrix least-squares on F^2	
Data / restraints / parameters	5495 / 0 / 356	
Goodness-of-fit on F^2	1.017	
Final R indices [$F^2 > 2\sigma(F^2)$]	$R1$ = 0.0630, $wR2$ = 0.1154	
R indices (all data)	$R1$ = 0.1230, $wR2$ = 0.1348	
Extinction coefficient	0.0089(14)	
Largest diff. peak and hole	0.583 and –0.568 e Å^{-3}	

Table A.51: Structure and refinement data.

Atom	x	y	z	U_{eq}	*S.o.f.*
C30	13382(5)	4885(4)	32(3)	31(1)	1
C31	13597(5)	3922(4)	-602(3)	33(1)	1
C32	15216(5)	4040(4)	-631(3)	33(1)	1
C1	9010(5)	6002(4)	4362(3)	29(1)	1
C2	8280(5)	6359(3)	3513(3)	27(1)	1
C3	6694(5)	6419(3)	3582(3)	31(1)	1
C4	6477(5)	6102(4)	4468(3)	35(1)	1
C5	7903(5)	5843(4)	4951(3)	32(1)	1
C6	5036(4)	3388(3)	2257(3)	22(1)	1
C7	4341(5)	3115(3)	3029(3)	28(1)	1
C8	5437(5)	2733(3)	3696(3)	26(1)	1
C9	6857(5)	2788(3)	3331(3)	26(1)	1
C10	6594(4)	3195(3)	2431(3)	21(1)	1
C11	7732(5)	3344(4)	1779(3)	27(1)	1
C12	9669(4)	2343(3)	1347(3)	20(1)	1
C13	10369(4)	1313(3)	1429(3)	18(1)	1
C14	10287(4)	400(3)	1996(2)	17(1)	1
C15	11366(4)	-265(3)	1779(2)	18(1)	1
C16	12066(4)	287(3)	1089(2)	18(1)	1
C17	13343(4)	143(3)	619(2)	20(1)	1
C18	9246(4)	177(3)	2685(2)	18(1)	1
C19	7522(4)	-624(3)	2321(3)	19(1)	1
C20	6498(4)	-778(3)	2951(3)	22(1)	1
C21	7194(4)	-144(3)	3936(3)	23(1)	1
C22	8910(5)	655(3)	4315(3)	23(1)	1
C23	9922(4)	818(3)	3688(3)	22(1)	1
C24	11676(4)	-1307(3)	2217(3)	19(1)	1
C25	11357(4)	-2531(3)	1616(3)	24(1)	1
C26	11669(4)	-3499(3)	2033(3)	27(1)	1
C27	12318(4)	-3261(4)	3053(3)	27(1)	1
C28	12614(4)	-2064(4)	3653(3)	26(1)	1
C29	12301(4)	-1094(3)	3237(3)	21(1)	1
N1	8448(4)	2331(3)	1776(2)	22(1)	1
N2	11453(4)	1227(3)	896(2)	19(1)	1
O1	10201(3)	3159(2)	895(2)	27(1)	1
O2	13878(3)	-792(2)	792(2)	25(1)	1
O3	13849(3)	873(2)	105(2)	23(1)	1
Fe1	6676(1)	4586(1)	3583(1)	19(1)	1

Table A.52: Atomic coordinates [↔10^4], equivalent isotropic displacement parameters [$Å^2$ ↔10^3] and site occupancy factors. U_{eq} is defined as one third of the trace of the orthogonalized U^{ij} tensor.

5-(Ferrocenyl-carbamoyl)-3,4-diphenyl-1*H*-pyrrole-2-carboxylic acid

Identification code	**(159)**	
Empirical formula	$C_{30}H_{27}Cl_3FeN_2O_5$	
Formula weight	657.74	
Temperature	120(2) K	
Wavelength	0.71073 Å	
Crystal system	Triclinic	
Space group	$P-1$	
Unit cell dimensions	$a = 11.0968(4)$ Å	$\alpha = 102.233(2)°$
	$b = 11.1517(4)$ Å	$\beta = 95.688(2)°$
	$c = 11.9917(5)$ Å	$\gamma = 92.374(3)°$
Volume	1440.14(9) $Å^3$	
Z	2	
Density (calculated)	1.517 Mg / m^3	
Absorption coefficient	0.845 mm^{-1}	
F(000)	676	
Crystal	Block; orange	
Crystal size	0.16 × 0.12 × 0.06 mm^3	
θ range for data collection	2.97 – 27.48°	
Index ranges	$-14 \le h \le 14$, $-14 \le k \le 14$, $-15 \le l \le 15$	
Reflections collected	21381	
Independent reflections	6433 [$R_{int} = 0.0476$]	
Completeness to $\theta = 27.48°$	97.4 %	
Absorption correction	Semi–empirical from equivalents	
Max. and min. transmission	0.9510 and 0.8766	
Refinement method	Full-matrix least-squares on F^2	
Data / restraints / parameters	6433 / 6 / 382	
Goodness-of-fit on F^2	1.029	
Final R indices [$F^2 > 2\sigma(F^2)$]	$R1 = 0.0551$, $wR2 = 0.1407$	
R indices (all data)	$R1 = 0.0746$, $wR2 = 0.1542$	
Extinction coefficient	0.0000(12)	
Largest diff. peak and hole	1.553 and –0.584 e $Å^{-3}$	

Table A.53: Structure and refinement data.

Atom	*x*	*y*	*z*	U_{eq}	*S.o.f.*
O5	16202(2)	3446(2)	4992(2)	29(1)	1
O4	15619(2)	5641(2)	6375(2)	35(1)	1
C30	15149(5)	5713(4)	5821(4)	51(1)	1
C1	7507(3)	5150(3)	8661(3)	23(1)	1
C2	8547(2)	5951(3)	8844(2)	21(1)	1
C3	9367(3)	5383(3)	8089(2)	21(1)	1
C4	8781(3)	4272(3)	7459(3)	22(1)	1
C5	6388(3)	5140(3)	9198(3)	25(1)	1
C6	8802(3)	7149(3)	9650(2)	22(1)	1
C7	8028(3)	8109(3)	9639(3)	25(1)	1
C8	8324(3)	9252(3)	10352(3)	30(1)	1
C9	9392(3)	9463(3)	11089(3)	32(1)	1
C10	10158(3)	8513(3)	11121(3)	31(1)	1
C11	9870(3)	7369(3)	10406(3)	26(1)	1
C12	10607(3)	5867(3)	8001(2)	20(1)	1
C13	11612(3)	5215(3)	8253(3)	25(1)	1
C14	12771(3)	5645(3)	8144(3)	32(1)	1
C15	12946(3)	6737(3)	7798(3)	37(1)	1
C16	11970(3)	7403(3)	7562(3)	38(1)	1
C17	10800(3)	6968(3)	7655(3)	29(1)	1
C18	9105(3)	3301(3)	6511(3)	23(1)	1
C19	10621(3)	2775(3)	5148(3)	24(1)	1
C20	10304(3)	1498(3)	4696(3)	28(1)	1
C21	11090(3)	1091(3)	3847(3)	32(1)	1
C22	11883(3)	2099(3)	3775(3)	34(1)	1
C23	11593(3)	3147(3)	4593(3)	29(1)	1
C24	12660(3)	1982(3)	7093(3)	32(1)	1
C25	12306(3)	731(3)	6601(3)	31(1)	1
C26	13036(3)	310(3)	5717(3)	34(1)	1
C27	13838(3)	1294(4)	5637(3)	37(1)	1
C28	13615(3)	2341(3)	6499(3)	36(1)	1
N1	7683(2)	4153(2)	7827(2)	24(1)	1
N2	10076(2)	3572(2)	5999(2)	23(1)	1
O1	6273(2)	6104(2)	10016(2)	30(1)	1
O2	5622(2)	4266(2)	8891(2)	30(1)	1
O3	8488(2)	2324(2)	6209(2)	33(1)	1
Fe1	12097(1)	1752(1)	5376(1)	25(1)	1
C29	4570(3)	9254(3)	1946(3)	33(1)	1
Cl1	3413(1)	8861(1)	2725(1)	32(1)	1
Cl2	4796(1)	10875(1)	2216(1)	53(1)	1
Cl3	4217(1)	8630(1)	475(1)	53(1)	1

Table A.54: Atomic coordinates [$\times 10^4$], equivalent isotropic displacement parameters [$Å^2 \times 10^3$] and site occupancy factors. U_{eq} is defined as one third of the trace of the orthogonalized U^{ij} tensor.

3,4-Diphenyl-1*H*-pyrrole-2,5-dicarboxylic acid 2-ferrocenylmethyl-amide 5-phenylamide

Identification code	**(160)**	
Empirical formula	$C_{35}H_{29}FeN_3O_2$	
Formula weight	579.46	
Temperature	120(2) K	
Wavelength	0.71073 Å	
Crystal system	Triclinic	
Space group	$P\bar{1}$	
Unit cell dimensions	a = 9.3589(7) Å	α = 86.856(12)°
	b = 16.076(2) Å	β = 89.616(12)°
	c = 17.627(3) Å	γ = 84.448(9)°
Volume	2635.6(6) Å^3	
Z	4	
Density (calculated)	1.460 Mg / m^3	
Absorption coefficient	0.612 mm^{-1}	
F(000)	1208	
Crystal	Orange Block	
Crystal size	0.25 × 0.15 × 0.10 mm^3	
θ range for data collection	4.62 – 24.11°	
Index ranges	$-10 \le h \le 10$, $-18 \le k \le 18$, $-20 \le l \le 20$	
Reflections collected	21862	
Independent reflections	21893 [R_{int} = 0.0000]	
Completeness to θ = 24.11°	95.6 %	
Max. and min. transmission	0.9413 and 0.8620	
Refinement method	Full-matrix least-squares on F^2	
Data / restraints / parameters	21893 / 0 / 740	
Goodness-of-fit on F^2	1.042	
Final R indices [$F^2 > 2\sigma(F^2)$]	$R1$ = 0.0591, $wR2$ = 0.1380	
R indices (all data)	$R1$ = 0.0833, $wR2$ = 0.1541	
Largest diff. peak and hole	0.534 and –0.375 e Å^{-3}	

Table A.55: Structure and refinement data.

Atom	x	y	z	U_{eq}	$S.o.f.$
Fe1	8045(1)	166(1)	3694(1)	17(1)	1
N1	7664(3)	−178(2)	1672(2)	16(1)	1
N2	7926(3)	896(2)	−176(2)	12(1)	1
N3	6097(3)	1814(2)	−1812(2)	15(1)	1
O1	9441(3)	−221(2)	811(1)	26(1)	1
O2	8498(3)	1730(2)	−1587(1)	20(1)	1
C1	6609(4)	1179(3)	3445(2)	25(1)	1
C2	7168(4)	1219(3)	4180(2)	26(1)	1
C3	6843(4)	500(3)	4611(2)	25(1)	1
C4	6082(4)	4(3)	4142(2)	26(1)	1
C5	5941(4)	429(3)	3426(2)	27(1)	1
C6	9653(4)	198(2)	2919(2)	20(1)	1
C7	10203(4)	219(2)	3657(2)	21(1)	1
C8	9869(4)	−505(2)	4077(2)	20(1)	1
C9	9115(4)	−986(2)	3589(2)	17(1)	1
C10	8983(4)	−545(2)	2866(2)	16(1)	1
C11	8326(4)	−843(2)	2177(2)	16(1)	1
C12	8245(4)	59(2)	1010(2)	13(1)	1
C13	7350(4)	658(2)	508(2)	13(1)	1
C14	5980(4)	1048(2)	552(2)	12(1)	1
C15	5713(4)	1540(2)	−130(2)	13(1)	1
C16	6943(4)	1420(2)	−571(2)	13(1)	1
C17	7284(4)	1681(2)	−1363(2)	15(1)	1
C18	6036(4)	1981(2)	−2609(2)	16(1)	1
C19	4751(4)	2346(2)	−2903(2)	23(1)	1
C20	4577(4)	2497(3)	−3678(2)	26(1)	1
C21	5709(4)	2275(3)	−4154(2)	25(1)	1
C22	6976(4)	1905(3)	−3863(2)	24(1)	1
C23	7149(4)	1750(2)	−3088(2)	18(1)	1
C24	4944(4)	1029(2)	1187(2)	14(1)	1
C25	4724(4)	1706(2)	1643(2)	17(1)	1
C26	3708(4)	1709(2)	2219(2)	20(1)	1
C27	2906(4)	1042(2)	2337(2)	21(1)	1
C28	3104(4)	377(3)	1883(2)	24(1)	1
C29	4112(4)	370(2)	1312(2)	20(1)	1
C30	3066(4)	1695(2)	−320(2)	20(1)	1
C31	1803(4)	2165(2)	−510(2)	19(1)	1
C32	1797(4)	3010(3)	−698(2)	22(1)	1
C33	3065(4)	3373(2)	−706(2)	19(1)	1
C34	4346(4)	2899(2)	−521(2)	16(1)	1
C35	4367(4)	2054(2)	−327(2)	12(1)	1
Fe2	2114(1)	4954(1)	1385(1)	16(1)	1
N4	3248(3)	5598(2)	3201(2)	18(1)	1
N5	3123(3)	5986(2)	5204(2)	14(1)	1
N6	1392(3)	6793(2)	6877(2)	15(1)	1

Table A.56: Continued overleaf

O3	4887(3)	5342(2)	4125(1)	20(1)	1
O4	3723(3)	6387(2)	6637(1)	23(1)	1
C36	1826(5)	3928(2)	2058(2)	26(1)	1
C37	1830(5)	3732(2)	1295(2)	25(1)	1
C38	701(4)	4231(3)	933(2)	26(1)	1
C39	–5(4)	4737(2)	1472(2)	24(1)	1
C40	701(4)	4553(3)	2173(2)	24(1)	1
C41	4221(4)	5089(2)	1202(2)	19(1)	1
C42	3397(4)	5399(2)	560(2)	19(1)	1
C43	2385(4)	6048(2)	794(2)	20(1)	1
C44	2585(4)	6141(2)	1576(2)	16(1)	1
C45	3712(4)	5544(2)	1835(2)	16(1)	1
C46	4304(4)	5411(3)	2620(2)	22(1)	1
C47	3654(4)	5588(2)	3929(2)	16(1)	1
C48	2601(4)	5913(2)	4492(2)	15(1)	1
C49	1156(4)	6196(2)	4495(2)	12(1)	1
C50	817(4)	6461(2)	5236(2)	13(1)	1
C51	2076(4)	6324(2)	5652(2)	12(1)	1
C52	2483(4)	6502(2)	6429(2)	15(1)	1
C53	1478(4)	7028(2)	7634(2)	14(1)	1
C54	2551(4)	6689(2)	8121(2)	19(1)	1
C55	2532(4)	6934(3)	8864(2)	22(1)	1
C56	1467(4)	7499(2)	9120(2)	22(1)	1
C57	396(4)	7835(2)	8629(2)	24(1)	1
C58	398(4)	7598(2)	7889(2)	21(1)	1
C59	186(4)	6744(2)	3228(2)	15(1)	1
C60	–777(4)	6740(2)	2641(2)	19(1)	1
C61	–1842(4)	6210(2)	2695(2)	19(1)	1
C62	–1971(4)	5697(2)	3344(2)	19(1)	1
C63	–1002(4)	5697(2)	3921(2)	16(1)	1
C64	114(4)	6214(2)	3868(2)	12(1)	1
C65	–1619(4)	6312(3)	5787(2)	21(1)	1
C66	–2982(4)	6644(3)	5972(2)	24(1)	1
C67	–3373(4)	7483(3)	5858(2)	26(1)	1
C68	–2393(5)	7998(3)	5550(2)	30(1)	1
C69	–1035(4)	7663(2)	5358(2)	22(1)	1
C70	–621(4)	6817(2)	5472(2)	14(1)	1

Table A.56: Atomic coordinates [$\times 10^4$], equivalent isotropic displacement parameters [Å^2 $\times 10^3$] and site occupancy factors. U_{eq} is defined as one third of the trace of the orthogonalized U^{ij} tensor.

3,4-Diphenyl-1*H*-pyrrole-2,5-dicarboxylic acid 2-ferrocenylamide 5-phenylamide

Identification code	**(161)**	
Empirical formula	$C_{35}H_{31}FeN_3O_3$	
Formula weight	597.48	
Temperature	120(2) K	
Wavelength	0.71073 Å	
Crystal system	Triclinic	
Space group	$P\bar{1}$	
Unit cell dimensions	a = 10.6570(5) Å	α = 88.074(2)°
	b = 10.9323(6) Å	β = 82.029(2)°
	c = 13.7118(10) Å	γ = 65.031(2)°
Volume	1433.65(15) Å^3	
Z	2	
Density (calculated)	1.384 Mg / m^3	
Absorption coefficient	0.568 mm^{-1}	
F(000)	624	
Crystal	Orange Blade	
Crystal size	0.25 × 0.20 × 0.03 mm^3	
θ range for data collection	3.00 – 23.25°	
Index ranges	$-11 \le h \le 11$, $-12 \le k \le 12$, $-15 \le l \le 15$	
Reflections collected	19514	
Independent reflections	4086 [R_{int} = 0.0787]	
Completeness to θ = 23.25°	99.6 %	
Absorption correction	Semi–empirical from equivalents	
Max. and min. transmission	0.9832 and 0.8711	
Refinement method	Full-matrix least-squares on F^2	
Data / restraints / parameters	4086 / 0 / 382	
Goodness-of-fit on F^2	1.016	
Final R indices [$F^2 > 2\sigma(F^2)$]	$R1$ = 0.0622, $wR2$ = 0.1560	
R indices (all data)	$R1$ = 0.0986, $wR2$ = 0.1782	
Extinction coefficient	none	
Largest diff. peak and hole	0.514 and –0.479 e Å^{-3}	

Table A.57: Structure and refinement data.

Atom	x	y	z	U_{eq}	*S.o.f.*
Fe1	7487(1)	2437(1)	4265(1)	48(1)	1
N1	9969(4)	1923(4)	2588(3)	47(1)	1
N2	12871(4)	-342(3)	908(3)	31(1)	1
N3	14958(4)	-1111(4)	-1491(3)	34(1)	1
O1	11455(4)	-217(4)	2845(3)	51(1)	1
O2	15343(3)	-2114(3)	-14(2)	40(1)	1
C1	6931(10)	895(9)	4172(8)	105(3)	1
C2	6107(10)	1752(11)	4943(6)	106(3)	1
C3	5430(8)	3004(10)	4662(9)	104(3)	1
C4	5776(9)	2973(10)	3632(9)	103(3)	1
C5	6720(8)	1631(10)	3338(6)	89(2)	1
C6	9557(7)	1564(9)	4415(5)	91(3)	1
C7	8745(8)	2397(12)	5225(6)	102(3)	1
C8	8073(8)	3717(10)	4894(6)	92(3)	1
C9	8409(6)	3685(6)	3832(5)	70(2)	1
C10	9337(6)	2343(6)	3562(4)	55(2)	1
C11	10991(5)	718(5)	2280(4)	40(1)	1
C12	11560(4)	617(4)	1226(3)	31(1)	1
C13	11050(4)	1382(4)	428(3)	30(1)	1
C14	12119(4)	888(4)	-395(3)	28(1)	1
C15	13237(4)	-191(4)	-62(3)	31(1)	1
C16	14612(4)	-1219(4)	-520(4)	32(1)	1
C17	16148(5)	-1986(5)	-2129(4)	38(1)	1
C18	17030(5)	-3268(5)	-1872(4)	52(1)	1
C19	18107(6)	-4076(6)	-2569(5)	65(2)	1
C20	18325(6)	-3643(7)	-3487(5)	66(2)	1
C21	17460(6)	-2353(7)	-3731(4)	63(2)	1
C22	16368(5)	-1523(5)	-3055(4)	48(1)	1
C23	9648(4)	2518(4)	429(3)	32(1)	1
C24	9424(5)	3839(5)	553(4)	48(1)	1
C25	8112(6)	4885(5)	562(4)	58(2)	1
C26	7008(5)	4634(5)	466(4)	49(1)	1
C27	7193(5)	3329(5)	338(5)	65(2)	1
C28	8512(5)	2270(5)	326(5)	56(2)	1
C29	12006(5)	1460(4)	-1387(3)	34(1)	1
C30	10904(5)	1579(5)	-1877(4)	51(1)	1
C31	10764(7)	2160(7)	-2786(5)	74(2)	1
C32	11702(9)	2631(6)	-3221(5)	76(2)	1
C33	12818(7)	2510(5)	-2764(4)	58(2)	1
C34	12960(5)	1946(4)	-1835(4)	41(1)	1
C35	13918(11)	-3509(10)	2405(8)	155(5)	1
O3	14003(4)	-2280(6)	2437(4)	94(2)	1

Table A.58: Atomic coordinates [↔10^4], equivalent isotropic displacement parameters [$Å^2$ ↔10^3] and site occupancy factors. U_{eq} is defined as one third of the trace of the orthogonalized U^{ij} tensor.

References

(1) Lehn, J. M.; *Angew. Chem. Int. Ed. Engl.* **1988**, *27*, 89.

(2) Beer, P. D.; Gale, P.A. *Angew. Chem. Int. Ed.* **2001**, *40*, 486.

(3) Gale, P. A. *Phil. Trans. R. Soc. Lond. A.* **2000**, *358*, 431.

(4) Fischer, E.; Ber. Dtsch. Chem. Ges. **1894**, 2985.

(5) Pedersen, C. J.; *J. Am. Chem. Soc.* **1967**, *89*, 2495.

(6) Pedersen, C. J.; *Angew. Chem. Int. Ed. Engl.* **1988**, *27*, 1021.

(7) Cram, D. J.; *Angew. Chem. Int. Ed. Engl.* **1988**, *27*, 1009.

(8) Sleiman, H.; Baxter, P. N. W.; Lehn, J.-M.; Rissanen, K. *J. Chem. Soc., Chem. Commun.* **1995**, 715.

(9) Harding, M. M.; Koert, U.; Lehn, J.-M.; Marquis-Rigault, A.; Piguet, C.; Siegel, J. *Helv. Chim. Acta* **1991**, *74*, 594.

(10) Youinou, M.-T.; Rahmouni, N.; Fischer, J.; Osborn, J. A. *Angew. Chem. Int. Ed. Engl.* **1992**, *31*, 733.

(11) Dietrich-Buchecker, C.; Rapenne, G.; Sauvage, J-P.; De Cian, A.; Fischer, J. *Chem. Eur. J.* **1999**, *5*, 1432.

(12) Simmons, H. E.; Park, C. H. *J. Am Chem. Soc.* **1968**, *90*, 2428.

(13) Mangani, S.; Ferraroni, M. *Supramolecular Chemstry of anions*; Wiley-VCH: New York, **1997**.

(14) Luecke, H.; Quiocho, F. A. *Nature* **1990**, *347*, 402.

(15) Higgins, C. *Nature* **1992**, *358*, 536.

(16) Calnan, B. J.; Tidor, B.; Biancalana, S.; Hudson, D.; Frankel, A. D. *Science* **1991**, *252*, 1167.

(17) Holloway, J. M.; Dahlgren, R. A.; Hansen, B.; Casey, W. H. *Nature.* **1998**, *395*, 785.

(18) Moss, B. *Chemistry & Industry* **1996**, 407.

(19) Beer, P.D.; Hopkins, P. K.; McKinney, J. D. *Chem. Commun.* **1999**, 1253.

(20) Gale, P. A. *Coord. Chem. Rev.* **2000**, *199*, 181.

(21) Gale, P. A. *Coord. Chem. Rev.* **2001**, *213*, 79.

(22) Gale, P. A.; Best, M. D.; Tobey, S. L.; Anslyn, E. V.; Sessler, J. L.; Camiolo, S.; Llinares, J. M.; Powell, D.; Bowman-James, K.; Bondy, C. R.; Loeb, S. J.; Choi, K.; Hamilton, A. D.; Wedge, T. J.; Hawthorne, M. F.; Lambert, T. N.; Smith, B. D.; Davis, A. P.; Joos, J-B.; Hosseini, M. W.; Beer, P. D.; Hayes, E. J. *Coord. Chem. Rev.* **2003**, *240*, 1-226.

(23) Gale, P. A. *Coord. Chem. Rev.* **2003**, *240*, 191.

(24) Wedge, T. J.; Hawthorne, M. F. *Coord. Chem. Rev.* **2003**, *240*, 111.

(25) Yang, X.; Knobler, C. B.; Hawthorne, M. F. *Angew. Chem. Int. Ed. Engl.* **1991**, *30*, 1507.

(26) Bondy, C. R.; Loeb, S. J. *Coord. Chem. Rev.* **2003**, *240*, 77.

(27) Lee, H-J.; Choi, Y-S.; Lee, K-B.; Park, J.; Yoon, C-J. *J. Phys. Chem. A.* **2002**, *106*, 7010.

(28) Alemán, C.; *J. Phys. Chem. A.* **2001**, *105*, 6717.

(29) Kavallieratos, K.; de Gala, S. R.; Austin, D. J.; Crabtree, R. H. *J. Am. Chem. Soc.* **1997**, *119*, 2325.

(30) Szumna, A.; Jurczak, J.; *Eur. J. Org. Chem.* **2001**, 4031.

(31) Inoue, Y.; Kanbara, T.; Yamamoto, T. *Tetrahedron Letters.* **2003**, *44*, 5167.

(32) Hossain, M. A.; Kang, S. O.; Llinares, J. M.; Powell, D.; Bowman-James, K. *Inorg. Chem.* **2003**, *42*, 5043.

(33) Kubik, S.; Kirchner, R.; Nolting, D.; Seidel, J. *J. Am. Chem. Soc.* **2002**, *124*, 12752.

(34) Kubik, S.; Goddard, R.; Kirchner, R.; Nolting, D.; Seidel, J. *Angew. Chem. Int. Ed. Engl.* **2001**, *40*, 2648.

(35) Tejeda, A.; Oliva, A. I.; Simón, L.; Grande, M.; Caballero, M. C.; Morán, J. R. *Tetrahedron Letters.* **2000**, *41*, 4563.

(36) De la Torre, M. F.; Campos, E. G.; González, S.; Caballero, M. C.; Morán, J. R. *Tetrahedron.* **2001**, *57*, 3945.

(37) Mei, M.; Wu, S. *New. J. Chem.* **2001**, *25*, 471.

(38) Ayling, A. J.; Perez-Payan, M. N.; Davis, A. P. *J. Am. Chem. Soc.* **2001**, *123*, 12716.

(39) Lee, D. H.; Lee, H. Y.; Lee, K. H.; Hong, J-I. *Chem. Commun.* **2001**, 1188.

(40) Best, M. D.; Tobey, S. L.; Anslyn, E. V. *Coord. Chem. Rev.* **2003**, *240*, 3-15.

(41) Metzger, A.; Anslyn, E. V. *Angew. Chem. Int. Ed. Engl.* **1998**, *37*, 649.

(42) Metzger, A.; Lynch, V.M.; Anslyn, E. V. *Angew. Chem. Int. Ed. Engl.* **1997**, *36*, 862.

(43) Baragaña, B.; Blackburn, A. G.; Breccia, P.; Davis, A. P.; de Mendoza, J.; Padrón-Carrillo, J. M.; Prados, P.; Riedner, J.; de Vries, J. G. *Chem. Eur. J.* **2002**, *8*, 2931.

(44) Lawless, L. J.; Blackburn, A. G.; Ayling, A. J.; Perez-Payan, M. N.; Davis, A. P. *J. Chem. Soc., Perkin Trans. 1.* **2001**, 1329.

(45) Beer, P. D.; Drew, M. G. B.; Smith, D. K. *J. Organomet. Chem.* **1997**, *543*, 259.

(46) Bell. R. A.; Christoph, G. G.; Fonczek, F. R.: Marsh, R.E. *Science.* **1975**, *190*, 151.

(47) Hosseini, M. W.; Lehn, J. M. *J. Am Chem. Soc.* **1982**, *104*, 3525.

(48) Hossain, M. A.; Llinares, J. M.; Miller, C. A.; Seib, L.; Bowman-James, K. *Chem. Commun.* **2000**, 2269.

(49) Kim, S. K.; Singh, N. J.; Kim, S. J.; Kim, H. G.; Kim, J. K.; Lee, J. W.; Kim, K. S.; Yoon, J. *Org. Lett.* **2003**, *5*, 2084.

(50) Schmidtchen, F. P. *Angew. Chem. Int. Ed. Engl.* **1977**, *16*, 720.

(51) Worm, K.; Schmidtchen, F. P. *Angew. Chem. Int. Ed. Engl.* **1995**, *34*, 65.

(52) Bondy, C. R.; Gale, P. A.; Loeb, S. J. *Chem. Commun.* **2001**, 729.

(53) Bondy, C. R.; Gale, P. A.; Loeb, S. J. *J. Supramol. Chem.* **2002**, *2*, 93.

(54) Mahoney, J. M.; Beatty, A. M.; Smith, B. D. *J. Am. Chem. Soc.* **2001**, *123*, 5847.

(55) Mahoney, J. M.; Marshall, R. A.; Beatty, A. M.; Smith, B. D.; Camiolo, S.; Gale, P. A. *Journal of Supramolecular Chemistry.* **2001**, *1*, 289.

(56) Coles, S. J.; Gale, P. A.; Hursthouse, M. B. *Cryst. Eng. Comm.* **2001**, 53.

(57) Gale, P. A.; Sessler, J. L.; Král, V.; Lynch, V. M. *J. Am. Chem. Soc.* **1996**, *118*, 5140.

(58) Sessler, J. L.; Camiolo, S.; Gale, P. A. *Coord. Chem. Rev.* **2003**, *240*, 17-55.

(59) Schmuck, C.; Lex, J. *Org. Lett.* **1999**, *1*, 1779. Schmuck, C. *Chem. Commun.* **1999**, 843. Schmuck, C.; Heil, M. *Org. Lett.* **2001**, *3*, 1253.

(60) Kavallieratos, K.; Bertao, C. M.; Crabtree, R. H. *J. Org. Chem.* **1999**, *64*, 1675.

(61) Gale, P. A.; Camiolo, S.; Chapman, C. P.; Light, M. E.; Hursthouse, M. B. *Tetrahedron Lett.* **2001**, *42*, 5095.

(62) Gale, P. A.; Camiolo, S.; Tizzard, G. J.; Chapman, C. P.; Light, M. E.; Coles, S. J.; Hursthouse, M. B. *J. Org. Chem.* **2001**, *66*, 7849.

(63) Camiolo, S.; Gale, P. A.; Hursthouse, M. B.; Light, M. E. *Tetrahedron Letters.* **2002**, *43,* 6995.

(64) Gale, P. A.; Sessler, J. L.; Allen, W. E.; Tvermoes, N. A.; Lynch, V. M. *Chem. Commun.* **1997**, 665.

(65) Sessler, J. L.; Anzenbacher, P. J.; Shriver, J. A.; Jurísková, K.; Lynch, V. M.; Marquez, M. *J. Am. Chem. Soc.* **2000**, *122*, 12061.

(66) Anzenbacher, P.; Try, A. C.; Miyaji, H.; Jursiková, K.; Lynch, V. M.; Marquez, M.; Sessler, J. L. *J. Am Chem. Soc.* **2000**, *122,* 10268.

(67) Camiolo, S.; Gale, P. A.; Hursthouse, M. B.; Light, M. E.; Shi, A. J. *Chem. Commun.* **2002**, 758.

(68) Gale, P. A.; Navakhun, K.; Camiolo, S.; Light, M. E.; Hursthouse, M. B. *J. Am. Chem. Soc.* **2002**, *124,* 11228.

(69) Sessler, J. L.; Maeda, H.; Mizuno, T.; Lynch, V. M.; Furuta, H. *Chem. Commun.* **2002**, 862.

(70) Baeyer, A. *Ber. Dtsch. Chem. Ges.* **1886**, *19*, 2184.

(71) Gutsche, C. D.; Bauer, L. J. *J. Am. Chem. Soc.* **1985**, *107*, 6052

(72) Floriani, C. In *The Porphyrin Handbook*; Kadish, K. M., Smith, K. M., Guilard, R., Eds.; Academic Press: San Diego, **2000**, Vol. 3, p. 405.

(73) Allen. W. E.; Gale, P. A.; Brown, C. T.; Lynch, V. M.; Sessler, J. L. *J. Am. Chem. Soc.* **1996**, *118*, 12471.

(74) Miyaji, H.; An, D.; Sessler, J. L. *Supramolecular Chemistry.* **2001**, *13,* 661.

(75) Yoon, D-W.; Hwang, H.; Lee, C-H. *Angew. Chem. Int. Ed. Engl.* **2002**, *41*, 1757.

(76) Lee, C-H.; Na, H-K.; Yoon, D-W.; Won, D-H.; Cho, W-S.; Lynch, V. M.; Shevchuk, S. V.; Sessler, J. L. *J. Am. Chem. Soc.* **2003**, *125*, 7301.

(77) Anzenbacher, P.; Jursikova, K.; Lynch, V. M.; Gale, P. A.; Sessler, J. L. *J. Am. Chem. Soc.* **1999**, *121*, 11020.

(78) Bonomo, L.; Solari, E.; Toraman, G.; Scopelliti, R.; Latronico, M.; Floriani, C. *Chem. Commun.* **1999**, 2413.

(79) Camiolo, S.; Gale, P. A. *Chem. Commun.* **2000**, 1129.

(80) Woods, C. J.; Camiolo, S.; Light, M. E.; Coles, S. J.; Hursthouse, M. B.; King, M. A.; Gale, P. A.; Essex, J. W. *J. Am. Chem. Soc.* **2002**, *124*, 8644.

(81) Turner, B.; Botoshansky, M.; Eichen, Y. *Angew. Chem. Int. Ed. Engl.* **1998**, *37*, 2475.

(82) Cafeo, G.; Kohnke, F. H.; La Torre, G. L.; White, A. J. P.; Williams, D. J. *Angew. Chem. Int. Ed. Engl.* **2000**, *39*, 1496.

(83) Turner, B.; Shterenberg, A.; Kapon, M.; Suwinska, K.; Eichen, Y. *Chem. Commun.* **2001**, 13.

(84) Cafeo, G.; Kohnke, F. H.; La Torre, G. L.; White, A. J. P.; Williams, D. J. *Chem. Commun.* **2000**, 1207.

(85) Bucher, C.; Zimmerman, R. S.; Lynch, V.; Sessler, J. L. *J. Am. Chem. Soc.* **2001**, *123*, 9716.

(86) Bucher, C.; Zimmerman, R. S.; Lynch, V.; Král, V.; Sessler, J. L. *J. Am. Chem. Soc.* **2001**, *123*, 2099.

(87) Andrievsky, A.; Ahuis, F.; Sessler, J. L.; Vogtle, F.; Gudat, D.; Moini, M. *J. Am. Chem. Soc.* **1998**, *120*, 9712.

(88) Bauer, V. J.; Clive, D. L. J.; Dolphin, D.; Paine, J. B.; Harris, F. L.; King, M. M.; Loder, J.; Wang, S-W. C.; Woodward, R. B. *J. Am. Chem. Soc.* **1983**, *105*, 6429.

(89) Sessler, J. L.; Cyr, M.; Lynch, V. *J. Am. Chem. Soc.* **1990**, *112*, 2810.

(90) Shionoya, M.; Furuta, H.; Lynch, V.; Harriman, A.; Sessler, J. L. *J. Am. Chem. Soc.* **1992**, *114*, 5714.

(91) Sessler, J. L.; Cyr, M.; Furuta, H.; Král, V.; Mody, T.; Morishima, T.; Shionoya, M.; Weghorn, S. *Pure & Appl. Chem.* **1993**, *65*, 393.

(92) Sessler, J. L.; Davis, J. M. *Acc. Chem. Res.* **2001**, *34*, 989.

(93) Köhler, T.; Seidel, D.; Lynch, V.; Arp, F. O.; Ou, Z.; Kadish, K. M.; Sessler, J. L. *J. Am. Chem. Soc.* **2003**, *125*, 6872.

(94) Seidel, D.; Lynch, V.; Sessler, J. L. *Angew. Chem. Int. Ed. Engl.* **2002**, *41*, 1422.

(95) Prasanna de Silva, A.; Fox, D. B.; Huxley, A. J. M. *Coord. Chem. Rev.* **2000**, *205*, 41-57.

(96) Lavigne, J. L.; Anslyn, E. V. *Angew. Chem. Int. Ed. Engl.* **2001**, *40*, 3118.

(97) Beer, P. D,; Gale, P. A,; Chen, G. Z. *J. Chem. Soc. Dalton Trans.* **1999**, 1897.

(98) Scherer, M.; Sessler, J. L.; Gebauer, A.; Lynch, V. *Chem. Commun.* **1998**, 85.

(99) Sessler, J. L.; Zimmerman, R. S.; Kirkovits, G. J.; Gebauer, A.; Scherer, M. *J. Organomet. Chem.* **2001**, *637-639*, 343-348.

(100) Sessler, J. L.; Gebauer, A.; Gale, P. A. *Gazz. Chim. Ital.* **1997**, *127,* 723.

(101) Kavallieratos, K.; Hwang, S.; Crabtree, R. H. *Inorg. Chem.* **1999**, *38,* 5184.

(102) Beer, P. D.; Hesek, D.; Nam, K. C. *Organometallics.* **1999**, *18,* 3933.

(103) Beer, P. D.: Berry, N.; Drew, M. G. B.; Fox, O. D.; Padilla-Tosta, M. E.; Patell, S. *Chem. Commun.* **2001**, 199.

(104) Berry, N. G.; Pratt, M. D.; Fox, O. D.; Beer, P. D. *Supramolecular Chemistry.* **2001**, *13,* 677.

(105) Antonisse, M. M. G.; Reinhoudt, D. N. *Chem. Commun.* **1998**, 443.

(106) Gutsche, C. D.; Bauer, L. J. *J. Am. Chem. Soc.* **1985**, *107*, 6052

(107) Floriani, C. *Chem. Commun.* **1996**, 1257.

(108) Gale, P. A.; Sessler, J. L.; Král, V. *Chem. Commun.* **1998**, 1.

(109) Hoorn, W. P. v.; Jorgensen, W. L. *J. Org. Chem.* **1999**, *64*, 7439.

(110) Schmidtchen, F. P. *Org. Lett.* **2002**, *4*, 431.

(111) de Namor, A. F. D.; Shehab, M. *J. Phys. Chem. B.* **2003**, *107*, 6462.

(112) Blas, J. R.; Márquez, M.; Sessler, J. L.; Luque, F. J.; Orozco, M. *J. Am. Chem. Soc.* **2002**, *124*, 12796.

(113) Gale, P. A.; Anzenbacher, P.; Sessler, J. L. *Coord. Chem. Rev.* **2001**, *222*, 57.

(114) Sessler, J. L.; Gale, P. A. In *The Porphyrin Handbook*; Kadish, K. M., Smith, K. M., Guilard, R., Eds.; Academic Press: San Diego, 2000; Vol. 6, p 257.

(115) Sessler, J. L.; Anzenbacher, P.; Miyaji, H.; Jursiková, K.; Bleasdale, E. R.; Gale, P. A. *Ind. Eng. Chem. Res.* **2000**, *39*, 3472.

(116) Miyaji, H.; Anzenbacher, P.; Sessler, J. L.; Bleasdale, E. R.; Gale, P. A. *Chem. Commun.* **1999**, 1723.

(117) Gale, P. A.; Twyman, L. J.; Handlin, C. I.; Sessler, J. L. *Chem. Commun.* **1999**, 1851.

(118) Hynes, M. J. *J. Chem. Soc., Dalton Trans.* **1993**, 311.

(119) Fielding, L. *Tetrahedron.* **2000**, *56*, 6151.

(120) Gale, P. A.; Hursthouse, M. B.; Light, M. E.; Sessler, J. L.; Warriner, C. N.; Zimmerman, R. S. *Tetrahedron Lett.* **2001**, *42*, 6759.

(121) Sessler, J. L.; Andrievsky, A.; Gale, P. A.; Lynch, V. *Angew. Chem. Int. Ed. Engl.* **1996**, *35*, 2782.

(122) Fischer, H.; Beyer, H.; Zaucker, E. *Justus. Liebigs. Ann. Chem.* **1931**, *33*, 55.

(123) Weber, H.; Rohn, T. *Z. Naturforsch. B.* **1990**, *45*, 701.

(124) Motekaitis, R. J.; Heinert, D. H.; Martell, A. E. *J. Org. Chem.* **1970**, *35*, 2504.

(125) Streith, J.; Blind, A.; Cassal, J-M.; Sigwalt, C. *Bull. Soc. Chim. Fra.* **1969**, 948.

(126) Lee, C-H.; Lindsey,J. S. *Tetrahedron.* **1994**, *50*, 11427.

(127) Littler, B. J.; Miller, M. A.; Hung, C-H.; Wagner, R. W.; O'Shea, D. F.; Boyle, P. D.; Lindsey,J. S. *J. Org. Chem.* **1999**, *64*, 1391.

(128) Wang, Q.M.; Bruce, D. W. *Synlett.* **1995**, 1267.

(129) Tayebani, M.; Conoci, S.; Feghali, K.; Gambarotta, S.; Yap, G. P. A. *Organometallics.* **2000**, *19*, 4568.

(130) Fox, O. D.; Rolls, T. D.; Drew, M. G. B.; Beer, P. D. *Chem. Commun.* **2001**, 1632.

(131) Gross, Z.; Galili, N.; Simkhovich, L.; Saltsman, I.; Botoshansky, M.; Bläser, D.; Boese, R.; Goldberg, I. *Org. Lett.* **1999**, *1*, 599.

(132) E.-H. Kim, B.-S. Koo, C.-E. Song and K.-J. Lee, *Synth. Comm.* **2001**, *31*, 3627.

(133) Warriner, C. N.; Gale, P. A.; Light, M. E.; Hursthouse, M. B. *Chem. Commun.* **2003**, 1810.

(134) Spartan '02, Wavefunction Inc. Irvine CA, USA.

(135) Abboud, J-L. M.; Roussel, C.; Gentric, E.; Sraidi, K.; Lauransan, J.; Guihéneuf, G.; Kamlet, M. J.; Taft, R. W. *J. Org. Chem.* **1988**, *53*, 1545.

(136) Laurence, C.; Berthelot, M.; Le Questel, J-Y.; El Ghomari, M. J. *J. Chem. Soc. Perkin Trans. 2.* **1995**, 2075.

(137) Bordwell, F. G.; Ji, G-Z. *J. Am. Chem. Soc.* **1991**, *113*, 8398.

(138) Bordwell, F. G.; Algrim, D. J.; Harrelson, J. A. *J. Am. Chem. Soc.* **1988**, *110*, 5903.

(139) Camiolo, S.; Gale, P. A.; Hursthouse, M. B.; Light, M. E.; Warriner, C. N. *Tetrahedron Letters.* **2003**, *44*, 1367.

(140) Backer, H. J.; Stevens, W. *Recl. Trav. Chim. Pays-Bas.* **1940**, *59*, 423.

(141) Yde, B.; Yousif, N. M.; Pedersen, U.; Thomsen, I.; Lawesson, S-O. *Tetrahedron.* **1984**, *40*, 2047. Cava, M. P.: Levinson, M. I. *Tetrahedron.* **1985**, *41*, 5061.

(142) Bisson, A. P.; Hunter, C. A.; Morales, J. C.; Young, K. *Chem. Eur. J.* **1998**, *4*, 845.

(143) Gale, P. A.; Hursthouse, M. B.; Light, M. E.; Warriner, C. N. *Collect. Czech, Chem. Comm.* **2004**, In Press.

(144) Job, P. *Ann. Chim.* **1928**, *9*, 113.

(145) Miyaji, H.; Sessler, J. L. *Angew. Chem. Int. Ed. Engl.* **2001**, *40*. 154.

(146) MacDowell, D. W. H.; Ballas, F. L. *J. Org. Chem.* **1977**, *42*, 3717.

(147) Galvez, C.; Garcia, F.; Garcia, J.; Soldevila, J. *J. Heterocyclic. Chem.* **1986**, *23*, 1103.

(148) Werner, F.; Schneider, H-J. *Helv. Chim. Acta.* **2000**, *83*, 465.

(149) Jeong, K-S.; Cho, Y. L. *Tetrahedron Letters.* **1997**, *38*, 3279.

(150) Camiolo, S.; Gale, P. A.; Hursthouse, M. B.; Mayer, T. A.; Paver, M. A. *Chem. Commun.* **2000**, 275.

(151) Camiolo, S.; Gale, P. A.; Hursthouse, M. B.; Light, M. E. *Org. Biomol. Chem. Commun.* **2003**, *1*, 741.

(152) Denuault, G. *Chemistry & Industry.* **1996**, *18*, 678.

(153) Denuault, G.; Gale, P. A.; Hursthouse, M. B.; Light, M. E.; Warriner, C. N. *New J. Chem.* **2002**, *26*, 811.

(154) Friedman, M. *J. Org. Chem.* **1965**, *30*, 859.

(155) Spencer, P. Polyaza redox-active acyclic and macrocyclic compounds designed to bind cations and anions, D.Phil Thesis, University of Oxford, **1994**.

(156) Knox, G. R.; Pauson, P. L.; Willison, D. *Organometallics.* **1990**, *9*, 301.

(157) Coles, S. J.; Denuault, G.; Gale, P. A.; Horton, P. N.; Hursthouse, M. B.; Light, M. E.; Warriner, C. N. *Polyhedron.* **2003**, *22*, 699.

(158) Beer, P. D.; Blackburn, C.; McAleer, J. F.; Sikanyika, H. *Inorg. Chem.* **1990**, *29*, 378.

(159) Beer, P. D.; Gale, P. A.; Chen, Z. *Adv. Phys. Org. Chem.* **1998**, *31*, 1.

(160) Gottlieb, H. E.; Kotlyer, V.; Nudelman, A. *J. Org. Chem.* **1997**, *62*, 7512.

(161) BDH Chemicals. Nuclear Magnetic Resonance.

(162) Amphlett, J. WinCV v2.1, University of Southampton, **1991**.